Fakulteit Ingenieurswese, Bou-omgewing & IT
Faculty of Engineering, Built Environment & IT

School of Engineering

Department of Materials Science and Metallurgical Engineering

**This report is completed in partial fulfilment of requirements for M.Eng (Metallurgical Engineering) at the University of Pretoria.**

# MEng: Upgrade of SLon Concentrate with the use of Froth Flotation on an Iron Ore Sample from Anglo American Kumba Iron Ore

Student: Morné Kruger 04421000

Supervisors: Dr N Naudè
Mr S Naik

Submission date: 3 May 2016

UNIVERSITEIT VAN PRETORIA
UNIVERSITY OF PRETORIA
YUNIBESITHI YA PRETORIA
Denkleiers • Leading Minds • Dikgopolo tša Dihlalefi

## Abstract

Pollution caused by mining practices is a growing concern worldwide. Although there are numerous contributing factors, discarded ultra-fine (-150 micron) material is regarded as one of the major challenges. Geological footprints, water pollution and dust generation are but some of the environmental challenges that are associated with the generation of ultra-fine (-150 micron) material.

To overcome the arising challenges, extensive research into the reduction of fines generation, as well as ultra-fines beneficiation, has been investigated. Although crushing circuits have been made more efficient by making use of improved mining techniques and novel processing technologies, the presence and the generation of ultra-fines are unavoidable. The environmental impact and the loss of material is thus forcing mining practices to consider new beneficiation techniques. Great benefits can be realised, as the ultra-fine material has no associated mining cost and has the potential of increasing production, effectively generating revenue.

Several techniques have been investigated over the last few decades to upgrade ultra-fine iron ore by making use of various differences in mineral characteristics. The major difference between beneficiation technologies is the cost involved and many technologies have therefore been uneconomical in the past. However, with the development of technologies, the beneficiation of iron ore ultra-fines has become more and more economically attractive. The most popular of these techniques include froth flotation, as well as magnetic separation - specifically the SLon concentrator.

Due to the selectivity and low operational costs, froth flotation has been used worldwide to produce a saleable product from the ultra-fine material. The use of flotation in South Africa's iron ore industry has been

unsuccessful in the past, due to the complexity of the ore body. The ore mineralogy complicates the use of flotation and the circuits involved. Therefore, Anglo American Kumba Iron Ore has conducted extensive research on the use of the SLon concentrator to upgrade the material found at its Sishen mine. However, this process alone has proved to be unsuccessful in producing a high grade product.

This study therefore investigated the use of froth flotation as a final upgrading process, after the SLon concentrator, to produce a high grade iron ore product with an iron content of more than 66,5%. Mineralogical studies of the feed material indicated that the material in the +38 micron material was unliberated and required milling of this size fraction prior to the use of flotation. Additionally, the -38 micron material was well liberated and was assayed to be close to the required product specification with a total Fe content of 66,3%. Based on the results, the process was determined to include de-sliming of the feed material (SLon concentrate) at 38 micron, and milling of the +38 micron material, which is then followed by froth flotation.

The use of starch, amines and inorganic chemicals as a depressant, collector and pH modifiers respectively, have proven successful in upgrading Sishen's iron ore ultra-fines during flotation. Results showed selective depression of hematite and the activation of quartz and kaolinite under specific conditions. Laboratory results indicated that the milled material can be upgraded to a Fe content of approximately 67% from a feed material containing less than 65% Fe at a yield to product of 60 to 65%. Finally, combining the flotation concentrate with the de-slimed -38 micron material, a total circuit yield of 82 % can be achieved with an Fe content of 66,5 % (w/w) and a total $SiO_2$ content of less than 2% as required for a high grade iron ore product. Therefore it was concluded that the SLon concentrate at Sishen can successfully be upgraded using froth flotation as a final concentrating step.

# Table of Contents

# List of Figures

# List of Tables

## Acknowledgement

It is with absolute pleasure that I extend my deepest gratitude to my mentor and supervisor **Dr N Naude** for her technical support and her personal interest to aid in my development, both academically and personally. I have learnt so much from her and for that I shall always be grateful. Her dedication and passion reflected through her willingness to guide me at even the most impossible hours, which truly inspired me and contributed to the successful completion of my work. I would also like to extend a special thanks to Sandip Naik for his continuous technical support throughout the study and therefore his contribution to the success thereof. Thank you very much. Gratitude to the University of Pretoria, more specifically the Department of Material Sciences and Metallurgical Engineering, for the opportunity, equipment and facilities to complete this study.

A special thank you to the sponsors of this study, Anglo American Kumba Iron Ore, for funding this study and making it possible. Furthermore, thank you to the Anglo American Kumba Iron Ore personnel for always being available for guidance and technical support where needed.

Thank you to Betachem for supplying reagents, as well as to Riaan Grobler for technical guidance. An additional thank you to Clarient for supplying reagents.

Thank you to Enprotec, my employer, for always supporting and encouraging me in terms of the time allocated to this study.

Then I would also like to lovingly thank my mother (Cathy Kruger) for always believing in me. She has been such an inspiration and role model in my life and I would never have come this far in my career if not for her.

Finally, with love, I would like to thank my wife for always being supportive, understanding and being there for me through the difficult times. Her love, compassion and encouragement has really made it a joyous experience.

# Chapter 1: Introduction

## 1.1 Iron Ore World Wide

World iron ore resources have been estimated to be 800 x $10^9$ tons, containing more than 230 x $10^9$ tons of iron (minerals.usgs.gov, 2014). Although the US iron ore reserve is of a low grade, it contains 27 billion tons of iron. Brazil, China and Australia are the leaders in iron ore production, accounting for more than 50% of world production (Papp *et al.,* 2008). China is a leader not only in production, but also in consumption of iron ore. The iron ore consumption of China exceeds 25% of world consumption.

Table 1 lists the production rate of various countries, as well as the reserves of that country. China is the largest producer with 1310 x $10^6$ tons produced in 2013. South Africa (SA) produced 67 x $10^6$ tons in 2013, making SA the 7$^{th}$ largest producer worldwide (Jorgenson, 2014).

**Table 1: Global iron ore production rate for 2012 and 2013, as well as the global reserves (Jorgenson, 2014)**

| | Mine production | | Reserves[7] | |
|---|---|---|---|---|
| | 2012 | 2013[e] | Crude ore | Iron content |
| United States | 54 | 52 | 6,900 | 2,100 |
| Australia | 521 | 530 | 35,000 | 17,000 |
| Brazil | 398 | 398 | 31,000 | 16,000 |
| Canada | 39 | 40 | 6,300 | 2,300 |
| China | 1,310 | 1,320 | 23,000 | 7,200 |
| India | 144 | 150 | 8,100 | 5,200 |
| Iran | 37 | 37 | 2,500 | 1,400 |
| Kazakhstan | 26 | 25 | 2,500 | 900 |
| Russia | 105 | 102 | 25,000 | 14,000 |
| South Africa | 63 | 67 | 1,000 | 650 |
| Sweden | 23 | 26 | 3,500 | 2,200 |
| Ukraine | 82 | 80 | [8]6,500 | [8]2,300 |
| Venezuela | 27 | 30 | 4,000 | 2,400 |
| Other countries | 96 | 88 | 14,000 | 7,100 |
| World total (rounded) | 2,930 | 2,950 | 170,000 | 81,000 |

## 1.2 Anglo American Kumba Iron Ore – Sishen

The high grade banded iron formation, which is currently mined at Anglo American Kumba Iron Ore (AAKIO), is situated in the Sishen-Postmasburg area of the Northern Cape Province. The bulk of the ore body at Sishen mine

consists of high grade, laminated and massive ores with most of the Sishen mining area covered with calcrete, limestone, clay, quaternary sand and detritus (Carney *et al.,* 2015).

### 1.3 Beneficiation Process

Generally the iron ore concentrating process involves an initial stage of crushing the run of mine material, such that the top size of the material can be treated with a concentrating unit (pers. Comm., 28 October 2015). The crushed product is then sized into various size ranges, as required by each unit operation. These size ranges are very dependent on the plant design and the mineralogy of the ore. Typically, the material is divided into very coarse (-90 to +25mm), medium coarse (-25 to +8mm), coarse (-8 to +5mm), fine (-5 to +212 micron) and ultra-fine (-212 micron) size fractions. The very coarse, medium coarse and coarse high grade fractions are concentrated with dense medium separation (DMS) processes, where ferrosilicon is utilised as the medium. The very coarse material is typically treated with a dense medium drum, whereas the coarse material is typically treated with a dense medium cyclone. Figure 1 gives an overview of the processing route employed at Sishen.

This process applies to the coarse material, whereas approximately 3 million tons per annum (Mt/a) of the ultra-fines (-212 micron) material is discarded as waste at Sishen mine (Dworzanowski, 2014). Due to the fact that there is still a lot of value in this discard stream, AAKIO has endeavoured to beneficiate hematite from this stream. One processing option includes the use of a SLon, which is a Wet High Intensity Magnetic Separator (WHIMS), to concentrate hematite that has been tested. However, the final product is still not on specification. This lead to the proposal of utilising froth flotation as a means of increasing the product grade to the desired specification.

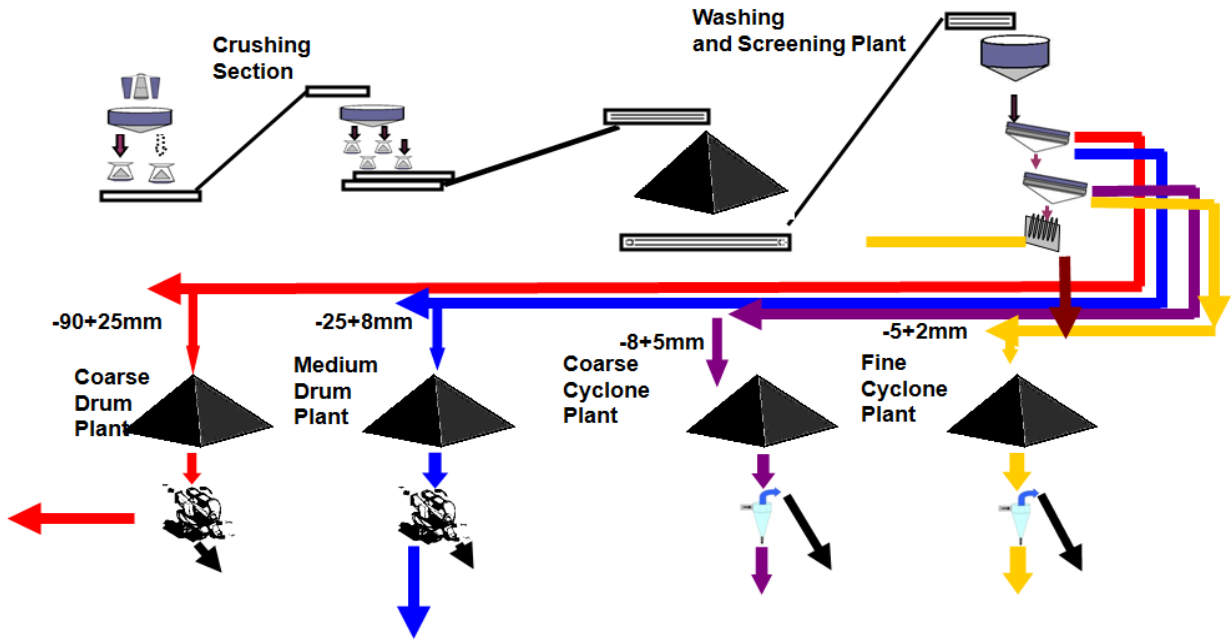


**Figure 1: Processing route employed at Sishen (pers. Comm., 28 October 2015)**

The motivation for concentrating iron ore can be explained by considering the unwanted elements, i.e. silicon, phosphorus, aluminium and sulfur and its effect on downstream processes. An understanding of the effects of trace elements in downstream processes is crucial in the beneficiation processes currently implemented in the iron ore industry (Roy *et al.*, 2008).

Quartz is known as a gangue phase which is always present in iron ore, and is reduced at temperatures above 1 300 ℃. Generally the higher the temperature, the more silicon will be present in the metal phase, but the higher the volume of quartz, the larger the slag volume which in turn raises coke consumption. In contrast, the silicon present in the metal phase has the main effect of promoting the formation of gray iron, which is finished with more ease than white iron. Additionally, silicon reduces the probability of forming blowholes and reduces shrinkage during casting.

Phosphorus is one of the most undesired trace elements in iron ore, as it drastically reduces ductility of steel and is not easily removed by fluxing or smelting. Even at very low concentrations, i.e. 0,5%, it has detrimental effects.

Al-bearing minerals has the benefit of being very hard to reduce, but has the negative effect of increasing the slag viscosity and therefore decreasing the descent of the furnace charge, and could quite possibly lead to a frozen furnace. It has also been determined that Al-bearing minerals has an adverse effect on sinter and pellet properties.

Sulfur in the iron causes the iron to be very brittle at high temperatures, and therefore cracks when hot worked. Concentrations of above 0,03% are therefore avoided.

## 1.4 Formulation of problem

The major challenge in processing ultra-fine iron ore in South Africa is the complexity of the ore body and the required high product specification. Flotation is the process generally used, but includes numerous stages of feed preparation, which in many cases is selective flocculation. The real challenge comes in when attempting to selectively float the gangue material.

By making use of the SLon, the raw feed material can be upgraded with good results in terms of yield to product and final product grades. However, this is not sufficient and requires the use of flotation to achieve the desired final grade. Therefore the aim is to successfully use flotation to upgrade the SLon concentrate.

## 1.5 Research objectives

In general there are two pellet type products typically produced with the following specification (pers. Comm., 28 October 2015):

- Direct reduction (DR) pellets with ($SiO_2$+$Al_2O_3$) < 2 and a maximum of 3%, as well as a Fe content of 67% with a minimum of 66%.
- Blast furnace (BF) pellets with a Fe content > 64% and a $SiO_2$ content of < 5%. Finally, an alumina ($Al_2O_3$) content of < 2% is required.

The research objectives are aimed at better understanding the froth flotation process, i.e. considering iron ore from Sishen. This entails extensive consideration and a detailed study of the mineralogical aspects of the ore, as well as a detailed study on flotation parameters, including the relative effect of these parameters in order to achieve a final concentrate grade of > 66,5% Fe and an $SiO_2$ content < 2%.

## 1.6 Hypothesis

***It is possible to treat and upgrade the ultra-fine iron ore SLon concentrate at Sishen by means of froth flotation to achieve a 66,5% Fe concentrate grade.***

## 1.7 Overview

- Chapter 2: Literature Review – The literature review discusses ultra-fine (-212 micron material) beneficiation in its entirety, including various minerals and methods used in various countries, as well as the various considerations brought into account regarding the mineralogy of the various ores specific to their geological location. The literature review also investigates the use of flotation in depth, including all of the various parameters and the influence thereof on the process. Additionally, various reagents and mechanisms thereof were also considered and discussed.

- Chapter 3: Methodology – The methodology describes the stepwise approach to completing the test program, including
  - materials characterisation;
  - flotation evaluation; and
  - process design.

- Chapter 4: Results and Discussion – This section discusses the results achieved, including the possible yields and product specification that can be realised when using froth flotation.

- Chapter 5: Proposed Solution – After determining the technical possibilities that can be realised when using froth flotation, the final proposal with regards to processing the SLon concentrate at AAKIO Sishen to produce a final saleable product can be generated.

- Chapter 6: Conclusion – This section summarises all results and achievements from the test program. It details the main findings from the test program.

# Chapter 2: Literature Review

The literature study on the beneficiation of fine hematite ore considers published data and reports to understand the minerals, the processing thereof and previous work that was completed, in order to structure the test program in the best possible way. It also ensures that various processing options are considered from a technical point of view. Specific attention is given to ultra-fine (-150 micron) iron ore beneficiation in general, followed by a more in-depth look at froth flotation and WHIMS as the main processing options for iron ore beneficiation, i.e. for the ultra-fine material.

## 2.1 Introduction

Extensive research has been done on ultra-fine material (typically < 150 µm), the production of which is unavoidable, and is being treated in many countries, including Brazil, USA, India, and South Africa, amongst other. Depending on the ore body, the ultra-fines can be treated in various ways, of which froth flotation and Wet Low Intensity Magnetic Separation (WLIMS) are probably the most popular processes for magnetite bearing ore bodies (Dworzanowski, 2014). In the case of hematite bearing ore bodies, froth flotation is predominantly used for the beneficiation of the -150 micron material in both Brazil and the USA. Brazilian ore bodies typically have low concentrations of impurities and therefore the general practice is to use reverse flotation (Peres, *et al.,* 1996). Typically, Brazilian flotation plant would de-slime prior to flotation, as the presence of -10 micron material substantially increases the reagent consumption deeming the option uneconomical.

In South Africa the challenges in treating these ultra-fines can be attributed to the extensive amount of -10 micron material present in the -150 micron fraction. Therefore the proposed processing route was to use the SLon concentrator (WHIMS), as this technology was proved successful (Dworzanowski, 2014).

## 2.2 Ultra-fines beneficiation

Producing ultra-fines during the mining and beneficiation process is unavoidable and pose a great challenge in iron ore production, as it is very difficult to beneficiate in some cases (Roy *et al.,* 2008). Fines are generally discarded into the environment, but with proper characterisation of the ore and the use of new technologies, it could be beneficiated in an environmentally friendly, potentially profitable manner.

The rest of this section focusses on previous testwork, results, challenges and processing possibilities for various iron ore types around the world. It also includes characterisation methods, conclusions based on the mineralogy of the specific ore types, and possible processing routes.

Iron ore from India is known to be different from the rest of the world due to a higher phosphorous and Al-bearing minerals content, which can have negative effects on downstream processes. Three different ore deposits were considered in an attempt to determine the amenability of fines beneficiation. The main aim was to characterise the ore body and test its amenability to beneficiation. The three ores considered were:

- Jilling-Langalota deposit, belonging to the Iron Ore Group (IOG)
- Chitradurga ores, belonging to the Dharwar Super group in India
- Krivoy Rog deposits, of Ukranian Sheild

Characterisation included determining the particle size distributions, liberation analysis and various microscopic analyses.

Figure 2 shows that all three samples were made up of extremely fine particles, all of which had 80% passing 50 µm and had more or less the same size distribution.

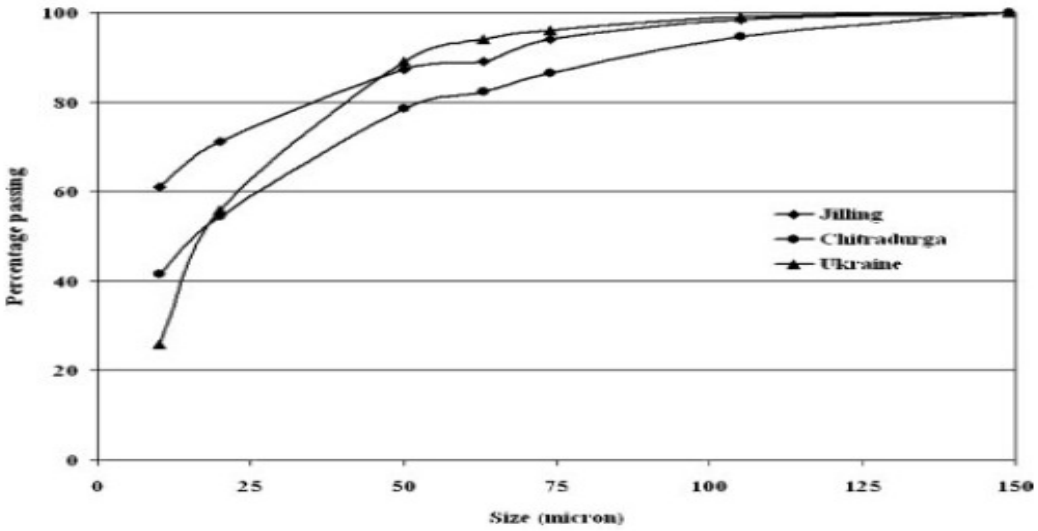


**Figure 2: Particle size distribution for three different iron ores (Roy *et al.,* 2008)**

Table 2 tabulates the assay data for the different ores, of which the Jilling ore can be upgraded by simply removing the material less than 20 µm. which had the majority of Al-bearing minerals present (Roy *et al.,* 2008). This was not true for the Chitradurga ore, as the Al-bearing minerals is evenly distributed over the entire size distribution. The Krivoy ore also showed good mineral distribution over the entire size range, as well as negligible amounts of Al-bearing minerals, and thus the ore is considered to be amenable to beneficiation.

**Table 2: Chemical analysis of three different iron ores (Roy *et al*., 2008)**

| | Jilling (assay%) | | | Chitradurga (assay%) | | | Krivoy Rog (assay%) | | |
|---|---|---|---|---|---|---|---|---|---|
| Size, µm | Fe | $Al_2O_3$ | $SiO_2$ | Fe | $Al_2O_3$ | $SiO_2$ | Fe | $Al_2O_3$ | $SiO_2$ |
| −150+50 | 52·70 | 8·12 | 5·62 | 56·28 | 4·43 | 7·26 | 29·07 | 1·04 | 54·82 |
| −50+20 | 45·92 | 9·08 | 14·06 | 53·03 | 6·12 | 8·57 | 28·43 | 1·38 | 55·10 |
| −20 | 33·40 | 16·72 | 22·61 | 45·91 | 10·11 | 12·07 | 28·12 | 2·27 | 54·68 |
| Head | 37·86 | 14·40 | 19·08 | 49·86 | 7·93 | 10·19 | 28·32 | 1·84 | 54·83 |

Table 3 lists the findings of the Scanning Electron Microscope (SEM) and Energy Dispersive Spectrum (EDS) analyses (Roy *et al*., 2008). Most importantly, the porous nature if the Jilling ore makes beneficiation by means

of flotation and density separation much more difficult and thus would require special attention.

**Table 3: Scanning electron microscope and energy dispersive spectroscopy data for three different iron ores (Roy *et al.*, 2008)**

| | Iron ores and slimes | | |
|---|---|---|---|
| Mineral phases | Jilling | Chitradurga | Ukraine |
| Iron-bearing minerals | Very porous and spongy. Contain some Al and Si in liberated particles major mineral | It contains some Al and Si in liberated particles | Almost regular smooth surface and compact grains. Relatively low Al and Si in liberated particles |
| Manganese minerals | Having some manganese content | Having some manganese content | No manganese, etc. |
| Gangue minerals | Kaolinite and gibbsite occur as ferruginous with traces of P. Quartz particles have negligible Fe | Kaolinite occurs as ferruginous with traces of P. Quartz particles have negligible Fe | Kaolinite is absent Quartz is the only gangue mineral |

Liberation graphs (Figure 3) show an increase in clay interlocked in hematite, with an increase in size fraction (Roy *et al.*, 2008). Although this is the case, the volume fraction of free hematite decreases with a decrease in particle size. This is due to the fact that the volume of gangue drastically increases with a decrease in size fraction, as illustrated in Figure 4. Interestingly enough there is minimal quartz associated with hematite in the Indian ores, but not in the case of the Ukrainian ore. Figure 5 also shows that the quartz is almost fully liberated and therefore it would be a much easier task to separate quartz from hematite in the case of the Indian ores.

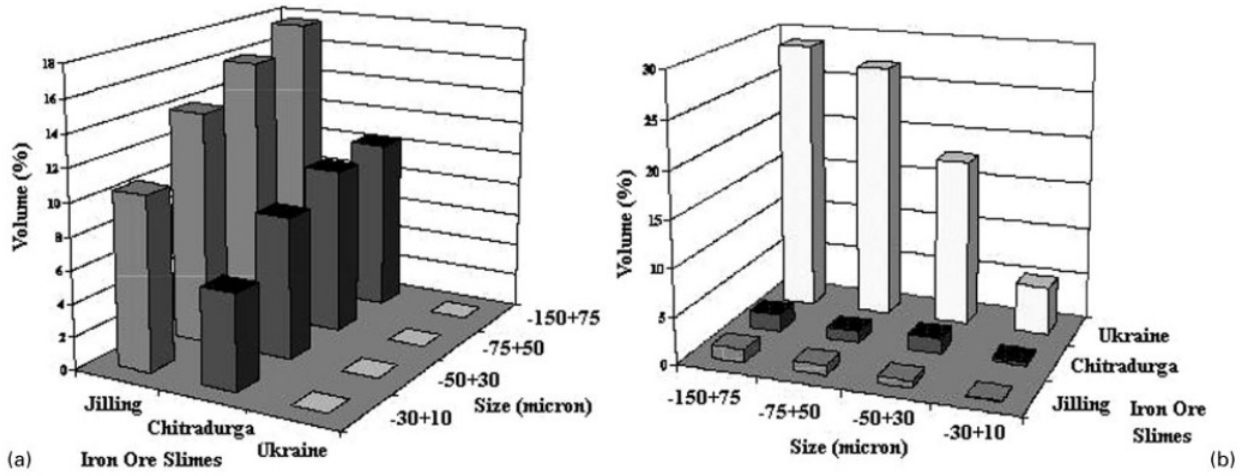


**Figure 3: Liberation graphs of a) hematite with clay interlocked b) hematite with quartz interlocked for three different iron ores (Roy *et al.*, 2008)**

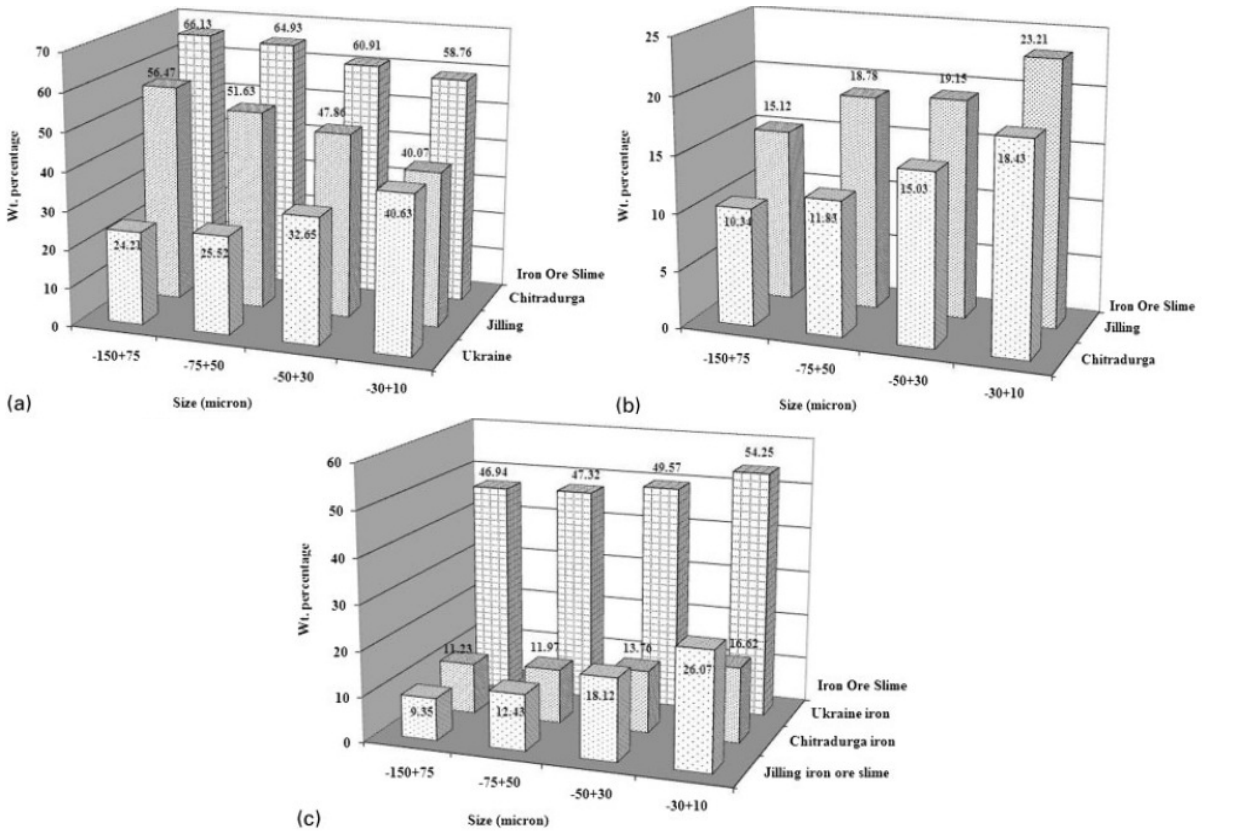


**Figure 4: Liberation graphs of a) free hematite b) free clay c) free quartz for three different iron ores (Roy *et al.*, 2008)**

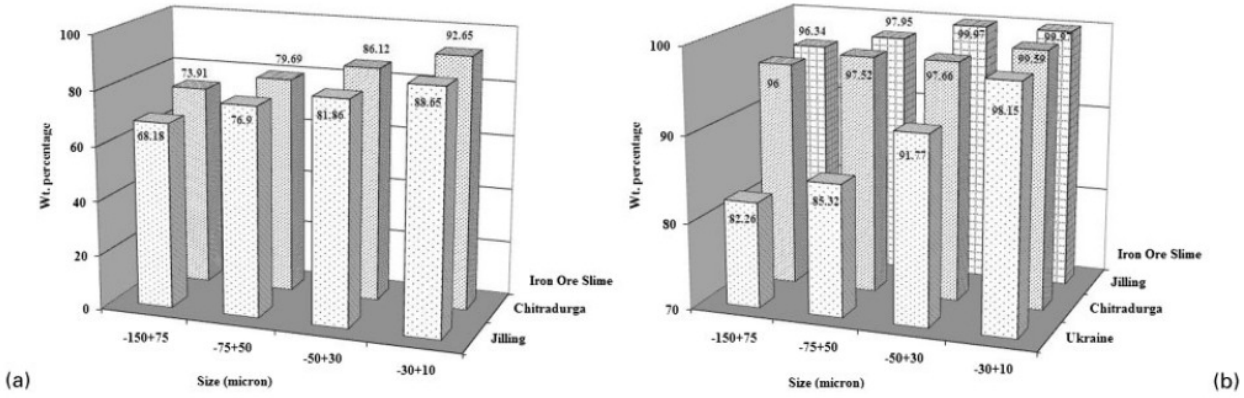


**Figure 5: Liberation graphs of a) percentage of clay liberated b) percentage of quartz liberated for three different iron ores (Roy *et al.*, 2008)**

Table 4 tabulates the volumetric distribution of different phases in the different size ranges for the three different ores.

**Table 4: Volumetric distribution of different phases in different size fractions for three different iron ores (Roy *et al.*, 2008)**

| | Volume per cent in different size fractions | | | |
|---|---|---|---|---|
| Mineral phases | −150+75 μm | −75+50 μm | −50+30 μm | −30+10 μm |
| Jilling iron ore slime | | | | |
| Hematite+goethite | 68·32 | 64·52 | 56·15 | 41·20 |
| Quartz | 11·35 | 13·83 | 22·73 | 34·36 |
| Kaolinite | 20·33 | 21·65 | 21·12 | 24·44 |
| Chitradurga iron ore slime | | | | |
| Hematite+goethite | 73·48 | 71·16 | 69·45 | 62·39 |
| Quartz | 14·25 | 15·51 | 16·49 | 20·73 |
| Kaolinite | 12·27 | 13·33 | 14·06 | 16·88 |
| Ukraine iron ore slime | | | | |
| Hematite+goethite | 30·48 | 30·49 | 30·27 | 29·66 |
| Quartz | 69·52 | 69·51 | 69·73 | 70·34 |

Based on the mineralogy of the various ores, specific beneficiation processes can be developed or considered for the specific characteristics of the ore. In this case, only three ore types where considered for illustration purposes.

In other parts of the world, other than South Africa, froth flotation is used to beneficiate ultra-fines produced from iron ore washing plants and slurry ponds (dos Santos *et al.*, 2007). One of these examples is Brazil, which uses reverse cationic flotation as the general method of beneficiation of these ultra-fines. It was stipulated that starch is considered as the general hematite depressant, but further studies showed that under specific conditions, humic acid provides a much more selective alternative (dos Santos *et al.*, 2007). It should be noted that once again this is only specific to some ore types. In this case it was proven that a concentrate grade with 86% hematite and a 90,7% recovery can be achieved from an ore with a quartz to hematite ratio of 1 to 3 under specific conditions.

Additional research was conducted on the implementation of column cells on some of the Brazilian ores, and showed a decrease in cost of between 25% and 40% compared to conventional cells (Flint *et al.*, 1992).

At the Kiriburu iron ore mines in India, a study aimed at upgrading the fines fraction was conducted. The study showed that the ore can be upgraded

assaying up to 60% Fe, 3,34% $SiO_2$, and 2,93% $Al_2O_3$ (Srivastava *et al.*, 2000). The experimental route included an initial characterisation process, after which possible processing routes were considered. These routes were modelled and the experimental testwork phase commenced. Characterisation showed a softer high clay ore with 80% passing 110 µm, and that the liberation of the minus 45 µm material was a function of particle size, in which case the ultra-fines show a lower degree of liberation. It was stipulated that high Al-bearing minerals content caused a great deal of operational problems during sintering and thus the challenge of upgrading the iron ore presented itself. One of the major problems of high Al-bearing mineral content is that a very viscous melt develops in the furnace which, amongst others, requires a high coke rate (Srivastava *et al.*, 2000).

The proposed final circuit was a hydro-cyclone and spiral circuit, which in this case upgraded the ore to such an extent that the product assay was 64,17% Fe with 1,15% alumina, with an Fe recovery of 53,7% (Srivastava *et al.*, 2000).

Although flocculation techniques were unsuccessful in this case, selectively flocculating hematite from quartz has been recorded in Michigan at the Tilden Mine (Mathur *et al.*, 1999). However, some challenges were experienced, such as heteroflocculation, as well as entrainment or entrapment, which could make implementing the process less attractive (Mathur *et al.*, 1999).

Another alternative is to leach Al-bearing minerals from iron ore in an attempt to upgrade the ore (Pradhan *et al.*, 2005). The aim of the research, on a sample from Bolani iron ore washing plant in India, was to leach Al-bearing minerals from the ore with bio-beneficiation, i.e. an in situ leaching process. The organisms considered were circulans MTCC 879 and niger MTCC 282. The chemical assay analysis resulted in an average of 75,7% $Fe_2O_3$, 9,95% $Al_2O_3$, 6,1% $SiO_2$ and a total Fe content of 52,94%. Results showed that 39%

of the alumina can be removed after six days with this specific bio-beneficiation technique.

There are many ways to concentrate iron ore ultra-fines, depending on the characteristics of the ore. In most instances flotation is a very selective process and has been used worldwide for many years to upgrade ultra-fine iron ore (Flippov, *et al* 2014). Additionally, the SLon concentrator, which is a modified version of conventional WHIMS machines, has also been tested on hematite bearing ore types.

## 2.3 Magnetic separation

A large amount of iron ore slimes is currently being discarded as waste material at Sishen, but there is a major requirement for liberation of hematite at smaller size fractions for low grade feed material (Dworzanowski, 2014). Liberating the material (milling) will lead to an increase in ultra-fine (-150 micron) material, effectively increasing the overall hematite loss of a complete processing plant. Therefore many different beneficiation processes have been investigated, of which the SLon concentrator and froth flotation have been determined to be the most viable.

### 2.3.1 SLon concentrator

A newly developed variation of the conventional WHIMS is the SLon concentrator, which has an additional pulsating action. The SLon concentrator was developed in 1988, but was only successfully scaled up in recent years (Zeng, *et al*., 2003). In 2003, more than 30 iron ore processing plants incorporated the SLon (Figure 6) into its processing circuits and used it to recover magnetic minerals in the -212 micron size fraction. The SLon concentrator makes use of a high magnetic field (in the order of 10000 G) to interact with the paramagnetic material's magnetic matrix (Dworzanowski, 2014). The forces involved during the process include the gravitational force, inertial force, hydrodynamic drag and interparticle forces. These forces all

need to be overcome by the magnetic force to ensure that the hematite particle adheres to the magnetic matrix.

Figure 6: Illustration of SLon concentrator (Autotec, 2013).

In a SLon system, the particles adhere to a magnetic matrix by means of magnetic force (Dworzanowski, 2014). The magnetic force on a particle is given by Equation 1:

Equation 1: $$F_m = k/\mu_0 (VB\nabla B)$$

Where:

k = the volumetric magnetic susceptibility of the particle

$\mu_0$ = the magnetic permeability of vacuum

V = volume of particle

B = external magnetic induction

$\nabla B$ = the gradient of the magnetic induction

To overcome the gravitational force, inertial force, hydrodynamic drag and interparticle forces, the SLon allows the user to change the magnetic force and the gradient of the magnetic induction, i.e. depending on the particle's

magnetic susceptibility, particle mass, particle volume as well as the slurry velocity and viscosity through the machine. Furthermore, the SLon incorporates a unique pulsating mechanism which increases the overall performance of the machine with high recoveries, a large beneficiation and no matrix clogging (Zeng *et al*., 2003 and Flippov *et al.,* 2014). This pulsating of slurry is generated using an actuated diaphragm in order to keep the particles in the loose state, effectively reducing entrapment (Autotec, 2013).

In a study conducted on Sishen's thickener underflow using the SLon as a concentrator, it was proven that, given the optimal process parameters, a mass yield of 41% at a Fe content of 67% can be achieved. However, it was concluded that the -10 micron material deemed problematic, but can be successfully recovered to some extent with a maximum mass yield of 37,6% (Dworzanowski, 2014).

A study by Zeng *et al*. included the implementation of the SLon concentrator into the processing circuit of Qidashan, which produces approximately eight million tons or iron ore per annum. The ore body at Qidashan mainly consists of hematite and magnetite. The main reason for implementing the SLon was to increase the processing capacity and efficiency of the circuit. Figure 7 shows the process flow diagram after implementing the SLon into the processing circuit. However, it is evident that the concentrate from the SLon is subjected to froth flotation in order to achieve the required final grade of 66% Fe from feed material containing 15,78% Fe. The case study reported that the use of the SLon in the processing circuit was a success, achieving 60% Fe recovery at an Fe content of approximately 30% in the SLon concentrate, i.e. prior to froth flotation.

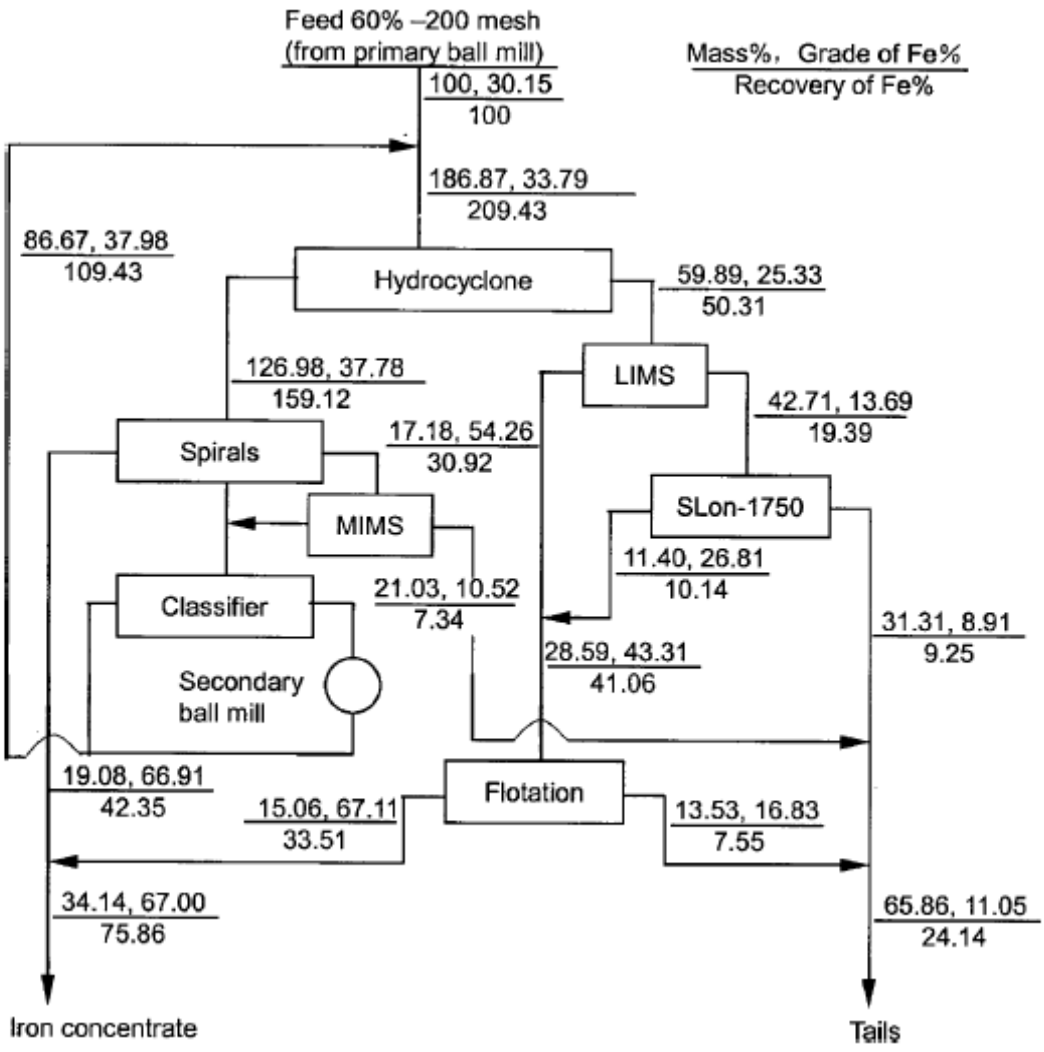


**Figure 7: Ultra-fine beneficiation circuit at Qidashan, illustrating the implementation of the SLon (Zeng *et al.*, 2003).**

## 2.4 Froth flotation

Flotation is utilised worldwide in many different applications, including sulphide and oxide ores (Deo *et al*., 1999). Sulphides are floated using alkyl xanthates, whereas iron ore, calcite, fluorite and quartzite industries make use of amines and fatty acids. It is a complex and selective process and thus should be fully understood together with the basic principles and the effects of different process variables (Naik *et al*., 2004). Even though this is the case, more than 200 Mt of material is processed worldwide every year by making use of froth flotation (Liu *et al*., 2009). In any basic flotation process, the main process

variables can be identified as the feed rate, concentration of solids in the feed, rate of air supplied to the system, froth depth, froth carrying capacity, particle size, reagent dosage and dispersion of material and air (Jena *et al*., 2008).

### 2.4.1 Flotation in general

The process of froth flotation, which separates minerals according to the surface properties, has been practised since 1860 (Taggart, 1956). Flotation is used in the treatment of fine ores, i.e. typically less than 212 micron (Kelly, 1982). The extent to which minerals are separated is known as recovery and the selectivity of the process is defined by grade (Morar *et al*., 2008). The recovery is thus defined as the mass ratio of the valuable mineral in the concentrate to the valuable mineral in the feed, while the grade is defined as the ratio of the mass of the valuable mineral in a processing stream to the total mass of that stream.

Water is used as a medium within the cell in which more dense particles would sink, except for the fact that the medium is agitated in the process, thus creating an upward velocity exceeding the settling velocity of the heaviest particle such that a suspension of solid particles within the solution is created (Morar *et al*., 2008). As the solid particles are suspended in solution, a second process related to the mineral's surface properties takes places, i.e. the particles are either hydrophobic (high affinity for air) or hydrophilic (high affinity for water) (Taggart, 1956). This process requires air to be either injected into the system or introduced by agitation of the solution, which produces bubbles within the solution (Pryor, 1965). Flotation reagents are additionally used (as a surface coating) in various ways to selectively render a particle surface hydrophobic or hydrophilic, depending on the process and final product. Reagents are further discussed later in this literature study.

Hydrophobic particles attach to the bubbles and are floated to the surface of the solution, as air is less dense than water (Pryor, 1965). This mechanism is also known as true flotation resulting from particle-bubble collision, adhesion and transportation to the froth phase. For a particle to stay attached to a bubble, the gravitational and dynamic forces within the system experienced by the particle must not overcome the adhesion to an air-water interface, i.e. a bubble. It is for this reason that very fine particles are required in the flotation process, but not too fine, as the particle must still maintain enough momentum to attach to a bubble. The processes and material flow is illustrated in Figure 8.

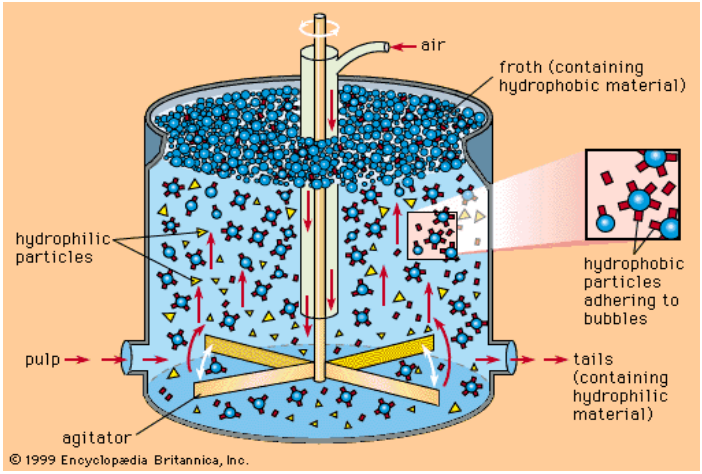


**Figure 8: A schematic representation of a typical flotation cell and the flow of material (cache.eb.com, 2009)**

Hydrophilic particles on the other hand do not float or attach to the bubbles and thus stay in suspension until removed from the system (Richards, 1940). However, hydrophobic particles can also report to the froth phase due to entrainment caused by water forcing the material to the froth phase. The efficient and cost effective separation of the two hydrophobic and hydrophilic material streams is the basis for the use of the froth flotation process and is used in industry to concentrate streams containing coal, gold, platinum group minerals and various other minerals.

It cannot be said that the hydrophilic sinking particles form part of the gangue material stream, as the respective streams depend on the ore processed, i.e. it might be that the valuable mineral is contained in the non-floating stream. When the valuable minerals are recovered to tails it is known as indirect or reverse flotation, while if recovered to the froth it is known as direct flotation.

The most common direct flotation applications are in the base metal sulphide industry, i.e. gold, platinum, lead, zinc, etc.

Indirect or reverse flotation is generally used in applications where large mass recoveries are required in the direct route, which is generally limited by the froth carrying capacity. For example, pyrite can be floated and coal depressed for a typical coal ore. Polysaccharides can be utilised to depress coal as well as dextrin, which also fails to depress pyrite. The use of dextrin and xanthate to depress coal and float pyrite is utilised in the Dow process (Richards, 1940).

The use of indirect or reverse flotation depends on the ore processed and product required (Liu, *et al*., 2007). Another example of an application for indirect flotation is the flotation of iron ore, where hematite is depressed and the gangue minerals floated to the concentrate. Quartz is typically floated to the froth, using amine and hematite depressed with causticised starch.

However, there are two limiting factors for the possible use of froth flotation as a beneficiation process, namely the particle size and mineral liberation (Rao, 1997). In essence the particle can be too large to float, or in the event that the material is extremely fine, entrainment can prevail, which is unselective. This concept can make flotation very difficult if the minerals are not well liberated (individual particles constituted of single free minerals), as grinding might be required, effectively generating more ultra-fine material and reducing flotation efficiency.

### *Flotation cells*

Different flotation cells have different mechanical characteristics and therefore different effects on the process (Jena *et al.*, 2008). Over the years many variations of flotation cells have been developed, some focused on recovery and some on concentrate grade. Of all the variations, two main categories of flotation cells can be identified, namely conventional and column flotation cells. Although the basic process stays the same, different mechanical implementations are made to alter the process mechanisms in different areas of the flotation cells. Conventional flotation cells incorporate mechanical agitation as opposed to its alternative pneumatically agitated column cell, as illustrated in Figure 9. The column cell is operated to maintain streamline conditions, where back mixing and entrainment of gangue are avoided to a greater extent than conventional cells. Therefore column cells are utilised to increase grade, as opposed to conventional mechanical cells aimed at recovery, which is typically used as cleaners within a sulphide (including Pt, Au, Cu, Zn, Pb, etc.) flotation circuit (Jena *et al.*, 2008).

a)

b)

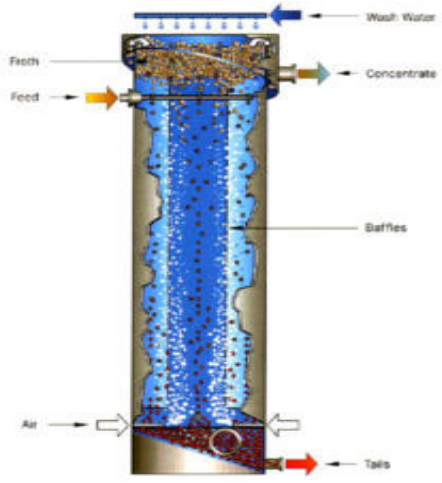


**Figure 9: a) Illustration of a conventional mechanically agitated cell (flsmidth.com, 2010) b) Illustration of a pneumatically agitated column cell (soloresources.co.za, 2010)**

### *Denver D12 laboratory flotation cell*

The Denver laboratory flotation machine comes in various sizes with various cell sizes and impeller/paddle sizes (Figure 10) (titanprocess.com, 2015). The Denver laboratory flotation machine is used to test the response of minerals on a laboratory scale, which is a fast and cost effective method of testing relative to large scale pilot plants.

However, there are limitations to batch scale machines, as the results can be a poor indicator of froth performance in full scale plants (Runge, 2010). On full scale flotation plants froth depths can be as deep as 50 cm relative to a bench top flotation test, which is significantly less. Therefore, bench top test work can lead to the selection of reagents that perform significantly different at froth depths of 50 cm, as the froth characteristics and performance could be significantly different.

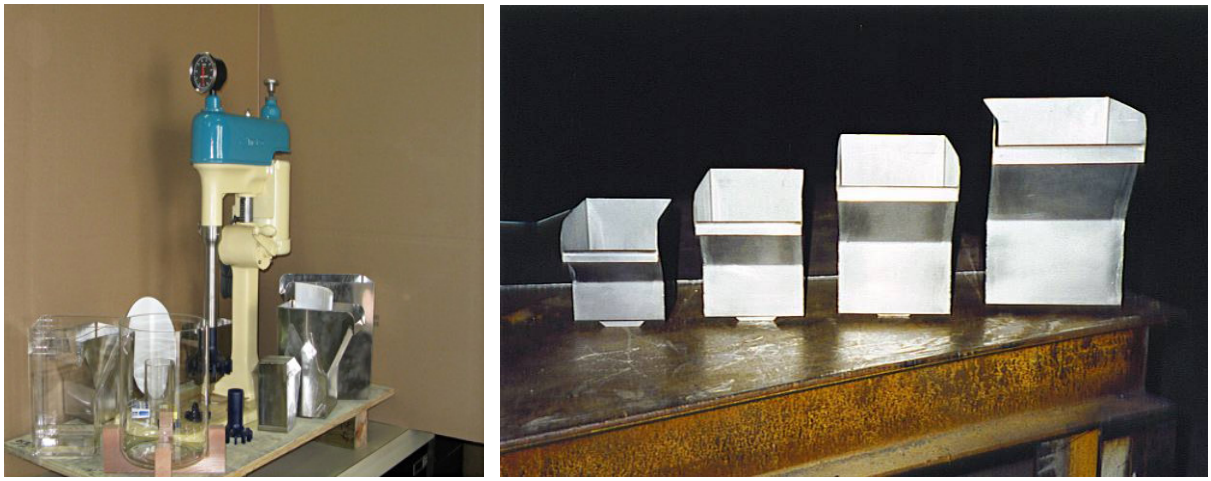

**Figure 10: Illustration of a Denver D12 laboratory flotation cell (titanprocess.com, 2015)**

### 2.4.2 Flotation reagents

The reagents used in froth flotation are critical to the performance of the system and are required in all flotation systems to selectively increase the hydrophobicity of particles to selectively depress particles, to stabilise the froth and to modify the system in terms of solution chemistry (Ding *et al.*, 2006).

The conditioning with reagents forms part of a complex and vital unit operation. This is due to the fact that the time required for physical and

chemical reactions is a direct function of the subsequent dispersion and agitation intensity, which is a function of many other parameters, including pH and reagent type.

The different reagents used to achieve a certain effect include:

- collectors
- depressants
- frothers
- modifiers

### *Collectors*

A mineral is not necessarily naturally floatable and thus some alteration is required (Taggart, 1956). In these instances a non-polar surface is created on the surface of the mineral by using an "activator" or "collector", which alters the surface properties of the mineral, producing a floatable particle (Gaudin, 1939). These substances are organic compounds like acids, bases and salts, which are normally highly selective to a specific mineral (Taggart, 1956).

The most common cationic collectors used in the iron ore flotation industry are the amine salts, which preferentially adsorb onto quartz surfaces (Araujo *et al.*, 2010). A typical ether amine is shown in Figure 11 (Lui *et al.*, 2015). The nitrogen/oxygen section of the molecule is the charged section and adheres to the mineral surface through electrostatic interaction. The carbon chain section is hydrophobic which, when attached to the surface, effectively renders the mineral hydrophobic for selective flotation, as illustrated in Figure 12.

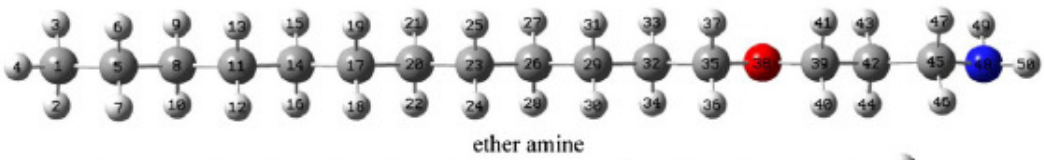


**Figure 11: Molecular structure of a typical ether amine (DDA) (Colour coding – blue, nitrogen – white, hydrogen – grey, carbon – red, oxygen) (Lui *et al.*, 2015)**

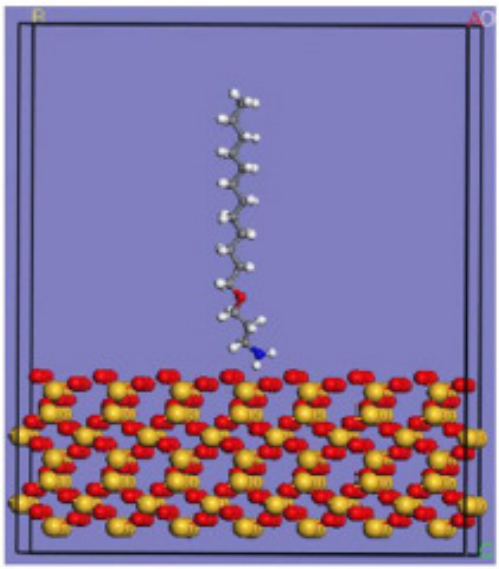

**Figure 12: Illustration of chemisorption of ether amine onto a quartz mineral surface (Colour coding - blue, nitrogen – white, hydrogen – grey, carbon – red, oxygen – yellow, silicon) (Lui *et al.,* 2015)**

Rodrigues *et al*. (2013), tested a variation of etheramines and ammonium quaternary salts on a Brazilian iron ore under various conditions. The test showed that etheramine Flotigam EDA supplied by Clarient performs the best in terms of selectivity at a pH of ten in the presence of corn starch as a depressant (Rodrigues *et al*., 2013). The study was mainly aimed at separating kaolinite from hematite, but quartz was also considered in the testwork conducted. Figure 13 illustrates the recovery of hematite and kaolinite to the froth phase at various EDA concentrations as a function of pH. The results show good recovery of kaolinite at higher dosages of EDA, achieving 90% to 100% recovery of kaolinite to the froth phase. However, the recovery of Fe to the concentrate was low at 40% to 50%.

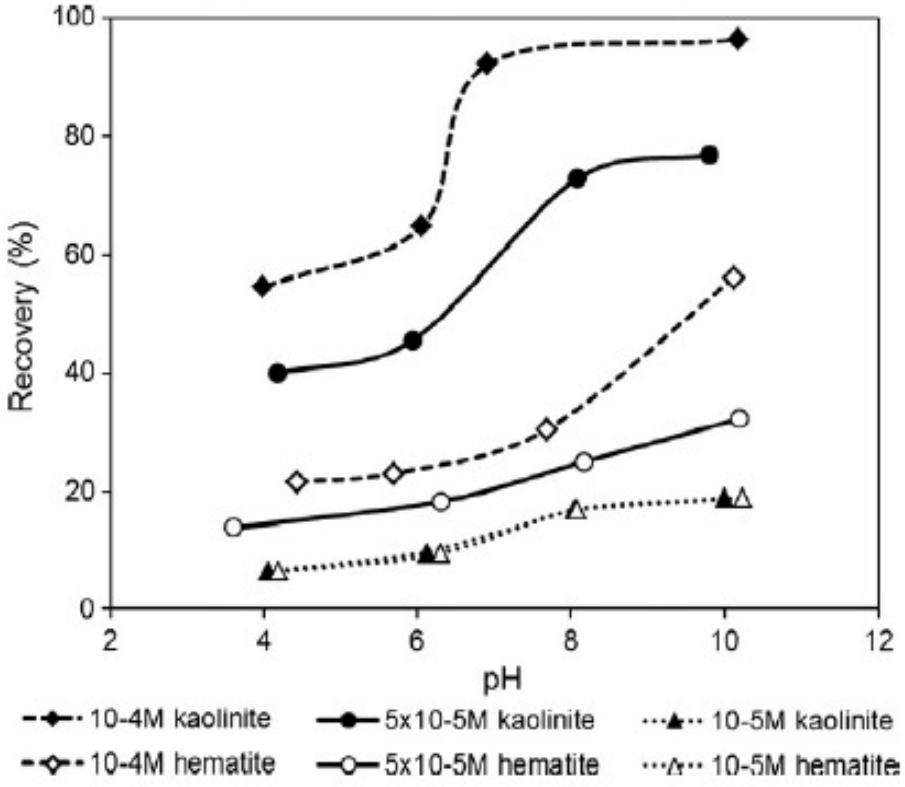


**Figure 13: Floatability of kaolinite and hematite as a function of pH and EDA concentration (Rodrigues *et al.*, 2013)**

Table 5 tabulates the results of three different tests, comparing the optimal results of three different sets of reagent suites (Rodrigues *et al.*, 2013). Results indicate that the EDA outperformed the other reagents, achieving a final product containing 67,4% Fe and 1,56% $SiO_2$ at a mass recovery of 37,94%.

**Table 5: Results of laboratory scale flotation tests with a feed size less than 45 micron (Rodrigues *et al.*, 2013)**

| Test | pH | Collector | Depressant | Product | Fe (%) | $SiO_2$ (%) | $Al_2O_3$ (%) | Fe Rec (%) | $Al_2O_3$ Rec (%) | Mass Rec (%) |
|---|---|---|---|---|---|---|---|---|---|---|
| 24 | 7 | DTAB 400 g/t | X | Reject | 59.22 | 6.96 | 5.04 | 23.83 | 4.21 | 21.47 |
| | | | | Concentrate | 67.76 | 1.02 | 0.81 | | | |
| | | | | Feed | 61.05 | 5.68 | 4.13 | | | |
| 33 | 10 | EDA 400 g/t | Corn starch 600 g/t | Reject | 57.55 | 8.06 | 5.92 | 41.72 | 10.53 | 37.94 |
| | | | | Concentrate | 67.40 | 1.56 | 1.14 | | | |
| | | | | Feed | 61.29 | 5.59 | 4.11 | | | |
| 38 | 10 | AQ142 400 g/t | Corn starch 400 g/t | Reject | 58.58 | 7.37 | 5.23 | 34.34 | 8.83 | 31.52 |
| | | | | Concentrate | 66.58 | 1.70 | 1.12 | | | |
| | | | | Feed | 61.10 | 5.58 | 4.00 | | | |

### *Depressants*

In some cases unwanted minerals are naturally floating, in which case depression is required, which is the converse of activation (Richards, 1940).

This can be done by either preventing adsorption of the collector on the mineral surface, or by making the mineral surface hydrophilic (Laskowski, 2003). These substances create an activation repelling surface or destroy an existing collector coating, producing a hydrophilic particle (Taggart, 1956).

Depressants in iron ore flotation include starch, consisting of a combination between amylose and amylopectin (Pavlovic *et al.*, 2003 and Flippov *et al.,* 2014). Both amylose and amylopectin are polymers of the monosacheride α-D-(+)-glucopyranose, as illustrated in Figure 14 (Weissenborn *et al.*, 1995). The polymer contains various hydroxyl groups, as well as –CH groups. The hydroxyl groups are free and can thus rotate to one side of the molecule, effectively rendering that side hydrophilic. As these groups are on the same side, the other side of the molecule is rendered hydrophobic due to the exposed –CH groups. When amylose is introduced to an aqueous solution, a helix is formed, in which case the interior is hydrophobic and the outside hydrophilic.

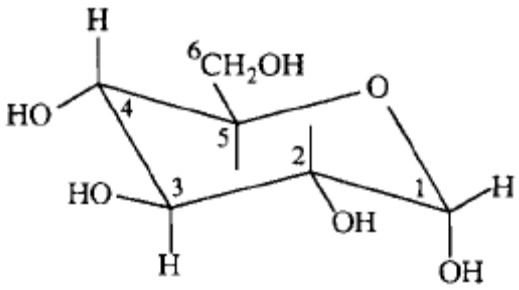


**Figure 14: Structure of a typical glucopyranose molecule (Weissenborn *et al.,* 1995)**

The proposed mechanism by Weissenborn (1995) is given in Figure 15, illustrating the adsorption of starch onto the hematite surface. Interaction (complex formation) between the OH-groups that exist in starch molecules and hydrolysed Fe sites that are present on the hematite surface allows for selective flocculation and depressing of hematite.

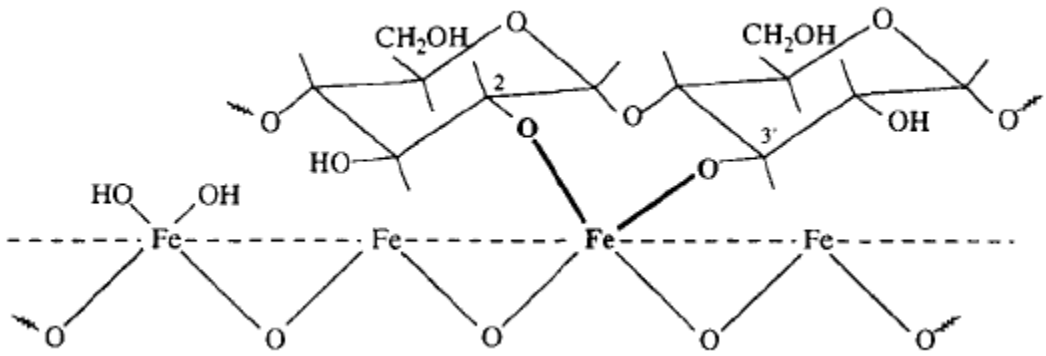


**Figure 15: Proposed mechanism of adsorption of starch onto the hematite surface (Weissenborn *et al.*, 1995)**

This interaction between the starch molecule and the hematite surface is known as chemisorption and has been proven to be very selective, as it has a limited affinity for adsorption onto quartz surfaces, effectively allowing selective depression of hematite (Weissenborn *et al*., 1995). Furthermore, starch can also be used for the dispersion of clay slimes and the depression of talc and calcite.

In an attempt to better understand the chemical interaction between depressants and the mineral surface, a coarse crystalline hematite ore from Brazil, various depressants and decyletheramine as collector were used to conduct a series of adsorption and flotation tests (Pavlovic *et al*., 2003).

Adsorption tests showed that the amylose had a much larger adsorption density onto quartz than both starch and amylopectin, even though the adsorption density onto hematite was almost the same as can be seen in Figure 16. It was speculated that amylose displays random coil behaviour in alkaline solution and could thus lead to higher adsorption densities.

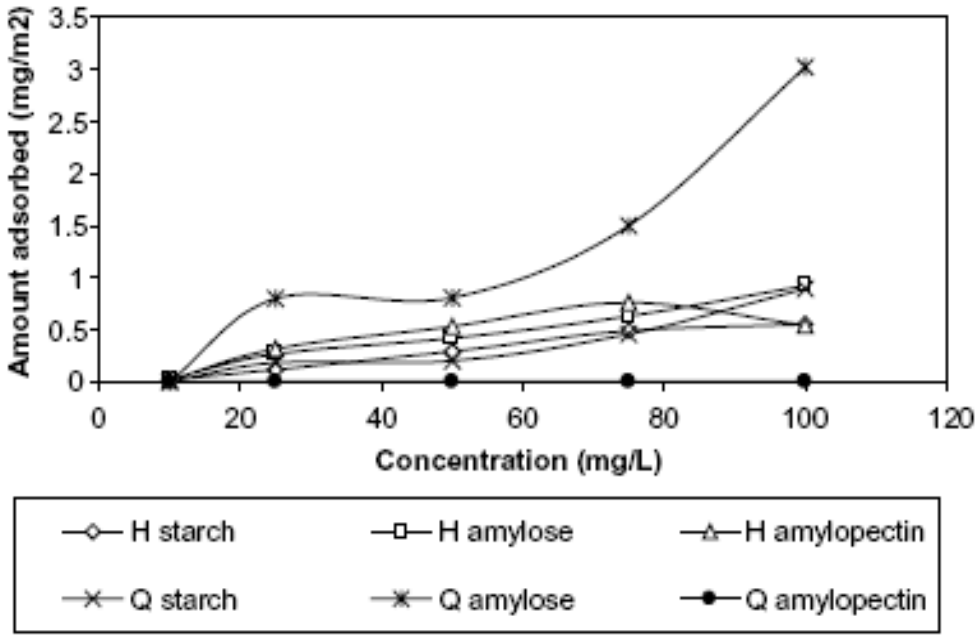


**Figure 16: Adsorption isotherms of various depressants onto hematite (H) and quartz (Q) (Pavlovic *et al.,* 2003)**

Flotation test results are given in Figure 17 and Figure 18, showing that all of the depressants have more or less the same effect on hematite and that recoveries differ quite severely in the case of quartz (Pavlovic *et al*., 2003). Additionally, as seen in Figure 16, amylose had the greatest adsorption density onto quartz, but had the least effect on the depression of quartz. The reason for the high adsorption density and the poor depression of quartz was thought to be the fact that amylose does not perform well as a flocculent. This phenomenon was tested by using only monomers as depressants, of which the results are given in Figure 18. These monomers should have no flocculation effect, but should still render the hematite surface hydrophilic. Therefore, if there is no depression of quartzwith the monomers, then the main mechanism of depression is the flocculation of quartz. This was indeed the case, as can be seen in Figure 18. The problem with these monomers is that they are extremely soluble in water, which explains the high concentrations used.

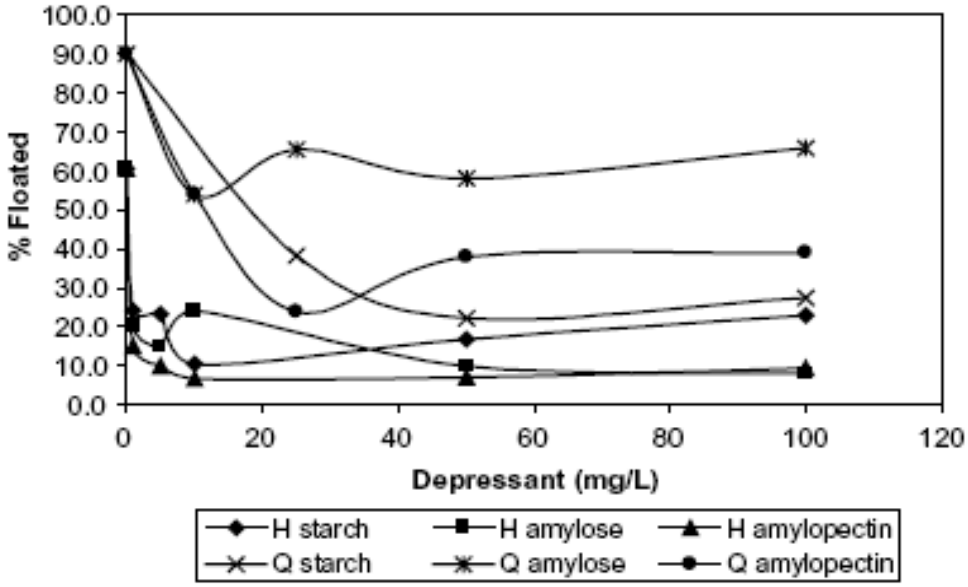


**Figure 17: The mass recovery to froth as a function of the depressant concentration in a hematite (H) and quartz (Q) float system for the three different depressants (Pavlovic *et al.*, 2003)**

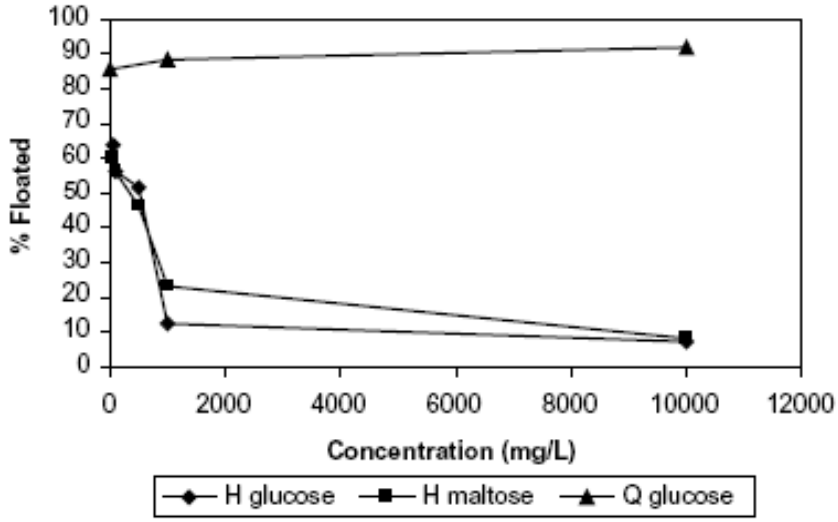


**Figure 18: The mass recovery to froth as a function of depressant concentration in a hematite (H) and quartz (Q) float system for two different monomers (Pavlovic *et al.*, 2003)**

Similar to the study done on the phosphate production plant in Canada, a study was conducted on the depression of hematite using guar gums as opposed to starch (Nanthakumar *et al.*, 2009). The results are given in Figure 19. The guar gums resulted in an increase in depression efficiency as compared to only using starch, effectively reducing the recovery of hematite

by approximately 4%. However, it should be noted that the feed was of a very low grade, making it difficult to see a significant difference in performance.

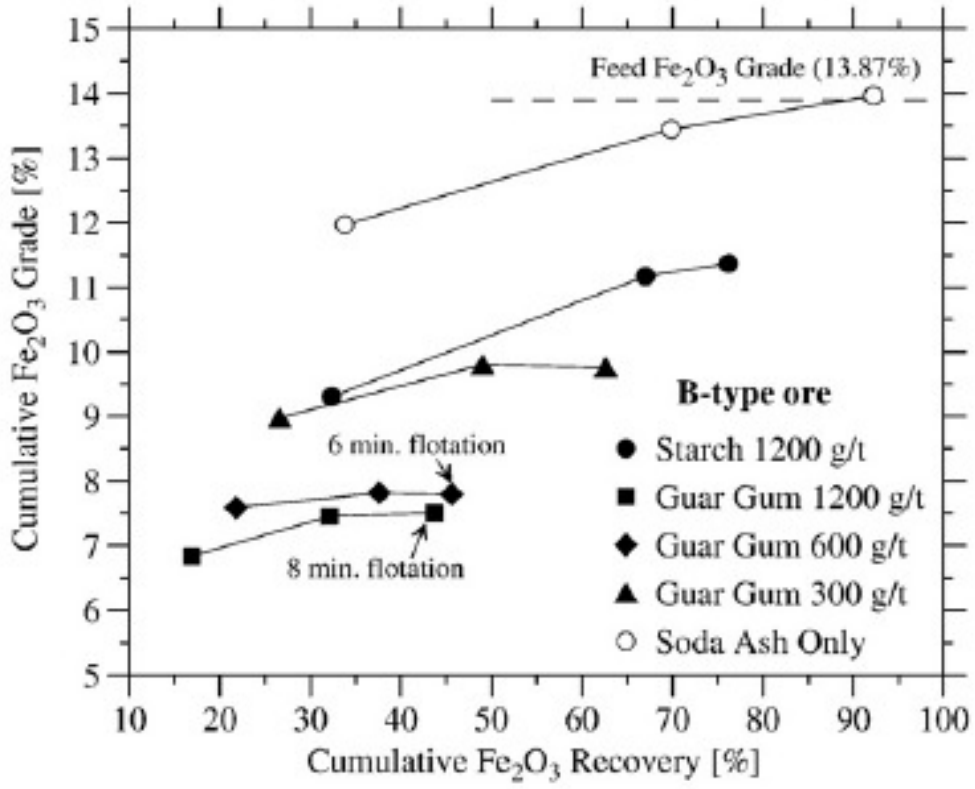


**Figure 19: Cumulative grade as a function of cumulative recovery with various depressant dosages, points on curve represents individual cumulative flotation times unless otherwise stated (Nanthakumar *et al.,* 2009)**

In the same study conducted by Rodrigues (2013) as was discussed in terms of collectors used in iron ore flotation, the use of corn starch was also tested. The results are given in Figure 20 and show that the EDA is unselective without the presence of starch. However, with the addition of starch the selectivity is drastically improved. Furthermore, the results also suggest that the starch selectively flocculates the hematite at low dosages, but can act as a dispersant at higher dosages. An optimal exists for the depression of hematite when considering the use of corn starch as a depressant.

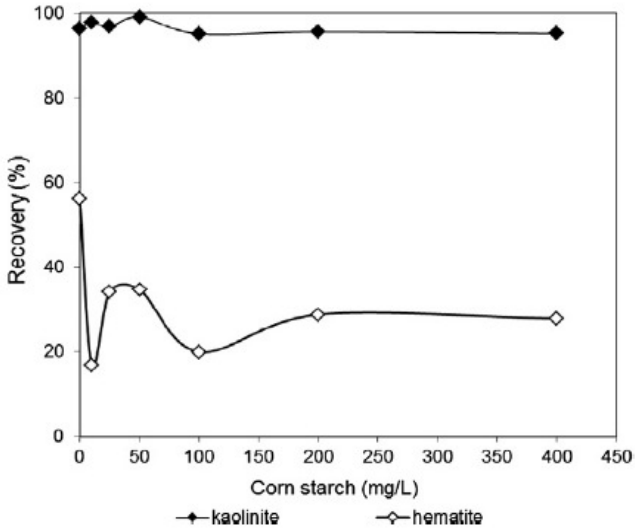


**Figure 20: Floatability of kaolinite and hematite, as a function of starch concentration, with EDA (1 x $10^{-4}$ mol/L) at pH = 10 (Rodrigues *et al.,* 2013)**

### *Frothing reagents*

During the literature study, no published article was found where frothing reagents are used for the flotation of iron ore. However, for completeness of this study, the frothing reagent was included in the literature, but no frothing reagents were used in the test program.

Bubbles have a natural tendency to break the air-water interface, as soon as the water surface is reached (Richards, 1940). This is not a desired effect in the flotation process, because the valuable minerals need to be removed from the cell before the interface is destroyed. Therefore a frother is used to facilitate air dispersion into fine bubbles and increase froth stability to prevent the destruction of the air water interface (Gupta *et al*., 2006; Boylu *et al*., 2007). This keeps the material floating above the pulp surface long enough for froth removal or drainage of mechanically trapped particles (Taggart, 1956). An illustration of froth produced within a cell is shown in Figure 21.

Figure 21: An illustration of the froth at the surface of the pulp in a floatation cell (metallurgy.utah.edu, 2008)

A schematic representation of a typical frother molecule distinguishing between the hydrophobic and hydrophilic constituents is given in Figure 22.

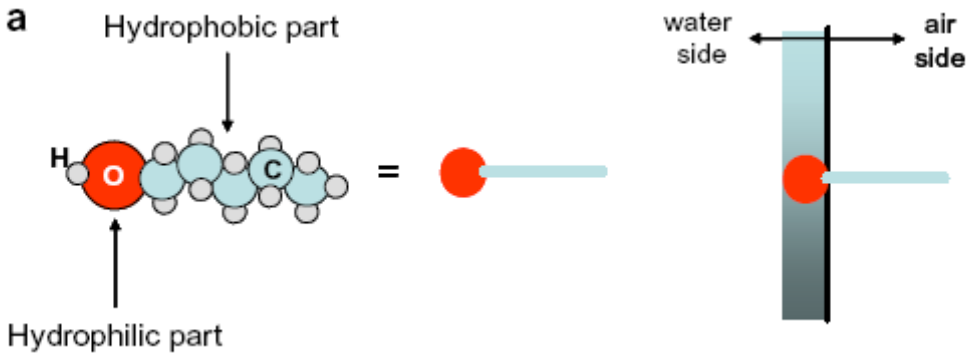


Figure 22: An illustration of a typical frother molecule (Laskowski, 2003)

Frother molecules preferentially orientate at the water/air interface (Laskowski, 2003). This characteristic is enabled by the fact that polar and nonpolar groups are distributed unevenly.

There has been significant testwork done in flotation, but it has only been realised in the last few decades that the characteristics of the froth are essential to performance (Tao *et al.*, 2000; Hadler, 2006). The froth characteristics that should be considered are as follows:

- Froth stability
- Selectivity

### *a) Froth stability*

Froth stability is defined as the persistence of the froth (Morar *et al*., 2006). The stability of the froth phase should be considered as an important process variable, because the more stable the froth, the less froth breakdown is experienced (Gupta *et al*., 2006). If the froth breaks down, the material attached to that air liquid interface is reintroduced to the system, thus reducing the process performance. In addition, with a more stable froth phase, a larger froth depth is possible. This means that a longer retention time in the froth phase is possible, which allows for drainage of entrained particles, effectively increasing the grade of the concentrate. The flotation rate constantly decreases with an increase in froth height, as some of the material drops back into the pulp as the froth becomes less stable at large froth heights (Laskowski, 2003). Therefore, there is a trade-off between grade and recovery (Morar *et al*., 2006), which is illustrated in Figure 23.

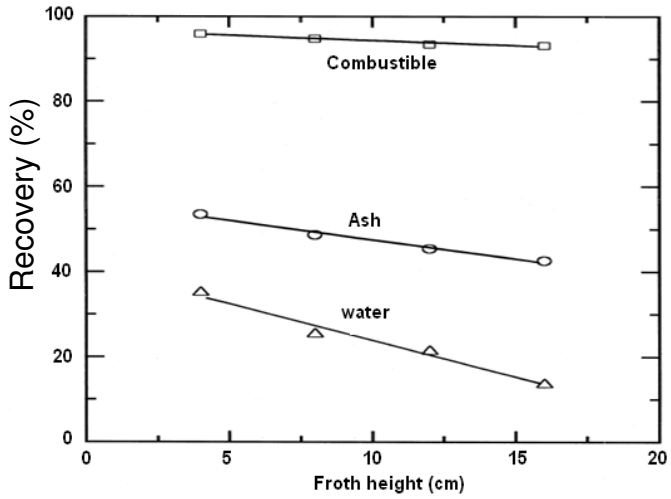


**Figure 23: The effect of froth height on the flotation performance (Tao *et al*., 2000)**

The stability of the froth phase is mainly determined by the particle size, particle wetting characteristics and particle shape. Smaller particles, especially particles that have a critical degree of wetting, increase the stability of the froth (Pugh, 2006). It is also mentioned that the smaller the particles, the larger the degree of entrainment (Peng et al, 2006). Considering the

wetting characteristic, it is postulated that if the contact angle is greater than 90 degrees, it will destabilise the froth.

Two additional parameters, namely pH and solids concentration of hydrophobic particles, also affect froth stability, but to a lesser extent (Pugh, 2006). It was shown that the foam stabilises with an increase in solids concentration of hydrophobic particles. Gupta *et al*. (2006) conducted a study on froth stability, using three different frothing reagents in a coal flotation application. It showed that the stability of the froth phase increases with the solution pH and the frothing reagent concentration (Gupta *et al*., 2006). This is illustrated in Figure 24 and Figure 25, which could possibly be explained by a change in surface charge on the particle surface throughout the pH range (Pugh, 2006). Very important to note is that each frother has a curve specific to that frother.

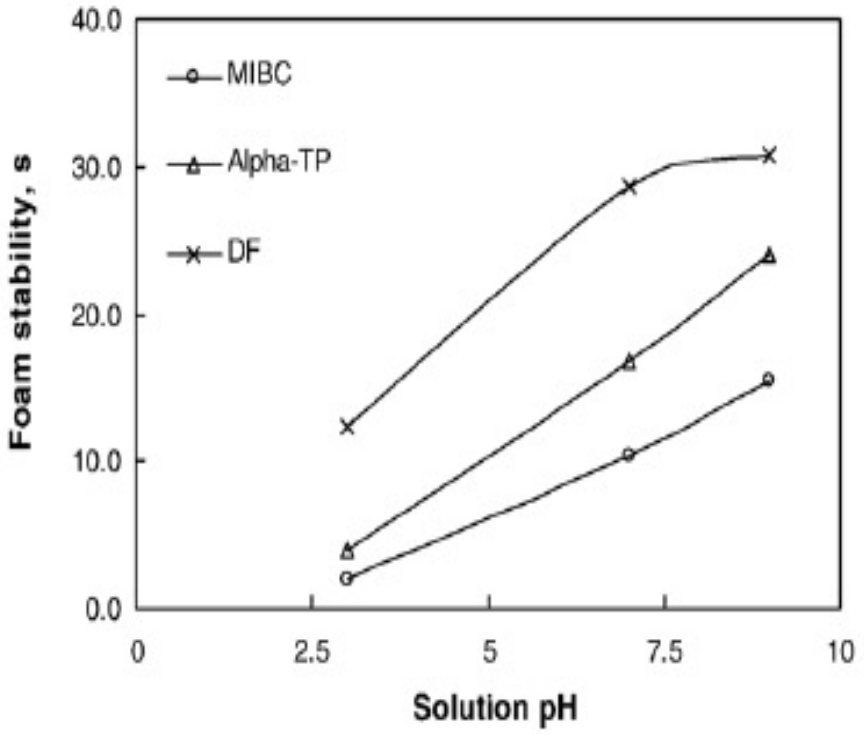


**Figure 24: Different frothing reagents illustrating the froth stability as a function of the solution pH (Gupta *et al*., 2006)**

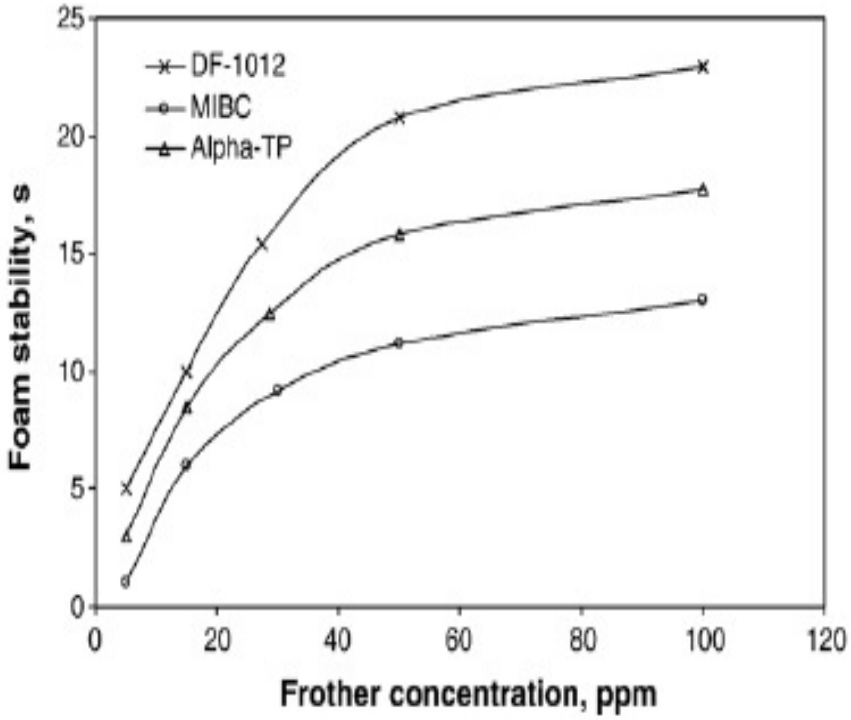


**Figure 25: Different frothing reagents illustrating the froth stability as a function of the frothing reagent concentration (Gupta *et al.*, 2006)**

### *b) Froth selectivity*

Froth selectivity can be related to the potential of the froth phase to drain water and thus entrained particles, which is a function of the frother type, even though there are other parameters that affect the degree of water recovery to the concentrate and entrainment, such as the superficial gas velocity and solids concentration in the froth phase (Nguyen *et al.*, 2006; Morar *et al.*, 2008).

It was shown that water recovery and mobility of the froth phase increases with an increase in frother dosage (Sripriya *et al.*, 2002; Boylu *et al.*, 2007). This was experimentally confirmed by increasing the frother dosage and measuring the amount of water reporting to the froth (Boylu *et al.*, 2007). The results are graphically illustrated below in Figure 26.

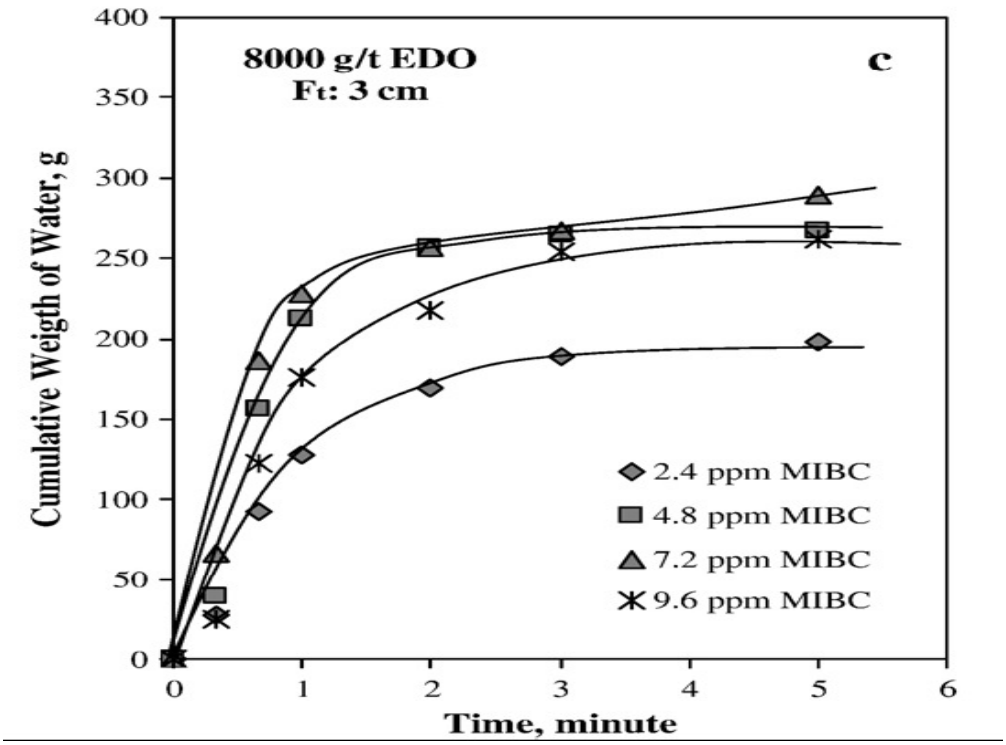


**Figure 26: The effect of frother dosage on the water recovered to the concentrate (Boylu *et al.*, 2007)**

Together with an increase in water recovery, there is an increase in entrained gangue particles and thus also a decrease in froth selectivity (Sripriya *et al.*, 2002; Boylu *et al.*, 2007). This is illustrated in Figure 27.

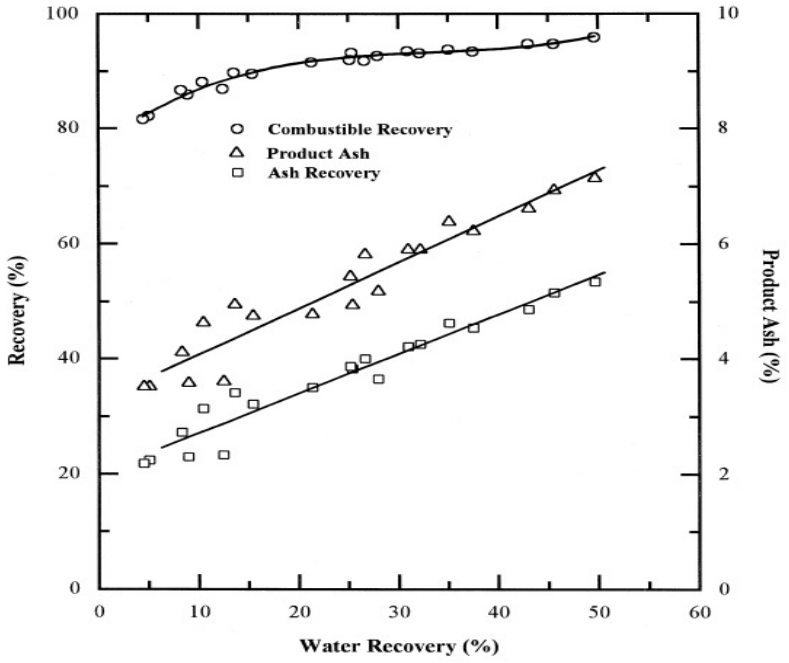


**Figure 27: The correlation between combustible recovery, ash recovery or product ash and water recovery (Tao, 2000)**

In a 23 factorial study conducted on a coal sample, the ash and combustible recovery as a function of the pH and two collectors, namely kerosene and dodecylamine (DDA), was investigated (Kelebek *et al.*, 2008). It was concluded that a beneficial effect is experienced at a high pH, due to the impact of the frothing reagent. This can be related to the possibility of a frother to be both a collector and a frother when processing coal.

#### *Modifiers*

Modifiers are substances used to alter the pulp in some or other way and in most cases are used to control the pH of the system (Richards, 1940). Controlling the pH is of tremendous importance as the selectivity of many reagents is pH dependent, for instance in applications like platinum, lead, zink, iron ore, etc. Furthermore, modifiers affect the solution chemistry and can effectively change the charge density of a surface, control the metallic ion concentration within the system, alter the mineral surface chemistry and modify the oxidation state of ions in the solution (Rao, 1997). Therefore, a modifying agent can act as an activator, regulator or depressant, depending on the flotation system.

### 2.4.3 Process water

Process water quality is generally viewed as an environmental issue and is generally made up of recirculating streams and make up water (Gupta *et al.*, 2008). Typical process water streams are the tailing and concentrate thickener overflows, filtrate from filter plants and tailing dam return water. Environmental issues increase the need to reduce the amount of fresh water or makeup water used, and thus increase the recirculating water streams. The increase in recirculating water affects the process water quality and thus the processes involved. An increase in reagent consumption will be experienced, as well as the presence of excessive slimes in the water, which also affects the separation process.

When considering direct iron ore flotation, a high concentration of calcium and magnesium polyvalent cations, present in almost all process water streams, generally affect the collecting efficiency of fatty acids on phosphate minerals (Nanthakumar et al, 2009). The challenge with calcium and magnesium are the formation of hydroxyl complexes and water insoluble precipitates with fatty acids. While the insoluble precipitates increases reagent consumption, the hydroxyl complexes adsorb onto all mineral surfaces, in which case the surface charge is rendered as positive. This process of charge reversal reduces the collector's adsorption selectivity, reducing the process efficiency. In general, process water should also be considered when conducting testwork, as this could influence the results.

## 2.5 Iron ore flotation

Iron ore flotation is grouped directly with the oxide flotation class, as most of the major minerals in the ore are oxides, i.e. Al-bearing minerals, quartz and hematite (Liu et al, 2009). The most common flotation technique used is reverse cationic flotation, which incorporates the concept of surface charge and collector adsorption as a function of pH.

In general, when considering the flotation of quartz from a hematite bearing ore (reverse cationic flotation), it is desired to coat the quartz mineral with a monolayer of amine through chemisorption and coat the hematite mineral with caustecised starch through physical adsorption, for selective separation of the two minerals (Rao, 1997).

Physical adsorption, in this case adsorption of starch onto the hematite surface, is characterised by a physical process where the absorbate (starch) is concentrated onto the substrate (hematite) surface without undergoing any alteration in terms of its chemical species or electric charge (Rao, 1997). In the case of amine collecting onto quartz is due to electrostatic attraction between the positively charged amine onto a negatively charge quartz

surface. Furthermore, the efficiency of both of these mechanisms are affected by the solution pH.

Figure 28 shows a recovery curve as a function of the solution pH for hematite and quartz. The tests were conducted in a 40 ml flotation cell with the synthetic collector N-dodecylethylenediamine. Sodium hydroxide and hydrochloric acid were used to regulate the pH. It can be seen that pH has a major effect on the quartz recovery. Therefore, the optimum pH for the flotation of quartz is within more alkaline conditions.

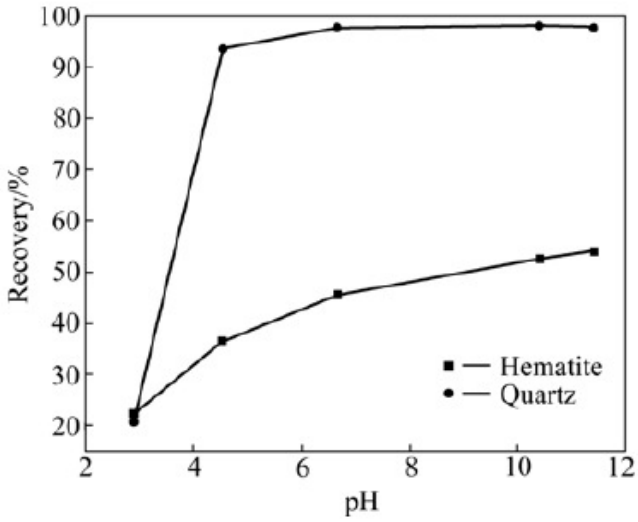


**Figure 28: Hematite and quartz recovery as a function of pH (Liu *et al.*, 2009)**

Quast (2000) conducted a study on an iron ore from the middle back area in South Australia, assaying 69% $Fe_2O_3$. The ore was used to test hematite flotation with 12-carbon chain collectors (Quast, 2000). Firstly, the surface properties of the ore were determined, which are illustrated in Figure 29. A 1 g hematite sample was used to determine the electrophoretic mobility, which was then used to draw up the graph using the rationalised Smoluchowski equation. It can be seen that the PZC in this case was at a pH of approximately 6,7 and the isoelectric point (IEP) was at a pH of 2,7.

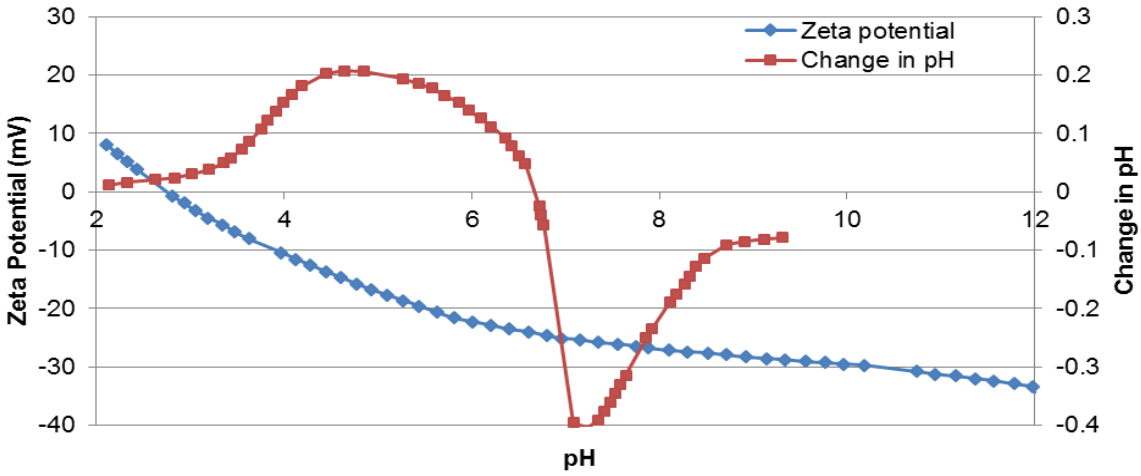


**Figure 29: Zeta potential and change in pH as a function of pH of a hematite ore from the middle back range area in South Australia (Quast, 2000)**

The feed sample used to construct the plots in Figure 29 was subjected to a flotation system with various reagents and different reagent addition rates (Quast, 2000). Figure 30 shows the results of a single reagent at different reagent addition rates. The possible flotation pH ranges are between five and eight and above ten. The reason for this is the ionisation of the collector above a pH of five and the positively charged surface of the mineral. The electrostatic interaction between the surface charge and the ionised collector is known as physical adsorption.

Flotation at a pH above ten can be attributed to other adsorption mechanisms, but with chemisorption of the collector onto the mineral surface as the dominant mechanism.

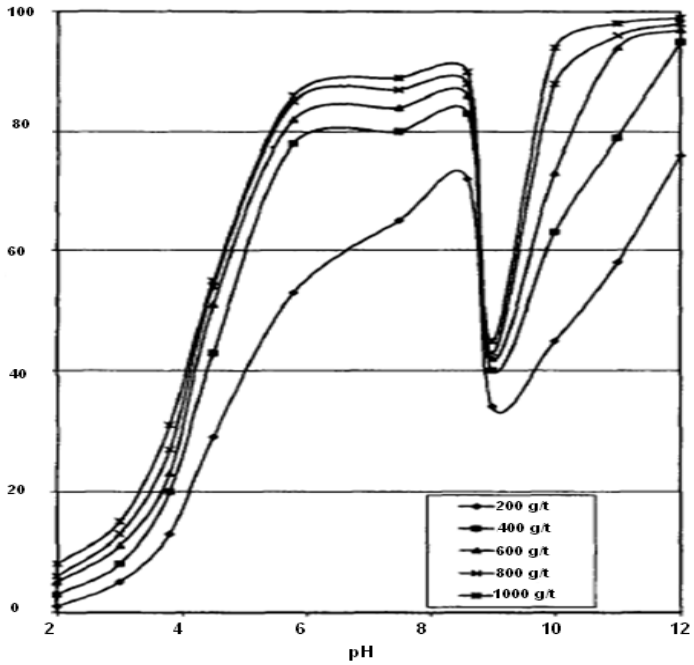


**Figure 30: Hematite recovery as a function of pH using dodecanoic acid as collector with multiple addition rates (Quast, 2000)**

Quast (2000) compared the reagent requirements of two different collectors, namely ammonium laurate and lauric acid, to achieve 80% hematite recovery (Quast, 2000). Results showed an increase in reagent requirements from 90 to 200 g/t, with ammonium laurate and lauric acid respectively. The floatable pH range was also tested as a function of the collector concentration, in which case the pH range decreased with a decrease in collector concentration.

Another concept employed in iron ore flotation is that of flocculation, which consists of using surfactants to flocculate or coagulate extremely fine particles to form large particles. Larger particles greatly increase the separation efficiency of various processes. It has been proposed that sodium oleate, a superior hematite collector, have both collection and flocculation properties, which lead to an investigation of the mechanisms involved (Shibata *et al.*, 2003). Initially, the dependence of flocculation and dispersion was measured with variation in pH and sodium oleate concentration, of which the findings are given in Figure 31. The figure shows that sodium oleate can be used both as a flocculent and a dispersant, depending on the pH of the system. Increasing

the sodium oleate concentration increases the pH range for flocculation and creates more stable flocs.

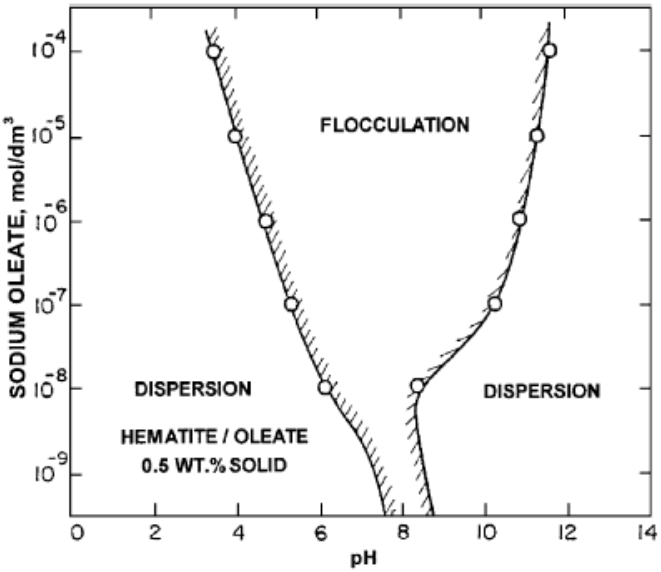


**Figure 31: Sodium oleate concentration as a function of pH indicating the mechanisms involved (Shibata *et al.*, 2003)**

The hematite recovery during flotation was then measured over the pH range, of which the results are given in Figure 32. Although the initial particle size was not specified, it is clear that the hematite recovery drastically increased within the specified flocculation region, which is due to the increase in particle size, i.e. floc size.

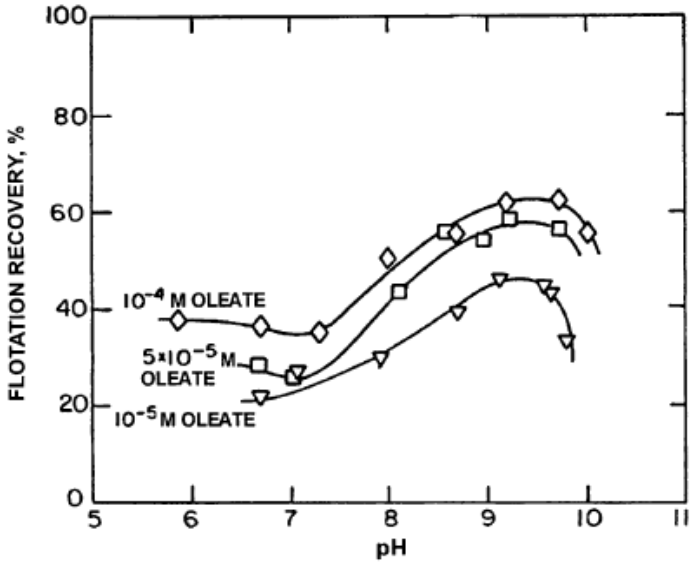


**Figure 32: Recovery as a function of pH in the presence of various concentrations of sodium oleate (Shibata *et al.*, 2003)**

In 2011, Ma published a paper discussing a Vale iron ore which was floated to determine the possibility to employ reverse anionic flotation (Ma *et al.*, 2011). In this case, reverse cationic flotation using a traditional ether amine as collector at a pH of 10.5 was compared to reverse anionic flotation, using initial lime additions to activate the quartz and then and fatty acids as collectors. The main motivation for the testwork included high tolerances of fines when employing the reverse anionic flotation, as reported in China's major iron ore area of Anshan, as well as lower operation expenditure.

For the tests, a Vale iron ore was selected and characterised. Phase analysis showed the contributing phases to be hematite, quartz, kaolinite, muscovite and talc. The chemical analysis is given in Table 6.

**Table 6: Chemical analysis for a Vale iron ore (Ma *et al.*, 2011)**

| Vale iron ore sample | Component (%) | | | | | | | |
|---|---|---|---|---|---|---|---|---|
| | Fe | $SiO_2$ | CaO | $Mn_3O_4$ | $Al_2O_3$ | $TiO_2$ | P | MgO |
| Cyclone feed | 40.36 | 39.01 | 0.025 | 0.649 | 1.390 | 0.092 | 0.015 | 0.178 |
| Cyclone underflow | 39.60 | 41.40 | 0.025 | 0.364 | 0.641 | 0.089 | 0.009 | 0.141 |

Except for the talc, this ore compares well to the ore body of Anglo American Kumba Iron Ore's Sishen ore in terms of flotation, as the talc and muscovite is easily floated. In this study Ma therefore only referred to the grade and recovery of hematite and quartz. Figure 33 shows the size-by-size recoveries for Fe and $SiO_2$ separately. The figure shows that the reverse anionic flotation promoted the effective flotation of the -10 micron material, compared to that of the reverse cationic flotation. However, there was an increase in Fe recovery in the -10 micron fraction, which was speculated to be due to entrainment with higher amounts of fine material floating and a more stable froth bed forming (Ma *et al.*, 2011). Additionally, the reverse cationic flotation performed better on the coarse $SiO_2$ at above 75 micron.

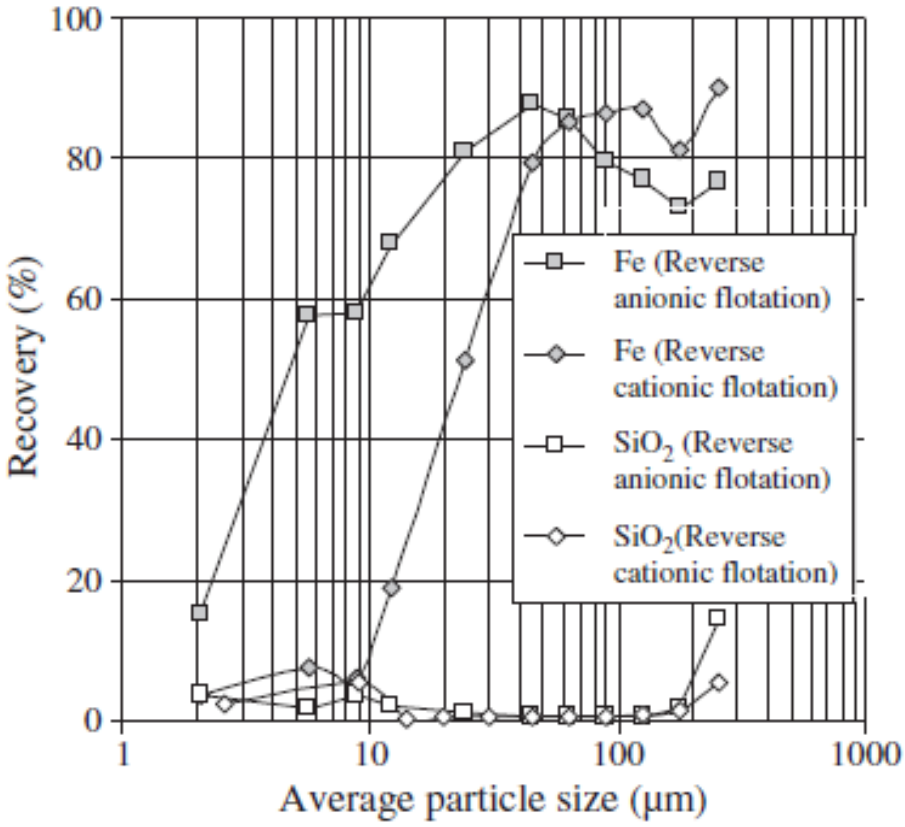


**Figure 33: Size-by-size recovery for Fe and $SiO_2$ using reverse anionic and cationic flotation (Ma *et al.*, 2011)**

Irrespective of the comparison between anionic and cationic flotation, it was reported that a 50% to 55% Fe recovery can be achieved with a product Fe grade of 66% to 67,5% from a feed containing 40% Fe. Due to the composition of the ore, it is a good reference for flotation tests conducted on Sishen's iron ore material. The results are given in Table 7.

**Table 7: Grade and recovery for Fe and $SiO_2$ for reverse cationic flotation tests (Ma *et al.*, 2011)**

| Starch dosage (g/t) | The grade and recovery of Fe and $SiO_2$ in concentrates (%) | | |
|---|---|---|---|
| | | Fe | $SiO_2$ |
| 1000 | Grade | 45.19 | 34.52 |
| | Recovery | 38.85 | 28.98 |
| 1250 | Grade | 66.11 | 5.18 |
| | Recovery | 54.81 | 4.4 |
| 1500 | Grade | 67.86 | 2.64 |
| | Recovery | 50.35 | 1.99 |

### 2.5.1 Reagents and the environment

It was mentioned that amines are generally used as a cationic collector within the iron ore flotation process (Araujo *et al*., 2010; Deo *et al*., 1999). These reagents have to leave the system, which in this case leads to the tailings dam where it remains. The amine compounds are harmful to aquatic life and thus should be controlled, considering that, for example, in Brazil alone an estimated 5500 tons of amines are consumed annually. In an attempt to reduce the amine concentration, a detailed study was conducted on the biodegradation of amine compounds. This was done by taking water samples from the tailings dams and testing for the degradation of these amines, using bacteria. The reagents used were Flotigam EDA 3B and Flotigam 2835, both produced by Clariant (Brazil). Results showed that, with the right type of bacteria and enough time, the concentration of amines can be reduced from 29,3 to 1,37 mg per litre, as shown in Figure 34.

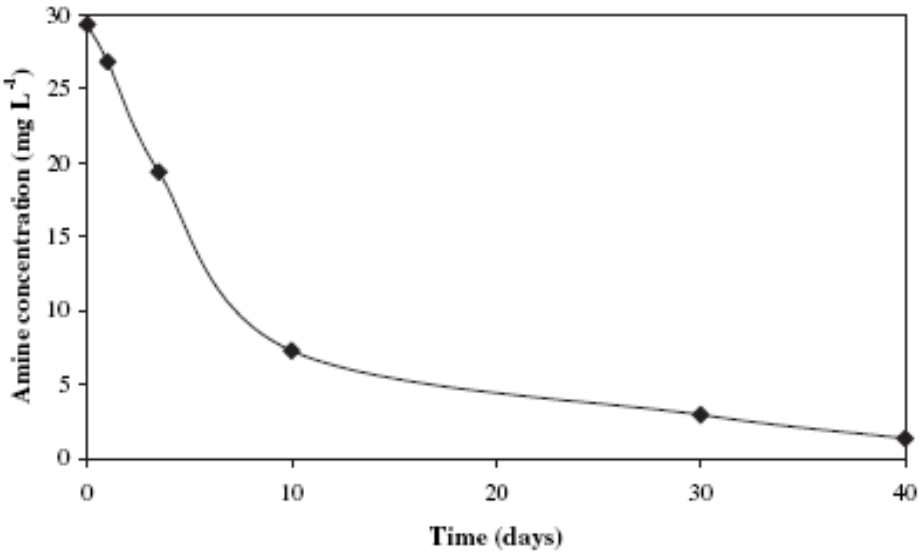


**Figure 34: The amine concentration as a function of time using biodegradation (Araujo *et al*., 2010)**

In the same manner as above, by testing for the remaining collector concentration with a variation of contact times, graphs were constructed with different collectors in the presence of Bacillus Polymyxa (Deo *et al*., 1999). Collectors used include isopropyl xanthate, sodium oleate, DA 16 and DAA, of

which the biodegradation graphs are given in Figure 35 to Figure 38. It can clearly be seen that residual concentrations of reagents can be eliminated and therefore it is absolutely necessary to remove these toxic chemicals in order to preserve the environment.

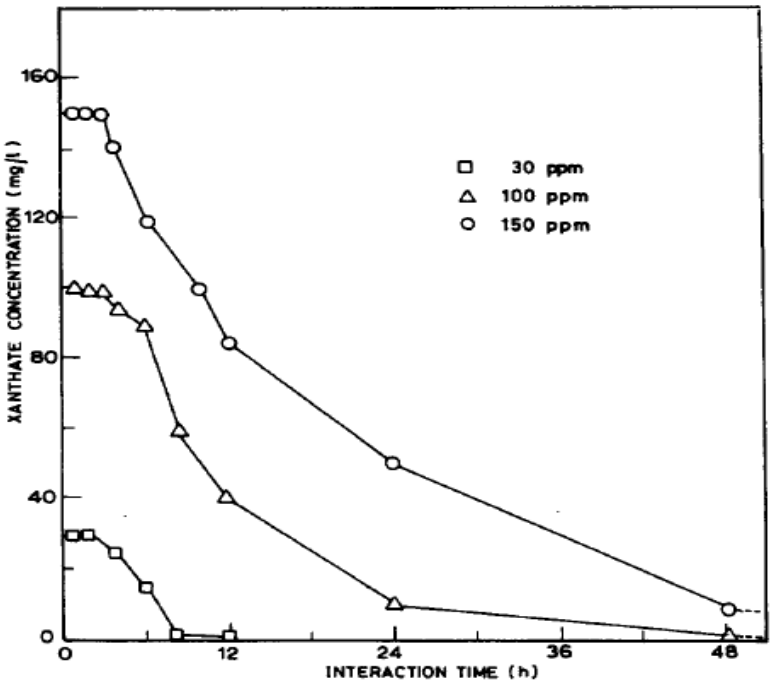


**Figure 35: Biodegradation of isopropyl xanthate in the presence of Bacillus Polymyxa (Deo *et al.*, 1999)**

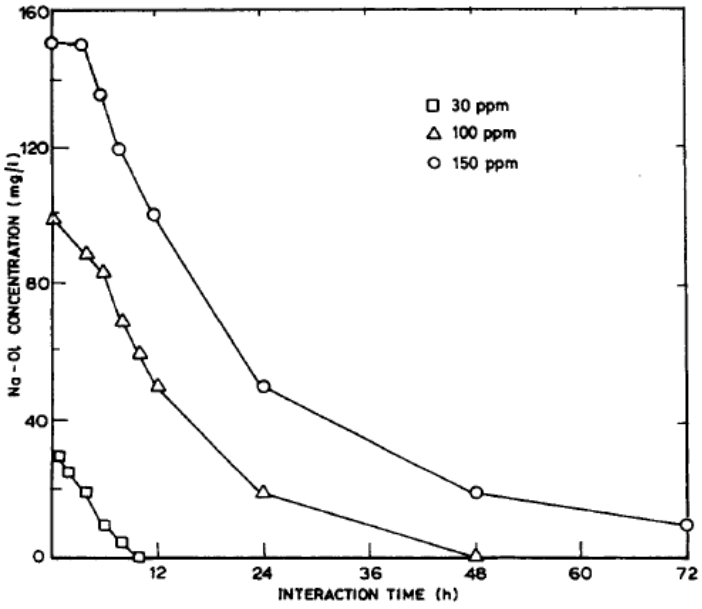


**Figure 36: Biodegradation of sodium oleate in the presence of Bacillus Polymyxa (Deo *et al.*, 1999)**

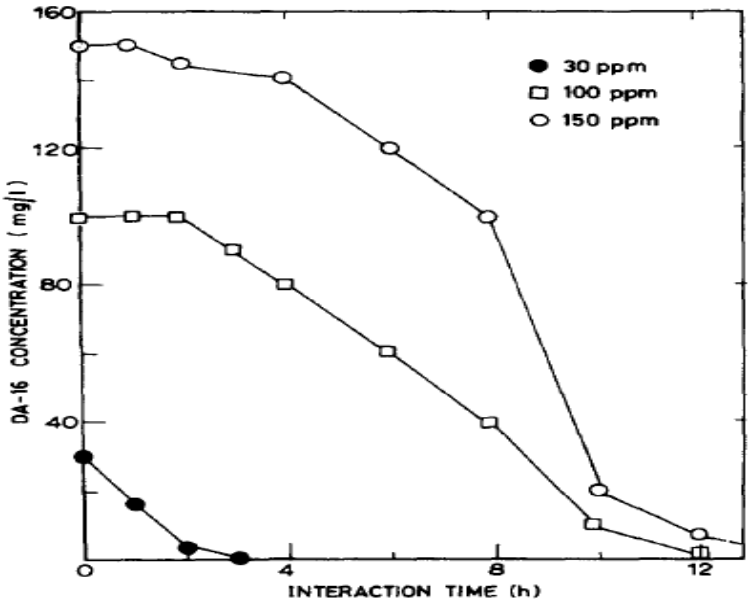


Figure 37: Biodegradation of DA-16 in the presence of Bacillus Polymyxa (Deo *et al.*, 1999)

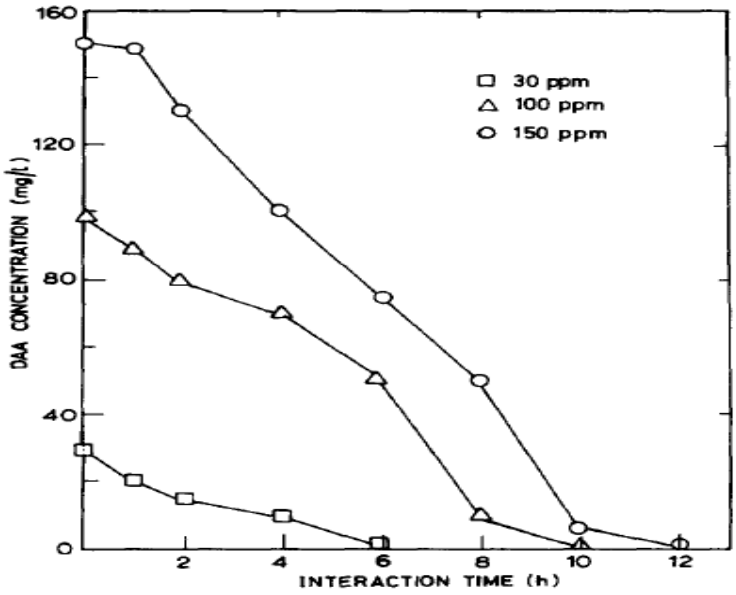


Figure 38: Biodegradation of DAA in the presence of Bacillus Polymyxa (Deo *et al.*, 1999)

## 2.6 Conclusions

If it can be proven that the iron ore at AAKIO can be upgraded using reverse froth flotation, a reduction in ultra-fine iron ore discard and an increase in revenue can be realised with froth flotation. While froth flotation is employed

in many countries for the same reasons, the difference in the case of AAKIO Sishen is the complexity of the ore body.

It is evident that a clear understanding of the mineralogy of the ore body is of great importance in order predict the ore's amenability to flotation and reagents to be used. Therefore, a complete mineralogical study is required prior to flotation.

When considering iron ore flotation, it can be concluded that the process is very dependent on the species present and the possible flotation pH ranges. This is true for most of the oxide species involved and is related to the surface charge of the different minerals.

# Chapter 3: Methodology

The methodology describes the various steps and processes used from the point where the sample was taken, handled and tested in order to achieve the required product specifications. The sample used for this specific test work was taken from the final concentrate of the SLon concentrate at AAKIO Sishen during June 2012. The sample, with an approximate mass of 400kg, was taken over a two day period.

The sample, with an approximate mass of 400 kg, was received from Kumba's Sishen plant which was sampled from the SLon concentrate stream. The sample was taken over 2 day period.

No additional information was provided and thus it was necessary to follow the proper standards and procedures to determine the characteristics of the sample received. AAKIO uses the ISO standards and therefore this sponsored project also made use of it. Procedures for determining the particle size distribution, liberation characteristics and phase composition were developed and discussed with AAKIO's quality control department. However, in some instances no standards were available and thus were discussed and agreed upon. This was true for flotation tests including conditioning time, as well as the standard for milling of material.

## 3.1 Materials handling

The materials handling, i.e. sample preparation, was considered to be one of the most important stages of the test work, as incorrect implementation of these procedures could result in project failure or doubtful results.

The key to the successful sample preparation campaign was to minimise or eliminate any biases. This was achieved by using the ISO 3082 (2009) standard for sample splitting. Competence also played an enormous part, as some biases like spillage and sample contamination, as well as incorrect

delineation and extraction of increments, could possibly be eliminated (ISO 3082:2009). Minimisation therefore could be applied to the loss of dust and particle degradation.

### *Gross sample division*

Keeping the above in mind, the sample was to be thoroughly mixed prior to the commencement of the materials handling campaign. The 400 kg sample received from Kumba, sampled at the SLon test facilities, was split into ten increments by making use of a 10-way Dickie and Stockler rotary splitter. The increments were then added and the process repeated two more times to ensure proper mixing of the sample (ISO 3082:2009). The ten-way rotary splitter is shown in Figure 39.

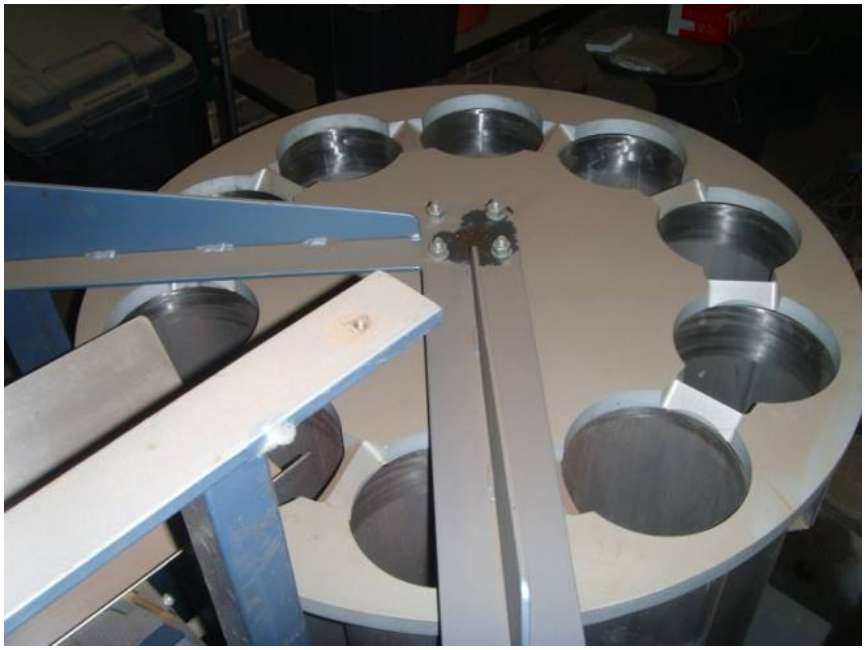

**Figure 39: Image of a Dickie and Stockler ten-way rotary sample divider**

The minimum sample mass in kilograms was calculated according to equation 1, which yielded a minimum divided-gross-sample mass of 1,44 g at a 212 micron top size and a 0,1% Fe standard deviation (ISO 3082:2009). Although the minimum mass was calculated to be 1,44 g, there was a set minimum

mass of 0,5 kg. However, for this study the set minimum divided-gross-sample mass was set to be 1 kg.

Equation 2: $$m_s = \frac{0.00032\, d^{2.5}}{\sigma_D{}^2}$$

Where

$m_s$ = Minimum mass of divided sample (kg)
$d$ = the nominal top size of the sample (mm)
$\sigma_D$ = the desired standard deviation of sample deviation (%Fe)

For proper sample splitting, a maximum 2% error was allowed during splitting. For instance, if the gross sample had a mass of 400 kg and was split into ten increments, then each increment must weigh 40 ± 0,8 kg.

An illustration of the splitting procedure to achieve 400 samples of 1 kg each from the gross sample is given in Figure 40. Cross selection of samples was employed for mixing of sub samples throughout the splitting procedure.

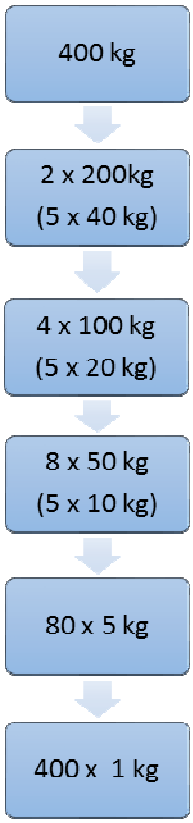


Figure 40: Graphical illustration of the splitting campaign

NOTE: A temperature of less than 105 ˚C for drying samples where necessary was used throughout the project (ISO 3082, 2009).

## 3.2 Material characterisation

The sample characterisation forms the basis of the project, as it is required to determine the chemical composition of the feed ore, the phases present, and the physical nature of the ore body – all of which are the most important factors when considering flotation as an upgrading process. Gangue minerals, even if present in small quantities, can drastically affect the outcomes and results of flotation testwork.

Therefore, after the sample was split into 1 kg sub-samples, five random samples were selected, split into 10 g sub-samples using a Dickie and Stockler rotary splitter, and dispatched to AAKIO and X-ray diffraction (XRD) analytical and consulting department for chemical and phase analysis, respectively. The remainder of the sample was then used for particle size

distribution (PSD) analysis, size by size chemical analysis, and Scanning Electron Microscope (SEM) analysis at the University of Pretoria.

### 3.2.1 Particle size distribution (PSD)

By making use of a ten-way rotary splitter, 500 g of material was split from one of the 1 kg samples. By employing cross selection, five sub-samples were added together to yield a single 500 g sample. The sample was then introduced to a set of Taylor sieves. The sieve sizes used in the particle size distribution analysis started at a mesh size of 212 micron and decreased in size with a factor of $\sqrt{2}$ down to 38 micron.

The -38 micron material was caught in a bucket, filtered, dried and weighed. The difference in weighed total mass and the initial sample mass provided a good indication of material loss, if any. Due to the fact that dry sieving is inefficient at sizes lower than 150 micron, wet sieving was employed.

Each size fraction from the PSD was submitted for elemental analysis to achieve and determine the distribution of elements within the feed sample as a function of size.

### 3.2.2 Chemical analysis (XRF analysis)

X-ray fluorescence (XRF), also known as X-ray emission spectrography, is a technique where a sample is irradiated with X-rays generated in a high intensity X-ray tube. The sample, which is ground to a fine powder and compressed into a pellet together with binder, absorbs the X-rays to some extent according to Beer's Law. As the sample absorbs X-ray energy, an X-ray emission spectrum, which is characteristic to each specific element, is generated. A detector is used to determine the specific elements present and to compare the X-ray intensity to that of a standard of known composition, resulting in a quantitative elemental analysis.

Each of the randomly chosen 1 kg sub-samples were split once more into 10 g samples using a small ten-way Dickie and Stockler rotary splitter. A single 10 g sample from each of the five randomly chosen 500 g samples were dispatched for XRF analysis at Anglo American Technical Services (AATS). The analytical technique was used to determine and quantify the specific elements present in the sample.

During the test programme, all samples were analysed (chemical analysis) at the University of Pretoria with a benchtop XRF machine. This machine was calibrated under the supervision of AATS and formed part of a "round robin" calibration exercise conducted by AATS to ensure accuracy of the results.

### 3.2.3 Phase analysis (XRD analysis)

In the exact same manner as the chemical analysis, ten samples of 10 g each taken from the 1 kg sub-samples were dispatched for XRD analysis. The analytical technique identifies and quantifies the various phases present in the sample.

X-ray diffraction is used to study crystal structures and to identify minerals. The analytical technique makes use of a cathode ray tube whereby electrons collide with a target material to produce X-rays. The generated X-rays, which are directed at the analytical sample, reflects at a certain angles of incidence. When considering mineral identification, the powder method is used. This requires the specimen to be ground as fine as possible. The mount is rotated in the path of the collimated X-ray beam, during which the diffracted X-ray signals are detected via an arm mounted detector. The signals are then analysed and minerals present determined.

### 3.2.4 Liberation analysis

#### *3.2.4.1 Scanning electron microscope*

The valuable and gangue minerals' degree of liberation analysis was conducted using a scanning electron microscope (SEM). Five randomly chosen 1 kg samples were subjected to proper splitting, as was done before. Five samples of 10 g each were mounted in resin, with the help of Betachem. Due to segregation of the sample during mounting, each sample was split in half (after mounting), such that one can see the cross section of the sample. The samples were then analysed with a SEM at the University of Pretoria. In this case the mineral association and thus the liberation characteristics were determined with the use of backscatter electron technology. By using the scanning electron microscope, the composition and size of each separate phase was also analysed.

The SEM generates a large amount of information by scanning the specimen with an electron beam, which generates various types of radiation signals including secondary electrons, backscatter electrons, X-rays and cathodoluminescence radiation. A series of varying detectors are used to filter through the information, such that a specific analysis can be conducted. With the use of backscatter electrons, various minerals can be determined according to the specific mineral's atomic number. Once the various minerals have been delivered, an estimate can be made regarding the liberation characteristics of the sample.

Additionally, the sample was also subjected to a mineral liberation analysis (MLA) at AATS, which makes use of energy dispersed spectra (EDS) from X-rays produced during interaction with electrons. Two samples were submitted for the MLA:

- Flotation feed sample: In this case the as received feed material was submitted for MLA analysis in order determine if there is unliberated

material in the coarser fractions of the feed. This was expected, as the XRF analysis showed that the -38 micron material was already on specification and that froth flotation did not necessarily upgrade the material.

- Milled flotation feed sample: Flotation tests were conducted on the raw feed material and showed difficulty in processing to achieve an upgraded product. Furthermore, it was also determined the -38 micron material was already close to specification. Therefore, as a test, the +38 micron material was screened from the raw feed and milled for various time intervals. The flotation results showed positive results, which then suggested that a comparative sample were to be submitted for MLA analysis. Therefore, the sample submitted as “milled flotation feed sample” was an as received flotation feed sample, which was screened at 38 micron. The +38 micron material was then milled for 20 minutes and submitted for MLA analysis.

The aim of the investigation was to determine the bulk mineralogy, hematite and gangue mineral liberation, association and grain size distributions. Furthermore, the sample was screened into the following size fractions for analysis:

- -38 micron
- +38 -75 micron
- +75 micron

The data will present the percentage liberated material in each size fraction, as well as the extent of association with a specific mineral.

### 3.3 Laboratory flotation testing

The ore characterisation provided enough information to continue with the flotation process as a means of beneficiation. The next step was to identify

reagents that could aid in the process. The reagents considered here are depressants, collectors and modifiers.

From literature it was concluded that for all tests the following reagent suite at various dosages was used to conduct flotation test to generate release curves:

- Sodium hydroxide and sulphuric acid as modifiers, i.e. for pH adjustment
- Corn starch as depressant
- Flotigam EDA3 and Flotigam 2385-2L as amine collectors suggested and supplied by Clariant.

## 3.4 Laboratory flotation tests (D12 Denver Cell)

### 3.4.1 Sample preparation

For each test a 10 kg sample (ten of 1 kg samples thoroughly mixed) was screened at 38 micron as a de-sliming step in the process. The reason for this was that the characterisation of the material indicated that the -38 micron material was already close to specification at an Fe content of 66,3% (w/w). Additionally, the PSD showed that approximately 60% of the feed material was -38 micron. The challenge with the screening step, i.e. de-sliming, was that the practicality of this process in a processing plant is not as efficient as when screened in a laboratory.

Therefore, it was assumed that a series of cyclone banks will typically be used for de-sliming, and as such, there should be separation inefficiencies calculated into the screening process. To simulate a real plant scenario, a 30% inefficiency was assumed, i.e. 30% (w/w) of material was misplaced. A flow diagram of the process that was followed is given in Figure 41. First, the sample was completely screened at 38 micron. Thereafter, the -38 micron material was split until a mass equating to 30% (w/w) of the total -38 micron

material was achieved. The 30% mass was then added to the +38 micron material to achieve the final flotation feed sample.

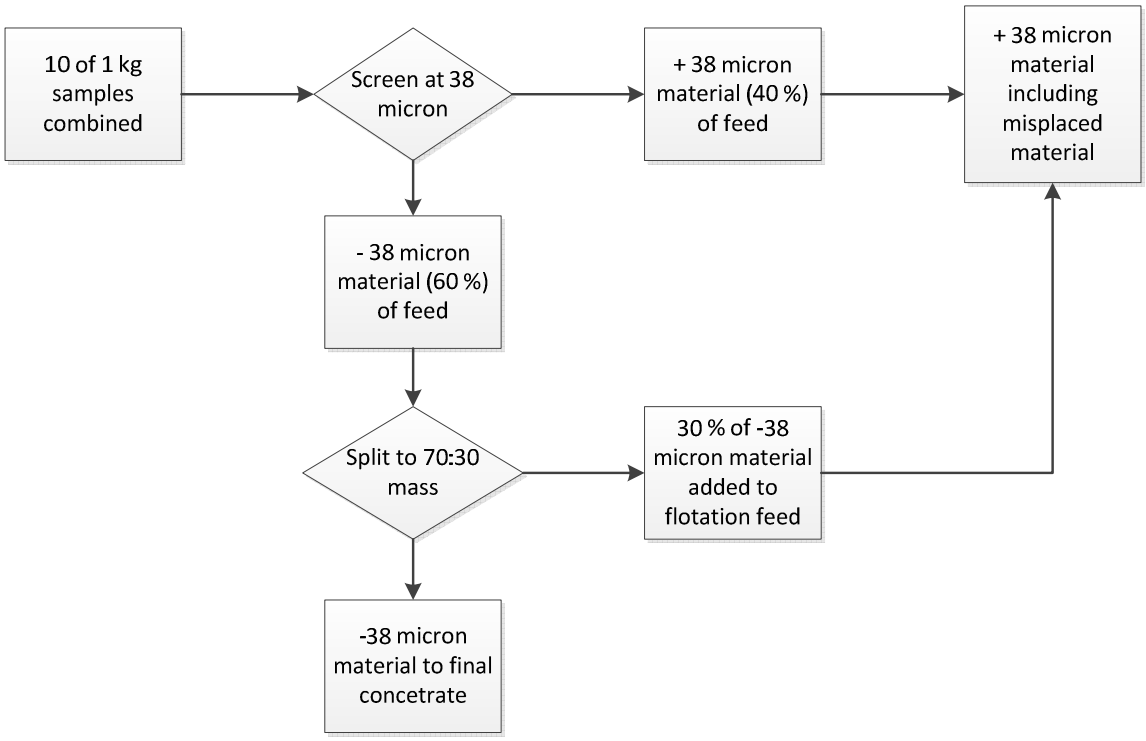


Figure 41: Process flow for preparation of laboratory flotation feed material

In this case a large sample was screened and prepared according to the procedure described above, then split to achieve 600 g samples, which was subjected to flotation tests.

Flotation tests were conducted without milling as an initial step, in order to determine if it is possible to selectively upgrade the feed material as received in order to save on capital and operational expenditure as part of the final solution.

Additionally, the liberation analysis (as discussed in detail later on) indicated that the material was not completely liberated. Therefore, tests were conducted with milled material to indicate any additional upgrading of material with a variation of milling time. In these instances the mass of material (flotation feed as per the sample preparation flow sheet) was weighed and introduced to a laboratory ball mill. Material was mixed with synthetic plant

water at 30% solids (w/w) and subjected to various durations of milling. The material milled at various milling times, were then subjected to flotation and the recovery as a function of milling time plotted in order to determine the required milling time.

To mill the material, 50 mm steel balls were added at 40% of the mill volume (the 40% included voids). The mill was operated at 90% of the critical rotational speed.

### 3.4.2 Reagent preparation

#### *3.4.2.1 Depressants*

The depressant, in this case causticised starch, was prepared by adding a 10% (w/v) chemical grade NaOH to 10 g of Sigma-Aldrich corn starch and 100 ml of distilled water. Initially, the starch is added to water and mixed. A total of 16.6 ml of 10% (w/v) NaOH was added to initiate the causticisation process. The solution was stirred continuously for 30 minutes at 300 rpm using an overhead stirrer.

Finally, after 30 minutes, distilled water was added to the solution to achieve a 2% (w/w) causticised starch solution, i.e. a total of 500 ml.

In the case of using dextrin, which is soluble in water, 10 g of dextrin was weighed, added to distilled water and stirred for 30 minutes to achieve the 2% (w/w) dextrin solution.

Please note that in both the cases of starch and dextrin, a new solution was prepared daily to ensure no degradation of the solution over time.

#### *3.4.2.2 Collectors*

As with the depressants (starch and dextrin), a fresh solution of collecting agents were prepared daily for tests conducted. In this case, industrial grade Flotigam EDA3 (ether mono-amine) and Flotigam 2385-2L (alkyl ether di-amine) supplied by Clariant were used as collectors. For all tests, a 0.058%

(w/w) concentration collector solution was prepared using the standard procedure as described by Clarient for both Flotigam EDA3 and Flotigam 2385-2L. This was achieved by adding 0,175 g of collector to 300 ml distilled water. The solution was stirred for a total of five minutes.

#### *3.4.2.3 Modifiers*

Sulphuric acid and sodium hydroxide were prepared at 1 molar solution by dissolving the sodium hydroxide and sulphuric acid in distilled water. Solutions were stored in air tight containers and were used as required to achieve the correct solution pH.

#### *3.4.2.4 Synthetic plant water*

"Synthetic" plant water was produced to resemble the expected available plant water at Sishen, in terms of its two largest contaminants, dissolved Ca and Mg ions. Distilled water was used as base liquid before 6,32g $CaCl_3$ and 5,4g MgCl were added to make up a 20 litre solution, as prescribed by AAKIO. At least 40 litres of synthetic plant water was made in a batch, and the supply was replenished weekly/as needed between flotation tests.

### 3.4.3 Flotation test (D12 Denver Cell)

Distilled water was combined with the sample into a 2,6 litre D12 Denver flotation cell to achieve a 30% (w/w) solids containing slurry. All tests were conducted in ambient temperatures. The impeller was then started at a rotational speed of 800 rpm after which the starch (depressant) was added to the system. The starch was conditioned for five minutes under these conditions to ensure sufficient contact with the material. During the conditioning of the slurry, the pH was adjusted to ensure a pH of 9,5 for all tests conducted.

The collector was then added to the system and conditioned for an additional two minutes. Thereafter, the rotor speed was adjusted to 1200 rpm prior to

flotation. At this point in time, the flotation process was initiated by injecting air into the system.

Once the flotation process commenced, froth phase (flotation tails – concentrated quartz stream) samples were collected every 15 seconds for the first two samples, and then every 30 seconds for the next three samples. In the cases where there was still flotation taking place, i.e. material overflowing the lip of the cell, an additional one minute sample was taken as a final sample. Therefore the total time allowed for flotation was three minutes.

### 3.4.4 Froth phase sample preparation for analysis

The concentrate samples were weighed, dried, reweighed, bagged and dispatched for XRF analysis. All data was recorded as part of the procedure for evaluation and construction of release curves. The release curves should clearly indicate the technical possibilities in terms of upgrading the sample by making use of froth flotation.

The concentrate samples were prepared by adding 5% (w/w) PVA binder to the material and mixed thoroughly. The sample was then put under a mechanical pressure of ten tons for two minutes and then cured for 30 minutes at 90 ºC.

## Chapter 4: Results and Discussion

The results and discussion has been divided into two sections, namely “Initial Sample Characterisation and Flotation Testwork”, which is discussed in section 4.1, and “Sample Characterisation and Flotation Testwork Revised”, discussed in section 4.2. Due to various challenges encountered during initial stages of the test program, changes were made to the test program which subsequently lead to acceptable results. This is discussed in section 4.2.

## 4.1 Initial feed material characterisation

The as received material (400 kg) was dried, combined, mixed and split, after which five random samples were selected and subjected to the following analyses, such that the material characteristics could be determined:

- particle size distribution
- chemical analysis by size
- chemical analysis
- SEM analysis
- phase analysis (only phases determined)

### 4.1.1 Particle size distribution

Figure 42 (raw data given in Appendix A) shows the particle size distribution for five randomly chosen samples after the splitting of the bulk sample of 400 kg as received. The PSD shows 60% passing 38 micron, which is very fine for flotation. Additionally, it is evident that the particle size distributions are similar for all the samples, indicating that the materials handling and splitting of the bulk sample was done representatively.

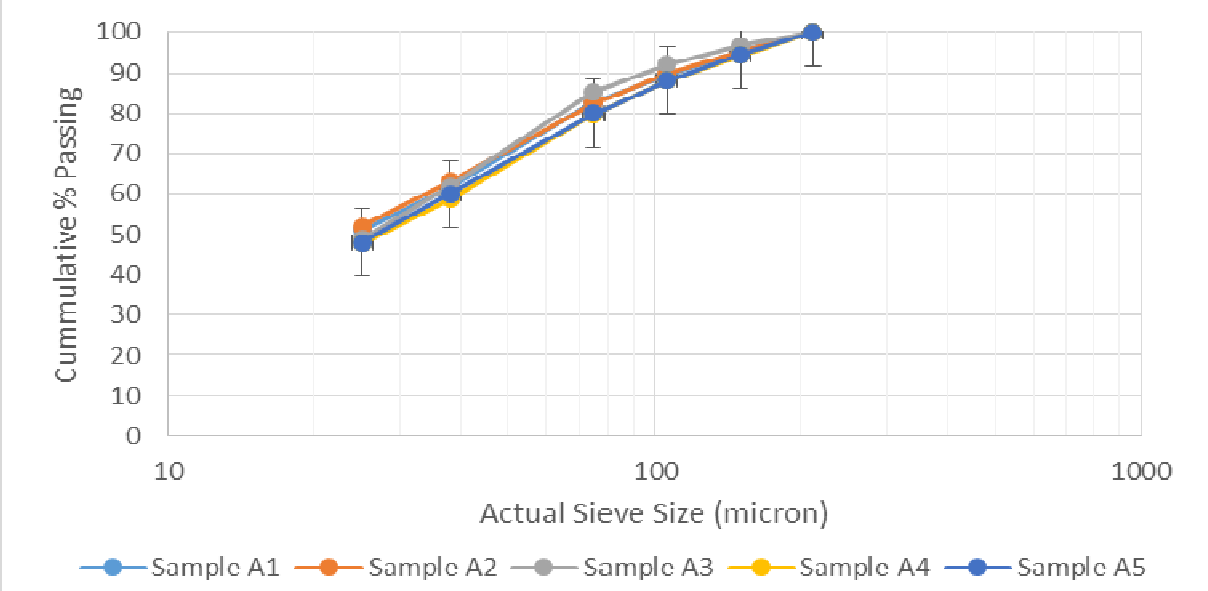


**Figure 42: Particle size distribution of the raw as received SLon concentration**

As an additional confirmation test for the splitting of the gross/bulk sample, ten randomly selected samples were subjected to the Malvern particle size analyser. Results showed that the materials handling campaign was successful and that all samples were representative of the bulk/gross sample (Appendix A).

### 4.1.2 Chemical analysis by size fraction

As part of the characterisation of the feed material, each size fraction was submitted for chemical analysis at Anglo American Research and Development to indicate the distribution of hematite and quartz as a function of the size fraction. Figure 43 shows the cumulative Fe content as a function of particle size. It is evident that the -38 micron has a total Fe content of 66,3%, which is close to the final concentrate grade required, which is 66,5%. Additionally, the cumulative Fe content indicates a feed Fe content of approximately 65,8% (w/w).

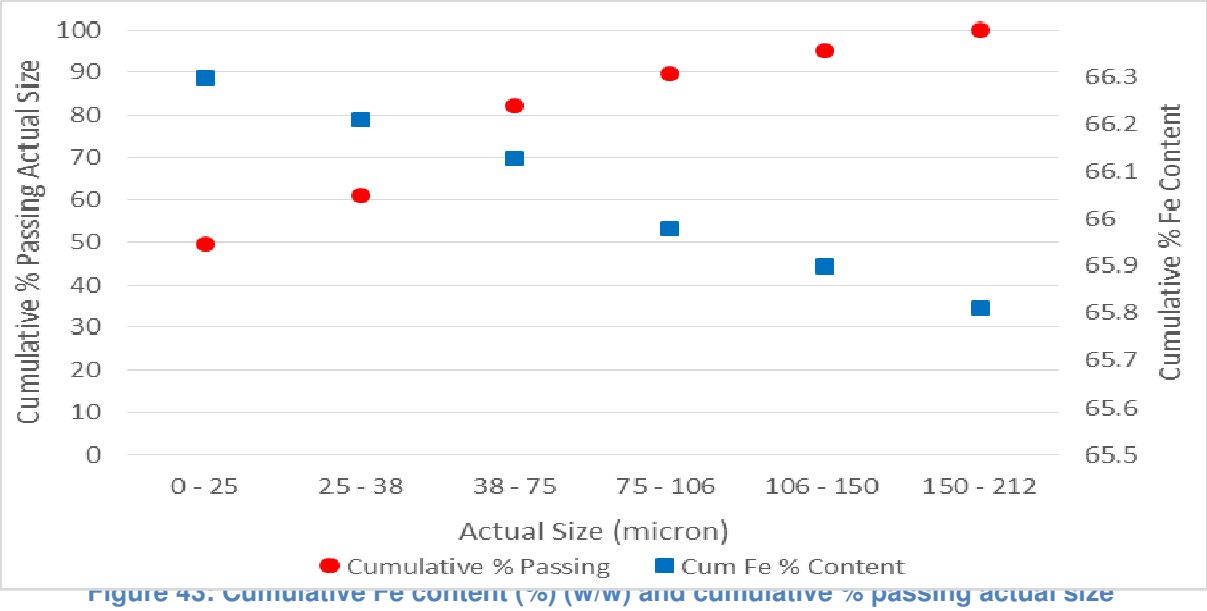


Figure 43: Cumulative Fe content (%) (w/w) and cumulative % passing actual size

### 4.1.3 Chemical analysis of feed

Five randomly selected samples were subjected to XRF analysis to determine the Fe and $SiO_2$ content of the bulk/gross sample, and to confirm that all of the split samples are representative (raw data is given in Appendix B). In Table 8

the Fe and $SiO_2$ content is given for each of the individual samples. Results indicate a total Fe content of approximately 65,8%, as well as a $SiO_2$ content of approximately 4,2%. Finally, the results show once more that the sample handling and splitting was conducted according to standard.

Table 8: Fe and SiO2 content of the feed material (five random samples chosen)

| Sample | Fe Content | $SiO_2$ Content |
|---|---|---|
| **A1-1** | 65.85 | 4.26 |
| **A1-2** | 65.78 | 4.24 |
| **A1-3** | 65.77 | 4.21 |
| **A1-4** | 65.82 | 4.28 |
| **A1-5** | 65.83 | 4.16 |
| | | |
| **Minimum** | 65.77 | 4.16 |
| **Maximum** | 65.85 | 4.28 |
| **Standard Error** | 0.015 | 0.021 |

### 4.1.4 SEM analysis

The SEM analysis indicated that there was segregation taking place when preparing the SEM sample (the raw data is given in Appendix C). The analysis also indicated liberation of most material, as can be seen in Figure 44. However, small traces of unliberated material was observed in some instances (shown in Figure 45). Due to the small amount detected, it was decided to continue with the flotation, as the effect on flotation and the results was expected to be negligible.

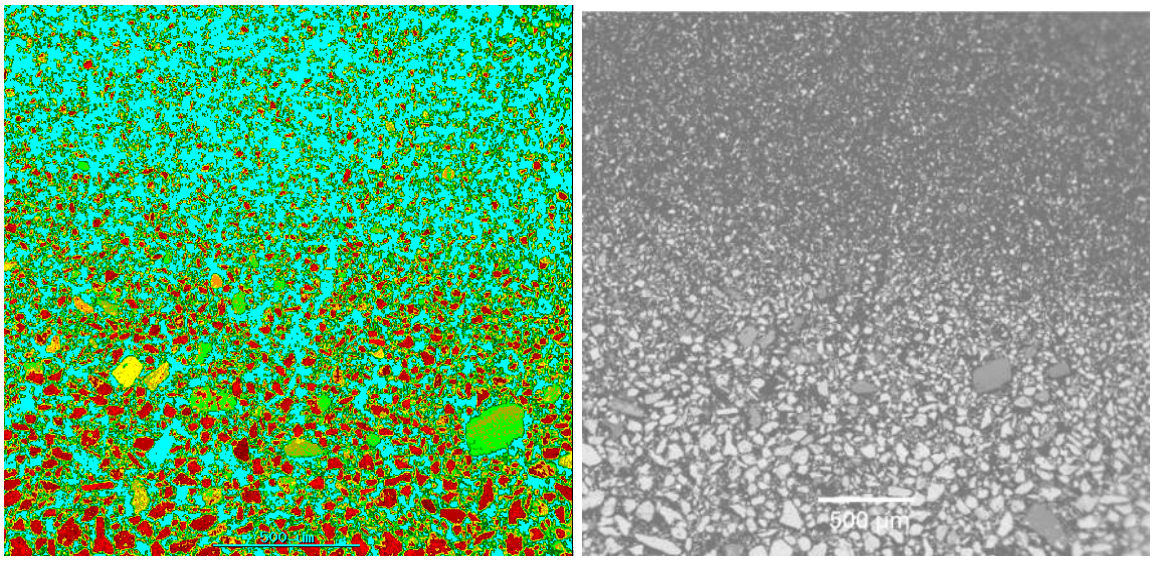


Figure 44: SEM backscattered-electron image shown of the gross sample cross section (hematite – red [bright phase] phase and quartz – green phase [dark phase])

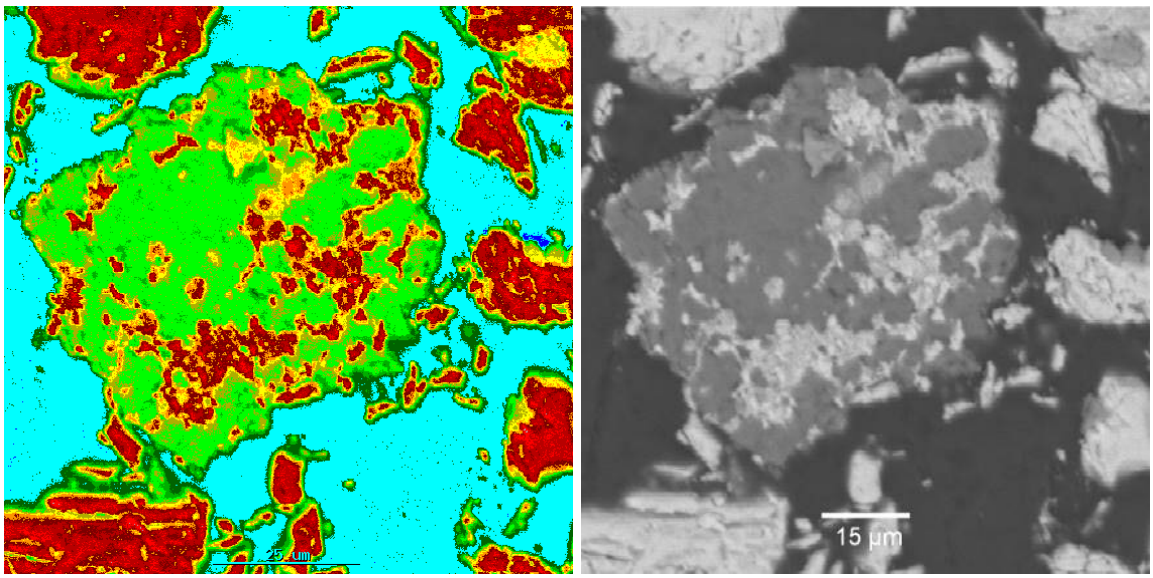


**Figure 45: SEM (backscattered-electron images) analysis indicating hematite associated with quartz (hematite – red [bright phase] phase and quartz – green phase [dark phase])**

### 4.1.5 Phase analysis of feed

The phase analysis conducted on the feed sample (raw data given in Appendix D), to the degree that can be detected by XRD analysis, showed the following phases to be present:

- hematite ($Fe_2O_3$)
- quartz ($SiO_2$)
- kaolanite ($Al_2Si_2O_5(OH)_4$)
- chlorite ($(Mg,Fe)_5Al(Si_3Al)O_{10}(OH)_8$)

This was not quantified, but only identified to be present within the sample.

### 4.1.6 Preliminary flotation test work

Flotation tests and repeatability test work were to be conducted on selected tests as part of the experimental procedure, such that process consistency could be proven. The tests were conducted using the process parameters (as per agreement with AAKIO) as tabulated in Table 9 (the raw data is given in Appendix E).

**Table 9: Fixed parameters and set points for the conducted flotation tests**

| Parameter | Set point |
|---|---|
| **Feed solids concentration (w/w)** | 30 % |

| | |
|---|---|
| **Cell volume** | 2,6 litre |
| **Impeller speed** | 1200 RPM |
| **Starch conditioning time** | 5 min |
| **Amine conditioning time** | 2 min |
| **pH** | 9,5 |

In this case, only the combined concentrate samples were collected i.e. float to completion. The reagent system for the various tests is tabulated in Table 10:

**Table 10: Reagent dosages for the various tests conducted at 180 g/t amine**

| Test No | Dextrin g/t |
|---|---|
| 1 | 30 |
| 2 | 30 |
| 3 | 30 |
| 4 | 30 |
| 5 | 120 |
| 6 | 120 |
| 7 | 120 |
| 8 | 120 |
| 9 | 180 |
| 10 | 180 |
| 11 | 180 |

For each individual test, the feed, concentrate (sunk material) and discard (floated material – froth phase) were sampled and subjected to chemical analyses. The results are given in Figure 46 to Figure 48, in which case the specific mineral is plotted according to the test number. From the graphs it can be seen that a “T-piece” effect (no upgrading was achieved, i.e. the feed, product and tailings stream has the same composition) was achieved and in most instances the amount of quartz is higher than that in the concentrate.

It is important to note that this is not due to misplaced fines, as these were removed from the system via screening.

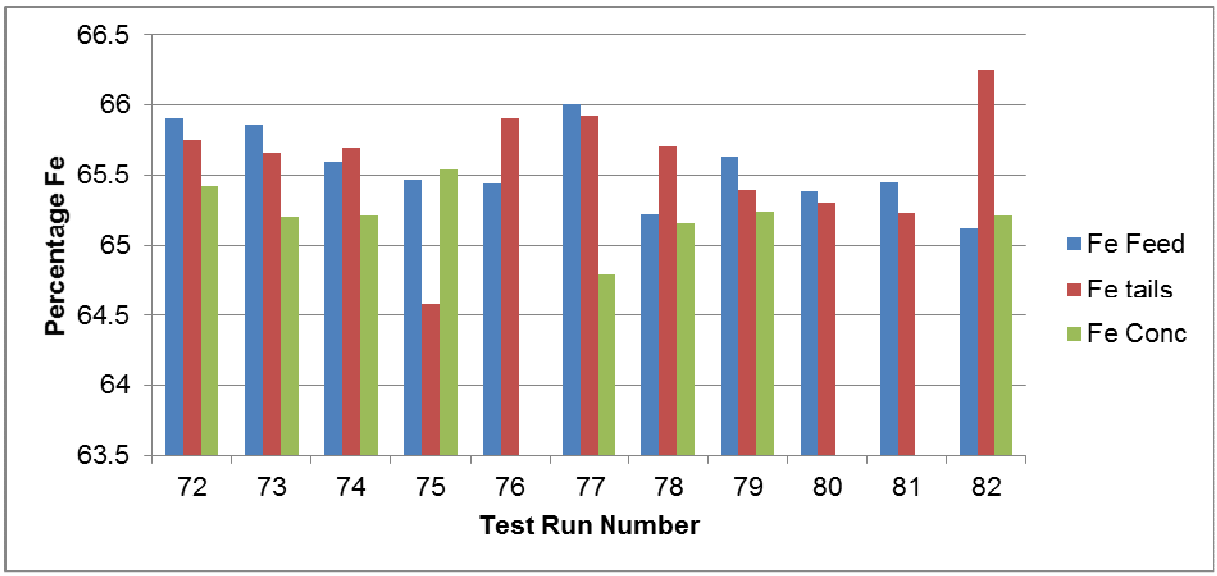


Figure 46: Fe content of the feed, tails and product material for each individual test conducted

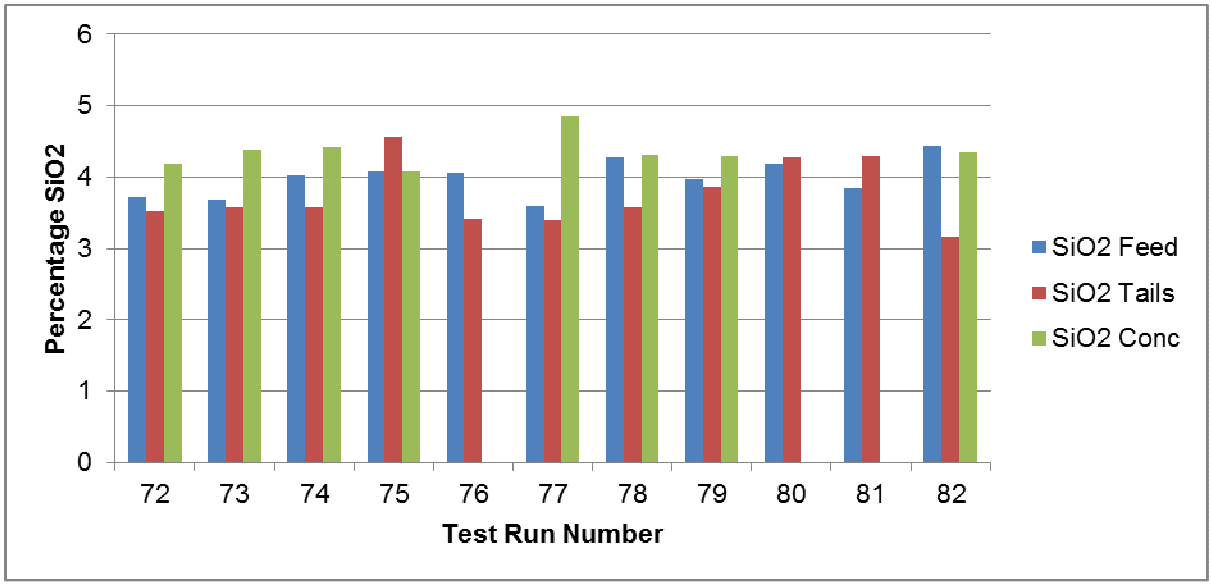


Figure 47: Quartz content of the feed, tails and product material for each individual test conducted

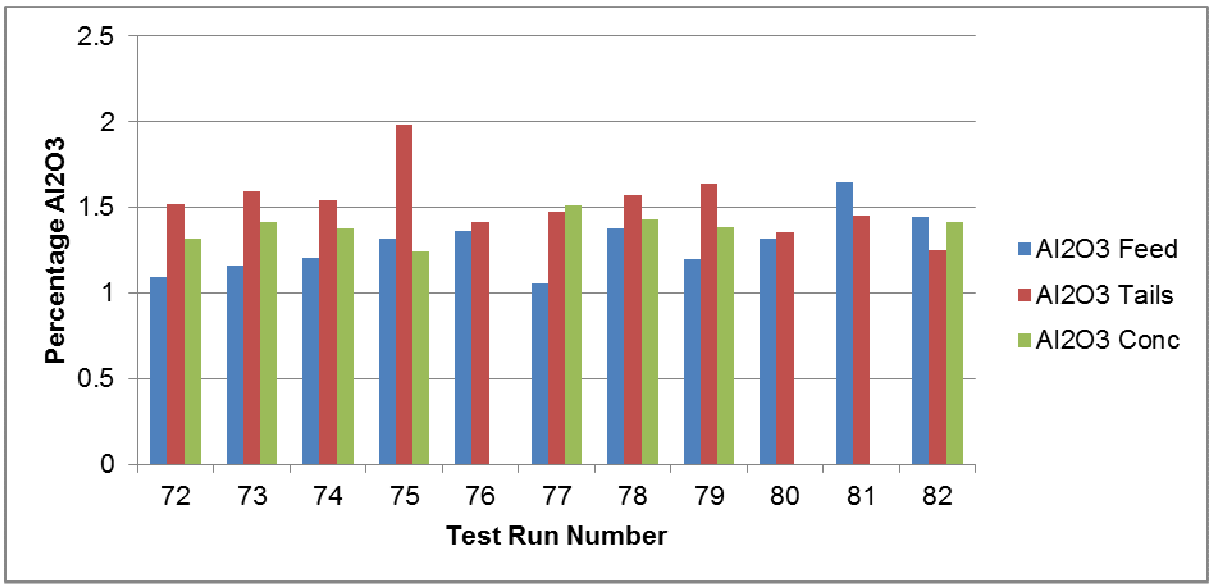


**Figure 48: Al-bearing minerals content of the feed, tails and product material for each individual test conducted**

### 4.1.7 Conclusion – preliminary flotation testwork (repeatability testwork)

From the results it is concluded that a T-piece split was realised. Therefore, there was no upgrading of the stream and no repeatability was achieved. This led to revisiting of the liberation study. In this case, the liberation study was conducted using an MLA analysis procedure instead of a SEM analysis, because the contribution of quartz to the bulk sample is not enough to conclude on the liberation.

## 4.2 Test program realignment

The laboratory testwork was carried out using various reagent suites, during which it was found that there was no upgrading by making use of froth flotation. In addition, there was no repeatability in terms of the results. This led to reanalysing the feed material by making use of the SEM, as well as submitting a sample for a mineral liberation analysis (MLA).

Results indicated that there was a substantial amount of unliberated hematite as well as unliberated quartz within the sample. This was not concluded during the initial characterisation, as the mass contribution of Quartz was only 4-5% of the feed material (therefore very difficult to detect).

After concluding that the material required additional liberation, tests were repeated, including milling the +38 micron material. The repeated liberation analysis as well as flotation results are discussed in the following sections.

### 4.2.1 Sample characterisation and flotation tests

Due to the fact that a "T-piece" effect was experienced, there were different speculations as to what the next step should be. The most obvious was to revisit the liberation study. Therefore, a sample was submitted to the Department of Physics at the University of Pretoria for another SEM analysis, using a SEM with a higher resolution. In Figure 49 it can be seen that there seems to be, to some degree, material that is not liberated as previously noted (Figure 45). However, it is important to understand that the low quartz content of the feed material, that is 4%, increases the difficulty of detecting liberation challenges.

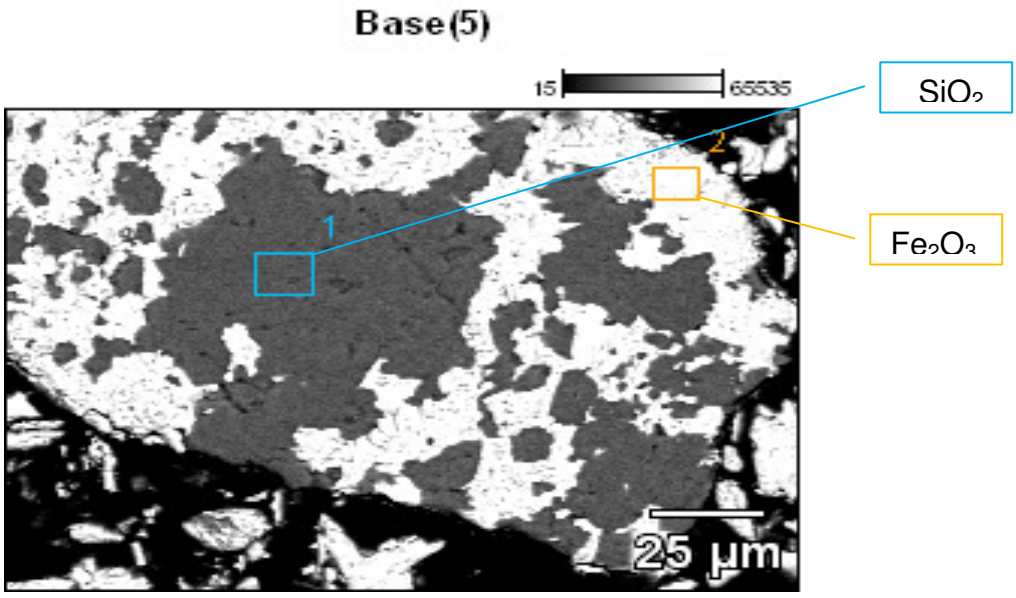


Figure 49: Image of unliberated quartz with hematite material (hematite – bright phase and quartz – dark phase)

### 4.2.2 Mineral liberation analysis (MLA)

The MLA uses energy dispersion spectra from X-rays produced by the sample during interaction with an electron beam which gives the chemical composition of a specific phase. Furthermore the use of backscattered electron images

(specific to the intensity i.e. the brightness in the image) together with the chemical composition is used to produce mineral maps in order to characterise the mineral. In this specific analysis not enough sample was available for XRD analysis, however the mineral phases were compared to the original XRD analysis conducted.

For the MLA, two samples were submitted to Anglo American Technical Solutions (AATS MLA report is given in Appendix F):

- Feed sample – raw feed sample that was not screened or altered.
- Milled sample – the feed sample was screened at 38 micron, of which the +38 micron material was ground for 25 minutes before submission.

Both samples were screened into three size fractions for the MLA, including -25 micron, +25 -75 micron, and +75 micron. Please note that the milled sample had no +75 micron material and thus only two size fractions were analysed.

As part of the MLA, the phases present were determined during the analysis and is given in Table 11. The main mineral phases identified were hematite ($Fe_2O_3$), quartz ($SiO_2$), kaolinite ($Al_2Si_2O_5(OH)_4$), and chlorite ($((Mg,Fe)_5Al(Si_3Al)O_{10}(OH)_8$), as was initially identified with XRD.

For quantification purposes, Table 11 indicates the PSD of the flotation feed sample, as well as the milled flotation feed sample. As a check, the PSD as per the sizing fractions was compared to the actual PSD determined during characterisation. From Table 11 the P50 is estimated at 25 micron, which correlate with the PSDs conducted on the raw feed samples and is therefore considered to be representative.

**Table 11: Bulk modal mineralogy for the flotation feed and the milled flotation feed sample**

| | Flotation Feed Sample | | | | Milled Flotation Feed Sample | | |
|---|---|---|---|---|---|---|---|
| Mineral | Combined | +75 µm | +25 µm | -25 µm | Combined | +25 µm | -25 µm |
| Hematite | 97.68 | 95.56 | 97.11 | 98.82 | 95.46 | 96.14 | 95.42 |
| Quartz | 1.38 | 2.84 | 1.73 | 0.61 | 3.01 | 2.08 | 3.06 |
| Kaolinite | 0.13 | 0.30 | 0.15 | 0.06 | 0.16 | 0.23 | 0.16 |
| Chlorite | 0.42 | 0.69 | 0.53 | 0.25 | 0.92 | 1.09 | 0.91 |
| Other | 0.39 | 0.61 | 0.48 | 0.25 | 0.45 | 0.46 | 0.45 |
| Total | 100.00 | 100.00 | 100.00 | 100.00 | 100.00 | 100.00 | 100.00 |
| PSD | 100.00 | 18.89 | 31.11 | 50.00 | 100.00 | 5.28 | 94.72 |

Figure 50 shows the mass contribution of various minerals (in the oxidised state) for the various screened size fractions and the combined material. Firstly, it can be seen that the -25 micron material of the feed sample has almost 99% hematite (w/w), which confirms the fact that the ultra-fine material -38 micron was already on specification and could therefore be removed from the flotation feed material. Secondly, the hematite content of the combined milled sample is lower than that of the feed sample, which is due to the fact that the -38 micron material was removed from the sample. Finally, the feed material shows an increase in quartz content with an increase in size fraction. This could be due to unliberated quartz reporting to the SLon concentrate.

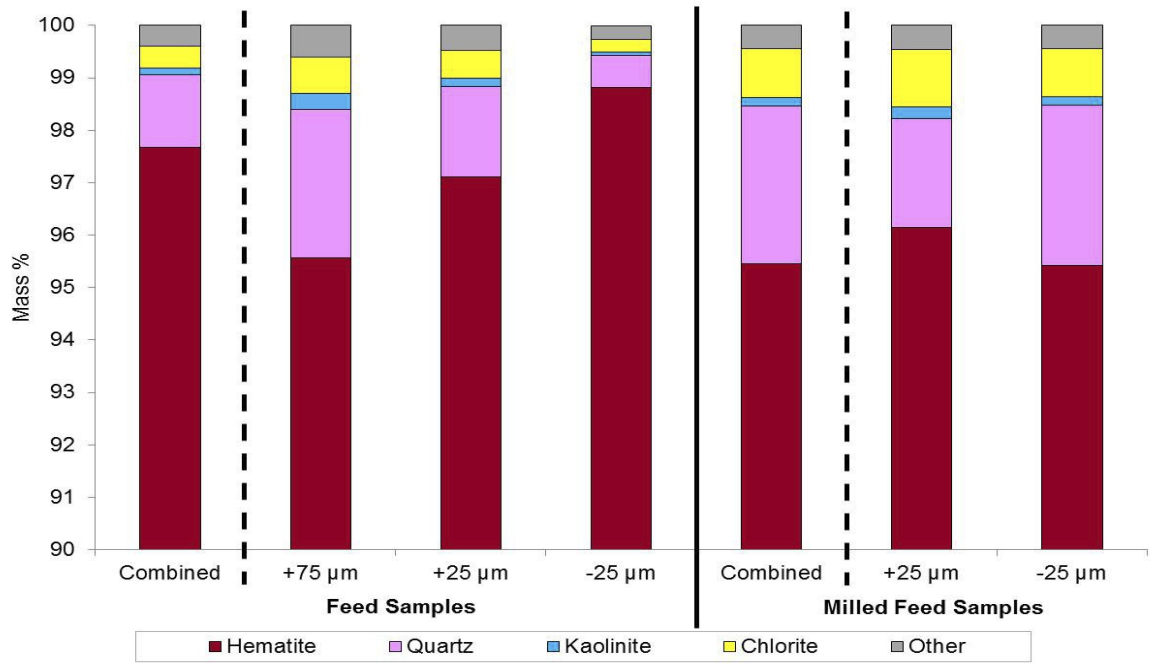


**Figure 50: Mass % contribution as a function of sized sample for various minerals**

When considering the data from the MLA, the liberation is calculated in terms of the area percentage of the mineral of interest present in a particle. For example, if a particle is determined to be 20% to 40% liberated, the specific particle will have less than 40% and more than 20% area percentage of the mineral of interest.

Note that the size given refers to the instrument-measured sectional area of a grain (not screen size) and is calculated based on the equivalent circle diameter (ECD).

Figure 51 illustrates the liberation of hematite of the combined as received feed material, which indicate that 94% of the total material, i.e. of the full size range, is well liberated.

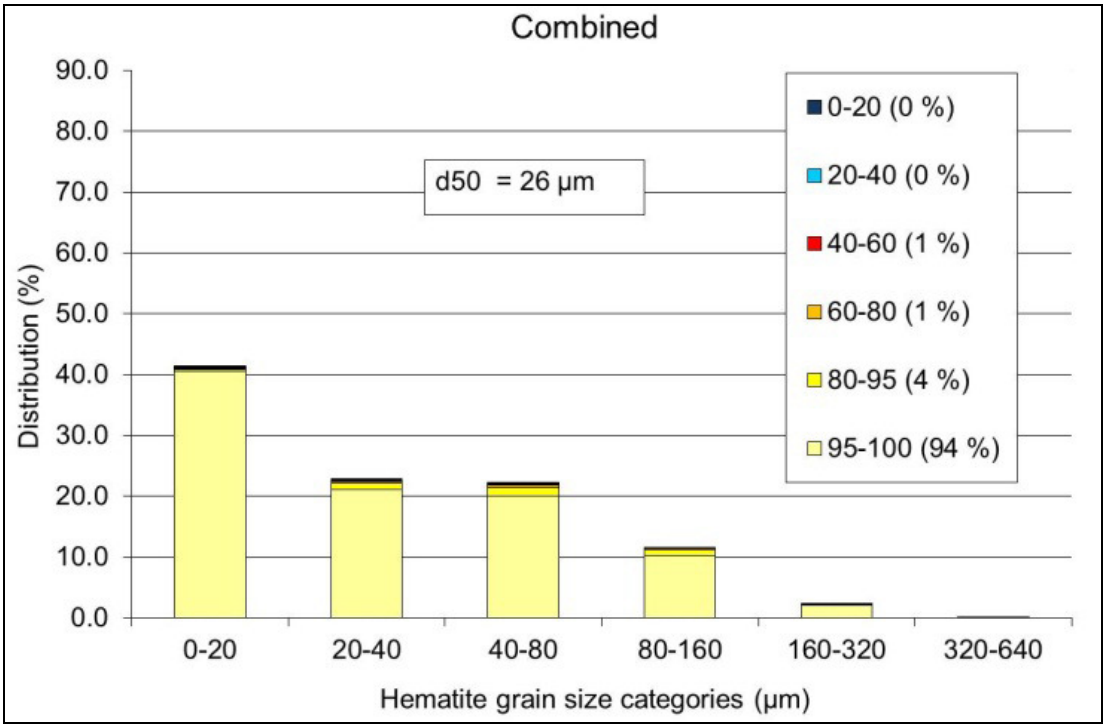


**Figure 51: Liberation of hematite within the distribution as a function of grain size (micron) for the combined feed material (feed material)**

However, if one considers the +75 micron material (Figure 52), only 87% of the hematite is well liberated. These results are compared with both the +25 micron analysis (92% well liberated - Figure 53) and the -25 micron analysis

(98% well liberated - Figure 54). Therefore it is evident that the unliberated hematite is in the coarser size fraction.

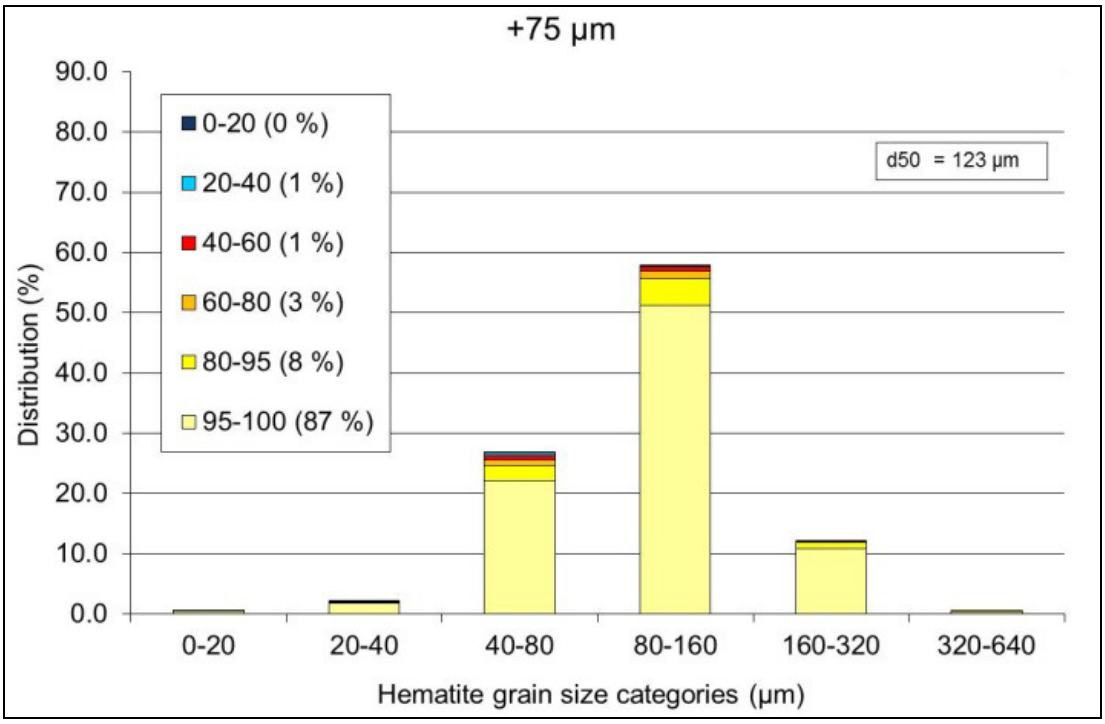


**Figure 52: Liberation of hematite within the distribution as a function of grain size (micron) for the +75 material (feed material)**

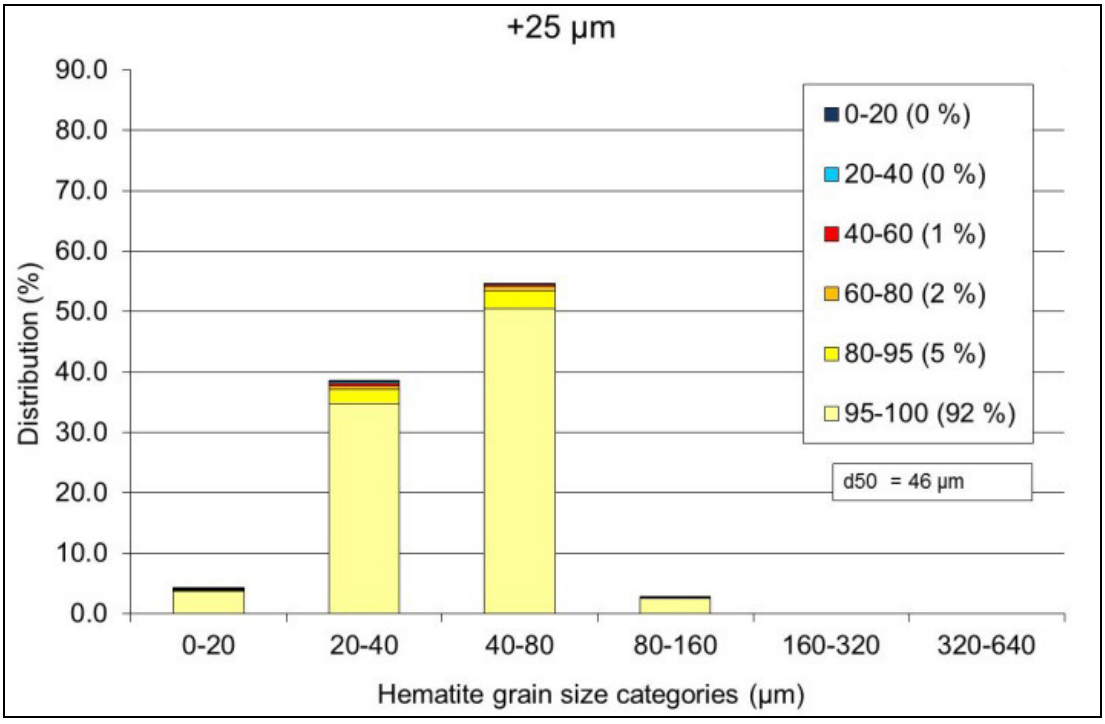


**Figure 53: Liberation of hematite within the distribution as a function of grain size (micron) for the +25 material (feed material)**

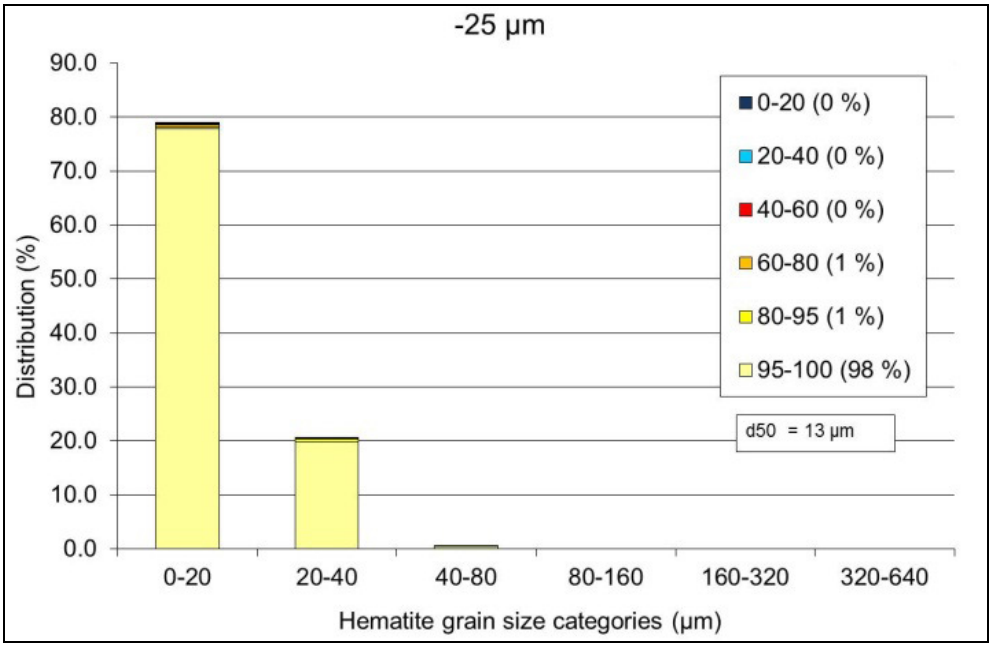


**Figure 54: Liberation of hematite within the distribution as a function of grain size (micron) for the -25 material (feed material)**

Figure 55 illustrates the liberated hematite after milling the +38 micron material. In this case, the well liberated hematite is 93%, which is a significant difference in liberation relative to the approximate 87% of the coarse fraction from Figure 51.

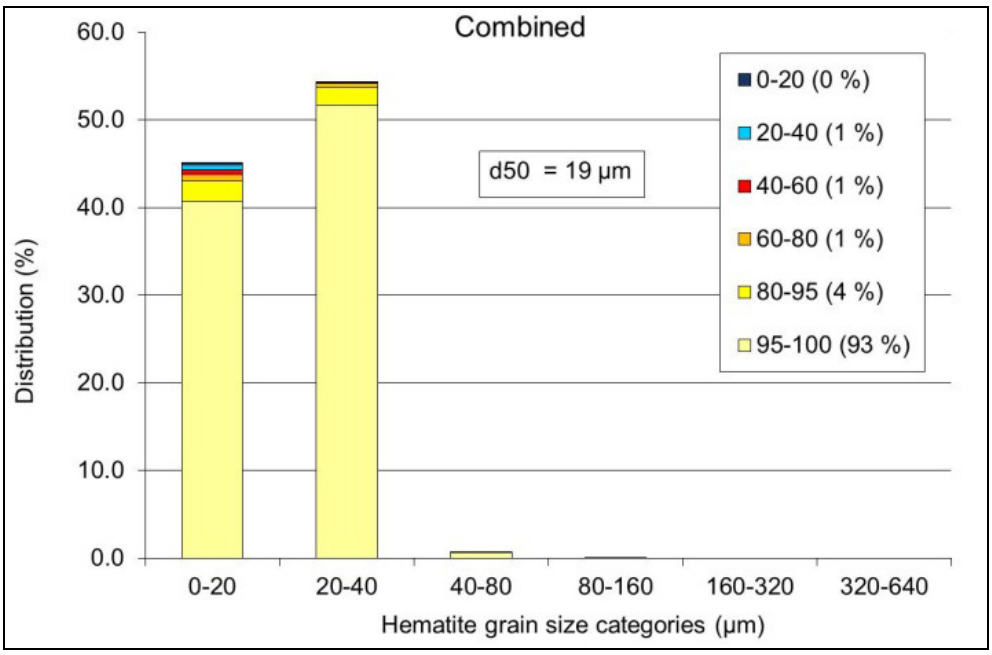


**Figure 55: Liberation of hematite within the distribution as a function of grain size (micron) for the combined feed material (milled material)**

In the same manner as for the liberation of hematite, the gangue minerals were also considered. Figure 56 illustrates the liberation for various grain size categories and shows that 26% of the material is well liberated, when considering the combined raw flotation feed material.

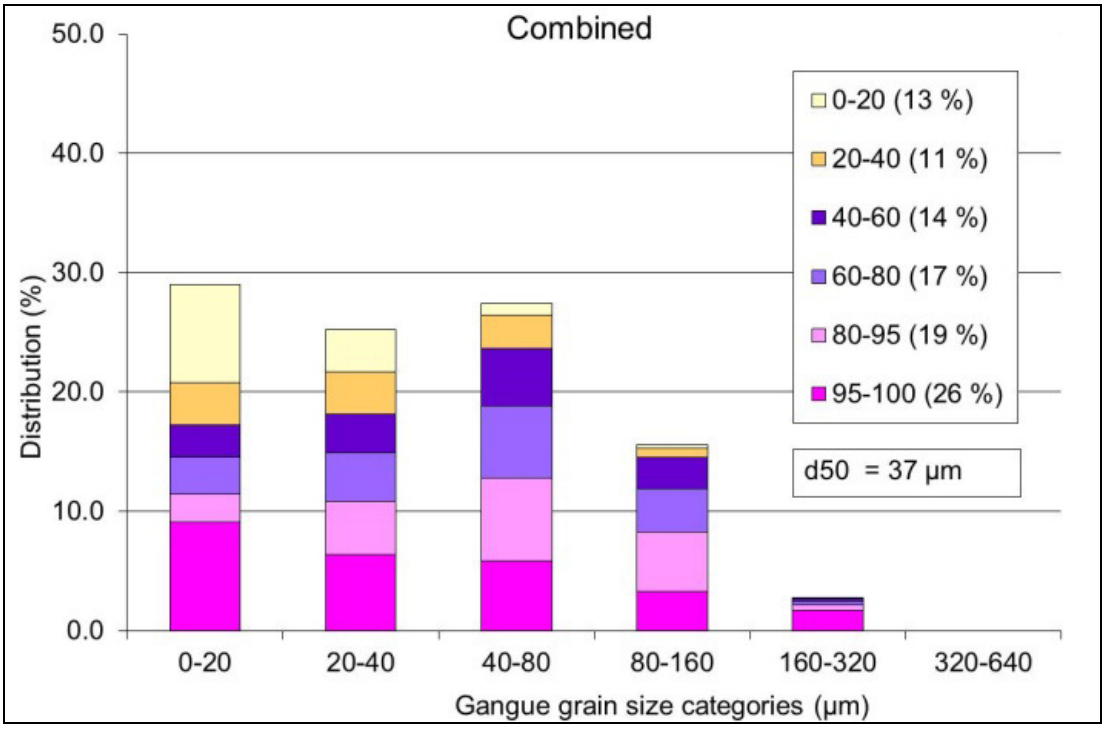


**Figure 56: Liberation of gangue material within the distribution as a function of grain size (micron) for the combined feed material (feed material)**

Figure 57 and Figure 58 show the liberation of the gangue minerals as a percentage for a specific degree, i.e. the fully liberated contribution for the +75 micron material, and was determined to be 18%, whereas for the +25 micron material it was determined to be 22%.

The liberation analysis of the +38 micron material that was subjected to milling shows an increase in liberation of the gangue mineral to a total of 45& to 55%, as given in Figure 59 and Figure 60.

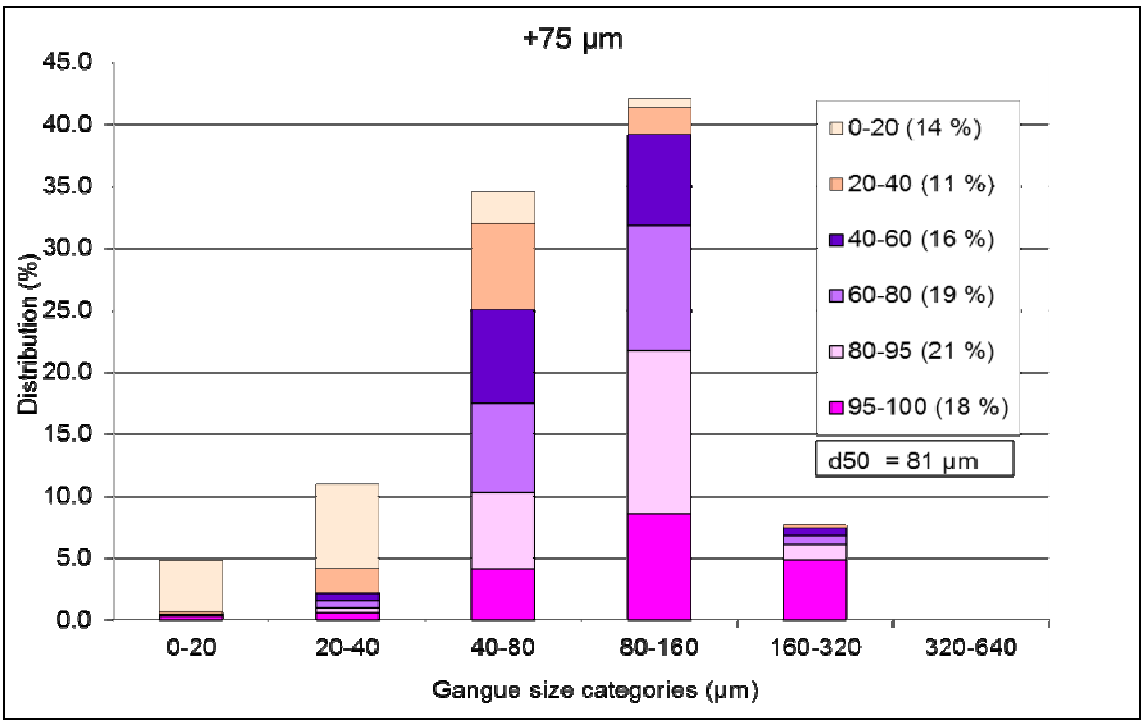


**Figure 57: Liberation of gangue material within the distribution as a function of grain size (micron) for the +75 micron material (feed material)**

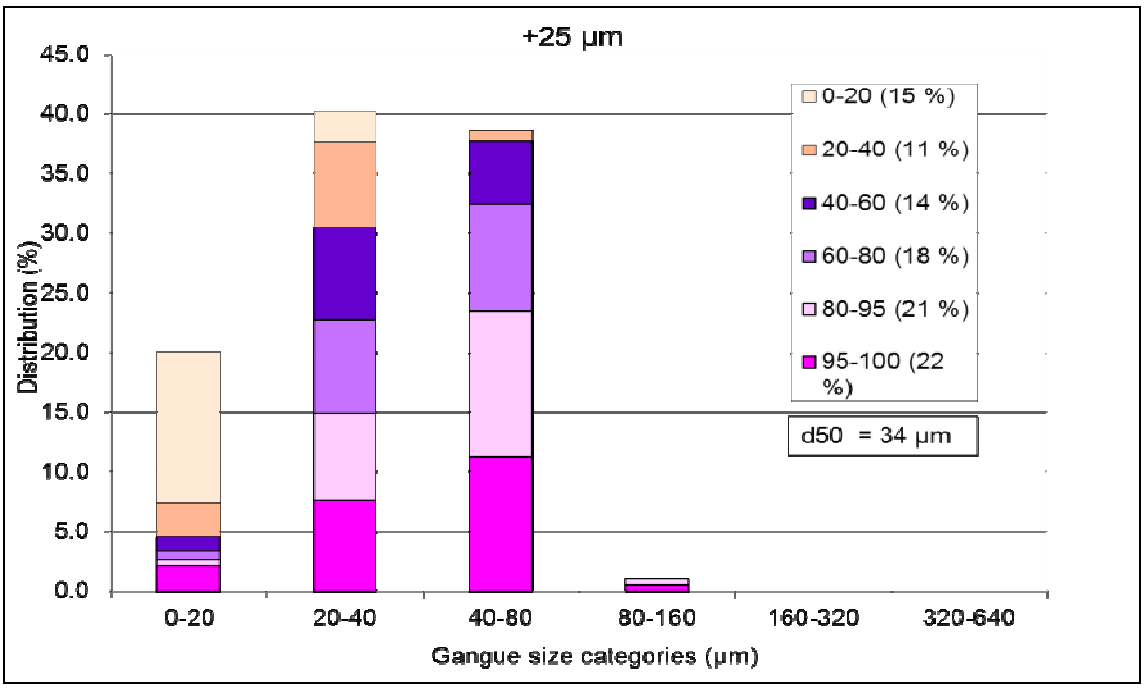


Figure 58: Liberation of gangue material with the distribution as a function of grain size (micron) for the +25 micron material (feed material)

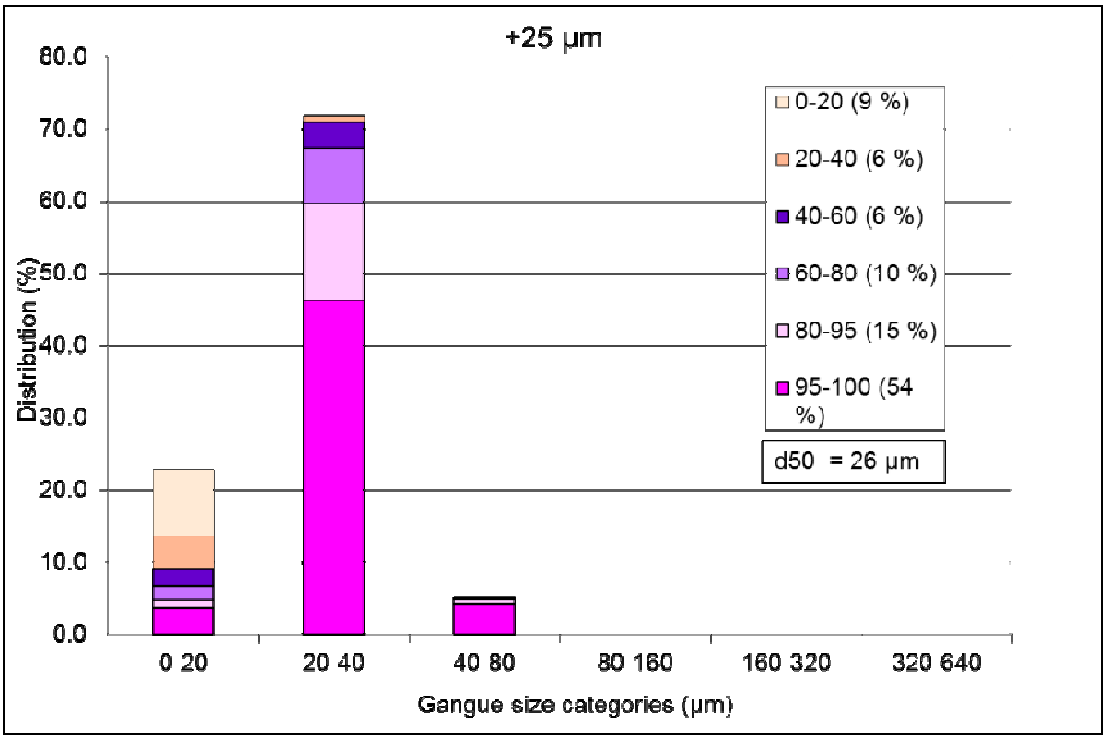


Figure 59: Liberation of gangue material with the distribution as a function of grain size (micron) for the +25 micron material (milled material)

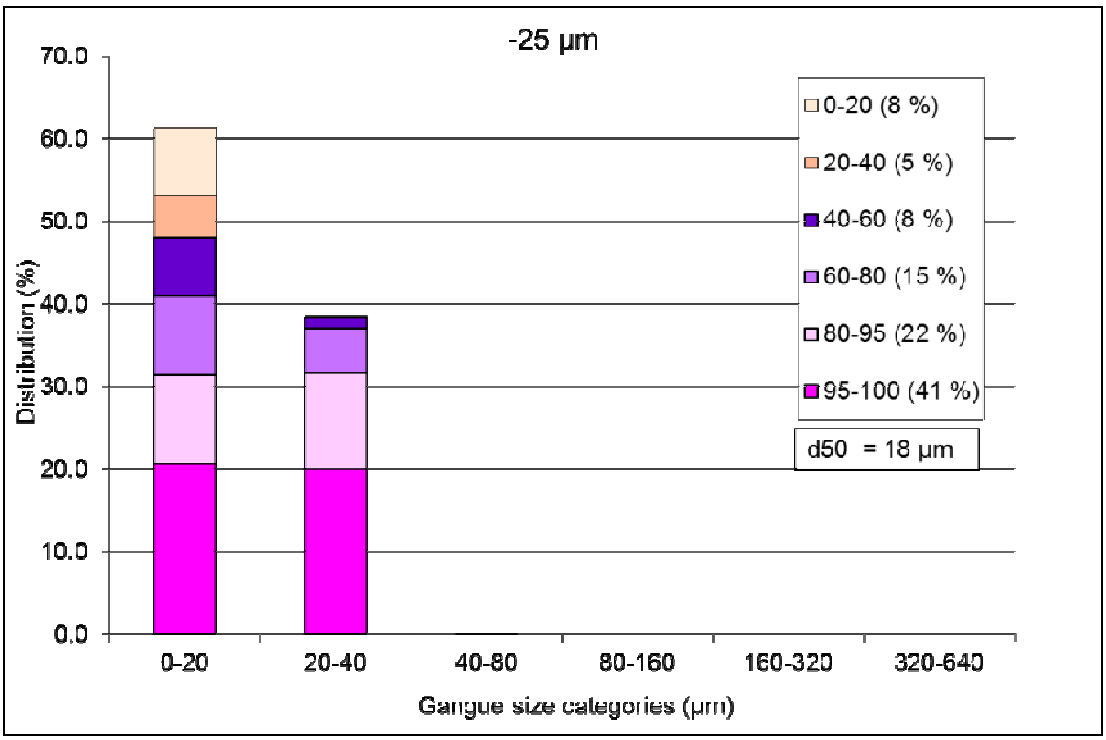


**Figure 60: Liberation of gangue material with the distribution as a function of grain size (micron) for the - 25 micron material (milled material)**

To illustrate the shift in liberation, the cumulative mass percentage of hematite as a function of the liberation class or degree of liberation is graphed. Figure 61 represents the data for the raw flotation feed material, whereas Figure 62 gives the data for the milled (+38 micron) material. In this case, an estimated curve between the +25 micron and +75 micron material for the raw flotation feed material is compared to the combined curve of the milled flotation feed curve, as shown in Figure 62. A shift to the top right hand side of the curve can be seen in Figure 61 and Figure 62, indicating an increase in hematite liberation.

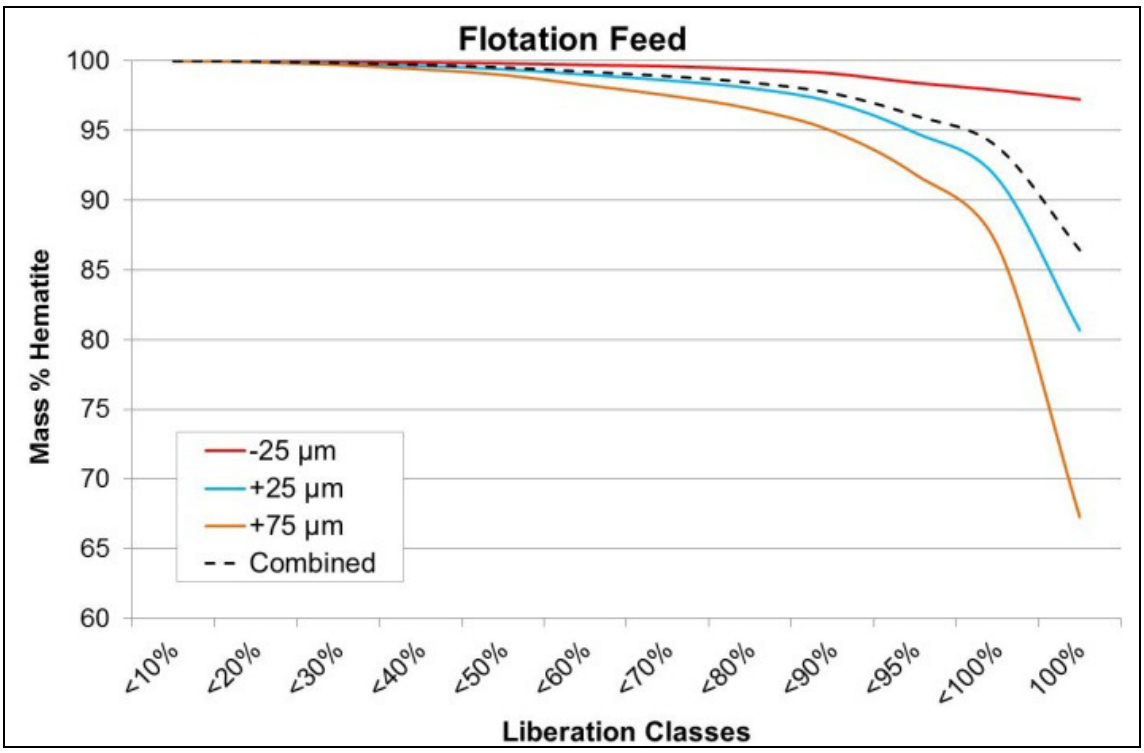


**Figure 61: Cumulative hematite liberation represented as mass % hematite as a function of the liberation class for the raw flotation feed material**

The same procedure is followed for the gangue mineral and is given in Figure 63 and Figure 64. Once again the a shift of the curve to the top right hand side can be seen in Figure 63 and Figure 64, also indicating that an increase in liberation was realised.

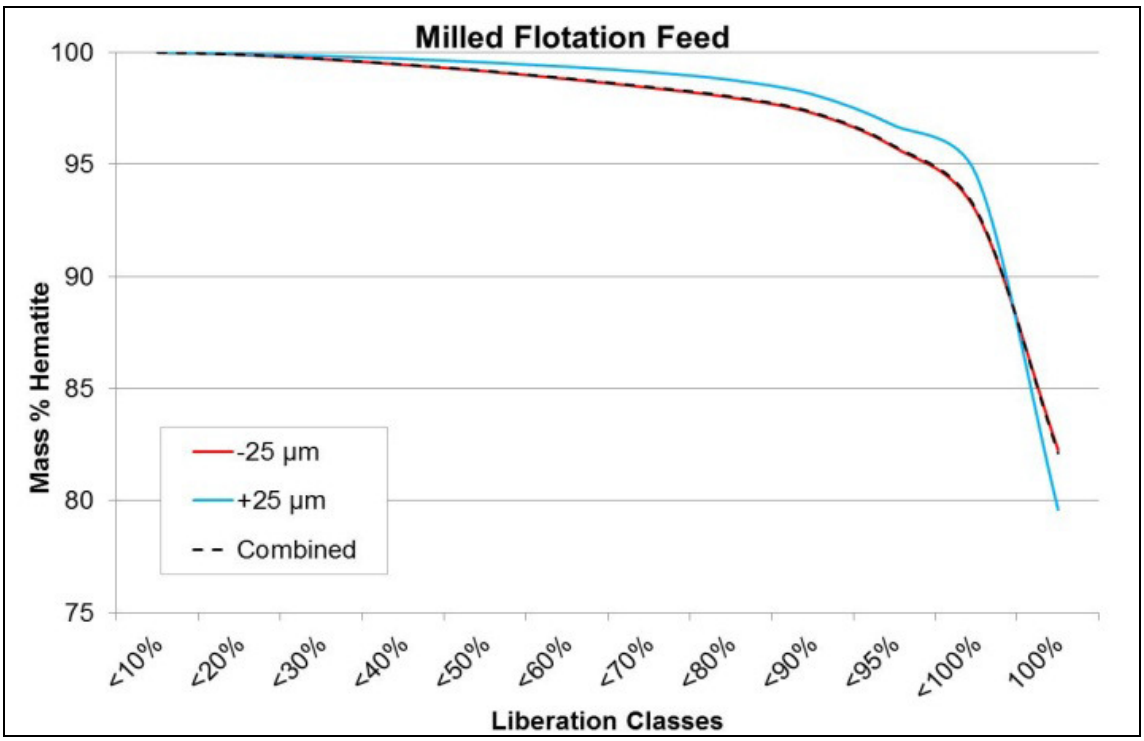


Figure 62: Cumulative hematite liberation represented as mass % hematite as a function of the liberation class for the milled flotation feed material

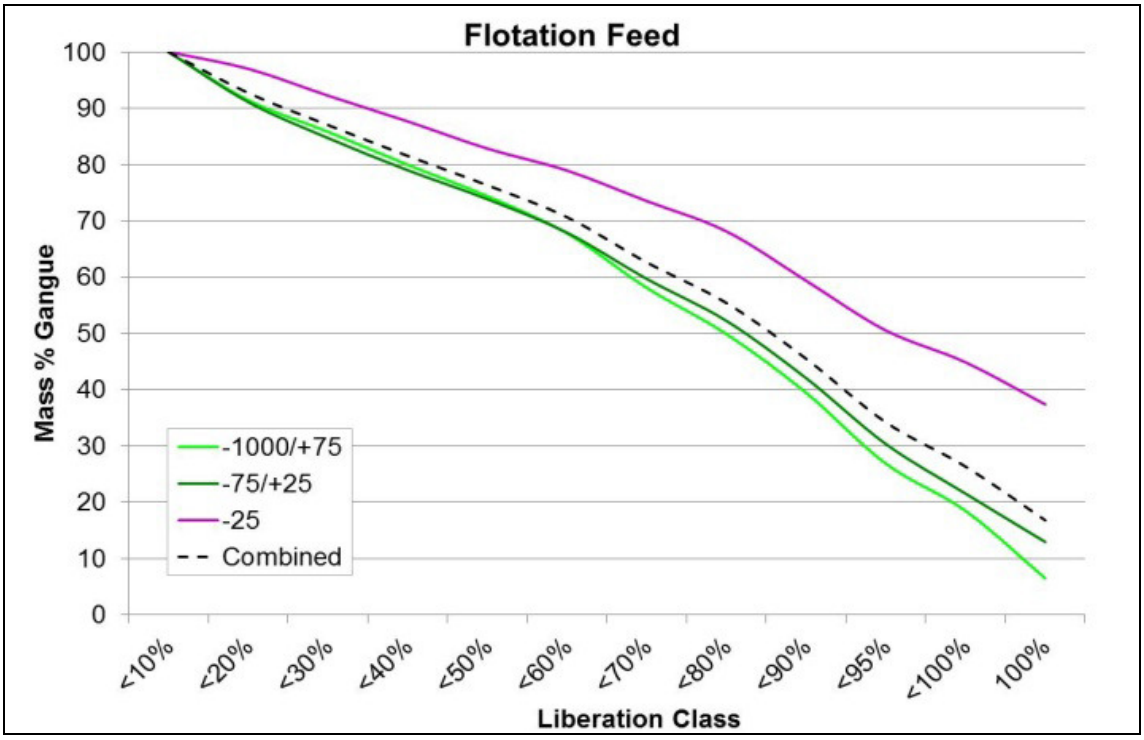


Figure 63: Cumulative gangue liberation represented as mass % gangue as a function of the liberation class for the raw flotation feed material

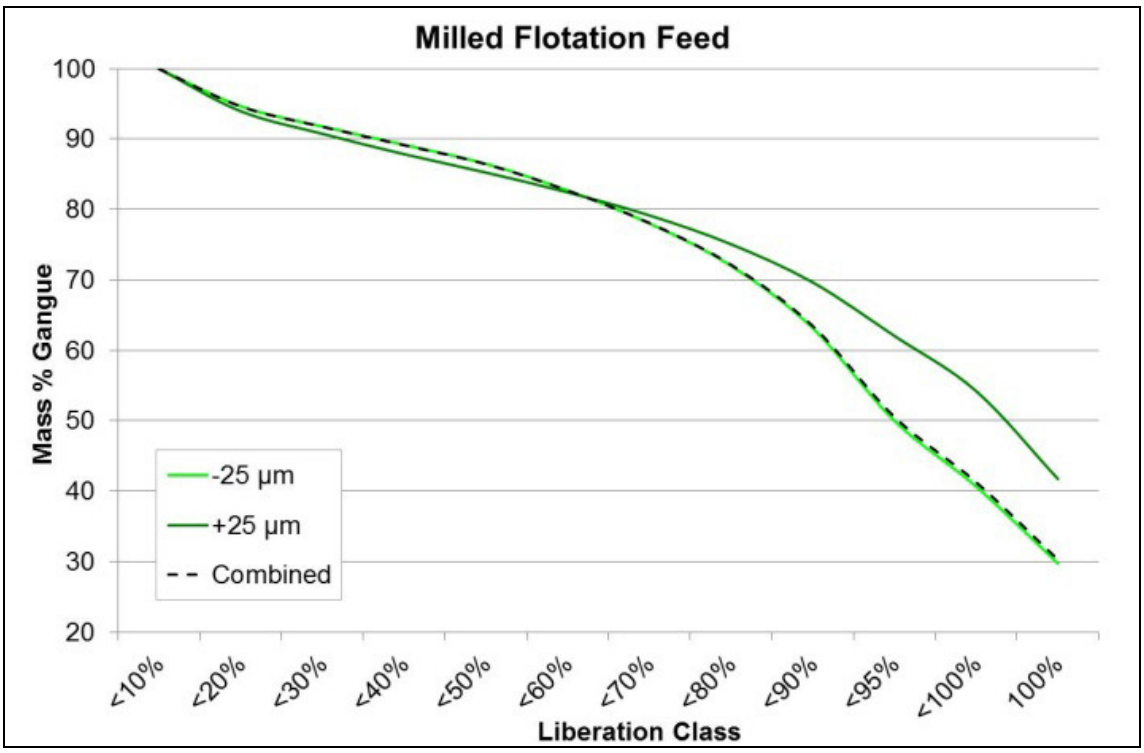


Figure 64: Cumulative gangue liberation represented as mass % gangue as a function of the liberation class for the milled flotation feed material

In summary, the flotation feed sample was coarser than the milled flotation feed material, as can be expected, with an average hematite grain size of 26 micron. The hematite in the milled flotation sample had an average grain size of approximately 19 micron. In the case of the gangue material, the average grain size was determined to be 37 and 8 micron for the flotation feed sample and the milled flotation feed sample, respectively.

Additionally, the milled flotation feed material showed 41% of the gangue material liberated and reporting to the 95% to 100% liberated category. In the case of the flotation feed sample, only 26% of the gangue reported to the 95% to 100% liberated category, with most of the gangue associated with hematite.

During initial testwork, prior to milling, there was no upgrading achieved and the product material had the same composition as that of the feed material. This is known as the “T-piece” effect, caused by the lack of liberation of the feed material.

### 4.2.3 Sample characterisation revised conclusion

It is evident from the liberation analysis that there is a definite increase in liberation of the gangue material when the +25 micron material from the feed is milled. This will also explain the increase in selectivity when introducing milling to the circuit. Additionally, the mineral surface is also cleaned with the introduction of milling, effectively increasing the chemisorption efficiency of the collector and depressant within the system.

Liberation analysis, flotation test results and the relative shift in PSD to the flotation feed material (+38 micron material screened from the raw feed material) suggested that a 25 minute grind is sufficient for liberation of the +25 micron material to achieve the required grade without overgrinding the material. This is shown in section 4.2.4.

### 4.2.4 Flotation testwork - revisited

After it was determined that there could be a liberation challenge with the feed material, it was determined that additional flotation tests were to be conducted on a control sample, a milled sample which is milled for five minutes and a milled sample which is milled for 15 minutes. The results are given in Figure 65 to Figure 69 (the raw data is given in Appendix G). Results show that a T-piece scenario was once more experienced in the case of the feed material. However, with the milled material there was a clear indication of upgrading to 67% Fe in the concentrate. The challenge at that point was the low mass yield to product at the required concentrate grade. Figure 65 shows the final concentrate Fe concentration (%) as well as the $SiO_2$ as a function of the milling time applied to the screened feed material. The increase in final concentrate Fe content can be seen with an increase in milling time. This relates to the liberation of both hematite and quartz within the feed material.

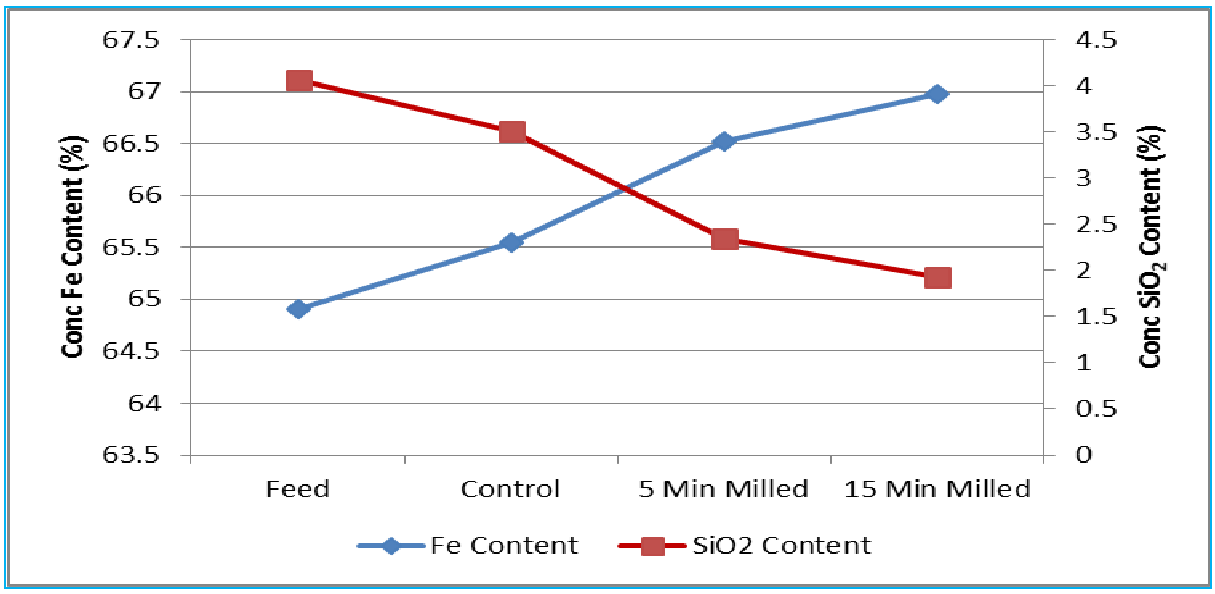


**Figure 65: Final Fe and SiO2 content of flotation concentrate for the different streams vs that of the feed**

Figure 66 shows the cumulative Fe and $SiO_2$ content (in the concentrate) as a function of time for the feed material milled for a total of five minutes.

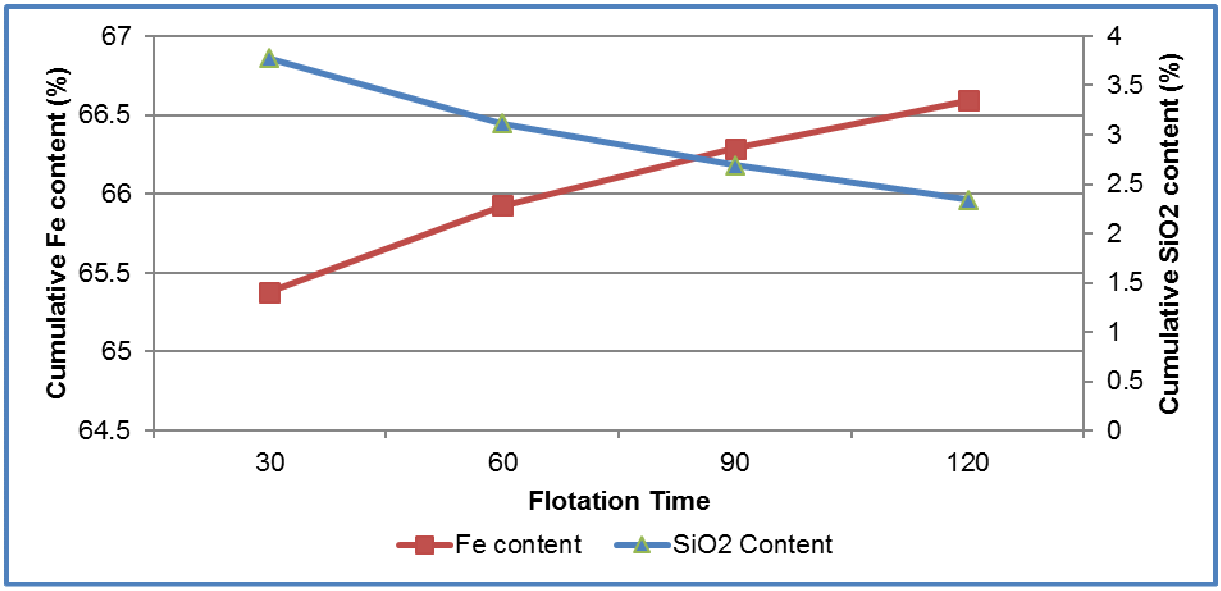


**Figure 66: Fe and SiO2 content as a function of time – sample milled for five minutes**

The cumulative Fe content in the concentrate and cumulative mass yield to the discard (froth phase) are given in Figure 67 as a function of time. Results indicate that a total mass yield to product of 60% with a Fe content of 66,5% can be achieved when the feed material is milled for five minutes.

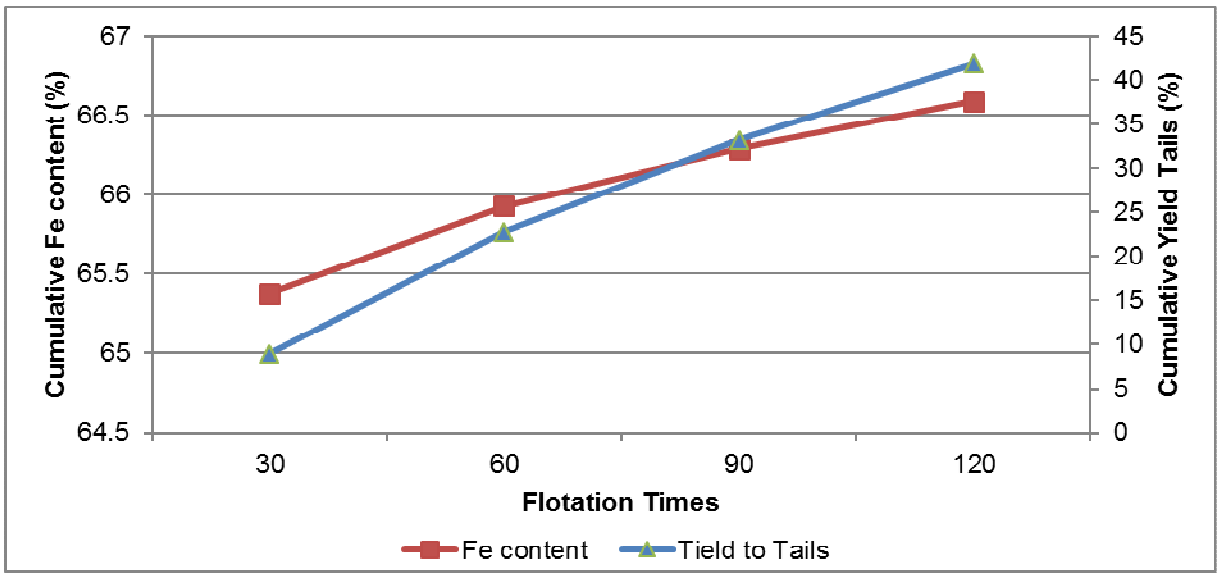


Figure 67: Fe content and yield to concentrate as a function of time - sample milled for five minutes

Figure 68 shows the results as the cumulative Fe and $SiO_2$ as a function of time, when milling the feed material for a total of 15 minutes. With the increased milling time, leading to better liberation, a final concentrate with a Fe content of 67% can be achieved at a mass yield to product of 50% (Figure 69).

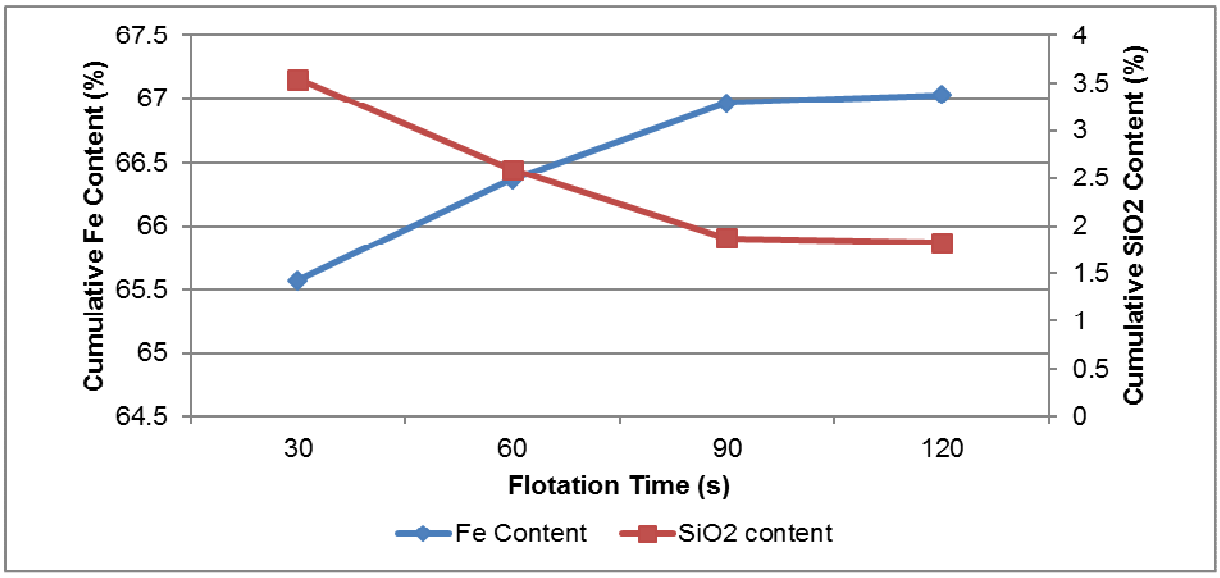


Figure 68: Fe and SiO2 content as a function of time - sample milled for 15 minutes

The cumulative yield to discard and concentrate Fe content as a function of time is given in Figure 69.

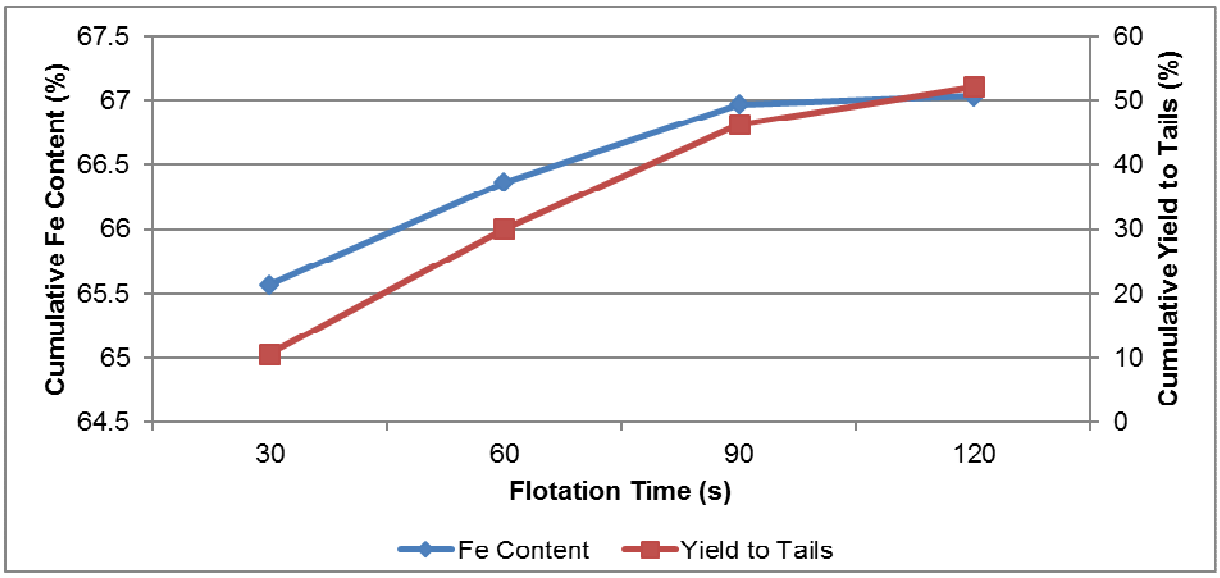


**Figure 69: Fe content and yield to concentrate as a function of time - sample milled for 15 minutes**

Figure 65 to Figure 69 suggest that there is a correlation between milling time and final concentrate grade, as well as recovery to tailings. This can be expected, as the more additional fines are produced during milling, the more stable the froth phase becomes and the yield thus increases. Additionally, as the grinding time increases, the final concentrate grade improves, which can be related to a better degree of liberation achieved with an increase in milling time. The milled materials' PSD as determined with the Malvern particle sizer is given in Figure 70.

From the PSDs of the various samples, the size distribution is moved to the left (shifting more with a longer grinding time), indicating that the material is reduced in size. By grinding the material, locked and hematite associated with gangue is liberated and can therefore selectively be floated.

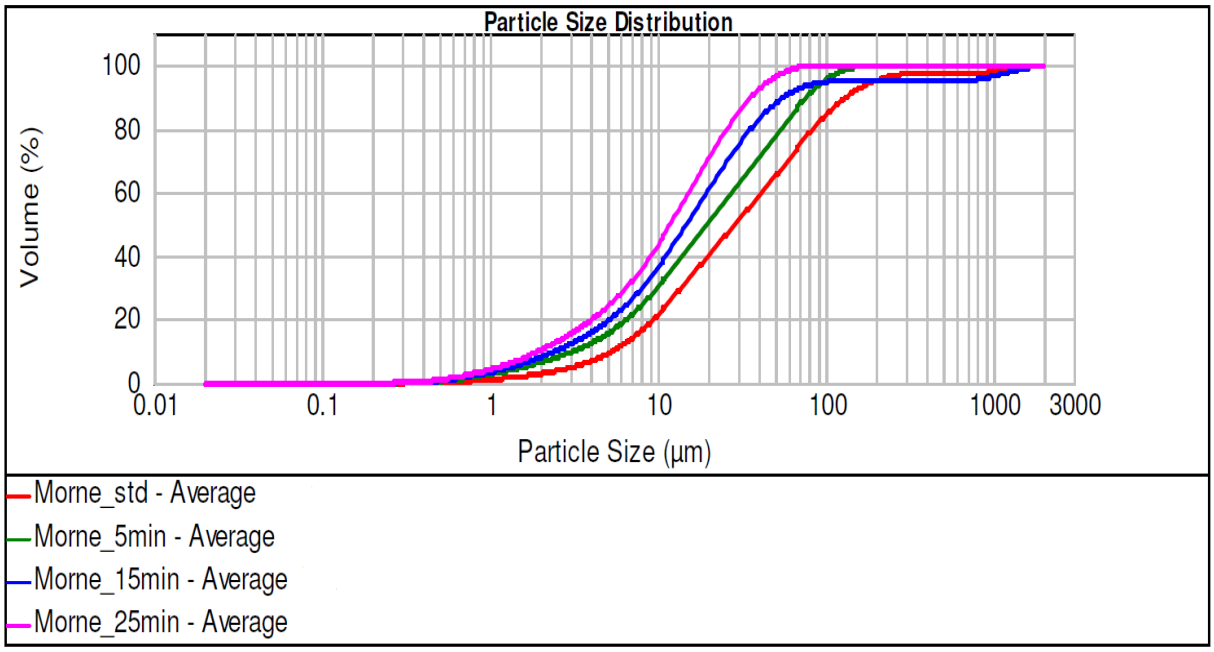


Figure 70: Particle size distributions for various milling times

After achieving good results with the milling of material, a 25min grind was used to investigate the influence of various dosages of starch, as well as amines. The tests were conducted by milling the screened feed material for 25 minutes to ensure sufficient milling time, after which the starch dosage and amine dosage were varied. Note that all tests were conducted at a pH of 9,5 and the starch dosage set at 400 g/t. The cumulative yield to concentrate and cumulative Fe content of the concentrate as a function of amine dosage is given in Figure 71.

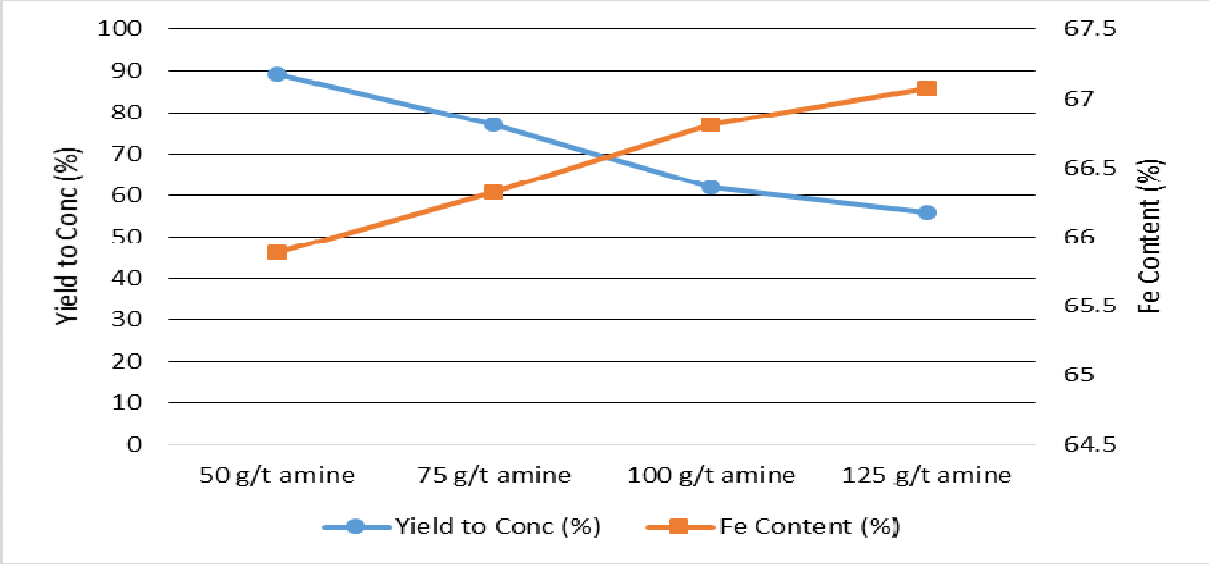


Figure 71: Yield to concentrate and Fe content of concentrate as a function of reagent dosage

Figure 72 shows the $SiO_2$ content as a function of amine dosage.

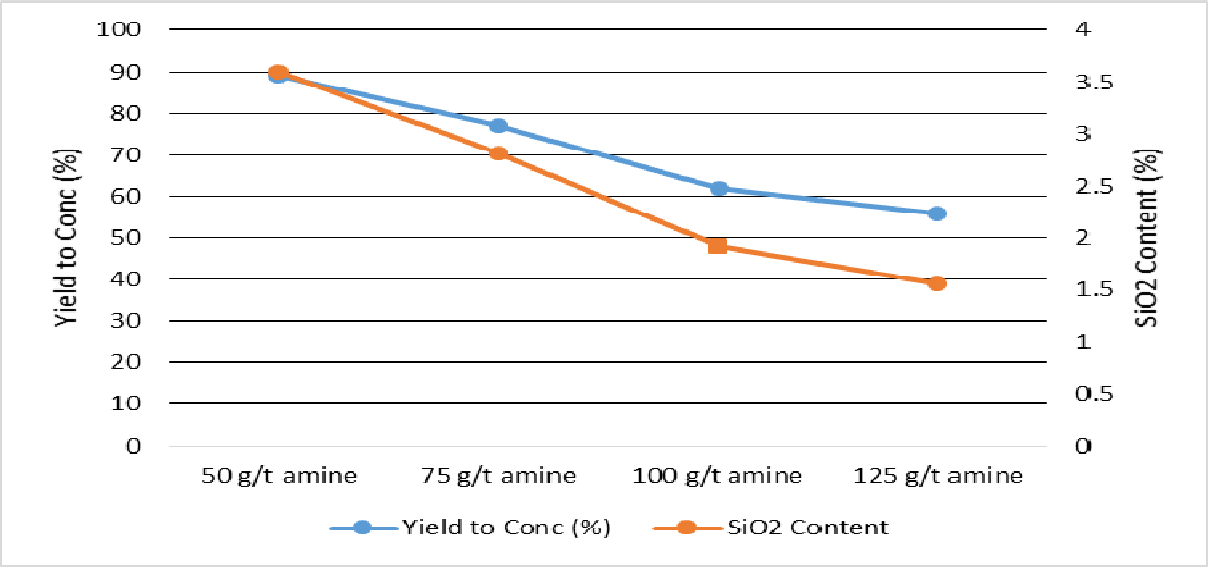


**Figure 72: Yield to concentrate and SiO2 content in concentrate as a function of amine dosage**

When considering an increase in amine dosage with a constant starch dosage, results indicate that a steady increase in concentrate quality in terms of Fe content was achieved, while a steady decline in $SiO_2$ content was realised. This is to be expected due to higher amine (collector) dosage, as well as the fact that higher yield to the tailings will increase the product quality, due to the selective flotation of quartz. However, a very high yield to tailings was required due to the fact that the tailings contained only 8% to 10% $SiO_2$. Therefore, the process is not extremely selective and could typically be attributed to the fine nature of the material, i.e. 80% passing approximately 50 micron (entrainment). That being said, the final target product grade was achieved. Please note that 60% of the feed material was screened and was said to be already on specification. Therefore the total yield to product will be between 75% and 85%.

Figure 73 and Figure 74 show a parabola being generated with the increase in starch dosage. The results show an optimum starch dosage to achieve

selective flocculation of the hematite material, and therefore achieve the required product grade. This can be referenced to the testwork conducted by Rodrigues *et al*. (2013), who suggested that the starch could possibly, in the event of "overdosing", react either as a dispersant – which will reduce the selectivity of the system – or reduce the selectivity of flocculation, meaning quartz can also be depressed. The fact that the yield to concentrate steadily increases would suggest the latter of the two suggestions.

This, however, is not part of the scope of this specific study and would require in-depth additional testwork to be conducted.

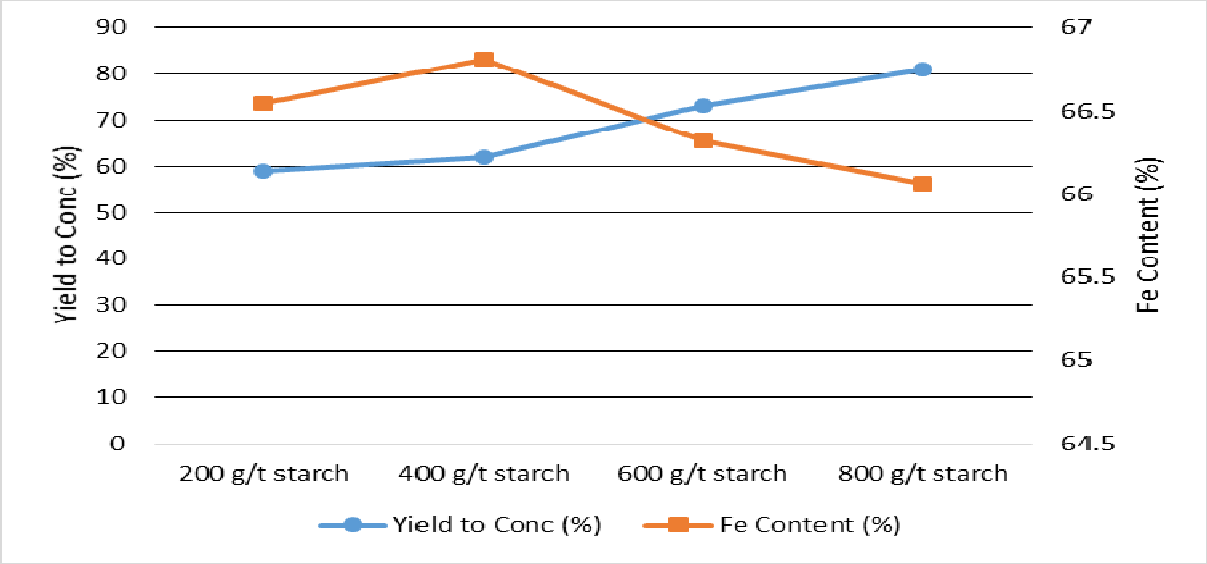


**Figure 73: Yield to concentrate and Fe content in concentrate as a function of starch dosage**

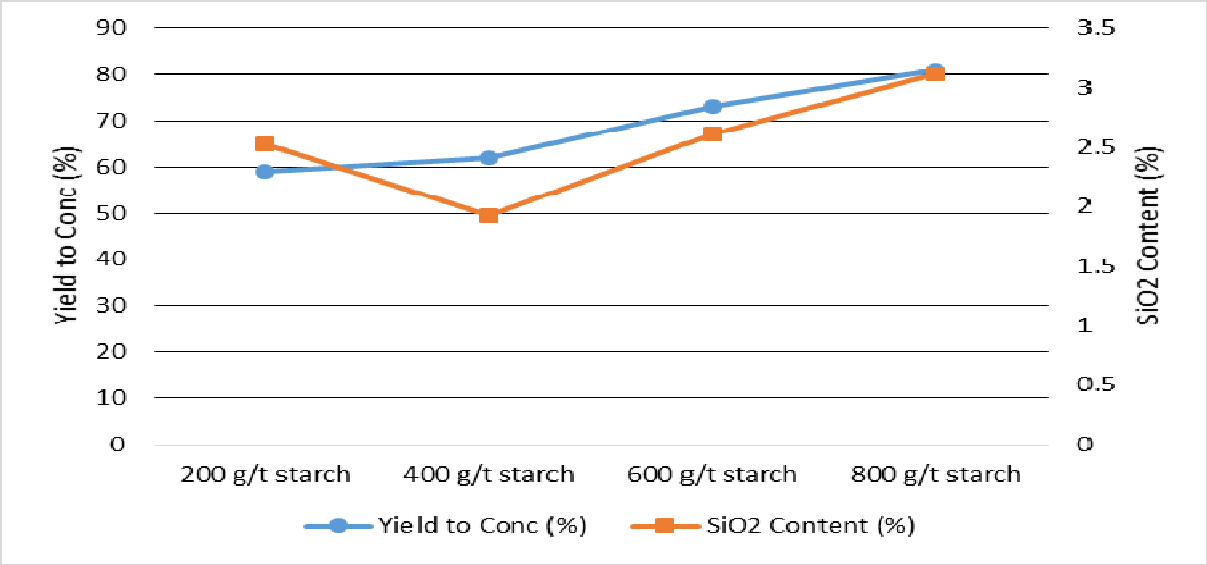


**Figure 74: Yield to concentrate and SiO2 content in concentrate as a function of starch dosage**

Figure 74 shows the cumulative $SiO_2$ content in the concentrate as a function of starch dosage.

Finally, a specific set of flotation tests were repeated in order to illustrate repeatability of the test results. Therefore, the test conducted at 100 g/t amine and 400 g/t starch was repeated three times. The yield to concentrate and Fe content in the concentrate are given in Figure 75.

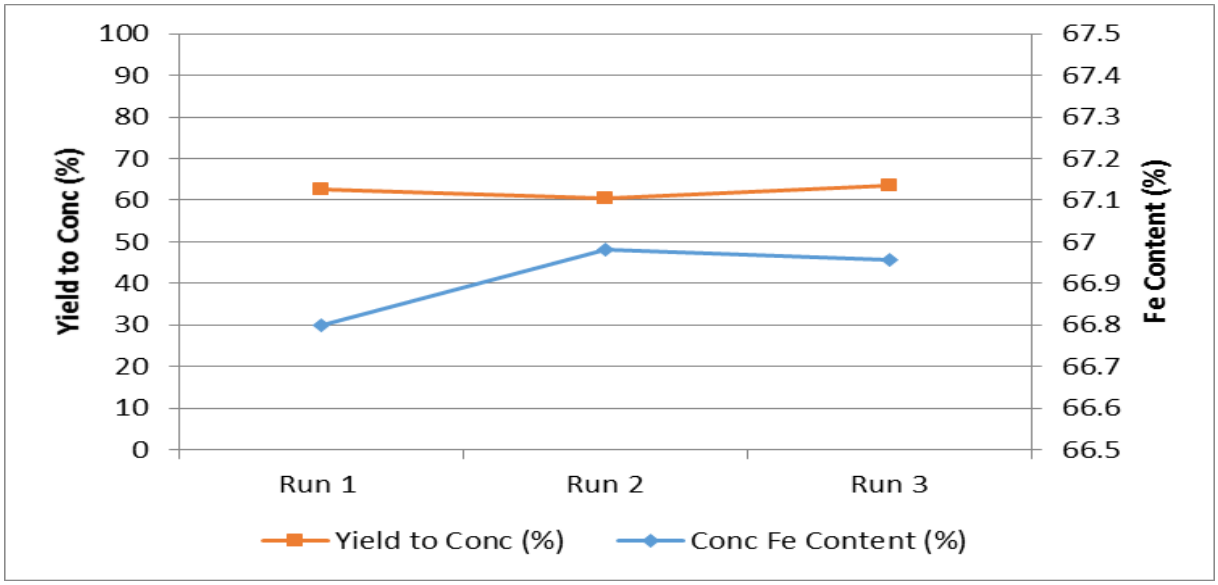


Figure 75: Yield and Fe content for three repeated tests

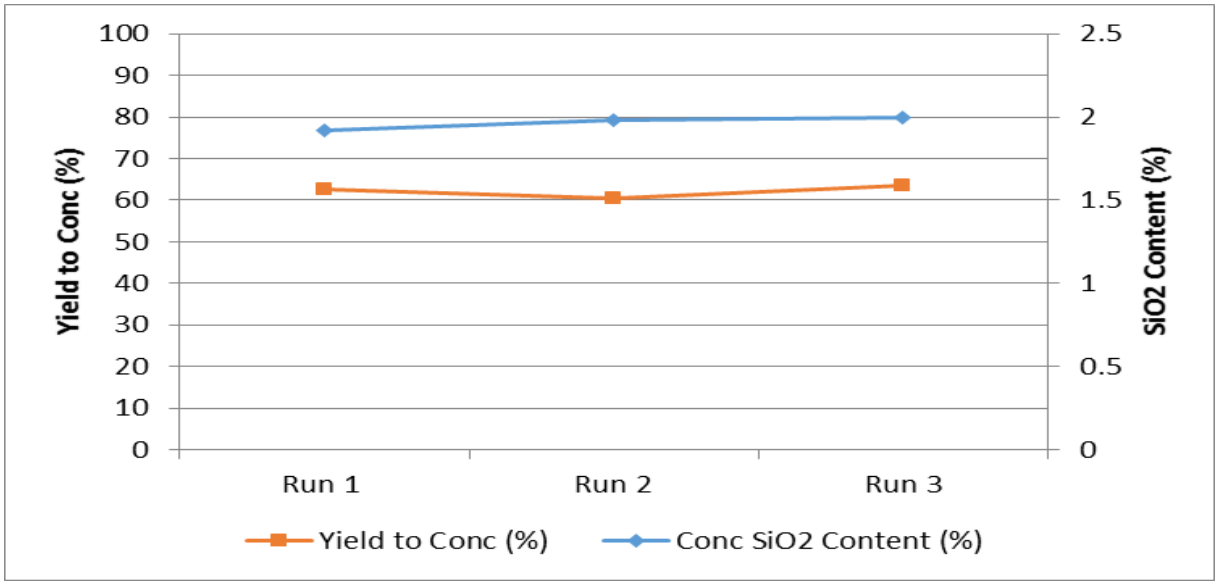


Figure 76: Yield and SiO2 content for three repeated tests

Figure 76 also indicates good repeatability with regards to the $SiO_2$ content in the concentrate.

Repeatability testwork showed a variance between 66,7 and 67,0% Fe in the concentrate and a yield between 60% and 63% to the concentrate. The quartz also showed good repeatability with a variance between 1,8% and 2% $SiO_2$ in the concentrate. In terms of laboratory flotation tests, this is acceptable for repeatability and thus indicate that the required concentrate grade off 66,5% Fe is achievable.

# Chapter 5: Proposed Solution

With the support of the test program and the results achieved, a process flow diagram (PFD) was constructed together with a complete mass balance to determine the possibilities in terms of final yield to product, as well as Fe recovery to concentrate.

The PFD is given in Figure 77. In this case, the feed material is first de-slimed (removal of ultra-fine material) at between 25 and 35 micron by making use of a hydro cyclone system. The overflow of these cyclones is already at product specification and therefore reports directly to the final concentrate. The total yield to product in this case is approximately 60% of the bulk feed with a 100% Fe recovery within this portion.

One of the important aspects to consider in this case is that this reduces the capacity required for milling as well as flotation with 60%, which is a large cost saving in terms of operational expenditure and capital expenditure. Additionally, the footprint of the specific plant is also drastically decreased. However, the cost of the de-sliming cyclones and the operational expenditure thereof need to be considered, as well as the efficiency and operability of this section.

After de-sliming, the underflow (+25, +35 micron) material is subjected to milling to liberate the hematite and quartz, as indicated by the mineral liberation study. The milled material is then conditioned with the reagents, starch and amine, prior to entering the flotation system. The quartz is then floated to the froth phase, while the upgraded hematite is removed from the slurry discharge of the cell and mixed with the final concentrate material. The final concentrate must then be filtered for dewatering.

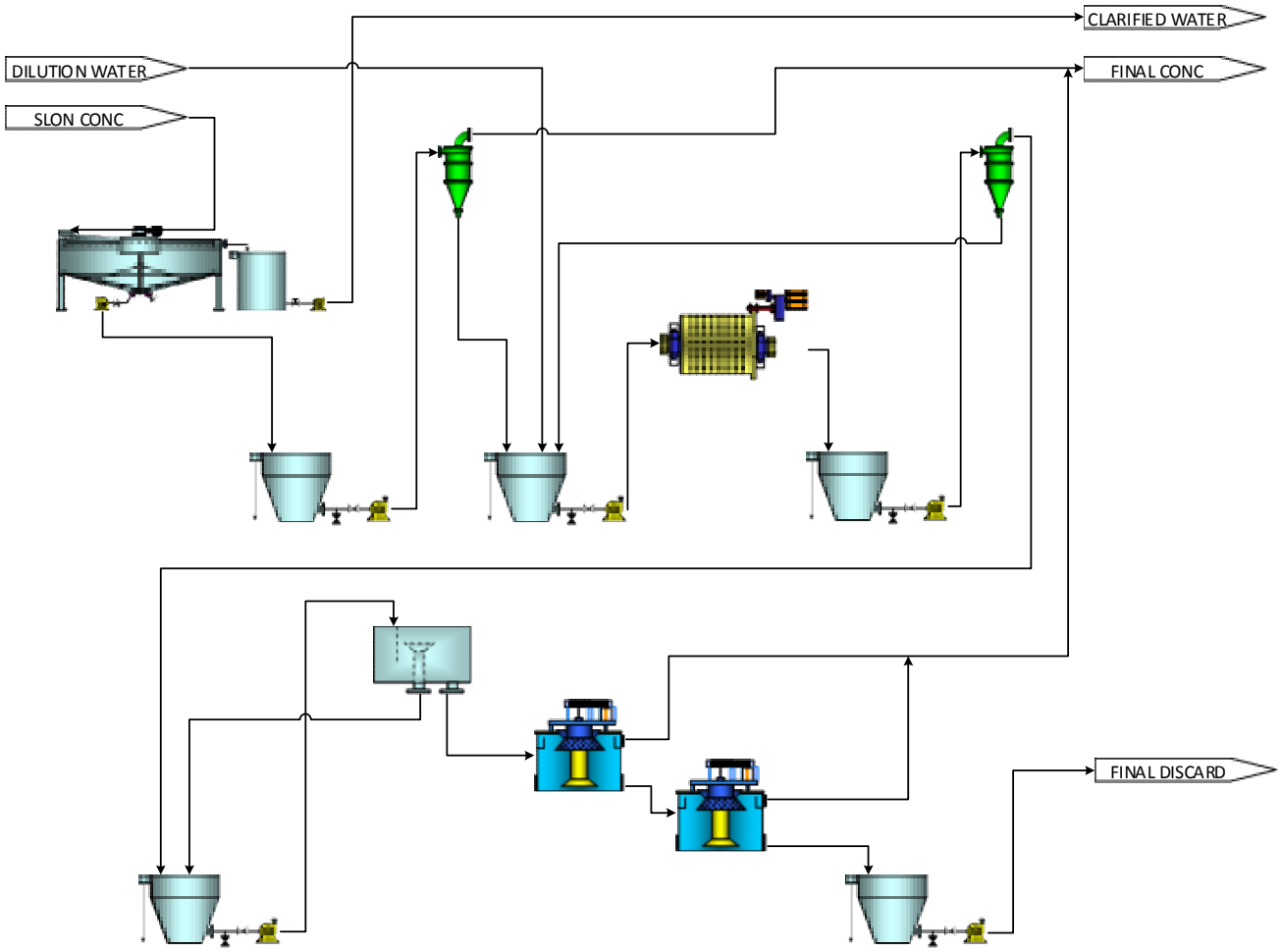


Figure 77: Proposed process flow diagram

From the mass balance conducted on this system and the results achieved in testwork, a gross mass yield to product of 75% to 80% can be realised with a Fe recovery of 80% to 90%. The mass balance is given in Table 12.

Table 12: Mass balance as per process flow diagram (Figure 77)

| | Thickener U/F | Dilution Water | Cyclone 1 Feed | Cyclone O/F | Cyclone U/F | Cyclone 2 Recirc | Mill Feed | Mill Product | Cyclone 2 Feed | Cyclone 2 O/F | Cyclone 2 U/F | Float Feed | Float Product | Float Tails | Final Product |
|---|---|---|---|---|---|---|---|---|---|---|---|---|---|---|---|
| Total T (tph) | 100.00 | 0.00 | 100.00 | 58.90 | 41.10 | 4.70 | 45.80 | 45.80 | 45.80 | 41.10 | 4.70 | 41.10 | 20.96 | 20.14 | 79.86 |
| Fe T (tph) | 65.77 | 0.00 | 65.77 | 39.07 | 26.70 | 3.05 | 29.75 | 29.75 | 29.75 | 26.70 | 3.05 | 26.70 | 14.04 | 12.66 | 53.11 |
| SiO2 (tph) | 3.77 | 0.00 | 3.77 | 1.35 | 2.42 | 0.28 | 2.70 | 2.70 | 2.70 | 2.42 | 0.28 | 2.42 | 0.42 | 2.00 | 1.77 |
| Water (m3/h) | 59.07 | 73.84 | 132.91 | 108.63 | 24.28 | 2.77 | 27.05 | 27.05 | 27.05 | 24.28 | 2.77 | 24.28 | 12.38 | 11.90 | 121.01 |
| M (m3/h) | 84.39 | 73.84 | 158.23 | 123.54 | 34.68 | 3.96 | 38.65 | 38.65 | 38.65 | 34.68 | 3.96 | 34.68 | 17.69 | 17.00 | 141.23 |
| RD (m3/h) | 1.89 | 1.00 | 1.47 | 1.36 | 1.89 | 1.89 | 1.89 | 1.89 | 1.89 | 1.89 | 1.89 | 1.89 | 1.89 | 1.89 | 1.42 |
| SG (t/m3) | 3.95 | 3.95 | 3.95 | 3.95 | 3.95 | 3.95 | 3.95 | 3.95 | 3.95 | 3.95 | 3.95 | 3.95 | 3.95 | 3.95 | 3.95 |
| Fe Content (%) | 65.77 | 65.77 | 65.77 | 66.33 | 64.96 | 64.96 | 64.96 | 64.96 | 64.96 | 64.96 | 64.96 | 64.96 | 67.00 | 62.84 | 66.50 |
| SiO2 (%) | 3.77 | 3.77 | 3.77 | 2.30 | 5.89 | 5.89 | 5.89 | 5.89 | 5.89 | 5.89 | 5.90 | 5.89 | 2.00 | 9.93 | 2.22 |
| % Solids (v/v) | 30.00 | 0.00 | 16.00 | 12.07 | 30.00 | 30.00 | 30.00 | 30.00 | 30.00 | 30.00 | 30 | 30.00 | 30.00 | 30.00 | 14.32 |
| % Solids (w/w) | 62.86 | 0.00 | 42.93 | 35.16 | 62.86 | 62.86 | 62.86 | 62.86 | 62.86 | 62.86 | 62.86 | 62.86 | 62.86 | 62.86 | 39.76 |

## 5.1 Financial evaluation

Based on the proposed solution and process flow, a financial evaluation was conducted, including both capital expenditure (CAPEX) as well as operational expenditure (OPEX), and was based on the following base conditions:

- CAPEX and OPEX model was based on a 100 ton per hour feed rate
- Operational time – 24 hours per day, 7 days per week.
- 90% availability inclusive of one day per week maintenance, that is one shift (eight hours)
- All prices based on 2015 prices
- CAPEX was estimated within a 20% margin, as this is the industry norm for budget purposes
- CAPEX includes:
    - design and engineering
    - civil works
    - structural fabrication and installation
    - mechanical equipment
    - electrical works
- CAPEX excludes all infrastructure and terracing

Taking this into consideration, a proposal was requested from AZMET (PTY) LTD and Environmental and Process Technologies (PTY) LTD for the total CAPEX (20% budget cost) of a 100 ton per hour feed processing plant (for the proposed solution), which was estimated to be R235 750 000,00. The estimated operational expenditure was also given in the proposals (proposals are given in Appendix I). The estimated CAPEX includes the following sections:

- de-sliming plant (removal of 38 micron material)
- milling plant, including sizing cyclone and recirculation stream
- flotation plant

- flotation product thickener
- flotation product filtration plant
- flotation tailings thickener
- flotation tailings filtration plant

Furthermore, this budget estimate was used within the financial model to determine the rand per ton payback per ton of feed material into the plant. Additionally, the repayment of the capital investment was based on an interest rate of 9,5% and a repayment period of ten years (120 months).

In terms of OPEX, two models were simulated, including the use of the current price per saleable product ton iron ore (69 USD per product ton), and estimated minimum price of $50 per product ton. Table 13 summarises all operational costs per processing section, as well as the capital expenditure as a rand per feed ton value.

In summary, the total operational expenditure is estimated at R272,44 per product ton inclusive of electricity, railage, labour, consumables, maintenance, etc. Based on a selling price of $69,00 per product ton and an exchange rate of $13,00 to R1,00 a total profit of R 590,06 per product ton can be realised. Based on this, a payback on the capital expenditure was estimated at eight months, deeming the process economically viable. Note that the CAPEX and OPEX model considered does not include any capital and operational expenditure for the SLon processing plant, as this will be a separate study.

Table 14 uses the same input values as in Table 13, however the selling price per ton of iron ore product was varied from an estimated minimum of $50,00 per product ton and up to $80,00 per product ton. In the worst case scenario, the profit is reduced to R290,06 per product ton and the capital investment has a payback of approximately 13 months and is still considered to be economically viable. Note that the CAPEX and OPEX model considered does

not include any capital and operational expenditure for the SLon processing plant.

**Table 13: Financial evaluation based on an iron ore selling price of $69,00 per product ton**

| | | | |
|---|---|---|---|
| CAPEX | | | |
| Total estimated capital expenditure | R235 750 000.00 | | |
| Interest (prime) | 9,5% | | |
| Payment period (term) | 120 | Months (10 Years) | |
| Payment | R 3 050 547.42 | | |
| R/t | R 48,42 | Per feed ton | |
| OPEX | | | |
| Flotation amine | R1,40 | R/feed ton | |
| Flotation starch | R1,44 | R/feed ton | |
| Flotation modifier | R10,00 | R/feed ton | |
| Flotation plant maintenance | R1,48 | R/feed ton | |
| Milling | R24,00 | R/feed ton | |
| Milling plant maintenance | R20,00 | R/feed ton | |
| Product thickener | R1,32 | R/feed ton | |
| Product filter plant | R4,40 | R/feed ton | |
| Tailings thickener | R0,33 | R/feed ton | |
| Tailings filter plant | R1,50 | R/feed ton | |
| Electricity | R28,00 | R/feed ton | |
| Railage | R76,00 | R/feed ton | |
| Labour | R5,11 | R/feed ton | |
| Total operational expenditure | R174,98 | R/feed ton | |
| Total monthly expenditure (incl. CAPEX repayment) | R 223,40 | R/feed ton | |
| Total monthly expenditure (incl. CAPEX repayment) | R 272,44 | R/Prod ton | |
| | | | |
| Selling price USD | $ 69,00 | per product ton | |
| Selling price ZAR | R862,50 | per product ton | |
| | | | |
| Profit after CAPEX repayment | R 590,06 | R/prod ton | |
| | | | |
| Total yearly profit | R 365 791 590,97 | R/annum | |
| | | | |
| Possible payback on capital | 7,8 | Months | |

**Table 14: Financial evaluation based various iron ore selling prices in USD per product ton**

| USD/t (selling price) | Payback Period (Months) | Profit R/t (after CAPEX repayment) | Yearly Profit |
|---|---|---|---|
| **45** | 16 | R 290,06 | R 179 815 590,00 |
| **50** | 13 | R 352,56 | R 218 560 590,97 |
| **55** | 11 | R 415,06 | R 257 305 590,97 |
| **60** | 9.6 | R 477,56 | R 296 050 590,97 |
| **65** | 8.5 | R 540,06 | R 334 795 590,97 |
| **70** | 7.6 | R 602,56 | R 373 540 590,97 |
| **75** | 6.9 | R 665,06 | R 412 285 590,97 |
| **80** | 6.3 | R 727,56 | R 451 030 590,97 |

# Chapter 6: Conclusions

In conclusion, ultra-fine (-150 micron) iron ore material that is not beneficiated has a negative environmental effect and is also considered to be a loss in possible revenue. Furthermore, this ultra-fine stream, which is an “already mined” stream, has been and is currently being beneficiated in most parts of the world, using SLon technology or froth flotation and in some cases a combination of both.

Currently, Sishen mine is still considering this stream as a waste stream, but is also considering alternative options to upgrade this material to generate additional revenue and alleviate environmental challenges. The alternative options include the use of SLon circuit, froth flotation or, in this case, a combination of both, i.e. flotation of the SLon concentrate.

The mineralogical study conducted on the SLon concentrate showed that the -38 micron material was well liberated and almost on specification with a Fe content of approximately 66,3%. Therefore, the -38 micron material can be removed prior to further processing as final concentrate.

The liberation analysis conducted on the +25 micron material showed a lack of complete liberation of both hematite and quartz. In this case, the material was milled using a ball mill to increase the liberation of quartz from 26% to 41%, i.e. at 95% to 100% liberated. The material was then subjected to flotation tests and compared to the results from the initial flotation test sample, which was not milled. Results indicated a definite increase in selective flotation of the liberated (milled) sample, achieving a concentrate containing more than 67% Fe.

Once the possibility of upgrading the material was proven, optimisation testwork was conducted by varying the amine and starch content. In these cases, release curves were constructed. Results showed that a yield (within

the flotation circuit) to concentrate of 60% to 63% can be realised with a Fe content of between 66,7% and 67%.

Using the flotation data, a mass balance was constructed to simulate the overall technical solution, which included de-sliming the -38 micron material and milling the oversize material, which is then floated. The final combination of the cyclone overflow and the flotation concentrate was then considered to be the final concentrate. The final mass balance indicated that a final yield to concentrate of 82% with a Fe content of 66,5% and a SiO2 content of less than 2% can be achieved, as per the original target set out for this project.

Based on these results and considering the CAPEX and OPEX for a 100 ton per hour feed plant, including the capital repayment with an iron ore selling price of both $69,00 and $50,00 per ton, the proposed process of milling and flotation was determined to be economically viable. However, the solution should be further evaluated by considering the CAPEX and OPEX of the SLon concentrating plant as preconditioning for the flotation.

References

1. Araujo, D.M., Yoshida, M.I., Takahashi, J.A., Carvalho, C.F. & Stapelfeldt, F. 2010. Biodegradation studies on fatty amines used for reverse flotation of iron ore. *International Biodeterioration & Biodegradation,* vol. 64, no 2, pp. 151-155.
2. Boylu, F. & Laskowski, J.S. 2007. Rate of water transfer to flotation froth in the flotation of low-rank coal that also requires the use of oily collector, *International Journal of Mineral Processing,* vol. 83, no. 3-4, pp. 125-131
3. Carney, M.D. & Mienie PJ. 2015. A Geological comparison of the Sishen and Sishen South (Welgevonden) Iron Ore Deposit, Northern Cape Province, South Africa. *Applied Earth Science: Transactions of the Instritute of Mining and Metallurgy: Section B,* vol 112, No 1, pp. 81-88.
4. Deo, N. & Natarajan, K.A. 1999. Biodegradation of Some Organic Flotation Reagents by Bacillus polymyxa. *Process Metallurgy,* vol. 9, pp. 687-696.
5. Ding, K. & Laskowski, J.S. 2006**.** Coal reverse flotation Part I: Separation of a mixture of sub bituminous coal and gangue minerals. *Minerals Engineering,* vol. 19, no. 1, pp. 72-78
6. Dos Santos, I.D. & Oliveira, J.F. 2007. Utilization of humic acid as a depressant for hematite in the reverse flotation of iron ore. *Minerals Engineering*, vol. 20, No. 10, pp.1003-1007
7. Dworzanowski, M. 2014. Maximising heamatite recovery within a fine and wide particle-size distribution using wet high-intensity magnetic separation. *The Journal of The South African Institute of Mining and Metallurgy,* vol. 114, no. 7, pp. 559-567
8. Flint, I.M., Wyslouzil, H.E., De Lima Andradef, V.L. & Murdockj, D.J. 1992. Column Flotation of Iron Ore. *Minerals Engineering*, vol. 5, no. 10-12, pp. 1185-1194.
9. Flippov, L.O., Severov, V.V., Filippova, I.V., 2014, An overview of the beneficiation of iron ores via reverse cationic flotation, *International Journal of Minerals Processing,* vol. 127, pp. 62-69.
10. Gaudin, A.M. 1939. *Principles of Mineral Dressing*. McGraw-Hill.
11. Gupta, A.K., Banerjee, P.K., Mishra, A. & Satish, P., Pradip. 2006. Effect of alcohol and polyglycol ether frothers on foam stability, bubble size and coal flotation. *International Journal of Mineral Processing,* vol. 82, no. 3, pp. 126–137.
12. Gupta, K.R. & Banerjee, P.K. 2008. Role of process water quality on coal flotation – a new look. , *IMPC.*
13. Hadler, K., Barbian, N. & Cilliers, J.J.. 2006. The relationship between froth stability and flotation performance down a bank of cells. *IMPC.*
14. http://cache.eb.com/eb/image?id=1534&rendTypeId=4, Accessed on: 5-4-2009

15. http://minerals.usgs.gov/minerals/pubs/commodity/iron_ore/mcs-2010-feore.pdf Accessed on: 29-011-2014
16. http://www.flsmidth.com/en-US/Products/Product+Index/All+Products/Flotation, Accessed on: 5/11/2010
17. http://www.metallurgy.utah.edu/galleries/photo.2006-08-16.2540861271/variant/original, Accessed on: 5-4-2009
18. http://www.soloresources.co.za/cpt-flotation.htm, Accessed on: 5/11/2010
19. http://www.titanprocess.com/flotation-machines, Accessed on: 10/08/2015
20. Jena, M.S., Biswal, S.K., Das, S.P. & Reddy, P.S.R. 2008. Comparative study of the performance of conventional and column flotation when treating coking coal fines. *Fuel Processing Technology,* vol. 89, no. 12, pp. 1409-1415
21. Jorgenson, D. 2014. Iron Ore. *U.S. Geological survey*.
22. Kelebek, S., Demir, U., Sahbaz, O., Ucar, A., Cinar, M., Karaguzel, C. & Oteyaka, B. 2008. The effects of dodecylamine, kerosene and pH on batch flotation of Turkey's Tuncbilek coal. *International Journal of Mineral Processing,* vol. 88, no. 3-4, pp. 65-71
23. Kelly, E.G. & Spottiswood, D.J. 1992. *Introduction to mineral processing*. New York: John Wiley & Sons.
24. Laskowski, J.S. 2003. Coal flotation and fine coal utilisation, *University of Cape Town*, Randburg, 2003
25. Laskowski, J.S.. 2006. Coal flotation – the future. *IMPC,*
26. Liu, G., Zhong, H., Hu, Y., Zhao, S. & Xia L. 2007. The role of cationic polyacrylamide in the reverse flotation of diasporic bauxite. *Minerals Engineering*, vol. 20, no. 13, pp.1191-1199.
27. Liu, W., Wei, D., Wang, B., Fang, P., Wang, X. & Cui, B. 2009. A new collector used for flotation of oxide minerals. *Transactions of Nonferrous Metals Society of China,* vol.19, no. 5, pp. 1326-1330.
28. Lui, A.N., Fan, J. & Fan, M. 2015. Quantum chemical calculations and molecular dynamics simulations of amine collector adsorption on quartz (0 0 1) surface in the aqueous solution. *International Journal of Minerals Processing,* vol. 134, pp. 1-10
29. Ma, X., Marques, M. & Gontijo, C. 2011. Comprehensive studies of reverse cationic/anionic flotation of Vale iron ore. *International Journal of Minerals Processing*,
30. Mathur, S., Singh, P. & Moudgil, B.M. 1999. Advances in selective flocculation technology for solid-solid separations. *International Journal of Minerals Processing,* vol. 58, no. 1-4, pp. 201-222
31. Morar, S.H., Bradshaw, D.J. & Harris, M.C. 2008. Assessment of froth stability down a flotation bank. *IMPC*

32. Morar, S.H. & Hatfield, D.P. 2006. A comparison flotation froth stability measurements and their use in the prediction of concentrate grade. *IMPC,*
33. Naik, P.K., Reddy, P.S.R. & Misra, V.N. 2004.'Interpretation of interaction effects and optimization of reagent dosages for fine coal flotation. *International Journal of Mineral Processing,* vol. 75, no. 1-2, pp.83-90
34. Nanthakumar, B., Grimm, D. & Pawlik, M. 2009. Anionic flotation of high-iron phosphate ores—Control of process water chemistry and depression of iron minerals by starch and guar gum. *International Journal of Minerals Processing*, vol. 92, no. 1-2, pp. 28-33
35. Nguyen, A.V., Karakashev, S.I. & Jameson, G.J. 2006. Effect of interfacial properties on water drainage and recovery in a froth column. *IMPC*
36. Papp, J.F., Bray, E.L., Edelstein, D.L., Fenton, M.D., Guberman, D.E., Hedrick, J.B., Jorgenson, J.D., Kuck, P.H., Shedd, K.B. & Tolcin, A.C. 2008. Factors that influence the price of Al, Cd, Co, Cu, Fe, Ni, Pb, Rare Earth lements, and Zn. *U.S. Geological survey.*
37. Pavlovic, S. & Brandao, P.R.G. 2003. Adsorption of starch, amylose, amylopectin and glucose monomer and their effect on the flotation of hematite and quartz. *Minerals Engineering,* vol. 16, no. 11, pp. 1117-1122
38. Pers. Comm. K. Vreugtenberg; 28 October 2015
39. Peng, Y. & Ourriban, M. 2006. Reduction of fine quartz entrainment in chalcopyrite flotation by polymer depressants. *IMPC,*
40. Peres, A.E.C. & Correa, M.I. 1996. Depression of iron oxides with corn starch. *Minerals Engineering,* vol. 9, no 12, pp. 1227-1234
41. Pradhan, N., Das, B., Gahan, C.S., Kar, R.N. & Sukla, L.B. 2005. Beneficiation of iron ore slime using Aspergillus niger and Bacillus circulans. *Bioresource Technology,* vol. 97, no. 15, pp. 1876-1879
42. Pryor, E.J. 1965. *Mineral Processing.* 3rd ed. Elsevier.
43. Pugh, R.J. 2006. Surface chemical studies on particle stabilized froths. *IMPC,*
44. Quast, K.B. 2000. A review of hematite flotation using 12-carbon chain collectors. *Minerals Engineering,* vol. 13, no. 13, pp. 1361-1376
45. Rao, K.H. & Forssberg, K.S.E. 1997. Mixed collector systems in flotation. *International Journal of Minerals Processing,* vol. 51, no. 1-4, pp. 67-79
46. Richards, R.H. 1940. *Textbook of ore dressing*. McGraw-Hill.
47. Rodrigues, O.M.S., Peres, A.E.C., Martins, A.H. & Pereira, C.A. 2013. Kaolinite and Hematite Flotation Separation Using Etheramine and Ammonium Quartenary Salts. *Minerals Engineering,* vol. 40, pp.12-15
48. Roy, S., Das, A. & Venkatesh, A.S. 2008. A comparative mineralogical and geochemical characterisation of iron ores from two Indian Precambrian

deposits and Krivoy rog deposit, Ukraine: implications for the upgrading of lean grade ore. *AusIMM*

49. Runge, K., Crosbie, R., Rivett, T. & McMaster, J. 2010. An evaluation of froth recovery measurement techniques; *International Minerals Processing Congress.*
50. Shibata, J. & Fuerstenau, D.W. 2003. Flocculation and flotation characteristics of fine hematite with sodium oleate. *International Journal of Minerals Processing,* vol. 72, no. 1-4, pp. 25-32
51. SLon Operational Manual. 2013. *SLon Vertically Pulsating High-Gradient Magnetic Separator*. Available: www.autotec.co.za.
52. Sripriya, R., Rao, P.V.T. & Choudhury, B.R. 2002. Optimisation of operating variables of fine coal flotation using a combination of modified flotation parameters and statistical techniques. *International Journal of Mineral Processing,* vol. 68, no. 1-4, pp. 109-127
53. Srivastava, M.P., Pan, S.K., Prasad, N. & Mishra, B.K. 2000. Characterization and processing of iron ore fines of Kiriburu deposit of India. *International Journal of Mineral Processing*, vol. 61, no. 2, pp. 93-107
54. Taggart, A.F. 1956. *Handbook of mineral dressing*. New York: John Wiley & Sons.
55. Tao, D., Luttrell, G.H. & Yoon, R.H. 2000. A parametric study of froth stability and its effect on column flotation of fine particles. *International Journal of Mineral Processing,* vol. 59, no. 1, pp.25-43.
56. Vieira, A.M. & Peres, A.E.C. 2007. The effect of amine type, pH and size range in the flotation of quartz. *Minerals Engineering,* vol. 20, no. 10, pp. 1008-1013
57. Weissenborn, P.K., Warren, L.J. & Dunn, J.G. 1995. Selective flocculation of ultrafine iron ore. 1. Mechanism of adsorption of starch onto hematite. *Colloids and Surfaces A: Physiccochemical and Engineering Aspects,* vol. 99, no. 1, pp. 11-27.
58. Zeng, W. & Dahe, X. 2003. The latest application of SLon vertical ring and pulsating high-gradient magnetic separator. *Minerals Engineering,* vol. 16, no. 6, pp. 563-565

# Appendices

Appendix A: Particle size distribution results (material characterisation)

Appendix B: Raw data XRF results (material characterisation)

Appendix C: Raw data SEM analysis

Appendix D: Raw data XRD results (material characterisation)

Appendix E: Initial flotation test raw data results

Appendix F: AR report on mineral liberation analysis

Appendix G: Revised flotation test raw data results

Appendix H: Safety and chemical disposal

Appendix I: AZMET and ENPROTEC LSTK proposals

## 7.1 Appendix A: Particle size distribution results (material characterisation)

Five randomly selected samples were taken from the bulk/gross sample after splitting for particle size distribution analysis. A total of 400 g of material was taken for all particle size distribution analyses, of which the raw data (results) is tabulated.

| PSD 1 | | | | | |
|---|---|---|---|---|---|
| **mass(g)** | 400 | | | | |
| | | | | | |
| **Size(µm)** | Mass of sieve(g) | Mass of sample and sieve(g) | Mass of sample(g) | Mass % retained | Cum % passing |
| **212** | 283.2 | 283.20 | 0.00 | 0.0 | 100.0 |
| **150** | 451.3 | 470.14 | 18.84 | 4.8 | 95.2 |
| **106** | 488.6 | 511.37 | 22.77 | 5.8 | 89.4 |
| **75** | 265.4 | 290.91 | 25.51 | 6.5 | 82.9 |
| **38** | 261.8 | 345.80 | 84.00 | 21.4 | 61.5 |
| **25** | 328.8 | 370.01 | 41.21 | 10.5 | 51.0 |
| **Pan** | 338.2 | 538.38 | 200.18 | 51.0 | 0.00 |
| **Total** | | | 392.5 | | |

| PSD 2 | | | | | |
|---|---|---|---|---|---|
| **mass(g)** | 400 | | | | |
| | | | | | |
| **Size(µm)** | Mass of sieve(g) | Mass of sample and sieve(g) | Mass of sample(g) | Mass % retained | Cum % passing |
| **212** | 283.2 | 283.20 | 0.00 | 0.0 | 100.0 |
| **150** | 451.3 | 468.83 | 17.53 | 4.5 | 95.5 |
| **106** | 488.6 | 510.03 | 21.43 | 5.5 | 90.0 |
| **75** | 265.4 | 293.84 | 28.44 | 7.3 | 82.7 |
| **38** | 261.8 | 338.16 | 76.36 | 19.6 | 63.1 |
| **25** | 328.8 | 372.05 | 43.25 | 11.1 | 52.0 |
| **Pan** | 338.2 | 540.79 | 202.59 | 52.0 | 0.0 |
| **Total** | | | 389.6 | | |
| | | | | | |
| **PSD 3** | | | | | |
| **mass(g)** | 402 | | | | |
| | | | | | |
| **Size(µm)** | Mass of sieve(g) | Mass of sample and sieve(g) | Mass of sample(g) | Mass % retained | Cum % passing |
| **212** | 283.2 | 283.20 | 0.00 | 0.0 | 100.0 |
| **150** | 451.3 | 464.20 | 12.90 | 3.2 | 96.8 |
| **106** | 488.6 | 507.15 | 18.55 | 4.6 | 92.2 |
| **75** | 265.4 | 292.82 | 27.42 | 6.8 | 85.4 |
| **38** | 261.8 | 356.55 | 94.75 | 23.5 | 61.9 |

| | | | | | |
|---|---|---|---|---|---|
| **25** | 328.8 | 381.22 | 52.42 | 13.0 | 48.9 |
| **Pan** | 338.2 | 535.36 | 197.16 | 48.9 | 0.0 |
| **Total** | | | 403.2 | | |

| | | | | | |
|---|---|---|---|---|---|
| | | | **PSD 4** | | |
| **mass(g)** | 400 | | | | |
| | | | | | |
| **Size(µm)** | Mass of sieve(g) | Mass of sample and sieve(g) | Mass of sample(g) | Mass % retained | Cum % passing |
| **212** | 283.2 | 283.20 | 0.00 | 0.0 | 100.0 |
| **150** | 451.3 | 474.17 | 22.87 | 5.7 | 94.3 |
| **106** | 488.6 | 513.48 | 24.88 | 6.2 | 88.1 |
| **75** | 265.4 | 298.71 | 33.31 | 8.3 | 79.8 |
| **38** | 261.8 | 346.07 | 84.27 | 21.0 | 58.8 |
| **25** | 328.8 | 372.94 | 44.14 | 11.0 | 47.8 |
| **Pan** | 338.2 | 530.02 | 191.82 | 47.8 | 0.0 |
| **Total** | | | 401.3 | | |
| | | | | | |
| | | | **PSD 5** | | |
| **mass(g)** | 400 | | | | |
| | | | | | |
| **Size(µm)** | Mass of sieve(g) | Mass of sample and sieve(g) | Mass of sample(g) | Mass % retained | Cum % passing |
| **212** | 283.2 | 283.20 | 0.00 | 0.0 | 100.0 |
| **150** | 451.3 | 473.17 | 21.87 | 5.5 | 94.5 |
| **106** | 488.6 | 513.65 | 25.05 | 6.3 | 88.2 |
| **75** | 265.4 | 298.00 | 32.60 | 8.2 | 80.0 |
| **38** | 261.8 | 341.32 | 79.52 | 20.0 | 60.0 |
| **25** | 328.8 | 376.51 | 47.71 | 12.0 | 48.0 |
| **Pan** | 338.2 | 529.05 | 190.85 | 48.0 | 0.0 |
| **Total** | | | 397.6 | | |

Additionally, Anglo American Technical Solutions also conducted a particle size distribution analysis on the MLA samples submitted, of which the results are summarised as follows. Sample KB-75 (A) is the unmilled material.

| | | | |
|---|---|---|---|
| **SAMPLE NUMBER:** | KB-75 (A) | | |
| **SAMPLE DESCRIPTION:** | | | |
| **WEIGTHS USED (g):** | 82.40 | | |

| Size (µm) | Wt 1 | Wt 2 | Wt 3 | Wt % 1 | Wt % 2 | Wt % 3 |
|---|---|---|---|---|---|---|
| **Starting wt** | 0.00 | 0.00 | 0.00 | | | |
| **+212** | 1.02 | 0.00 | 0.00 | 1.24 | 0.00 | 0.00 |
| **+75** | 14.34 | 0.00 | 0.00 | 17.40 | 0.00 | 0.00 |
| **+25** | 25.55 | 0.00 | 0.00 | 31.01 | 0.00 | 0.00 |
| **Calc. -25** | 40.91 | 0.00 | 0.00 | 49.65 | 0.00 | 0.00 |
| **TOTALS** | 82.40 | 0.00 | 0.00 | 100.00 | 0.00 | 0.00 |
| **Actual -10** | 40.00 | 0.00 | 0.00 | 48.54 | 0.00 | 0.00 |

Sample number KB75-2 is the milled material after screening as part of the MLA analysis.

| | | | |
|---|---|---|---|
| **SAMPLE NUMBER:** | KB75-2 | | |
| **SAMPLE DESCRIPTION:** | | | |
| **WEIGTHS USED (g):** | 179.47 | | |

| Size (µm) | Wt 1 | Wt 2 | Wt 3 | Wt % 1 | Wt % 2 | Wt % 3 |
|---|---|---|---|---|---|---|
| **Starting wt** | 0.00 | 0.00 | 0.00 | | | |
| **+212** | 0.00 | 0.00 | 0.00 | 0.00 | 0.00 | 0.00 |
| **+75** | 0.06 | 0.00 | 0.00 | 0.03 | 0.00 | 0.00 |
| **+25** | 9.48 | 0.00 | 0.00 | 5.28 | 0.00 | 0.00 |
| **Calc. -25** | 169.93 | 0.00 | 0.00 | 94.68 | 0.00 | 0.00 |
| **TOTALS** | 179.47 | 0.00 | 0.00 | 100.00 | 0.00 | 0.00 |
| **Actual -10** | 168.39 | 0.00 | 0.00 | 93.83 | 0.00 | 0.00 |

The bulk/gross sample as received from Sishen, that is the SLon concentrate, was subjected to sample splitting in order to achieve a set of smaller

representative samples for use during testwork. As an additional test to ensure that the split material was representative of the bulk/gross sample, ten randomly chosen samples were subjected to a Malvern particle size analyser, of which the results are given in Figure 78. The results show that the material was adequately split.

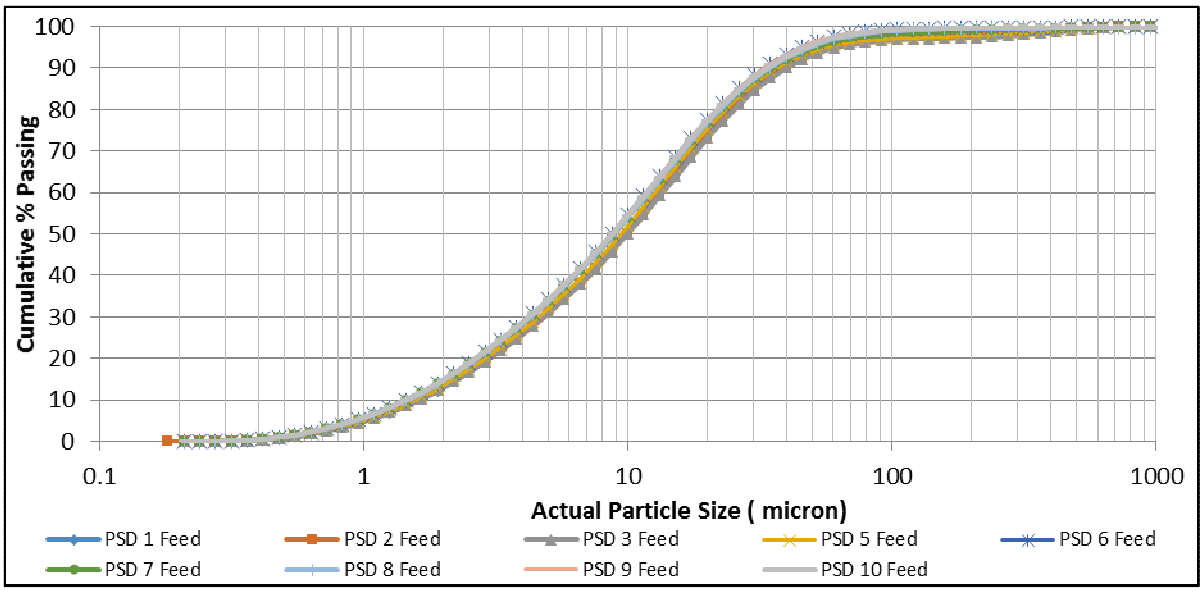


Figure 78: Comparative particle size distributions for the ten randomly chosen samples

## 7.2 Appendix B: Raw data XRF results (material characterisation)

In general, five samples were subjected for sample characterisation and comparison. However, in the case of the XRF (chemical) analysis, the results were considered crucial for the test program as the flotation results will be measured according to chemical analysis. Therefore ten samples were considered in this case. The table gives all as received raw data.

| SAMPLE ID | Fe | | $SiO_2$ | $Al_2O_3$ | $K_2O$ | P | Mn | CaO | MgO | $TiO_2$ | $Na_2O$ |
|---|---|---|---|---|---|---|---|---|---|---|---|
| | % | | % | % | % | % | % | % | % | % | % |
| **MK 1** | 61.20 | 87.50 | 3.90 | 4.47 | 0.79 | 0.112 | 0.03 | 0.38 | 0.08 | 0.16 | 0.15 |
| **MK 2** | 61.50 | 87.93 | 3.84 | 4.49 | 0.80 | 0.113 | 0.03 | 0.39 | 0.09 | 0.16 | 0.15 |
| **MK 3** | 61.30 | 87.64 | 3.92 | 4.50 | 0.79 | 0.111 | 0.03 | 0.39 | 0.07 | 0.16 | 0.15 |
| **MK 4** | 60.53 | 86.54 | 3.89 | 4.45 | 0.80 | 0.113 | 0.02 | 0.38 | 0.08 | 0.16 | 0.15 |
| **MK 5** | 61.80 | 88.36 | 3.94 | 4.50 | 0.80 | 0.114 | 0.02 | 0.38 | 0.07 | 0.16 | 0.15 |
| **MK 6** | 62.30 | 89.07 | 4.00 | 4.48 | 0.80 | 0.113 | 0.03 | 0.41 | 0.08 | 0.16 | 0.15 |
| **MK 7** | 62.10 | 88.79 | 4.11 | 4.55 | 0.80 | 0.114 | 0.03 | 0.40 | 0.09 | 0.16 | 0.15 |
| **MK 8** | 61.40 | 87.79 | 3.98 | 4.57 | 0.81 | 0.115 | 0.03 | 0.42 | 0.13 | 0.16 | 0.15 |
| **MK 9** | 61.40 | 87.79 | 3.90 | 4.51 | 0.80 | 0.114 | 0.03 | 0.39 | 0.10 | 0.16 | 0.15 |
| **MK 10** | 60.98 | 87.19 | 4.02 | 4.47 | 0.80 | 0.113 | 0.03 | 0.38 | 0.09 | 0.16 | 0.15 |

## 7.3 Appendix C: Raw data SEM analysis

Initially five randomly selected samples were taken after the bulk/gross sample was split, and subjected to a SEM analysis. The sample label and images (backscattered –electron images) are given for reference (hematite – red [bright phase] phase and quartz – green phase [dark phase]).

*Sample A1-1*

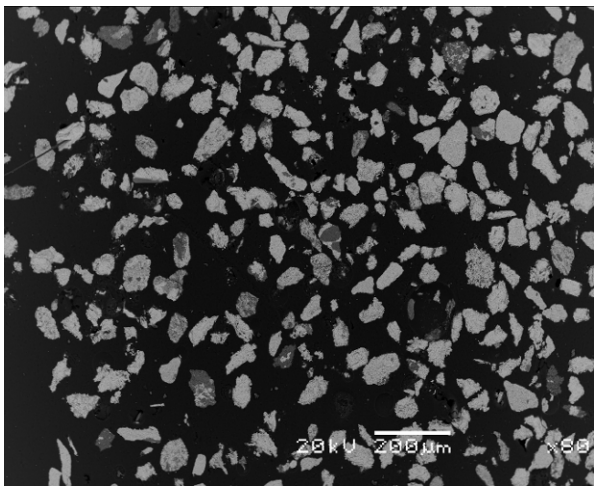


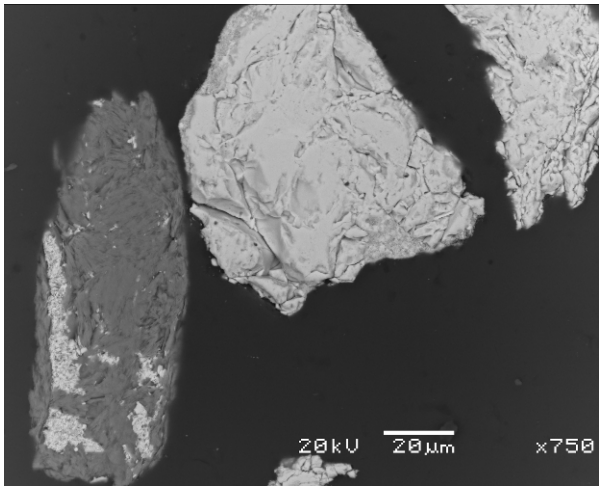


*Sample A2-1*

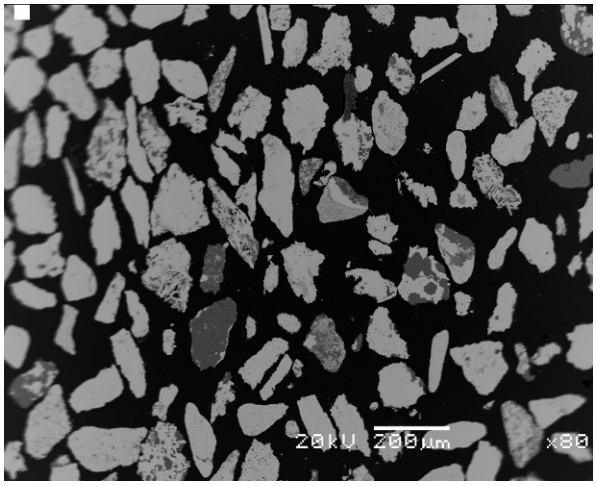


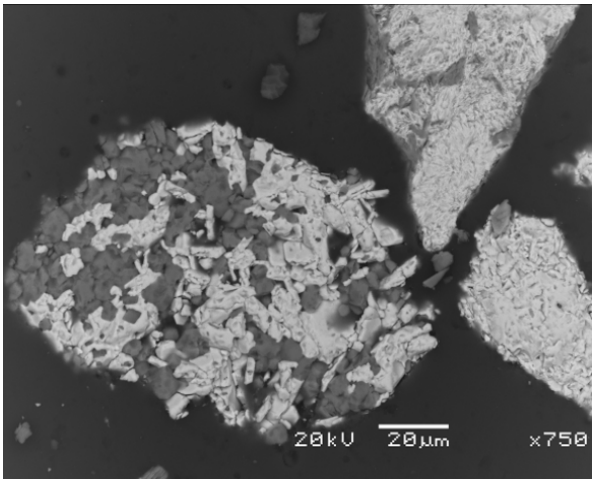

*Sample A3-1*

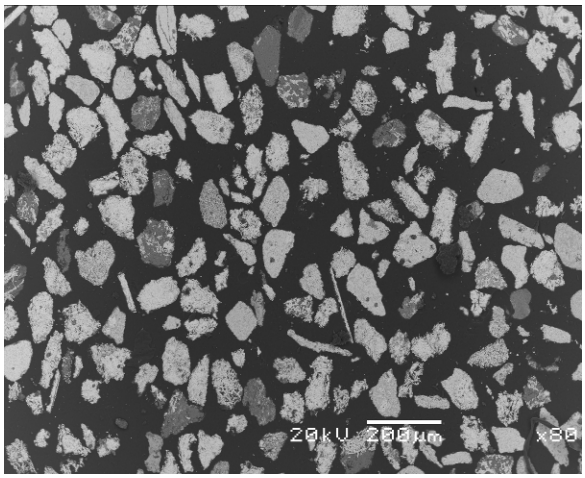


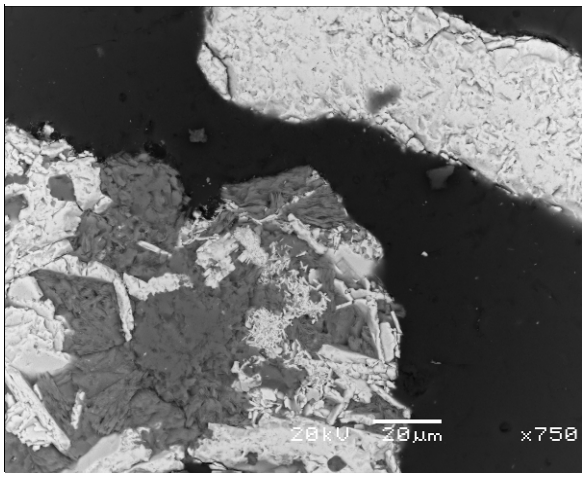


*Sample A4-1*

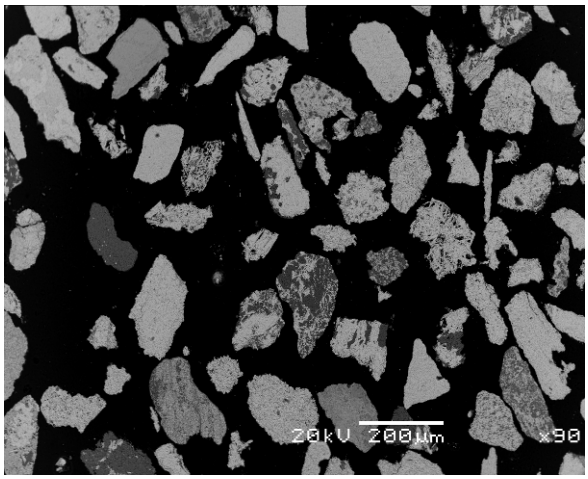


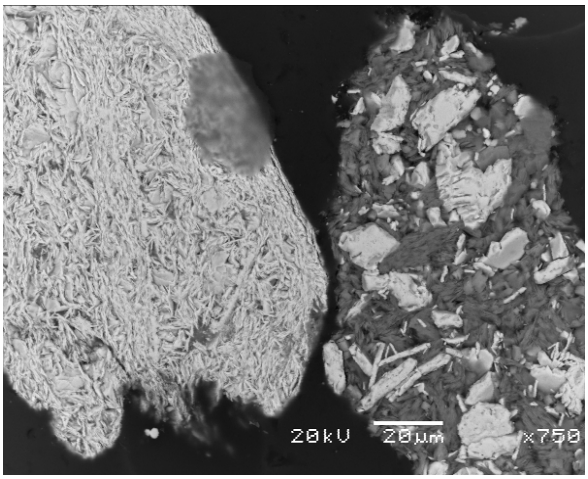


*Sample A5-1*

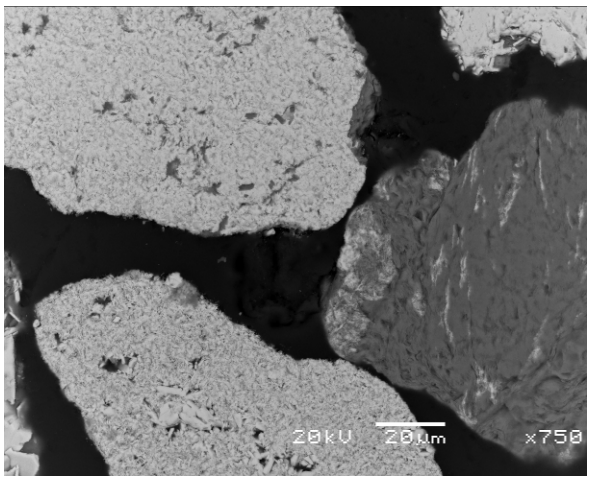
20kV
20µm
x750

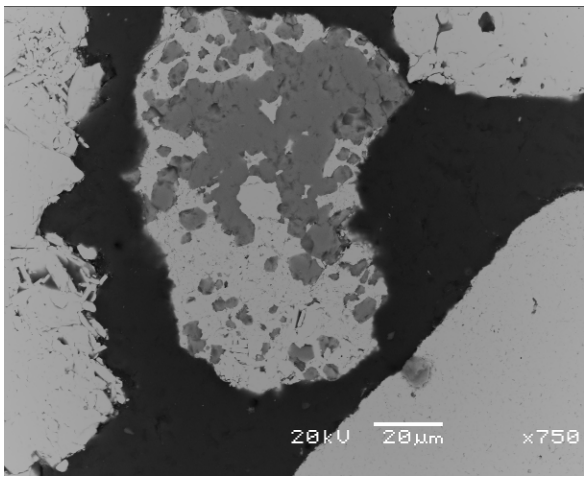
20kV
20µm
x750

## 7.4 Appendix D: Raw data XRD results (material characterisation)

Five randomly selected raw feed samples (after splitting the bulk/gross sample) were submitted for XRD analysis, of which the data below is the raw as received results.

| | **MK 1** | | | | **MK 2** | | |
|---|---|---|---|---|---|---|---|
| | weight% | 3σ error | Fe (%) XRD | | weight% | 3σ error | Fe (%) |
| **Kaolinite** | 1.17 | 0.66 | | Kaolinite | 1 | 0.45 | |
| **Hematite** | 89.38 | 0.84 | 62.52 | Hematite | 88.97 | 0.78 | 62.23 |
| **Other** | 5.24 | 0.66 | | Other | 5.63 | 0.63 | |
| **Quartz** | 4.21 | 0.23 | | Quartz | 4.4 | 0.36 | |

| | **MK 3** | | | | MK 4 | | |
|---|---|---|---|---|---|---|---|
| | weight% | 3σ error | Fe (%) | | weight% | 3σ error | Fe (%) |
| **Kaolinite** | 1.15 | 1.6 | | Kaolinite | 1.11 | 1.32 | |
| **Hematite** | 89.3 | 1.3 | 62.46 | Hematite | 89.2 | 1.35 | 62.39 |
| **Other** | 5.32 | 0.69 | | Other | 5.57 | 0.63 | |
| **Quartz** | 4.23 | 0.25 | | Quartz | 4.12 | 0.23 | |

| | **MK 5** | | |
|---|---|---|---|
| | weight% | 3σ error | Fe (%) |
| **Kaolinite** | 1.08 | 0.51 | |
| **Hematite** | 88.85 | 0.87 | 62.14 |
| **Other** | 5.82 | 0.78 | |
| **Quartz** | 4.25 | 0.45 | |

## 7.5 Appendix E: Initial flotation test raw data results

The raw data for the initial flotation test results indicating the ”T-piece” effect is tabulated.

| Sample | Fe2O3 (%) | Fe | SiO2 (%) | K2O (%) | Al2O3 (%) | P2O5 (%) | SO3 (%) | MnO (%) | TiO2 (%) | CaO (%) | |
|---|---|---|---|---|---|---|---|---|---|---|---|
| **MK72F** | 87.76 | 61.27 | 3.45 | 0.26 | 1.02 | 0.09 | 0.02 | 0.10 | 0.10 | 0.13 | 92.97 |
| | 94.40 | 65.90 | 3.71 | 0.28 | 1.09 | 0.10 | 0.02 | 0.11 | 0.11 | 0.14 | 100.00 |
| **MK72OF** | 93.19 | 65.06 | 3.49 | 0.27 | 1.50 | 0.09 | 0.03 | 0.09 | 0.09 | 0.10 | 98.94 |
| | 94.19 | 65.75 | 3.52 | 0.27 | 1.52 | 0.09 | 0.03 | 0.09 | 0.10 | 0.11 | 100.00 |
| **MK72UF** | 87.29 | 60.94 | 3.89 | 0.25 | 1.23 | 0.10 | 0.02 | 0.11 | 0.11 | 0.12 | 93.15 |
| | 93.71 | 65.42 | 4.18 | 0.27 | 1.32 | 0.11 | 0.02 | 0.11 | 0.11 | 0.13 | 100.00 |
| **MK73F** | 86.40 | 60.32 | 3.38 | 0.26 | 1.07 | 0.10 | 0.02 | 0.10 | 0.10 | 0.12 | 91.58 |
| | 94.35 | 65.87 | 3.69 | 0.28 | 1.16 | 0.11 | 0.02 | 0.11 | 0.11 | 0.14 | 100.00 |
| **MK73OF** | 91.48 | 63.86 | 3.49 | 0.29 | 1.55 | 0.08 | 0.03 | 0.09 | 0.10 | 0.09 | 97.25 |
| | 94.06 | 65.66 | 3.58 | 0.30 | 1.59 | 0.08 | 0.03 | 0.09 | 0.10 | 0.09 | 100.00 |
| **MK73UF** | 88.47 | 61.77 | 4.15 | 0.28 | 1.34 | 0.10 | 0.02 | 0.10 | 0.11 | 0.11 | 94.72 |
| | 93.41 | 65.21 | 4.38 | 0.30 | 1.42 | 0.10 | 0.02 | 0.11 | 0.12 | 0.12 | 100.00 |
| **MK74F** | 88.43 | 61.73 | 3.79 | 0.26 | 1.13 | 0.11 | 0.02 | 0.10 | 0.10 | 0.12 | 94.11 |
| | 93.96 | 65.60 | 4.02 | 0.28 | 1.20 | 0.11 | 0.02 | 0.11 | 0.11 | 0.13 | 100.00 |
| **MK74OF** | 92.83 | 64.81 | 3.52 | 0.28 | 1.52 | 0.08 | 0.03 | 0.10 | 0.10 | 0.11 | 98.64 |
| | 94.11 | 65.70 | 3.57 | 0.29 | 1.54 | 0.08 | 0.03 | 0.10 | 0.10 | 0.11 | 100.00 |
| **MK74UF** | 86.87 | 60.64 | 4.11 | 0.24 | 1.28 | 0.11 | 0.02 | 0.11 | 0.10 | 0.11 | 92.98 |
| | 93.42 | 65.22 | 4.42 | 0.26 | 1.38 | 0.11 | 0.02 | 0.11 | 0.11 | 0.12 | 100.00 |
| **MK75F** | 88.69 | 61.92 | 3.86 | 0.28 | 1.25 | 0.10 | 0.02 | 0.10 | 0.11 | 0.11 | 94.57 |
| | 93.78 | 65.47 | 4.08 | 0.29 | 1.32 | 0.11 | 0.02 | 0.11 | 0.12 | 0.12 | 100.00 |
| **MK75OF** | 90.92 | 63.47 | 4.48 | 0.39 | 1.95 | 0.10 | 0.04 | 0.11 | 0.11 | 0.12 | 98.28 |
| | 92.51 | 64.58 | 4.56 | 0.40 | 1.98 | 0.10 | 0.04 | 0.11 | 0.11 | 0.12 | 100.00 |
| **MK75UF** | 87.73 | 61.24 | 3.81 | 0.25 | 1.17 | 0.11 | 0.02 | 0.11 | 0.10 | 0.12 | 93.45 |
| | 93.87 | 65.54 | 4.08 | 0.27 | 1.25 | 0.12 | 0.02 | 0.12 | 0.11 | 0.12 | 100.00 |
| **MK76F** | 88.86 | 62.03 | 3.86 | 0.27 | 1.29 | 0.11 | 0.02 | 0.11 | 0.10 | 0.12 | 94.79 |
| | 93.74 | 65.44 | 4.07 | 0.28 | 1.37 | 0.12 | 0.02 | 0.12 | 0.11 | 0.12 | 100.00 |
| **MK76OF** | 93.74 | 65.44 | 3.39 | 0.29 | 1.41 | 0.07 | 0.03 | 0.10 | 0.10 | 0.10 | 99.29 |
| | 94.41 | 65.91 | 3.41 | 0.30 | 1.42 | 0.07 | 0.03 | 0.10 | 0.10 | 0.10 | 100.00 |
| **MK77F** | 86.87 | 60.64 | 3.30 | 0.26 | 0.97 | 0.10 | 0.02 | 0.11 | 0.11 | 0.11 | 91.87 |
| | 94.55 | 66.01 | 3.59 | 0.29 | 1.06 | 0.10 | 0.02 | 0.12 | 0.11 | 0.12 | 100.00 |
| **MK77OF** | 92.08 | 64.28 | 3.32 | 0.25 | 1.44 | 0.07 | 0.03 | 0.09 | 0.10 | 0.08 | 97.51 |
| | 94.43 | 65.93 | 3.40 | 0.26 | 1.48 | 0.07 | 0.03 | 0.09 | 0.10 | 0.08 | 100.00 |
| **MK77UF** | 88.84 | 62.02 | 4.64 | 0.29 | 1.45 | 0.12 | 0.02 | 0.10 | 0.11 | 0.12 | 95.72 |
| | 92.81 | 64.80 | 4.84 | 0.30 | 1.51 | 0.13 | 0.02 | 0.11 | 0.11 | 0.12 | 100.00 |
| **MK78F** | 88.77 | 61.97 | 4.06 | 0.29 | 1.31 | 0.11 | 0.02 | 0.11 | 0.16 | 0.12 | 95.01 |
| | 93.43 | 65.23 | 4.27 | 0.31 | 1.38 | 0.11 | 0.03 | 0.11 | 0.17 | 0.12 | 100.00 |
| **MK78OF** | 93.51 | 65.28 | 3.54 | 0.27 | 1.55 | 0.08 | 0.03 | 0.10 | 0.10 | 0.10 | 99.35 |
| | 94.13 | 65.71 | 3.56 | 0.28 | 1.56 | 0.08 | 0.03 | 0.10 | 0.10 | 0.10 | 100.00 |
| **MK78UF** | 89.53 | 62.50 | 4.13 | 0.29 | 1.37 | 0.12 | 0.02 | 0.11 | 0.17 | 0.13 | 95.93 |

| | | | | | | | | | | | |
|---|---|---|---|---|---|---|---|---|---|---|---|
| | 93.33 | 65.16 | 4.31 | 0.30 | 1.43 | 0.12 | 0.02 | 0.12 | 0.18 | 0.13 | 100.00 |
| **MK79F** | 87.99 | 61.42 | 3.73 | 0.27 | 1.12 | 0.10 | 0.02 | 0.11 | 0.10 | 0.13 | 93.60 |
| | 94.00 | 65.63 | 3.98 | 0.29 | 1.20 | 0.11 | 0.02 | 0.11 | 0.11 | 0.13 | 100.00 |
| **MK79OF** | 91.69 | 64.01 | 3.78 | 0.30 | 1.61 | 0.09 | 0.03 | 0.10 | 0.11 | 0.11 | 97.88 |
| | 93.68 | 65.40 | 3.86 | 0.31 | 1.64 | 0.09 | 0.03 | 0.11 | 0.11 | 0.11 | 100.00 |
| **MK79UF** | 88.19 | 61.57 | 4.06 | 0.27 | 1.31 | 0.12 | 0.03 | 0.12 | 0.11 | 0.14 | 94.37 |
| | 93.46 | 65.24 | 4.30 | 0.29 | 1.39 | 0.13 | 0.03 | 0.12 | 0.11 | 0.15 | 100.00 |
| **MK80F** | 87.33 | 60.97 | 3.90 | 0.27 | 1.23 | 0.10 | 0.02 | 0.11 | 0.11 | 0.13 | 93.24 |
| | 93.66 | 65.39 | 4.18 | 0.29 | 1.31 | 0.11 | 0.02 | 0.11 | 0.12 | 0.14 | 100.00 |
| **MK80UF** | 87.72 | 61.24 | 4.01 | 0.28 | 1.27 | 0.10 | 0.02 | 0.10 | 0.10 | 0.12 | 93.77 |
| | 93.55 | 65.31 | 4.27 | 0.29 | 1.35 | 0.11 | 0.02 | 0.11 | 0.11 | 0.13 | 100.00 |
| **MK81OF** | 92.51 | 64.58 | 3.79 | 0.29 | 1.63 | 0.08 | 0.03 | 0.10 | 0.10 | 0.10 | 98.68 |
| | 93.75 | 65.45 | 3.84 | 0.29 | 1.65 | 0.08 | 0.03 | 0.10 | 0.10 | 0.10 | 100.00 |
| **MK82F** | 88.36 | 61.69 | 4.20 | 0.29 | 1.37 | 0.10 | 0.02 | 0.11 | 0.11 | 0.12 | 94.74 |
| | 93.27 | 65.12 | 4.43 | 0.30 | 1.44 | 0.11 | 0.02 | 0.12 | 0.11 | 0.13 | 100.00 |
| **MK82OF** | 93.72 | 65.43 | 3.13 | 0.23 | 1.23 | 0.06 | 0.02 | 0.10 | 0.10 | 0.10 | 98.75 |
| | 94.91 | 66.26 | 3.17 | 0.23 | 1.25 | 0.06 | 0.02 | 0.10 | 0.11 | 0.10 | 100.00 |
| **MK82UF** | 89.88 | 62.75 | 4.18 | 0.27 | 1.36 | 0.12 | 0.02 | 0.11 | 0.11 | 0.12 | 96.22 |
| | 93.42 | 65.22 | 4.35 | 0.28 | 1.42 | 0.12 | 0.03 | 0.11 | 0.11 | 0.13 | 100.00 |

## 7.6 Appendix F: AR report on mineral liberation analysis

AngloAmerican

Real Mining. Real People. Real Difference.

RESEARCH

# MINERALOGICAL INVESTIGATION OF IRON ORE FLOTATION FEEDS

CONFIDENTIAL

PROJECT NO.: TR.1300179

REPORT NO.: MPR/14/114

BY: Y. SCHARNECK AND S. BRAMDEO

MAY 2014

Research
8 Schonland Street, Theta, Johannesburg 2091, South Africa
P.O. Box106, Crown Mines2025, South Africa
Tel: +27 11 377 4600
Fax: +27 11 835 1314
E-mail: info.research@angloamerican.com

**CONFIDENTIAL**

# MINERALOGICAL INVESTIGATION OF IRON ORE FLOTATION FEEDs

**REPORT NO. : MPR/14/114**


| | | |
|---|---|---|
| CLIENT | : | M. Kruger (University of Pretoria) |
| REPORTED BY | : | Y. Scharneck and S. Bramdeo |
| DEPARTMENT | : | Minerals and Process Research |
| INVESTIGATOR(S) | : | Y. Scharneck<br>S. Bramdeo<br>S. Mamabolo<br>T. Mohatjo |
| HEAD OF DEPARTMENT | : | Dr R. Schouwstra |
| DATE DISTRIBUTED | : | May 2014 |
| PROJECT No. | : | TR.1300179 |
| KEYWORDS | : | Flotation, hematite, liberation, association |

**P. Hey**
Manager –Base Metals and Research commodities


**DISTRIBUTION**

| | | |
|---|---|---|
| Mr R. De Pretto | Dr R. Schouwstra | Mr S. Naik |
| Mr M. Kruger | TKL/File | |

# MINERALOGICAL INVESTIGATION OF IRON ORE FLOTATION FEEDS

## SUMMARY

Flotation test work was carried out at the University of Pretoria by Morné Kruger as part of an MSc thesis. Two flotation feed samples, namely a flotation feed and a milled flotation feed were submitted for mineralogical analysis. The milled flotation feed was derived from the flotation feed by removing the -38µm and the balance (+38 µm fraction) was milled before submitting for mineralogical analysis. The aim of this investigation is to determine bulk mineralogy, hematite and gangue mineral liberation, association and grain size distribution

Both samples have very similar mineralogical compositions. The flotation feed contains ~98 % hematite and ~1 % quartz, whilst the milled flotation feed contains ~95 % hematite and ~3 % quartz.

The flotation feed sample is slightly coarser than milled flotation feed sample with the average hematite grain size at 26 µm and 19 µm respectively. Similarly the average grain size of the gangue in the flotation feed is 37 µm, whist in the milled flotation feed the average gangue grain size is 18 µm.

The milled flotation feed has a higher proportion of liberated gangue with 41 % of the gangue reporting to the 95-100 liberation category. The flotation feed contained only 26 % gangue reporting to the 95-100 liberation category. The unliberated gangue is mainly associated with hematite.

# MINERALOGICAL INVESTIGATION OF IRON ORE FLOTATION FEEDS

# MINERALOGICAL INVESTIGATION OF IRON ORE FLOTATION FEEDS

## 1 INTRODUCTION

Flotation test work was carried out at the University of Pretoria by Morné Kruger as part of an MSc thesis. Two flotation feed samples were submitted for mineralogical analysis. The first sample being a flotation feed sample and the second sample (milled flotation feed). The milled flotation feed was produced by screening the flotation feed sample at 38 µm; discarding the -38 µm portion and the balance was milled. The milled sample was submitted for mineralogy and was screened at 25 µm for mineralogical analysis. The aim of this investigation is to determine bulk modal mineralogy, hematite and gangue mineral liberation, association and grain size distribution.

## 2 METHODOLOGY

The feed sample was split into representative portions and screened into the following size fractions; +75 µm, +25 µm and -25 µm. The milled feed sample was screened into a +25 µm and -25 µm fraction. Polished sections from the individual size fractions were prepared and analysed using the MLA.

The MLA uses energy dispersed spectra (EDS) from X-rays produced by the sample when it interacts with an electron beam. These X-rays give the chemical composition and together with backscattered electron intensity of the mineral phases, mineral maps are produced which are used to characterize the material. There was insufficient sample to validate the results with XRD or chemistry

## 3 MINERALOGICAL RESULTS

### 3.1 Bulk Mineralogy

The bulk modal mineralogy of the feed and milled feed is presented in Table 1 and in Figure 1. The mineral phases identified include hematite ($Fe_2O_3$), quartz ($SiO_2$), kaolinite ($Al_2Si_2O_5(OH)_4$), and chlorite ($(Mg,Fe)_5Al(Si_3Al)O_{10}(OH)_8$) as well as other minor quartz phases.

*Table 1: Bulk modal mineralogy for the flotation feed and the milled feed sample.*

| | Flotation Feed Sample | | | | Milled Flotation Feed Sample | | |
|---|---|---|---|---|---|---|---|
| Mineral | Combined | +75 µm | +25 µm | -25 µm | Combined | +25 µm | -25 µm |
| Hematite | 97.68 | 95.56 | 97.11 | 98.82 | 95.46 | 96.14 | 95.42 |
| Quartz | 1.38 | 2.84 | 1.73 | 0.61 | 3.01 | 2.08 | 3.06 |
| Kaolinite | 0.13 | 0.30 | 0.15 | 0.06 | 0.16 | 0.23 | 0.16 |
| Chlorite | 0.42 | 0.69 | 0.53 | 0.25 | 0.92 | 1.09 | 0.91 |
| Other | 0.39 | 0.61 | 0.48 | 0.25 | 0.45 | 0.46 | 0.45 |
| Total | 100.00 | 100.00 | 100.00 | 100.00 | 100.00 | 100.00 | 100.00 |
| PSD | 100.00 | 18.89 | 31.11 | 50.00 | 100.00 | 5.28 | 94.72 |

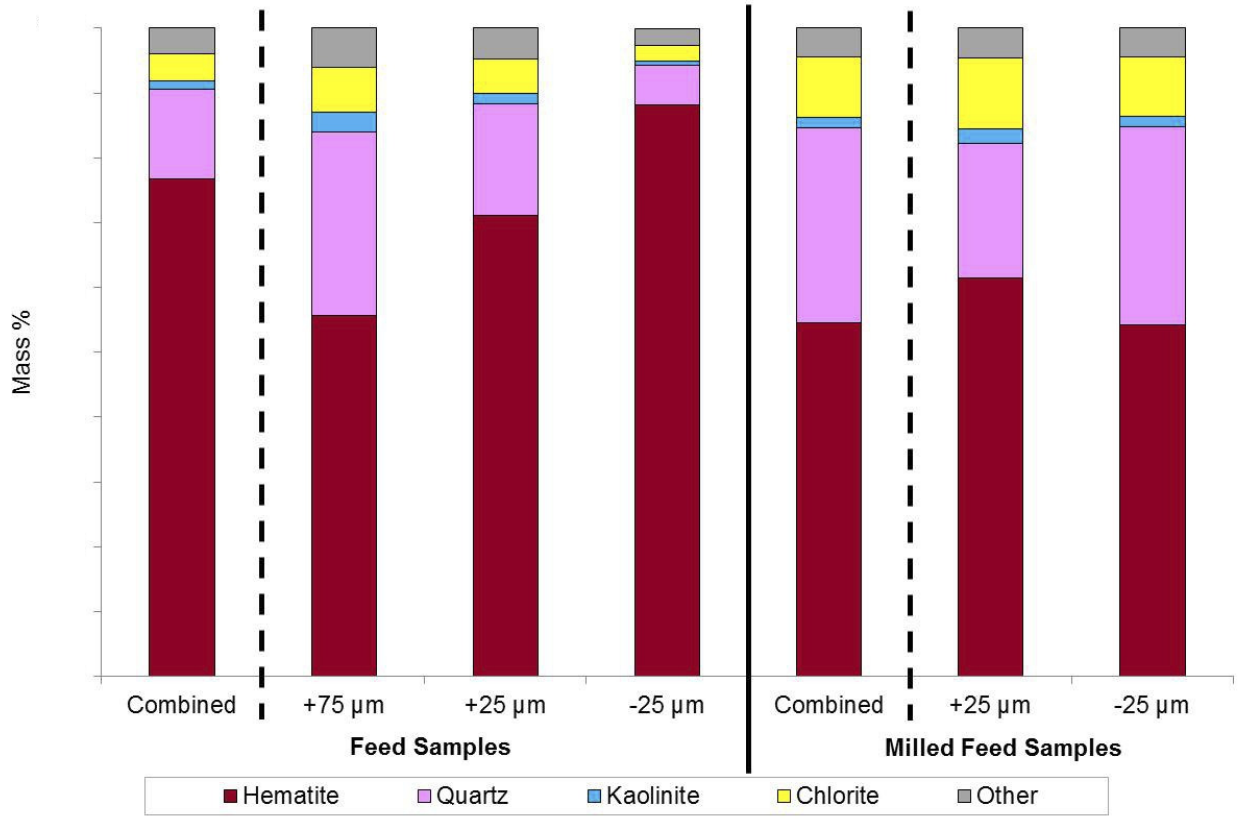


*Figure 1: Bulk modal mineralogy for the flotation feed sample. Note that the y-axis starts at 90 %.*

### 3.2 Mass percent in liberation class

The mass percent of the sample in each liberation class together with the calculated chemistry from the MLA bulk modal data (in mass percent and mass) as well as the grade and bulk modal mineralogy per density category for the flotation feed and the milled flotation feed (including size fractions) are shown in *Appendices I and II*. These tables also depict the proportion of minerals reporting to each liberation class. The elemental (Fe, Si, Al, K, P and Mn) distribution represents the actual elemental percent present in each liberation class. The elemental deportment denotes the total mass percent of the element present in the sample, distributed amongst the liberation classes. Mass elemental distribution presents the normalised elemental distribution between the liberation classes. Please note that values of 0.0 denote values that are <0.1. The density in each liberation class was calculated based on the minerals present.

### 3.3 Grade and yield vs. hematite liberation charts

The Fe grade (mass percent) and the yield (mass percent) were plotted for each liberation class in the flotation feed and milled flotation feed samples and are presented in *Appendices I and II*.

### 3.4 Grade and bulk modal mineralogy per density class

The elemental Fe and Si grade as well as modal mineralogy *vs.* density class data is presented in *Appendices I to II*.

### 3.5 Liberation vs. grain size distribution

Liberation is calculated in terms of the area percentage of the mineral of interest present in a particle. For example particles occurring in the 0-10 % liberation class will have particles that contain less than 10 area percent of the mineral of interest. The bar charts depict the measured sectional area of particles in each liberation class.

Note that the size given refers to instrument-measured sectional area of a grain (not screen sizes). The grain size is calculated based on the equivalent circle diameter (ECD) method, which uses the calculated diameter of a circle that would have an area equivalent to the sectional area of the grain measured. For the benefit of graphical representation liberation is expressed at 20 % liberation intervals based on the percentage the mineral of interest a particle contains.

The hematite liberation vs. grain size distribution charts for the flotation feed and the milled flotation feed is presented in Figure 2 and 3. The gangue mineral liberation vs. grain size distribution for the flotation feed and milled flotation feed sample is presented in Figure 4 and 5.

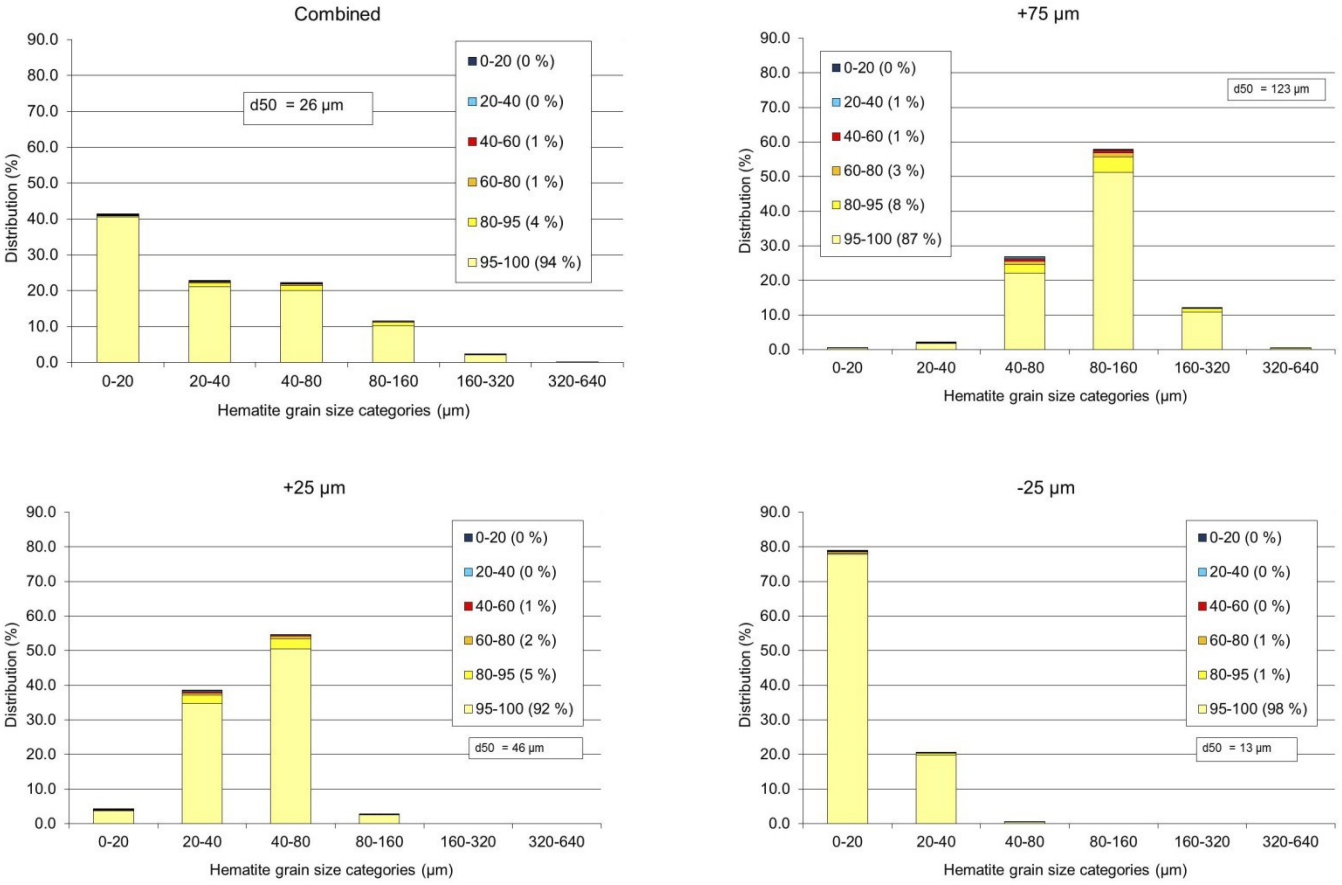


*Figure 2: Hematite liberation vs. grain size distribution for the flotation feed sample.*

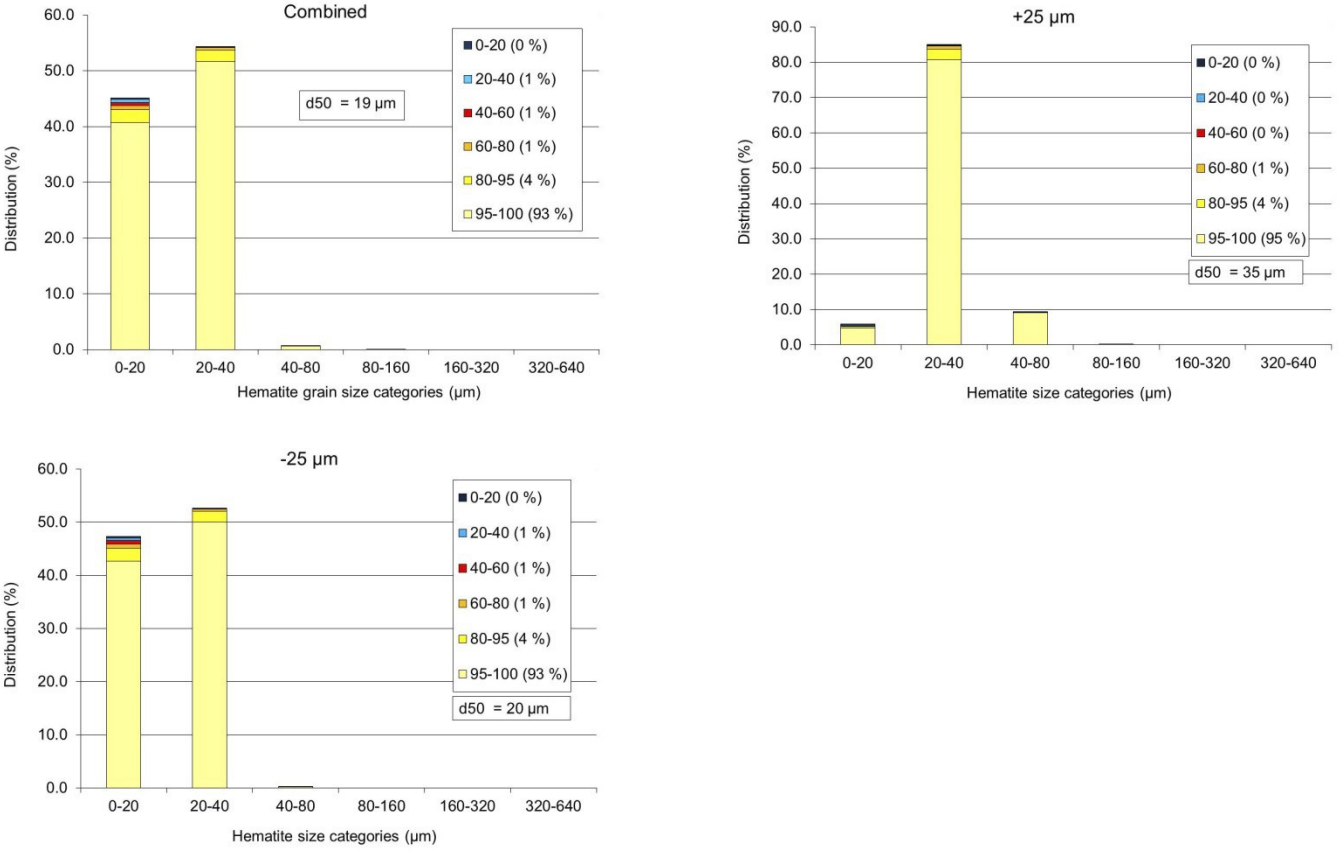


*Figure 3: Hematite liberation vs. grain size distribution for the milled flotation feed sample*

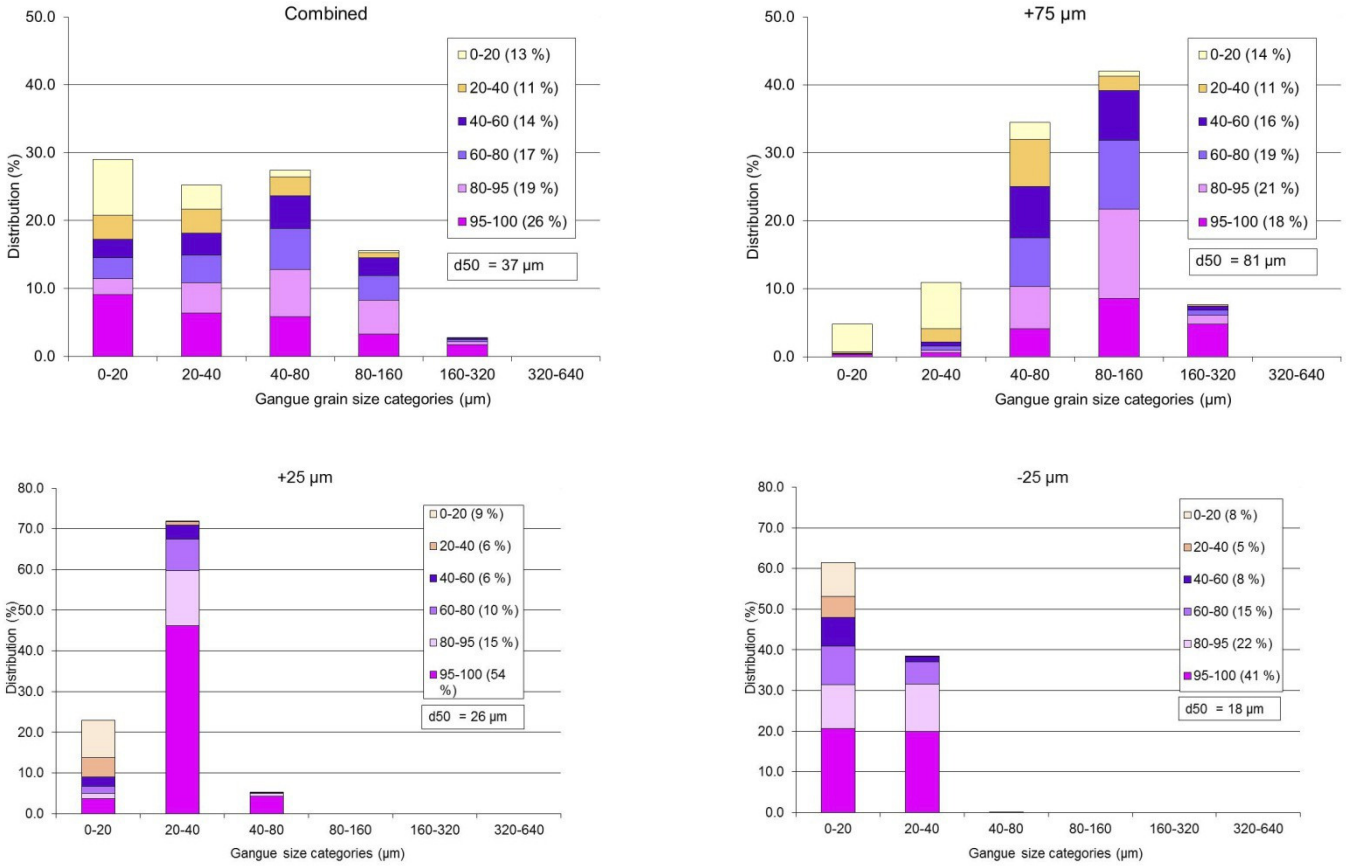


*Figure 4: Gangue liberation vs. grain size distribution for the flotation feed sample.*

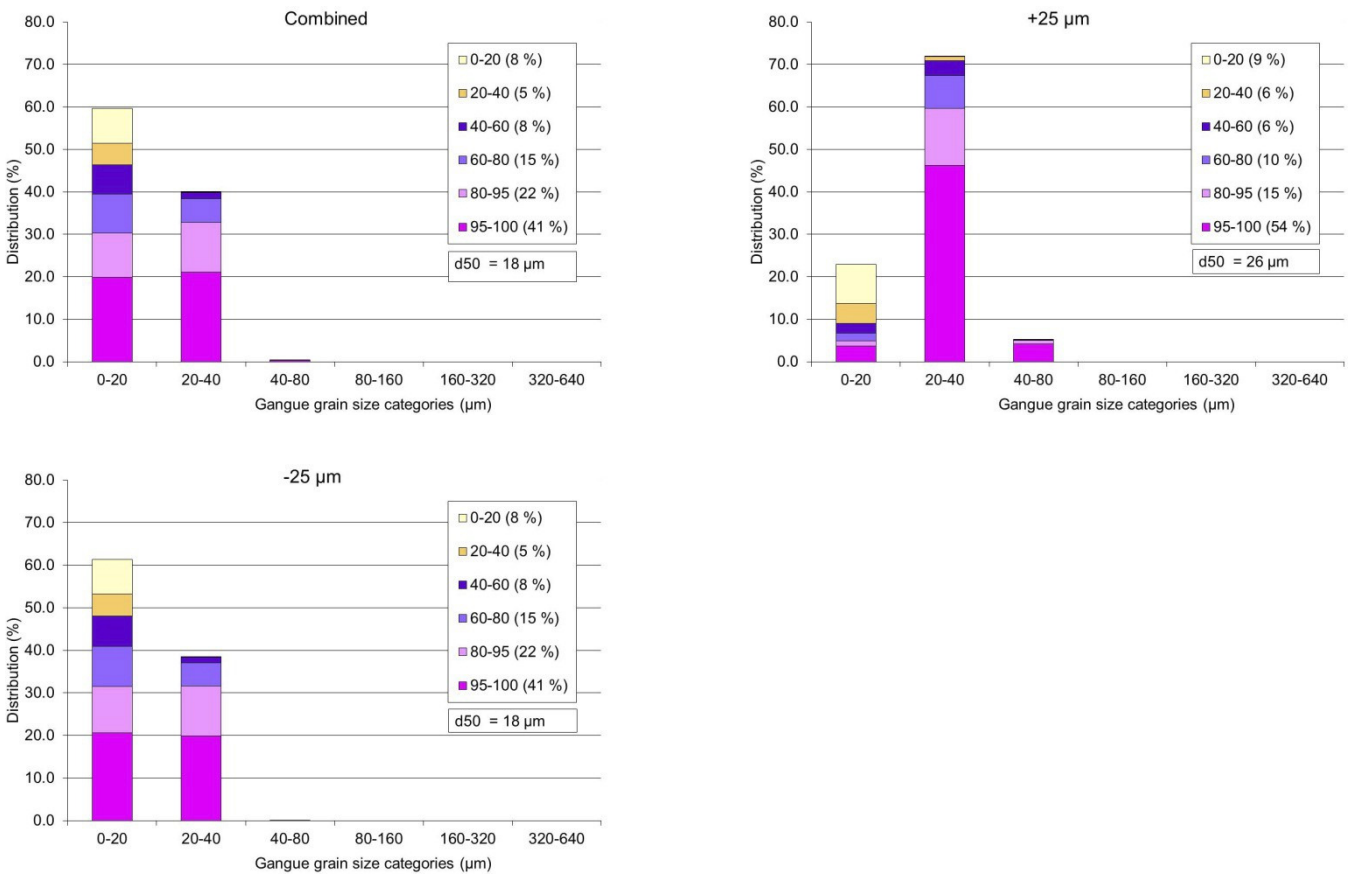


*Figure 5: Gangue liberation vs. grain size distribution for the milled flotation feed sample.*

### 3.6 Cumulative liberation

The cumulative hematite liberation for the flotation feed and the milled flotation feed is presented in Figure 6. The cumulative gangue liberation for the flotation feed and the milled flotation feed is presented in Figure 7.

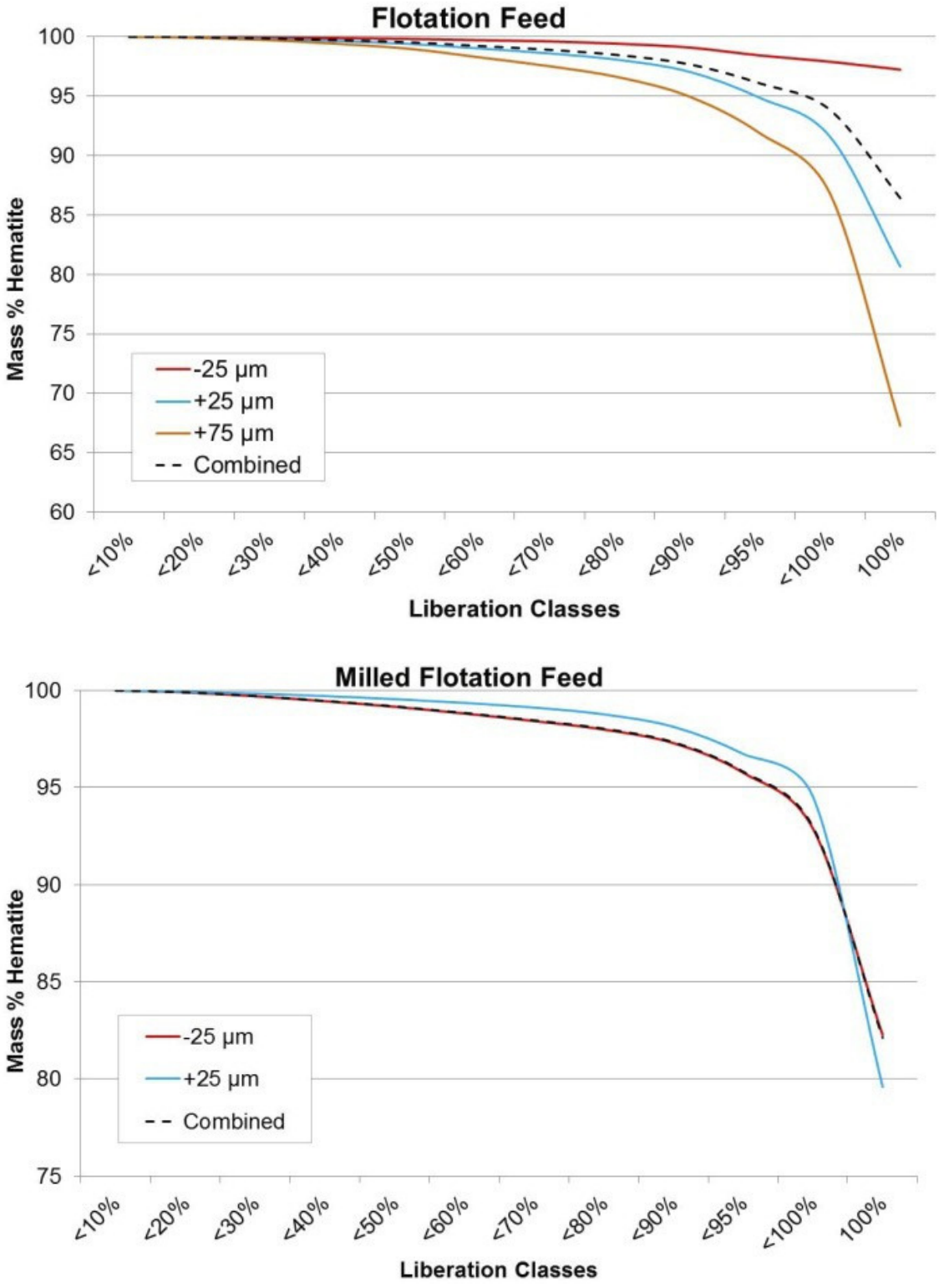


*Figure 6: Cumulative hematite liberation.*

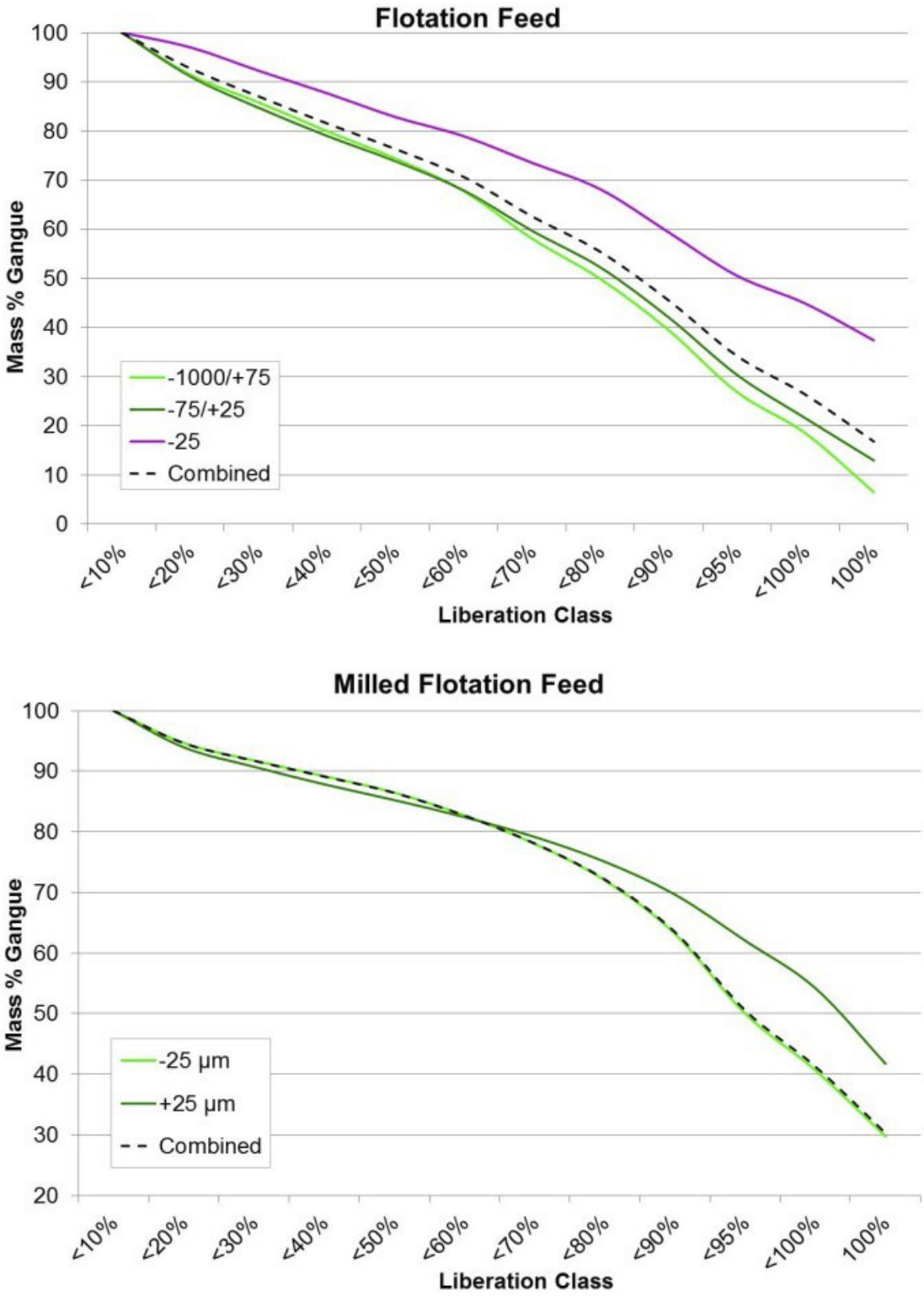


*Figure 7: Cumulative gangue liberation.*

### 3.7 Hematite Mineral Association

Hematite mineral association is calculated in terms of hematite deportment. Hematite in the 95-100 category contains >95 area percent hematite in a particle whilst a binary phase (e.g. hematite+kaolinite) contains only two mineral phases. The 'Other' association

category refers to complex particles where hematite is associated with two or more gangue minerals.

The hematite association data for the flotation feed and milled flotation feed samples is given in Tables 2 and 3 respectively and presented in Figures 8 and 9.

*Table 2: Hematite association for the flotation feed sample.*

| Sample | +75 µm | +25 µm | -25 µm | Combined |
|---|---|---|---|---|
| Hematite >95 | 86.77 | 91.58 | 97.90 | 93.89 |
| Hematite 80-95 | 8.18 | 5.47 | 1.19 | 3.81 |
| Hematite+quartz | 3.43 | 1.82 | 0.41 | 1.40 |
| Hematite+kaolinite | 0.33 | 0.21 | 0.04 | 0.15 |
| Hematite+chlorite | 0.66 | 0.50 | 0.32 | 0.44 |
| Ternary | 0.63 | 0.42 | 0.13 | 0.32 |
| Total | 100.00 | 100.00 | 100.00 | 100.00 |

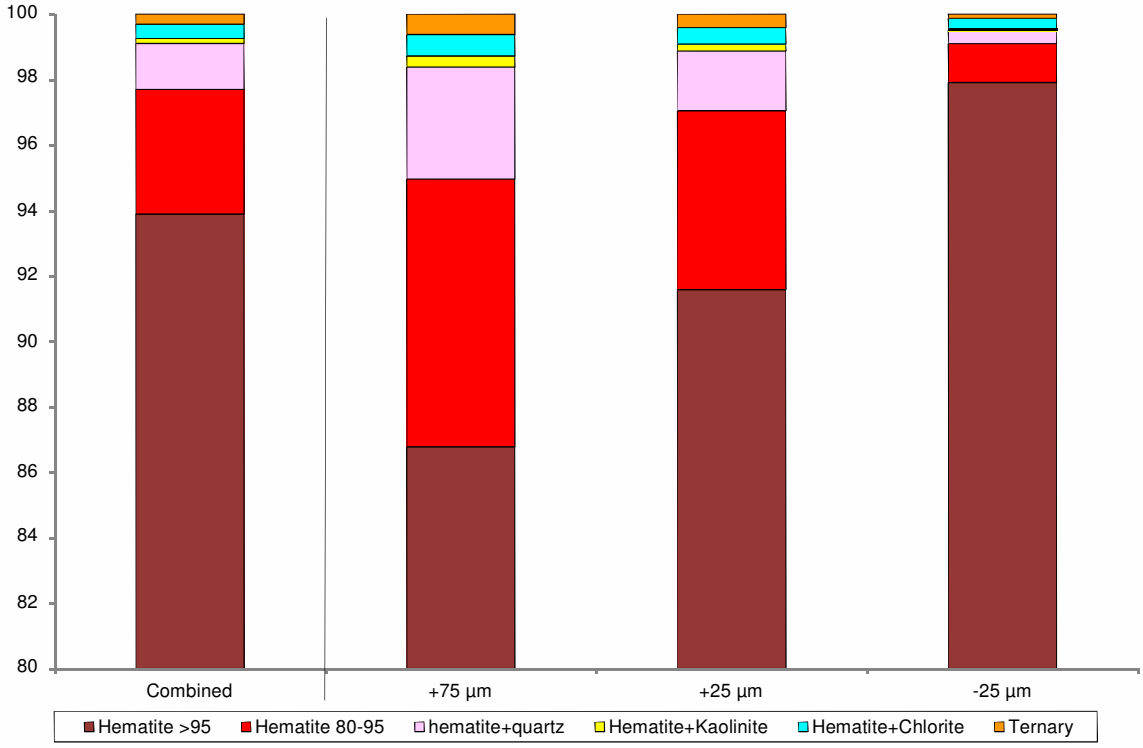


*Figure 8: Hematite association for the flotation feed sample. Note that the y-axis starts at 80 %.*

*Table 3: Hematite association for the milled flotation feed sample.*

| Sample | +25 µm | -25 µm | Combined |
|---|---|---|---|
| Hematite >95 | 94.54 | 92.89 | 92.98 |
| Hematite 80-95 | 3.60 | 4.41 | 4.35 |
| Hematite+quartz | 0.96 | 1.87 | 1.84 |
| Hematite+Kaolinite | 0.10 | 0.06 | 0.06 |
| Hematite+Chlorite | 0.60 | 0.52 | 0.52 |
| Ternary | 0.20 | 0.25 | 0.25 |
| Total | 100.00 | 100.00 | 100.00 |

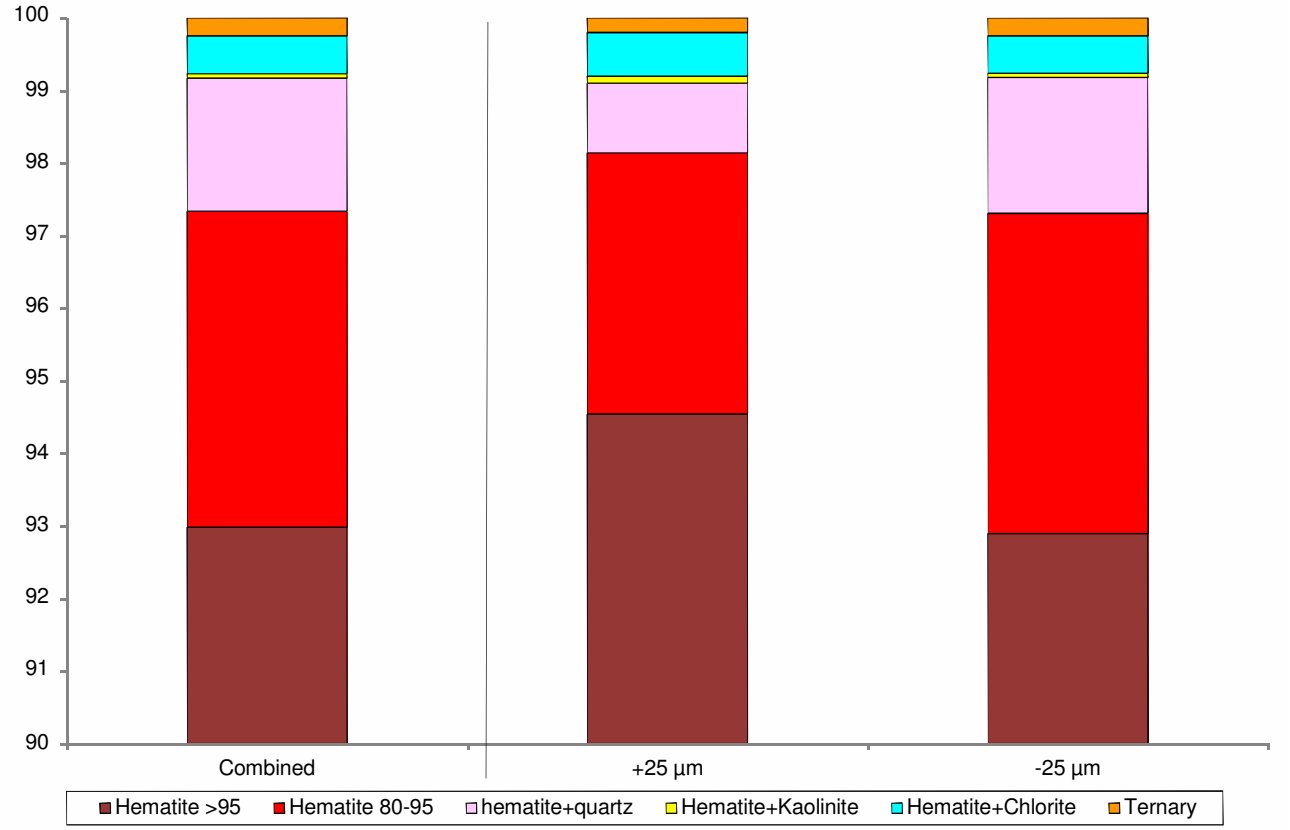


*Figure 9: Hematite association for the milled flotation feed sample. Note that the y-axis starts at 90 %.*

## 3.8 Gangue Mineral Association

Gangue mineral association is calculated in terms of gangue deportment. Gangue in the 95-100 category contains >95 area percent gangue in a particle whilst binary phase (*e.g.* gangue+hematite) contain only two mineral phases.

The gangue association data for the flotation feed and milled flotation feed samples is given in Tables 4 and 5 respectively and presented in Figures 10 and 11.

*Table 4: Gangue association for the flotation feed sample.*

| Sample | +75 µm | +25 µm | -25 µm | Combined |
|---|---|---|---|---|
| Gangue >95 | 18.50 | 21.56 | 44.89 | 26.36 |
| Gangue 80-95 | 20.97 | 20.51 | 14.48 | 19.15 |
| Quartz+hematite | 37.45 | 31.99 | 17.81 | 30.37 |
| Chlorite+hematite | 12.81 | 14.90 | 13.85 | 13.88 |
| Gangue+ hematite | 10.27 | 11.04 | 8.97 | 10.24 |
| Total | 100.00 | 100.00 | 100.00 | 100.00 |

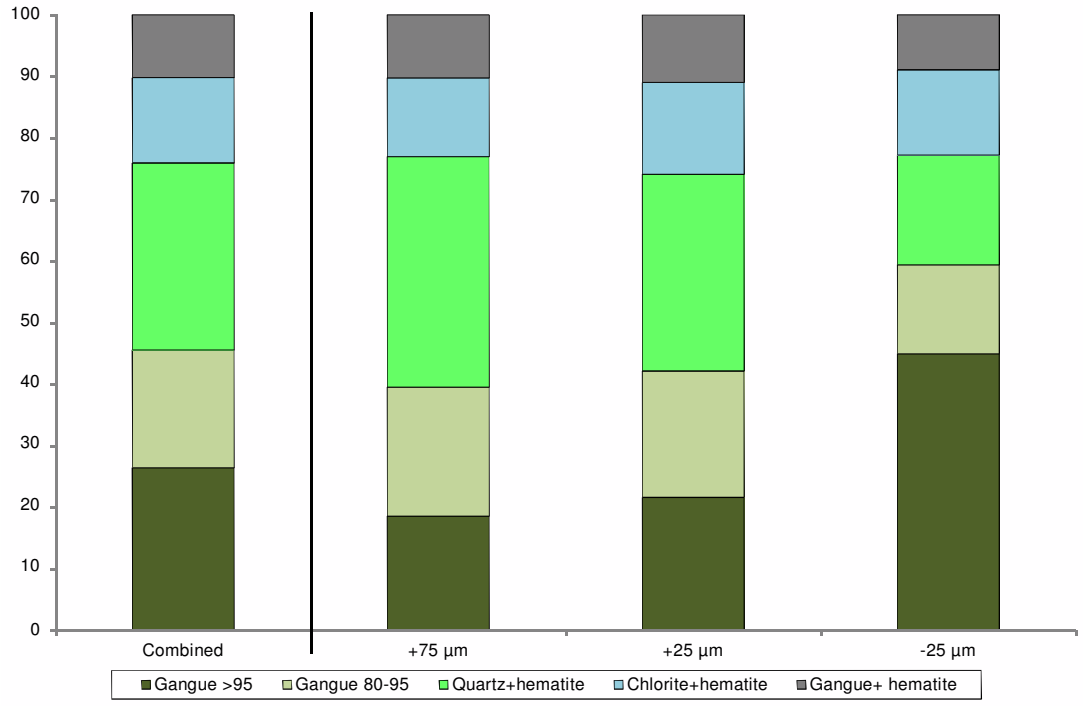


*Figure 10: Gangue association for the flotation feed sample.*

*Table 5: Gangue association for the milled flotation feed sample.*

| Sample | +25 µm | -25 µm | Combined |
|---|---|---|---|
| Gangue >95 | 54.22 | 40.68 | 41.27 |
| Gangue 80-95 | 15.45 | 22.50 | 22.19 |
| Quartz+hematite | 13.94 | 23.89 | 23.46 |
| Chlorite+hematite | 12.58 | 8.85 | 9.01 |
| Gangue+ hematite | 3.82 | 4.08 | 4.07 |
| Total | 100.00 | 100.00 | 100.00 |

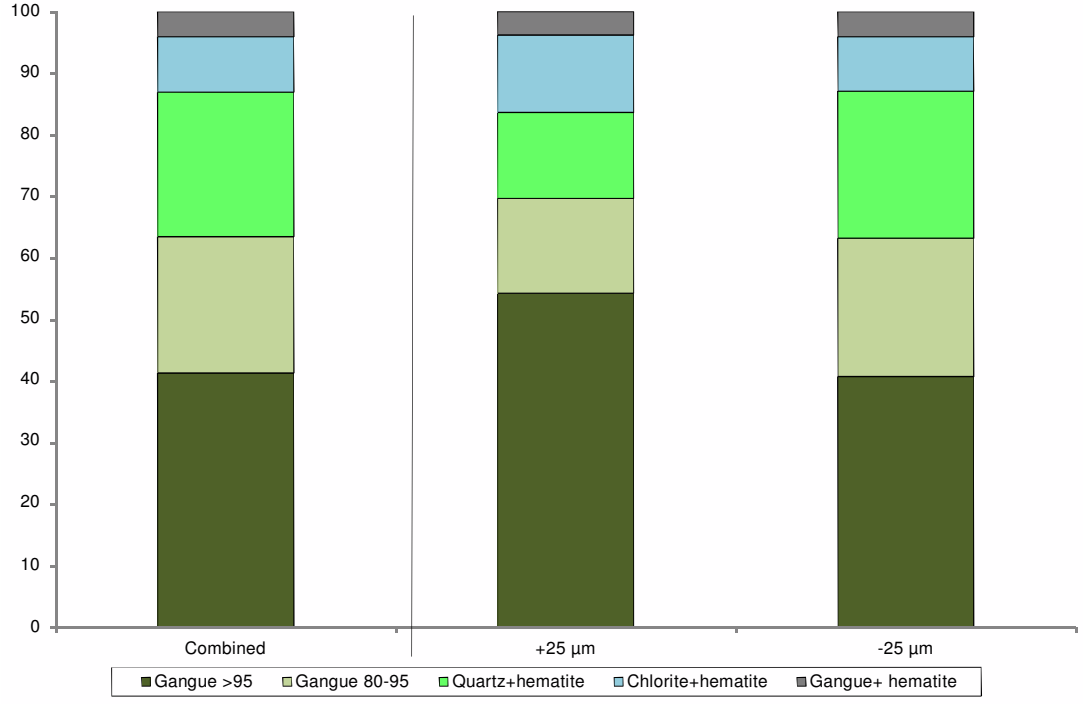


*Figure 11: Gangue association for the milled flotation feed sample.*

# 4 COMMENTS

- Both samples have very similar mineral compositions. The flotation feed sample comprises ~98 % hematite and ~1 % quartz. The milled flotation feed sample contains ~95 % hematite and ~3 % quartz.
- The hematite liberation by hematite grain sizes shows that the flotation feed sample is slightly coarser than milled flotation feed sample with the average grain size at 26 µm and 19 µm respectively.
- The gangue liberation by gangue grain size shows a similar trend, with the average grain size of the gangue in flotation feed at 37 µm and the average grain size of the milled flotation feed at 18 µm.
- The milled flotation feed has a higher proportion of liberated gangue with 41 % of the gangue reporting to the 95-100 liberation category. The flotation feed contained only 26 % gangue reporting to the 95-100 liberation category.
- The unliberated gangue is mainly associated with hematite.

# APPENDICES

APPENDIX I - Flotation Feed Sample

**Mass percent in liberation class - Hematite**

*Table i: Hematite liberation data for flotation feed sample (Combined Head).*

| | Hematite liberation class | | | | | | | | | | |
|---|---|---|---|---|---|---|---|---|---|---|---|
| | Combined | <10 | <20 | <30 | <40 | <50 | <60 | <70 | <80 | <90 | >90 |
| % Fe Distribution | 68.38 | 4.74 | 19.60 | 28.50 | 37.02 | 43.69 | 50.21 | 55.42 | 60.08 | 64.63 | 69.83 |
| Fe deportment | 68.38 | 0.04 | 0.07 | 0.11 | 0.13 | 0.21 | 0.22 | 0.31 | 0.53 | 1.09 | 65.67 |
| Mass Fe Distribution | 100.00 | 0.06 | 0.10 | 0.16 | 0.19 | 0.31 | 0.32 | 0.45 | 0.77 | 1.59 | 96.04 |
| % Si Distribution | 0.77 | 33.96 | 27.39 | 21.63 | 16.09 | 13.10 | 9.75 | 6.69 | 4.48 | 2.06 | 0.04 |
| Si deportment | 0.77 | 0.28 | 0.10 | 0.08 | 0.06 | 0.06 | 0.04 | 0.04 | 0.04 | 0.03 | 0.04 |
| Mass Si Distribution | 100.00 | 36.58 | 12.48 | 10.49 | 7.21 | 8.35 | 5.55 | 4.88 | 5.12 | 4.51 | 4.81 |
| % Al Distribution | 0.08 | 2.26 | 2.10 | 1.91 | 1.86 | 1.23 | 1.11 | 0.86 | 0.58 | 0.40 | 0.01 |
| Al deportment | 0.08 | 0.02 | 0.01 | 0.01 | 0.01 | 0.01 | 0.00 | 0.00 | 0.01 | 0.01 | 0.01 |
| Mass Al Distribution | 100.00 | 24.00 | 9.42 | 9.12 | 8.22 | 7.70 | 6.21 | 6.15 | 6.54 | 8.65 | 13.99 |
| % K Distribution | 0.01 | 0.22 | 0.24 | 0.36 | 0.28 | 0.24 | 0.25 | 0.16 | 0.11 | 0.08 | 0.00 |
| K deportment | 0.01 | 0.00 | 0.00 | 0.00 | 0.00 | 0.00 | 0.00 | 0.00 | 0.00 | 0.00 | 0.00 |
| Mass K Distribution | 100.00 | 14.09 | 6.45 | 10.43 | 7.45 | 9.00 | 8.37 | 7.05 | 7.40 | 10.25 | 19.50 |
| % P Distribution | 0.03 | 0.76 | 0.40 | 0.72 | 0.73 | 0.66 | 0.34 | 0.43 | 0.32 | 0.21 | 0.00 |
| P deportment | 0.03 | 0.01 | 0.00 | 0.00 | 0.00 | 0.00 | 0.00 | 0.00 | 0.00 | 0.00 | 0.00 |
| Mass P Distribution | 100.00 | 20.55 | 4.56 | 8.71 | 8.22 | 10.64 | 4.80 | 7.79 | 9.27 | 11.79 | 13.68 |
| Density | 5.19 | 2.78 | 3.06 | 3.36 | 3.62 | 3.90 | 4.14 | 4.41 | 4.67 | 4.95 | 5.29 |
| Mineral mass percent | | | | | | | | | | | |
| Hematite | 97.68 | 0.04 | 0.09 | 0.15 | 0.18 | 0.30 | 0.31 | 0.44 | 0.75 | 1.55 | 93.87 |
| Quartz | 1.38 | 0.54 | 0.18 | 0.15 | 0.10 | 0.12 | 0.07 | 0.06 | 0.07 | 0.05 | 0.04 |
| Kaolinite | 0.13 | 0.04 | 0.02 | 0.02 | 0.02 | 0.01 | 0.01 | 0.01 | 0.01 | 0.01 | 0.01 |
| Chlorite | 0.42 | 0.07 | 0.04 | 0.03 | 0.03 | 0.03 | 0.03 | 0.03 | 0.03 | 0.05 | 0.09 |
| Other | 0.39 | 0.14 | 0.03 | 0.03 | 0.03 | 0.03 | 0.02 | 0.02 | 0.02 | 0.03 | 0.04 |
| Total | 100.00 | 0.83 | 0.35 | 0.37 | 0.34 | 0.49 | 0.44 | 0.56 | 0.88 | 1.68 | 94.05 |
| Normalized mineral mass percent | | | | | | | | | | | |
| Hematite | 100.00 | 0.04 | 0.09 | 0.15 | 0.18 | 0.31 | 0.32 | 0.45 | 0.77 | 1.58 | 96.11 |
| Quartz | 100.00 | 39.17 | 13.10 | 10.78 | 7.13 | 8.49 | 5.40 | 4.64 | 4.84 | 3.66 | 2.79 |
| Kaolinite | 100.00 | 29.60 | 11.46 | 11.86 | 11.59 | 8.42 | 5.92 | 5.34 | 5.59 | 5.50 | 4.71 |
| Chlorite | 100.00 | 17.19 | 9.00 | 7.49 | 6.50 | 7.50 | 6.34 | 6.86 | 7.57 | 11.04 | 20.50 |
| Other | 100.00 | 35.33 | 6.64 | 8.00 | 6.72 | 7.77 | 5.05 | 5.59 | 6.06 | 8.12 | 10.72 |

**Grade and yield vs. hematite liberation.**

*Table ii: Mass percent cumulative Fe and mass percent cumulative sample yield versus hematite liberation class for flotation feed sample (Combined Head).*

| Discrete Analysis | | | | | | | | | | | |
|---|---|---|---|---|---|---|---|---|---|---|---|
| %Liberation | Combined | <10 | 10-20 | 20-30 | 30-40 | 40-50 | 50-60 | 60-70 | 70-80 | 80-90 | >90 |
| %Fe | 68.38 | 4.74 | 19.60 | 28.50 | 37.02 | 43.69 | 50.21 | 55.42 | 60.08 | 64.63 | 69.83 |
| %Si | 0.77 | 33.96 | 27.39 | 21.63 | 16.09 | 13.10 | 9.75 | 6.69 | 4.48 | 2.06 | 0.04 |
| Mass%(yield) | 100.00 | 0.83 | 0.35 | 0.37 | 0.34 | 0.49 | 0.44 | 0.56 | 0.88 | 1.68 | 94.05 |
| Density of Fraction | 5.19 | 2.78 | 3.06 | 3.36 | 3.62 | 3.90 | 4.14 | 4.41 | 4.67 | 4.95 | 5.29 |
| Cumulative Analysis | | | | | | | | | | | |
| Cumulative % Fe | | 68.38 | 68.91 | 69.08 | 69.24 | 69.35 | 69.48 | 69.57 | 69.65 | 69.74 | 69.83 |
| Cumulative % Si | | 0.77 | 0.49 | 0.40 | 0.32 | 0.26 | 0.20 | 0.15 | 0.12 | 0.07 | 0.04 |
| Cumulative mass % (yield) | | 100.00 | 99.17 | 98.82 | 98.45 | 98.10 | 97.61 | 97.17 | 96.61 | 95.73 | 94.05 |

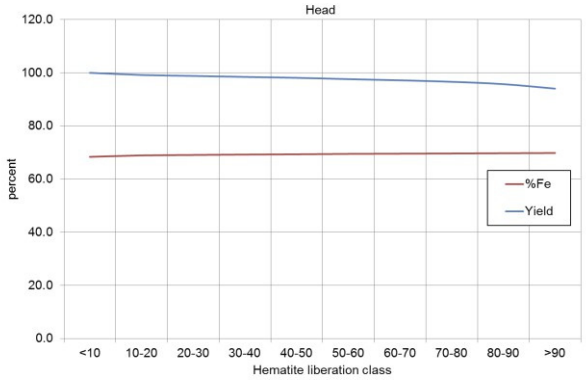


**Mass percent in density class**

*Table iii: Mass percent in density class together with elemental mass percent Fe and Si for flotation feed sample (Combined Head).*

| Density Class | | | | | | | | | | | | | | | |
|---|---|---|---|---|---|---|---|---|---|---|---|---|---|---|---|
| | <2.6 | <2.8 | <3.0 | <3.2 | <3.4 | <3.6 | <3.8 | <4.0 | <4.2 | <4.4 | <4.6 | <4.8 | <5.0 | <5.2 | >5.2 |
| % Fe | 3.26 | 3.08 | 13.82 | 21.69 | 28.88 | 32.09 | 39.17 | 44.79 | 49.69 | 52.23 | 56.72 | 59.97 | 63.64 | 67.32 | 69.83 |
| % Si | 5.25 | 41.34 | 32.03 | 28.45 | 22.19 | 18.16 | 15.91 | 13.92 | 10.56 | 8.49 | 6.07 | 4.19 | 2.33 | 0.79 | 0.03 |
| Average Density | 2.55 | 2.66 | 2.89 | 3.09 | 3.30 | 3.50 | 3.71 | 3.90 | 4.10 | 4.30 | 4.51 | 4.71 | 4.91 | 5.13 | 5.30 |
| Mineral mass percent | | | | | | | | | | | | | | | |
| Hematite | 0.00 | 0.01 | 0.05 | 0.07 | 0.10 | 0.12 | 0.16 | 0.21 | 0.23 | 0.29 | 0.41 | 0.60 | 1.02 | 3.55 | 90.84 |
| Quartz | 0.00 | 0.44 | 0.17 | 0.13 | 0.10 | 0.08 | 0.08 | 0.08 | 0.06 | 0.06 | 0.05 | 0.05 | 0.04 | 0.03 | 0.01 |
| Kaolinite | 0.00 | 0.03 | 0.01 | 0.01 | 0.01 | 0.01 | 0.01 | 0.01 | 0.01 | 0.00 | 0.01 | 0.01 | 0.01 | 0.01 | 0.00 |
| Chlorite | 0.00 | 0.05 | 0.04 | 0.02 | 0.03 | 0.02 | 0.02 | 0.02 | 0.02 | 0.02 | 0.03 | 0.03 | 0.03 | 0.06 | 0.03 |
| Other | 0.00 | 0.01 | 0.02 | 0.03 | 0.01 | 0.04 | 0.02 | 0.02 | 0.02 | 0.04 | 0.03 | 0.04 | 0.04 | 0.05 | 0.03 |
| Total | 0.00 | 0.55 | 0.29 | 0.26 | 0.26 | 0.28 | 0.30 | 0.33 | 0.34 | 0.41 | 0.52 | 0.71 | 1.13 | 3.70 | 90.92 |

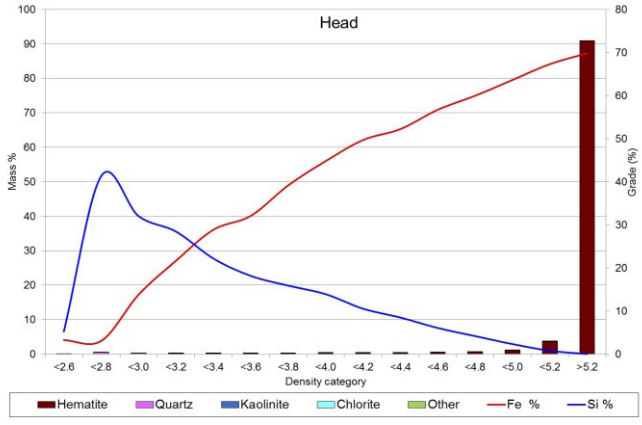

APPENDIX I - Flotation Feed Sample

**Mass percent in liberation class - Hematite**

*Table iv: Hematite liberation data for flotation feed sample (+75 µm).*

| | Hematite liberation class | | | | | | | | | | |
|---|---|---|---|---|---|---|---|---|---|---|---|
| | Combined | <10 | <20 | <30 | <40 | <50 | <60 | <70 | <80 | <90 | >90 |
| % Fe Distribution | 66.93 | 5.30 | 19.16 | 29.05 | 37.63 | 43.58 | 50.24 | 55.33 | 59.90 | 64.50 | 69.66 |
| Fe deportment | 66.93 | 0.07 | 0.14 | 0.22 | 0.28 | 0.49 | 0.51 | 0.64 | 1.09 | 2.07 | 61.43 |
| Mass Fe Distribution | 100.00 | 0.10 | 0.21 | 0.33 | 0.42 | 0.73 | 0.76 | 0.95 | 1.63 | 3.09 | 91.78 |
| % Si Distribution | 1.55 | 35.51 | 27.95 | 23.08 | 17.60 | 14.09 | 10.52 | 7.38 | 4.76 | 2.23 | 0.09 |
| Si deportment | 1.55 | 0.45 | 0.21 | 0.17 | 0.13 | 0.16 | 0.11 | 0.09 | 0.09 | 0.07 | 0.08 |
| Mass Si Distribution | 100.00 | 28.91 | 13.40 | 11.28 | 8.44 | 10.22 | 6.84 | 5.49 | 5.59 | 4.63 | 5.20 |
| % Al Distribution | 0.14 | 0.02 | 0.01 | 0.02 | 0.01 | 0.01 | 0.01 | 0.01 | 0.01 | 0.01 | 0.03 |
| Al deportment | 0.14 | 0.02 | 0.01 | 0.02 | 0.01 | 0.01 | 0.01 | 0.01 | 0.01 | 0.01 | 0.03 |
| Mass Al Distribution | 100.00 | 16.36 | 9.80 | 11.03 | 9.72 | 8.05 | 6.97 | 6.27 | 6.22 | 7.80 | 17.77 |
| % K Distribution | 0.02 | 0.00 | 0.00 | 0.00 | 0.00 | 0.00 | 0.00 | 0.00 | 0.00 | 0.00 | 0.01 |
| K deportment | 0.02 | 0.00 | 0.00 | 0.00 | 0.00 | 0.00 | 0.00 | 0.00 | 0.00 | 0.00 | 0.01 |
| Mass K Distribution | 100.00 | 11.20 | 6.59 | 10.72 | 6.62 | 8.58 | 9.74 | 7.56 | 5.89 | 8.50 | 24.60 |
| % P Distribution | 0.05 | 0.00 | 0.00 | 0.00 | 0.00 | 0.01 | 0.00 | 0.00 | 0.01 | 0.01 | 0.01 |
| P deportment | 0.05 | 0.00 | 0.00 | 0.00 | 0.00 | 0.01 | 0.00 | 0.00 | 0.01 | 0.01 | 0.01 |
| Mass P Distribution | 100.00 | 6.72 | 8.96 | 0.40 | 3.25 | 13.12 | 5.38 | 7.09 | 14.35 | 16.71 | 24.02 |
| Density | 5.08 | 2.75 | 3.04 | 3.31 | 3.55 | 3.88 | 4.13 | 4.39 | 4.67 | 4.95 | 5.28 |
| | Mineral mass percent | | | | | | | | | | |
| Hematite | 95.56 | 0.08 | 0.19 | 0.30 | 0.39 | 0.69 | 0.72 | 0.90 | 1.55 | 2.95 | 87.79 |
| Quartz | 2.84 | 0.88 | 0.40 | 0.32 | 0.24 | 0.30 | 0.19 | 0.15 | 0.16 | 0.12 | 0.08 |
| Kaolinite | 0.30 | 0.07 | 0.04 | 0.04 | 0.04 | 0.02 | 0.02 | 0.02 | 0.02 | 0.02 | 0.02 |
| Chlorite | 0.69 | 0.07 | 0.06 | 0.06 | 0.05 | 0.06 | 0.05 | 0.04 | 0.05 | 0.07 | 0.19 |
| Other | 0.61 | 0.16 | 0.05 | 0.03 | 0.02 | 0.05 | 0.03 | 0.04 | 0.05 | 0.06 | 0.11 |
| Total | 100.00 | 1.26 | 0.74 | 0.76 | 0.74 | 1.12 | 1.01 | 1.15 | 1.82 | 3.21 | 88.18 |
| | Normalized mineral mass percent | | | | | | | | | | |
| Hematite | 100.00 | 0.08 | 0.20 | 0.32 | 0.41 | 0.72 | 0.75 | 0.95 | 1.62 | 3.09 | 91.87 |
| Quartz | 100.00 | 31.04 | 14.08 | 11.36 | 8.40 | 10.60 | 6.80 | 5.38 | 5.51 | 4.07 | 2.76 |
| Kaolinite | 100.00 | 23.50 | 11.81 | 13.47 | 12.96 | 7.87 | 6.58 | 6.65 | 5.85 | 5.63 | 5.69 |
| Chlorite | 100.00 | 10.41 | 8.77 | 8.90 | 7.50 | 8.03 | 6.54 | 5.44 | 6.70 | 9.66 | 28.06 |
| Other | 100.00 | 25.75 | 9.02 | 4.86 | 3.89 | 8.84 | 5.68 | 6.18 | 8.06 | 10.20 | 17.53 |

**Grade and yield vs. hematite liberation.**

*Table v: Mass percent cumulative Fe and mass percent cumulative sample yield versus hematite liberation class for floation feed sample (+75 µm).*

| Discrete Analysis | | | | | | | | | | | |
|---|---|---|---|---|---|---|---|---|---|---|---|
| %Liberation | Combined | <10 | 10-20 | 20-30 | 30-40 | 40-50 | 50-60 | 60-70 | 70-80 | 80-90 | >90 |
| %Fe | 66.93 | 5.30 | 19.16 | 29.05 | 37.63 | 43.58 | 50.24 | 55.33 | 59.90 | 64.50 | 69.66 |
| %Si | 1.55 | 35.51 | 27.95 | 23.08 | 17.60 | 14.09 | 10.52 | 7.38 | 4.76 | 2.23 | 0.09 |
| Mass%(yield) | 100.00 | 1.26 | 0.74 | 0.76 | 0.74 | 1.12 | 1.01 | 1.15 | 1.82 | 3.21 | 88.18 |
| Density of Fraction | 5.08 | 2.75 | 3.04 | 3.31 | 3.55 | 3.88 | 4.13 | 4.39 | 4.67 | 4.95 | 5.28 |
| Cumulative Analysis | | | | | | | | | | | |
| Cumulative % Fe | | 66.93 | 67.72 | 68.08 | 68.39 | 68.63 | 68.92 | 69.12 | 69.29 | 69.48 | 69.66 |
| Cumulative % Si | | 1.55 | 1.12 | 0.91 | 0.74 | 0.61 | 0.45 | 0.34 | 0.26 | 0.17 | 0.09 |
| Cumulative mass % (yield) | | 100.00 | 98.74 | 98.00 | 97.24 | 96.50 | 95.37 | 94.36 | 93.21 | 91.39 | 88.18 |

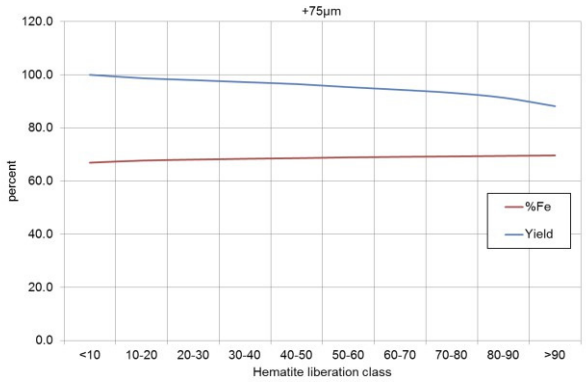


**Mass percent in density class**

*Table vi: Mass percent in density class together with elemental mass percent Fe and Si for floation feed sample (+75 µm).*

| Density Class | | | | | | | | | | | | | | | |
|---|---|---|---|---|---|---|---|---|---|---|---|---|---|---|---|
| | <2.6 | <2.8 | <3.0 | <3.2 | <3.4 | <3.6 | <3.8 | <4.0 | <4.2 | <4.4 | <4.6 | <4.8 | <5.0 | <5.2 | >5.2 |
| % Fe | 3.12 | 3.07 | 13.89 | 21.72 | 28.84 | 32.28 | 39.37 | 44.70 | 49.77 | 52.73 | 57.14 | 60.11 | 63.61 | 67.33 | 69.80 |
| % Si | 3.51 | 41.44 | 32.08 | 28.85 | 21.98 | 18.41 | 16.05 | 14.27 | 10.81 | 8.60 | 6.34 | 4.36 | 2.39 | 0.79 | 0.04 |
| Average Density | 2.55 | 2.68 | 2.90 | 3.10 | 3.30 | 3.50 | 3.71 | 3.89 | 4.10 | 4.30 | 4.51 | 4.70 | 4.92 | 5.13 | 5.29 |
| Mineral mass percent | | | | | | | | | | | | | | | |
| Hematite | 0.00 | 0.03 | 0.11 | 0.13 | 0.22 | 0.27 | 0.42 | 0.44 | 0.56 | 0.62 | 0.82 | 1.17 | 2.05 | 7.37 | 81.32 |
| Quartz | 0.00 | 0.69 | 0.38 | 0.25 | 0.23 | 0.20 | 0.22 | 0.19 | 0.16 | 0.13 | 0.12 | 0.11 | 0.09 | 0.07 | 0.02 |
| Mica | 0.00 | 0.05 | 0.04 | 0.02 | 0.04 | 0.03 | 0.02 | 0.01 | 0.02 | 0.02 | 0.01 | 0.01 | 0.01 | 0.02 | 0.00 |
| Kaolinite | 0.00 | 0.03 | 0.07 | 0.03 | 0.06 | 0.04 | 0.05 | 0.03 | 0.04 | 0.03 | 0.03 | 0.04 | 0.05 | 0.13 | 0.08 |
| Others | 0.01 | 0.02 | 0.02 | 0.01 | 0.03 | 0.06 | 0.05 | 0.03 | 0.03 | 0.04 | 0.03 | 0.05 | 0.06 | 0.10 | 0.07 |
| Total | 0.01 | 0.82 | 0.62 | 0.44 | 0.57 | 0.60 | 0.77 | 0.70 | 0.80 | 0.83 | 1.01 | 1.37 | 2.26 | 7.68 | 81.50 |

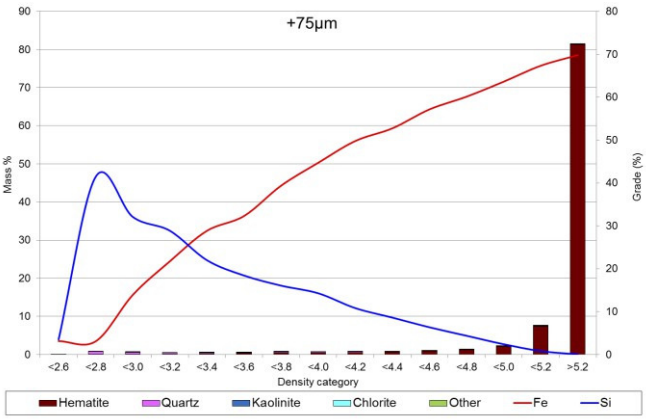

APPENDIX I - Flotation Feed Sample

**Mass percent in liberation class - Hematite**

*Table vii: Hematite liberation data for floation feed sample (+25 µm).*

| | Hematite liberation class | | | | | | | | | | |
|---|---|---|---|---|---|---|---|---|---|---|---|
| | Combined | <10 | <20 | <30 | <40 | <50 | <60 | <70 | <80 | <90 | >90 |
| % Fe Distribution | 68.00 | 5.16 | 19.46 | 28.52 | 36.59 | 43.74 | 49.81 | 55.30 | 60.14 | 64.59 | 69.77 |
| Fe deportment | 68.00 | 0.05 | 0.09 | 0.14 | 0.16 | 0.27 | 0.29 | 0.38 | 0.69 | 1.49 | 64.45 |
| Mass Fe Distribution | 100.00 | 0.07 | 0.13 | 0.20 | 0.24 | 0.39 | 0.42 | 0.56 | 1.01 | 2.20 | 94.78 |
| % Si Distribution | 0.96 | 35.12 | 27.50 | 22.41 | 15.93 | 13.24 | 9.74 | 6.95 | 4.42 | 2.04 | 0.06 |
| Si deportment | 0.96 | 0.32 | 0.12 | 0.11 | 0.07 | 0.08 | 0.06 | 0.05 | 0.05 | 0.05 | 0.06 |
| Mass Si Distribution | 100.00 | 33.62 | 12.83 | 11.05 | 7.43 | 8.38 | 5.82 | 4.93 | 5.25 | 4.89 | 5.79 |
| % Al Distribution | 0.10 | 0.02 | 0.01 | 0.01 | 0.01 | 0.01 | 0.01 | 0.01 | 0.01 | 0.01 | 0.02 |
| Al deportment | 0.10 | 0.02 | 0.01 | 0.01 | 0.01 | 0.01 | 0.01 | 0.01 | 0.01 | 0.01 | 0.02 |
| Mass Al Distribution | 100.00 | 18.43 | 9.73 | 8.95 | 7.79 | 7.73 | 6.88 | 5.32 | 7.10 | 10.33 | 17.76 |
| % K Distribution | 0.02 | 0.00 | 0.00 | 0.00 | 0.00 | 0.00 | 0.00 | 0.00 | 0.00 | 0.00 | 0.00 |
| K deportment | 0.02 | 0.00 | 0.00 | 0.00 | 0.00 | 0.00 | 0.00 | 0.00 | 0.00 | 0.00 | 0.00 |
| Mass K Distribution | 100.00 | 10.72 | 8.33 | 9.19 | 8.05 | 10.53 | 7.95 | 6.44 | 6.44 | 11.30 | 21.05 |
| % P Distribution | 0.04 | 0.00 | 0.00 | 0.00 | 0.00 | 0.00 | 0.00 | 0.00 | 0.00 | 0.01 | 0.01 |
| P deportment | 0.04 | 0.00 | 0.00 | 0.00 | 0.00 | 0.00 | 0.00 | 0.00 | 0.00 | 0.01 | 0.01 |
| Mass P Distribution | 100.00 | 12.54 | 5.05 | 7.90 | 11.22 | 10.98 | 6.42 | 7.69 | 9.47 | 14.08 | 14.66 |
| Density | 5.16 | 2.79 | 3.08 | 3.35 | 3.66 | 3.90 | 4.15 | 4.41 | 4.67 | 4.94 | 5.29 |
| | Mineral mass percent | | | | | | | | | | |
| Hematite | 97.11 | 0.05 | 0.12 | 0.19 | 0.23 | 0.37 | 0.40 | 0.54 | 0.98 | 2.13 | 92.11 |
| Quartz | 1.73 | 0.63 | 0.23 | 0.20 | 0.13 | 0.15 | 0.10 | 0.08 | 0.09 | 0.07 | 0.06 |
| Kaolinite | 0.15 | 0.03 | 0.02 | 0.02 | 0.01 | 0.01 | 0.01 | 0.01 | 0.01 | 0.01 | 0.01 |
| Chlorite | 0.53 | 0.07 | 0.05 | 0.03 | 0.04 | 0.03 | 0.03 | 0.03 | 0.04 | 0.07 | 0.14 |
| Other | 0.48 | 0.13 | 0.04 | 0.03 | 0.04 | 0.04 | 0.03 | 0.03 | 0.03 | 0.05 | 0.06 |
| Total | 100.00 | 0.92 | 0.45 | 0.48 | 0.45 | 0.61 | 0.58 | 0.68 | 1.14 | 2.31 | 92.37 |
| | Normalized mineral mass percent | | | | | | | | | | |
| Hematite | 100.00 | 0.05 | 0.12 | 0.19 | 0.24 | 0.39 | 0.42 | 0.55 | 1.01 | 2.19 | 94.85 |
| Quartz | 100.00 | 36.75 | 13.35 | 11.57 | 7.39 | 8.49 | 5.63 | 4.83 | 4.93 | 3.82 | 3.24 |
| Kaolinite | 100.00 | 21.69 | 12.62 | 13.97 | 9.83 | 9.20 | 8.53 | 4.19 | 6.67 | 7.37 | 5.92 |
| Chlorite | 100.00 | 13.77 | 8.70 | 6.20 | 6.80 | 6.53 | 5.97 | 6.11 | 7.96 | 12.39 | 25.58 |
| Other | 100.00 | 27.33 | 7.98 | 7.10 | 8.93 | 8.35 | 6.36 | 5.66 | 6.40 | 9.52 | 12.36 |

**Grade and yield vs. hematite liberation.**

*Table viii: Mass percent cumulative Fe and mass percent cumulative sample yield versus hematite liberation class for floation feed sample (+25 µm).*

| Discrete Analysis | | | | | | | | | | | |
|---|---|---|---|---|---|---|---|---|---|---|---|
| %Liberation | Combined | <10 | 10-20 | 20-30 | 30-40 | 40-50 | 50-60 | 60-70 | 70-80 | 80-90 | >90 |
| %Fe | 68.00 | 5.16 | 19.46 | 28.52 | 36.59 | 43.74 | 49.81 | 55.30 | 60.14 | 64.59 | 69.77 |
| %Si | 0.96 | 35.12 | 27.50 | 22.41 | 15.93 | 13.24 | 9.74 | 6.95 | 4.42 | 2.04 | 0.06 |
| Mass%(yield) | 100.00 | 0.92 | 0.45 | 0.48 | 0.45 | 0.61 | 0.58 | 0.68 | 1.14 | 2.31 | 92.37 |
| Density of Fraction | 5.16 | 2.79 | 3.08 | 3.35 | 3.66 | 3.90 | 4.15 | 4.41 | 4.67 | 4.94 | 5.29 |
| Cumulative Analysis | | | | | | | | | | | |
| Cumulative % Fe | | 68.00 | 68.58 | 68.81 | 69.00 | 69.15 | 69.31 | 69.43 | 69.53 | 69.64 | 69.77 |
| Cumulative % Si | | 0.96 | 0.65 | 0.52 | 0.42 | 0.35 | 0.26 | 0.21 | 0.16 | 0.11 | 0.06 |
| Cumulative mass % (yield) | | 100.00 | 99.08 | 98.63 | 98.15 | 97.70 | 97.09 | 96.52 | 95.83 | 94.69 | 92.37 |

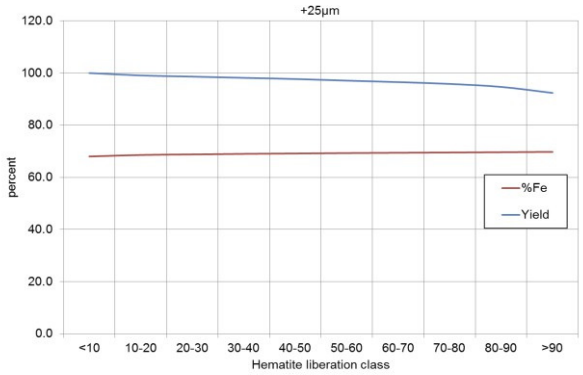


**Mass percent in density class**

*Table ix: Mass percent in density class together with elemental mass percent Fe and Si for floation feed sample (+25 µm).*

| Density Class | | | | | | | | | | | | | | | |
|---|---|---|---|---|---|---|---|---|---|---|---|---|---|---|---|
| | <2.6 | <2.8 | <3.0 | <3.2 | <3.4 | <3.6 | <3.8 | <4.0 | <4.2 | <4.4 | <4.6 | <4.8 | <5.0 | <5.2 | >5.2 |
| % Fe | 4.37 | 3.14 | 13.64 | 21.74 | 29.11 | 31.65 | 38.29 | 45.01 | 49.49 | 51.23 | 55.63 | 59.71 | 63.76 | 67.31 | 69.86 |
| % Si | 18.62 | 41.31 | 31.98 | 27.79 | 22.95 | 17.67 | 15.47 | 13.13 | 9.80 | 8.35 | 5.41 | 3.83 | 2.20 | 0.80 | 0.02 |
| Average Density | 2.56 | 2.67 | 2.90 | 3.11 | 3.31 | 3.50 | 3.71 | 3.90 | 4.10 | 4.30 | 4.52 | 4.71 | 4.91 | 5.13 | 5.29 |
| Mineral mass percent | | | | | | | | | | | | | | | |
| Hematite | 0.00 | 0.02 | 0.06 | 0.10 | 0.12 | 0.16 | 0.17 | 0.31 | 0.28 | 0.37 | 0.49 | 0.83 | 1.41 | 5.17 | 87.62 |
| Quartz | 0.00 | 0.50 | 0.22 | 0.18 | 0.13 | 0.12 | 0.09 | 0.11 | 0.06 | 0.08 | 0.06 | 0.06 | 0.05 | 0.05 | 0.02 |
| Mica | 0.00 | 0.02 | 0.01 | 0.02 | 0.02 | 0.01 | 0.01 | 0.01 | 0.01 | 0.00 | 0.01 | 0.01 | 0.01 | 0.01 | 0.00 |
| Kaolinite | 0.00 | 0.05 | 0.04 | 0.03 | 0.03 | 0.03 | 0.02 | 0.03 | 0.03 | 0.02 | 0.03 | 0.04 | 0.05 | 0.09 | 0.05 |
| Others | 0.00 | 0.01 | 0.03 | 0.02 | 0.01 | 0.06 | 0.03 | 0.03 | 0.02 | 0.04 | 0.04 | 0.05 | 0.04 | 0.07 | 0.04 |
| Total | 0.00 | 0.61 | 0.37 | 0.35 | 0.30 | 0.38 | 0.33 | 0.49 | 0.40 | 0.51 | 0.63 | 0.98 | 1.56 | 5.39 | 87.73 |

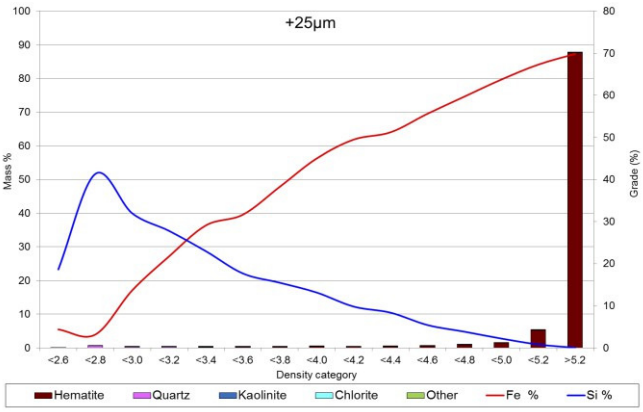

APPENDIX I - Flotation Feed Sample

**Mass percent in liberation class - Hematite**

*Table x: Hematite liberation data for flotation feed sample (-25 µm).*

| | Hematite liberation class | | | | | | | | | | |
|---|---|---|---|---|---|---|---|---|---|---|---|
| | Combined | <10 | <20 | <30 | <40 | <50 | <60 | <70 | <80 | <90 | >90 |
| % Fe Distribution | 69.16 | 3.90 | 20.75 | 27.51 | 36.59 | 43.86 | 51.15 | 55.74 | 60.31 | 64.92 | 69.92 |
| Fe deportment | 69.16 | 0.02 | 0.03 | 0.05 | 0.05 | 0.08 | 0.07 | 0.15 | 0.22 | 0.46 | 68.04 |
| Mass Fe Distribution | 100.00 | 0.03 | 0.04 | 0.07 | 0.07 | 0.11 | 0.10 | 0.21 | 0.32 | 0.67 | 98.38 |
| % Si Distribution | 0.35 | 31.64 | 26.05 | 17.70 | 13.22 | 10.42 | 7.66 | 5.12 | 4.06 | 1.83 | 0.01 |
| Si deportment | 0.35 | 0.19 | 0.04 | 0.03 | 0.02 | 0.02 | 0.01 | 0.01 | 0.01 | 0.01 | 0.01 |
| Mass Si Distribution | 100.00 | 54.28 | 10.40 | 8.23 | 4.80 | 5.22 | 2.97 | 3.78 | 4.14 | 3.69 | 2.50 |
| % Al Distribution | 0.04 | 2.91 | 2.58 | 1.81 | 2.20 | 1.75 | 1.36 | 1.18 | 0.73 | 0.44 | 0.00 |
| Al deportment | 0.04 | 0.02 | 0.00 | 0.00 | 0.00 | 0.00 | 0.00 | 0.00 | 0.00 | 0.00 | 0.00 |
| Mass Al Distribution | 100.00 | 41.43 | 8.52 | 6.99 | 6.62 | 7.26 | 4.36 | 7.20 | 6.19 | 7.41 | 4.02 |
| % K Distribution | 0.01 | 0.23 | 0.07 | 0.40 | 0.30 | 0.18 | 0.26 | 0.15 | 0.18 | 0.08 | 0.00 |
| K deportment | 0.01 | 0.00 | 0.00 | 0.00 | 0.00 | 0.00 | 0.00 | 0.00 | 0.00 | 0.00 | 0.00 |
| Mass K Distribution | 100.00 | 26.65 | 2.01 | 12.71 | 7.52 | 6.28 | 6.96 | 7.57 | 12.18 | 10.88 | 7.24 |
| % P Distribution | 0.02 | 1.39 | 0.00 | 2.08 | 1.42 | 0.90 | 0.34 | 0.65 | 0.25 | 0.13 | 0.00 |
| P deportment | 0.02 | 0.01 | 0.00 | 0.00 | 0.00 | 0.00 | 0.00 | 0.00 | 0.00 | 0.00 | 0.00 |
| Mass P Distribution | 100.00 | 42.43 | 0.00 | 17.17 | 9.17 | 7.99 | 2.38 | 8.55 | 4.45 | 4.66 | 3.18 |
| Density | 5.24 | 2.80 | 3.08 | 3.47 | 3.70 | 3.92 | 4.17 | 4.44 | 4.66 | 4.95 | 5.30 |
| | Mineral mass percent | | | | | | | | | | |
| Hematite | 98.82 | 0.01 | 0.04 | 0.06 | 0.06 | 0.11 | 0.10 | 0.20 | 0.31 | 0.66 | 97.27 |
| Quartz | 0.61 | 0.35 | 0.07 | 0.05 | 0.03 | 0.03 | 0.02 | 0.02 | 0.02 | 0.02 | 0.01 |
| Kaolinite | 0.06 | 0.03 | 0.01 | 0.00 | 0.01 | 0.00 | 0.00 | 0.00 | 0.00 | 0.00 | 0.00 |
| Chlorite | 0.25 | 0.07 | 0.02 | 0.02 | 0.01 | 0.02 | 0.02 | 0.02 | 0.02 | 0.03 | 0.01 |
| Other | 0.25 | 0.14 | 0.01 | 0.03 | 0.02 | 0.02 | 0.01 | 0.01 | 0.01 | 0.01 | 0.01 |
| Total | 100.00 | 0.61 | 0.14 | 0.16 | 0.13 | 0.18 | 0.14 | 0.26 | 0.36 | 0.71 | 97.31 |
| | Normalized mineral mass percent | | | | | | | | | | |
| Hematite | 100.00 | 0.02 | 0.04 | 0.06 | 0.07 | 0.11 | 0.10 | 0.21 | 0.31 | 0.67 | 98.43 |
| Quartz | 100.00 | 57.66 | 10.98 | 8.37 | 4.47 | 4.77 | 2.54 | 3.00 | 3.51 | 2.67 | 2.03 |
| Kaolinite | 100.00 | 54.36 | 8.90 | 5.29 | 11.74 | 8.23 | 0.40 | 4.67 | 3.34 | 2.22 | 0.85 |
| Chlorite | 100.00 | 28.83 | 9.65 | 7.70 | 5.07 | 8.21 | 6.63 | 9.34 | 7.98 | 10.71 | 5.89 |
| Other | 100.00 | 53.41 | 2.91 | 11.90 | 6.61 | 6.14 | 2.94 | 4.99 | 3.86 | 4.61 | 2.64 |

**Grade and yield vs. hematite liberation.**

*Table xi: Mass percent cumulative Fe and mass percent cumulative sample yield versus hematite liberation class for flotation feed sample (-25 µm).*

| Discrete Analysis | | | | | | | | | | | |
|---|---|---|---|---|---|---|---|---|---|---|---|
| %Liberation | Combined | <10 | 10-20 | 20-30 | 30-40 | 40-50 | 50-60 | 60-70 | 70-80 | 80-90 | >90 |
| %Fe | 69.16 | 3.90 | 20.75 | 27.51 | 36.59 | 43.86 | 51.15 | 55.74 | 60.31 | 64.92 | 69.92 |
| %Si | 0.35 | 31.64 | 26.05 | 17.70 | 13.22 | 10.42 | 7.66 | 5.12 | 4.06 | 1.83 | 0.01 |
| Mass%(yield) | 100.00 | 0.61 | 0.14 | 0.16 | 0.13 | 0.18 | 0.14 | 0.26 | 0.36 | 0.71 | 97.31 |
| Density of Fraction | 5.24 | 2.80 | 3.08 | 3.47 | 3.70 | 3.92 | 4.17 | 4.44 | 4.66 | 4.95 | 5.30 |
| Cumulative Analysis | | | | | | | | | | | |
| Cumulative % Fe | | 69.16 | 69.56 | 69.63 | 69.70 | 69.74 | 69.79 | 69.82 | 69.85 | 69.89 | 69.92 |
| Cumulative % Si | | 0.35 | 0.16 | 0.13 | 0.10 | 0.08 | 0.06 | 0.05 | 0.04 | 0.02 | 0.01 |
| Cumulative mass % (yield) | | 100.00 | 99.39 | 99.25 | 99.09 | 98.96 | 98.78 | 98.64 | 98.38 | 98.02 | 97.31 |

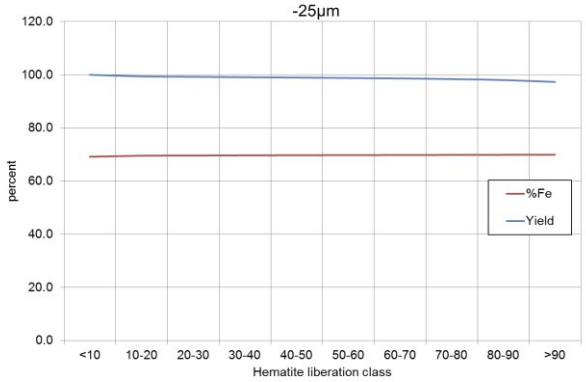


**Mass percent in density class**

*Table xii: Mass percent in density class together with elemental mass percent Fe and Si for flotation feed sample (-25 µm).*

| Density Class | | | | | | | | | | | | | | | |
|---|---|---|---|---|---|---|---|---|---|---|---|---|---|---|---|
| | <2.6 | <2.8 | <3.0 | <3.2 | <3.4 | <3.6 | <3.8 | <4.0 | <4.2 | <4.4 | <4.6 | <4.8 | <5.0 | <5.2 | >5.2 |
| % Fe | 0.00 | 2.40 | 13.04 | 19.00 | 27.11 | 30.31 | 41.50 | 43.90 | 47.78 | 43.70 | 55.32 | 57.64 | 62.57 | 67.15 | 69.94 |
| % Si | 0.00 | 38.96 | 29.77 | 24.30 | 20.59 | 13.36 | 12.97 | 11.63 | 8.04 | 5.38 | 4.56 | 3.06 | 1.85 | 0.97 | 0.00 |
| Average Density | 0.00 | 2.64 | 2.89 | 3.07 | 3.28 | 3.51 | 3.71 | 3.88 | 4.10 | 4.29 | 4.51 | 4.71 | 4.91 | 5.12 | 5.30 |
| Mineral mass percent | | | | | | | | | | | | | | | |
| Hematite | 0.00 | 0.00 | 0.02 | 0.03 | 0.04 | 0.04 | 0.06 | 0.06 | 0.08 | 0.11 | 0.21 | 0.24 | 0.39 | 1.09 | 96.44 |
| Quartz | 0.00 | 0.31 | 0.06 | 0.05 | 0.04 | 0.02 | 0.02 | 0.02 | 0.01 | 0.01 | 0.02 | 0.01 | 0.01 | 0.02 | 0.00 |
| Mica | 0.00 | 0.03 | 0.00 | 0.00 | 0.00 | 0.01 | 0.00 | 0.00 | 0.00 | 0.00 | 0.00 | 0.00 | 0.00 | 0.00 | 0.00 |
| Kaolinite | 0.00 | 0.06 | 0.02 | 0.02 | 0.02 | 0.01 | 0.02 | 0.01 | 0.01 | 0.01 | 0.02 | 0.02 | 0.02 | 0.02 | 0.00 |
| Others | 0.00 | 0.01 | 0.01 | 0.04 | 0.01 | 0.03 | 0.01 | 0.01 | 0.01 | 0.04 | 0.02 | 0.03 | 0.02 | 0.01 | 0.01 |
| Total | 0.00 | 0.41 | 0.12 | 0.14 | 0.12 | 0.11 | 0.11 | 0.09 | 0.12 | 0.18 | 0.27 | 0.30 | 0.43 | 1.14 | 96.45 |

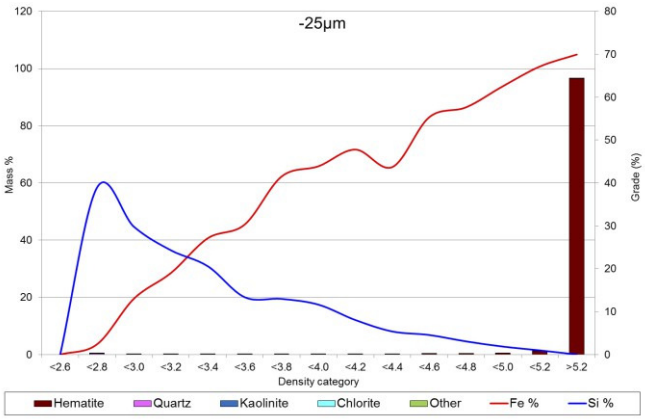

APPENDIX II - Milled Flotation Feed Sample

**Mass percent in liberation class - Hematite**

*Table i: Hematite liberation data for milled flotation feed sample (Head).*

| | Hematite liberation class | | | | | | | | | | |
|---|---|---|---|---|---|---|---|---|---|---|---|
| | Combined | <10 | <20 | <30 | <40 | <50 | <60 | <70 | <80 | <90 | >90 |
| % Fe Distribution | 66.87 | 4.03 | 18.37 | 27.43 | 35.49 | 42.78 | 48.51 | 54.15 | 59.28 | 63.89 | 69.75 |
| Fe deportment | 66.87 | 0.09 | 0.14 | 0.17 | 0.19 | 0.23 | 0.26 | 0.29 | 0.47 | 1.02 | 64.00 |
| Mass Fe Distribution | 100.00 | 0.14 | 0.21 | 0.26 | 0.29 | 0.35 | 0.39 | 0.44 | 0.70 | 1.53 | 95.70 |
| % Si Distribution | 1.59 | 36.86 | 27.86 | 21.71 | 17.26 | 14.02 | 9.75 | 7.39 | 4.69 | 2.35 | 0.07 |
| Si deportment | 1.59 | 0.85 | 0.21 | 0.14 | 0.09 | 0.08 | 0.05 | 0.04 | 0.04 | 0.04 | 0.06 |
| Mass Si Distribution | 100.00 | 53.18 | 13.18 | 8.62 | 5.88 | 4.79 | 3.25 | 2.52 | 2.33 | 2.35 | 3.88 |
| % Al Distribution | 0.13 | 2.19 | 1.50 | 1.26 | 1.30 | 1.15 | 1.03 | 0.87 | 0.64 | 0.50 | 0.02 |
| Al deportment | 0.13 | 0.05 | 0.01 | 0.01 | 0.01 | 0.01 | 0.01 | 0.00 | 0.01 | 0.01 | 0.02 |
| Mass Al Distribution | 100.00 | 39.66 | 8.90 | 6.29 | 5.56 | 4.94 | 4.31 | 3.74 | 3.98 | 6.30 | 16.33 |
| % K Distribution | 0.01 | 0.19 | 0.17 | 0.11 | 0.08 | 0.13 | 0.06 | 0.03 | 0.03 | 0.02 | 0.00 |
| K deportment | 0.01 | 0.00 | 0.00 | 0.00 | 0.00 | 0.00 | 0.00 | 0.00 | 0.00 | 0.00 | 0.00 |
| Mass K Distribution | 100.00 | 50.39 | 14.58 | 8.07 | 4.69 | 7.77 | 3.81 | 1.85 | 2.28 | 2.84 | 3.71 |
| % P Distribution | 0.05 | 0.58 | 0.90 | 1.34 | 0.83 | 0.44 | 0.73 | 0.30 | 0.26 | 0.15 | 0.00 |
| P deportment | 0.05 | 0.01 | 0.01 | 0.01 | 0.00 | 0.00 | 0.00 | 0.00 | 0.00 | 0.00 | 0.00 |
| Mass P Distribution | 100.00 | 27.63 | 14.11 | 17.58 | 9.38 | 4.93 | 8.09 | 3.36 | 4.26 | 4.90 | 5.77 |
| Density | 5.11 | 2.84 | 3.21 | 3.51 | 3.78 | 4.00 | 4.30 | 4.53 | 4.78 | 5.02 | 5.29 |
| Mineral mass percent | | | | | | | | | | | |
| Hematite | 95.46 | 0.09 | 0.18 | 0.24 | 0.27 | 0.32 | 0.36 | 0.41 | 0.66 | 1.45 | 91.46 |
| Quartz | 3.01 | 1.66 | 0.41 | 0.27 | 0.18 | 0.14 | 0.09 | 0.07 | 0.06 | 0.06 | 0.07 |
| Kaolinite | 0.16 | 0.12 | 0.01 | 0.01 | 0.01 | 0.00 | 0.00 | 0.00 | 0.00 | 0.00 | 0.00 |
| Chlorite | 0.92 | 0.25 | 0.08 | 0.06 | 0.06 | 0.05 | 0.04 | 0.04 | 0.05 | 0.08 | 0.21 |
| Other | 0.45 | 0.18 | 0.06 | 0.06 | 0.03 | 0.02 | 0.03 | 0.01 | 0.02 | 0.02 | 0.02 |
| Total | 100.00 | 2.30 | 0.75 | 0.63 | 0.54 | 0.54 | 0.53 | 0.54 | 0.79 | 1.60 | 91.76 |
| Normalized mineral mass percent | | | | | | | | | | | |
| Hematite | 100.00 | 0.10 | 0.19 | 0.25 | 0.28 | 0.34 | 0.38 | 0.43 | 0.70 | 1.52 | 95.82 |
| Quartz | 100.00 | 55.10 | 13.69 | 8.91 | 5.89 | 4.74 | 3.11 | 2.34 | 2.11 | 1.83 | 2.28 |
| Kaolinite | 100.00 | 70.95 | 8.86 | 6.16 | 4.03 | 2.99 | 3.04 | 1.71 | 0.70 | 0.98 | 0.57 |
| Chlorite | 100.00 | 27.06 | 8.86 | 6.37 | 6.37 | 5.44 | 4.88 | 4.84 | 5.30 | 8.43 | 22.46 |
| Other | 100.00 | 40.94 | 13.51 | 12.73 | 7.70 | 4.90 | 6.00 | 2.64 | 3.44 | 3.71 | 4.45 |

**Grade and yield vs. hematite liberation.**

*Table ii: Mass percent cumulative Fe and mass percent cumulative sample yield versus hematite liberation class for milled flotation feed sample (Head).*

| Discrete Analysis | | | | | | | | | | | |
|---|---|---|---|---|---|---|---|---|---|---|---|
| %Liberation | Combined | <10 | 10-20 | 20-30 | 30-40 | 40-50 | 50-60 | 60-70 | 70-80 | 80-90 | >90 |
| %Fe | 66.87 | 4.03 | 18.37 | 27.43 | 35.49 | 42.78 | 48.51 | 54.15 | 59.28 | 63.89 | 69.75 |
| %Si | 1.59 | 36.86 | 27.86 | 21.71 | 17.26 | 14.02 | 9.75 | 7.39 | 4.69 | 2.35 | 0.07 |
| Mass%(yield) | 100.00 | 2.30 | 0.75 | 0.63 | 0.54 | 0.54 | 0.53 | 0.54 | 0.79 | 1.60 | 91.76 |
| Density of Fraction | 5.11 | 2.84 | 3.21 | 3.51 | 3.78 | 4.00 | 4.30 | 4.53 | 4.78 | 5.02 | 5.29 |
| Cumulative Analysis | | | | | | | | | | | |
| Cumulative % Fe | | 66.87 | 68.35 | 68.74 | 69.01 | 69.20 | 69.35 | 69.47 | 69.56 | 69.65 | 69.75 |
| Cumulative % Si | | 1.59 | 0.76 | 0.55 | 0.41 | 0.32 | 0.24 | 0.19 | 0.14 | 0.11 | 0.07 |
| Cumulative mass % (yield) | | 100.00 | 97.70 | 96.95 | 96.31 | 95.77 | 95.23 | 94.69 | 94.15 | 93.36 | 91.76 |

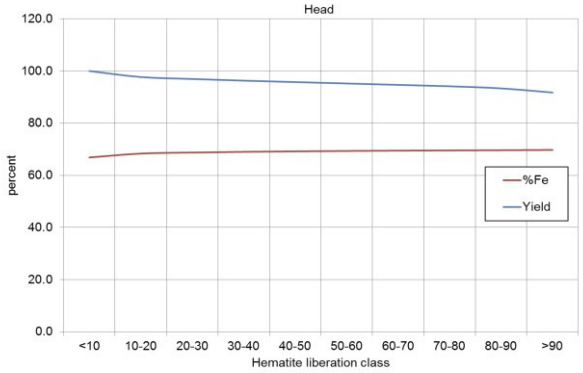


**Mass percent in density class**

*Table iii: Mass percent in density class together with elemental mass percent Fe and Si for milled flotation feed sample (Head).*

| Density Class | | | | | | | | | | | | | | | |
|---|---|---|---|---|---|---|---|---|---|---|---|---|---|---|---|
| | <2.6 | <2.8 | <3.0 | <3.2 | <3.4 | <3.6 | <3.8 | <4.0 | <4.2 | <4.4 | <4.6 | <4.8 | <5.0 | <5.2 | >5.2 |
| % Fe | 0.00 | 1.33 | 12.13 | 17.64 | 26.13 | 25.30 | 35.79 | 36.70 | 27.03 | 37.00 | 46.75 | 53.41 | 59.80 | 65.36 | 69.80 |
| % Si | 0.00 | 43.46 | 36.17 | 28.56 | 25.71 | 17.29 | 17.72 | 14.72 | 12.65 | 8.02 | 6.72 | 4.77 | 3.14 | 1.38 | 0.04 |
| Average Density | 0.00 | 2.66 | 2.89 | 3.09 | 3.30 | 3.50 | 3.71 | 3.90 | 4.07 | 4.30 | 4.50 | 4.70 | 4.90 | 5.13 | 5.30 |
| Mineral mass percent | | | | | | | | | | | | | | | |
| Hematite | 0.00 | 0.04 | 0.08 | 0.13 | 0.15 | 0.15 | 0.17 | 0.19 | 0.22 | 0.26 | 0.35 | 0.46 | 0.77 | 2.95 | 89.55 |
| Quartz | 0.00 | 1.46 | 0.35 | 0.29 | 0.21 | 0.15 | 0.11 | 0.10 | 0.07 | 0.06 | 0.05 | 0.04 | 0.04 | 0.05 | 0.02 |
| Kaolinite | 0.00 | 0.10 | 0.01 | 0.01 | 0.01 | 0.01 | 0.01 | 0.01 | 0.00 | 0.00 | 0.00 | 0.00 | 0.00 | 0.00 | 0.00 |
| Chlorite | 0.00 | 0.00 | 0.00 | 0.03 | 0.01 | 0.01 | 0.01 | 0.02 | 0.26 | 0.09 | 0.08 | 0.06 | 0.06 | 0.13 | 0.17 |
| Other | 0.00 | 0.02 | 0.01 | 0.03 | 0.01 | 0.04 | 0.02 | 0.01 | 0.02 | 0.09 | 0.07 | 0.04 | 0.03 | 0.03 | 0.02 |
| Total | 0.00 | 1.62 | 0.46 | 0.48 | 0.39 | 0.36 | 0.31 | 0.33 | 0.57 | 0.50 | 0.56 | 0.61 | 0.90 | 3.16 | 89.76 |

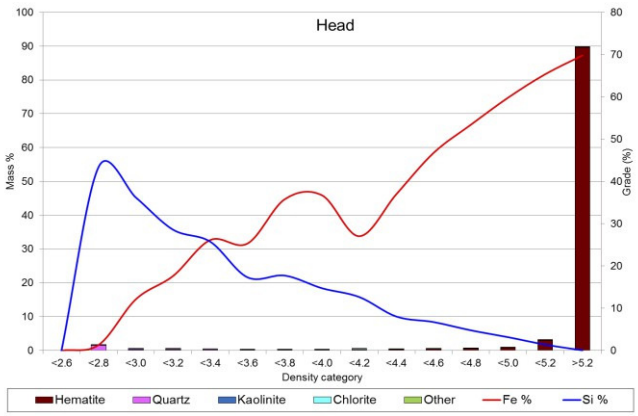

APPENDIX II - Milled Flotation Feed Sample

**Mass percent in liberation class - Hematite**

*Table iv: Hematite liberation data for milled flotation feed sample (+25 µm).*

| | Hematite liberation class | | | | | | | | | | |
|---|---|---|---|---|---|---|---|---|---|---|---|
| | Combined | <10 | <20 | <30 | <40 | <50 | <60 | <70 | <80 | <90 | >90 |
| % Fe Distribution | 67.37 | 3.64 | 18.89 | 27.81 | 35.44 | 42.29 | 48.36 | 54.07 | 59.08 | 63.83 | 69.76 |
| Fe deportment | 67.37 | 0.08 | 0.07 | 0.10 | 0.12 | 0.14 | 0.17 | 0.24 | 0.44 | 0.95 | 65.08 |
| Mass Fe Distribution | 100.00 | 0.13 | 0.11 | 0.14 | 0.17 | 0.20 | 0.25 | 0.36 | 0.65 | 1.41 | 96.59 |
| % Si Distribution | 1.20 | 34.07 | 24.09 | 18.62 | 13.44 | 11.95 | 8.78 | 6.35 | 4.15 | 2.09 | 0.06 |
| Si deportment | 1.20 | 0.79 | 0.09 | 0.06 | 0.04 | 0.04 | 0.03 | 0.03 | 0.03 | 0.03 | 0.05 |
| Mass Si Distribution | 100.00 | 65.78 | 7.71 | 5.29 | 3.64 | 3.20 | 2.52 | 2.34 | 2.56 | 2.58 | 4.38 |
| % Al Distribution | 0.17 | 0.08 | 0.01 | 0.01 | 0.01 | 0.01 | 0.01 | 0.01 | 0.01 | 0.01 | 0.02 |
| Al deportment | 0.17 | 0.08 | 0.01 | 0.01 | 0.01 | 0.01 | 0.01 | 0.01 | 0.01 | 0.01 | 0.02 |
| Mass Al Distribution | 100.00 | 48.10 | 7.92 | 6.02 | 4.88 | 3.80 | 3.48 | 3.24 | 4.05 | 5.03 | 13.49 |
| % K Distribution | 0.01 | 0.01 | 0.00 | 0.00 | 0.00 | 0.00 | 0.00 | 0.00 | 0.00 | 0.00 | 0.00 |
| K deportment | 0.01 | 0.01 | 0.00 | 0.00 | 0.00 | 0.00 | 0.00 | 0.00 | 0.00 | 0.00 | 0.00 |
| Mass K Distribution | 100.00 | 62.99 | 11.84 | 6.10 | 2.81 | 2.07 | 2.45 | 2.10 | 1.81 | 3.07 | 4.75 |
| % P Distribution | 0.04 | 0.01 | 0.00 | 0.00 | 0.00 | 0.00 | 0.00 | 0.00 | 0.00 | 0.00 | 0.00 |
| P deportment | 0.04 | 0.01 | 0.00 | 0.00 | 0.00 | 0.00 | 0.00 | 0.00 | 0.00 | 0.00 | 0.00 |
| Mass P Distribution | 100.00 | 36.62 | 7.72 | 7.22 | 10.12 | 6.16 | 5.43 | 5.14 | 5.60 | 8.38 | 7.62 |
| Density | 5.15 | 2.86 | 3.34 | 3.65 | 4.00 | 4.11 | 4.36 | 4.58 | 4.82 | 5.04 | 5.29 |
| | Mineral mass percent | | | | | | | | | | |
| Hematite | 96.14 | 0.06 | 0.09 | 0.12 | 0.15 | 0.19 | 0.23 | 0.33 | 0.62 | 1.34 | 93.00 |
| Quartz | 2.08 | 1.47 | 0.16 | 0.10 | 0.07 | 0.06 | 0.05 | 0.04 | 0.04 | 0.04 | 0.04 |
| Kaolinite | 0.23 | 0.17 | 0.02 | 0.01 | 0.00 | 0.01 | 0.01 | 0.00 | 0.00 | 0.00 | 0.00 |
| Chlorite | 1.09 | 0.34 | 0.09 | 0.08 | 0.08 | 0.05 | 0.05 | 0.05 | 0.06 | 0.08 | 0.22 |
| Other | 0.46 | 0.28 | 0.03 | 0.02 | 0.03 | 0.02 | 0.01 | 0.01 | 0.01 | 0.02 | 0.02 |
| Total | 100.00 | 2.32 | 0.39 | 0.34 | 0.33 | 0.32 | 0.35 | 0.44 | 0.74 | 1.48 | 93.29 |
| | Normalized mineral mass percent | | | | | | | | | | |
| Hematite | 100.00 | 0.06 | 0.09 | 0.13 | 0.16 | 0.19 | 0.24 | 0.35 | 0.64 | 1.40 | 96.73 |
| Quartz | 100.00 | 70.60 | 7.56 | 5.03 | 3.20 | 3.04 | 2.26 | 2.09 | 2.15 | 1.94 | 2.12 |
| Kaolinite | 100.00 | 73.03 | 8.97 | 4.81 | 1.90 | 3.19 | 2.52 | 2.05 | 1.59 | 1.45 | 0.49 |
| Chlorite | 100.00 | 31.60 | 8.05 | 7.32 | 6.91 | 4.51 | 4.31 | 4.16 | 5.71 | 7.15 | 20.27 |
| Other | 100.00 | 61.19 | 6.51 | 5.06 | 5.79 | 3.33 | 3.10 | 3.15 | 3.15 | 4.47 | 4.27 |

**Grade and yield vs. hematite liberation.**

*Table v: Mass percent cumulative Fe and mass percent cumulative sample yield versus hematite liberation class for milled flotation feed sample (+25 µm).*

| Discrete Analysis | | | | | | | | | | | |
|---|---|---|---|---|---|---|---|---|---|---|---|
| %Liberation | Combined | <10 | 10-20 | 20-30 | 30-40 | 40-50 | 50-60 | 60-70 | 70-80 | 80-90 | >90 |
| %Fe | 67.37 | 3.64 | 18.89 | 27.81 | 35.44 | 42.29 | 48.36 | 54.07 | 59.08 | 63.83 | 69.76 |
| %Si | 1.20 | 34.07 | 24.09 | 18.62 | 13.44 | 11.95 | 8.78 | 6.35 | 4.15 | 2.09 | 0.06 |
| Mass%(yield) | 100.00 | 2.32 | 0.39 | 0.34 | 0.33 | 0.32 | 0.35 | 0.44 | 0.74 | 1.48 | 93.29 |
| Density of Fraction | 5.15 | 2.86 | 3.34 | 3.65 | 4.00 | 4.11 | 4.36 | 4.58 | 4.82 | 5.04 | 5.29 |
| Cumulative Analysis | | | | | | | | | | | |
| Cumulative % Fe | | 67.37 | 68.89 | 69.09 | 69.23 | 69.35 | 69.44 | 69.51 | 69.58 | 69.67 | 69.76 |
| Cumulative % Si | | 1.20 | 0.42 | 0.33 | 0.26 | 0.22 | 0.18 | 0.15 | 0.12 | 0.09 | 0.06 |
| Cumulative mass % (yield) | | 100.00 | 97.68 | 97.29 | 96.95 | 96.62 | 96.30 | 95.96 | 95.51 | 94.77 | 93.29 |

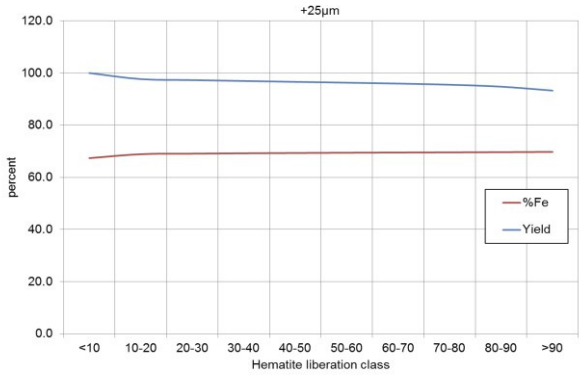


**Mass percent in density class**

*Table vi: Mass percent in density class together with elemental mass percent Fe and Si for milled flotation feed sample (+25 µm).*

| Density Class | | | | | | | | | | | | | | | |
|---|---|---|---|---|---|---|---|---|---|---|---|---|---|---|---|
| | <2.6 | <2.8 | <3.0 | <3.2 | <3.4 | <3.6 | <3.8 | <4.0 | <4.2 | <4.4 | <4.6 | <4.8 | <5.0 | <5.2 | >5.2 |
| % Fe | 0.00 | 1.11 | 11.62 | 16.12 | 24.69 | 19.94 | 33.58 | 32.74 | 24.37 | 35.96 | 47.46 | 53.10 | 59.66 | 65.16 | 69.80 |
| % Si | 0.00 | 43.30 | 35.34 | 26.66 | 24.78 | 14.24 | 17.42 | 14.24 | 12.56 | 7.89 | 6.92 | 4.70 | 3.08 | 1.37 | 0.04 |
| Average Density | 0.00 | 2.65 | 2.89 | 3.09 | 3.30 | 3.50 | 3.70 | 3.91 | 4.06 | 4.30 | 4.50 | 4.71 | 4.91 | 5.12 | 5.29 |
| Mineral mass percent | | | | | | | | | | | | | | | |
| Hematite | 0.00 | 0.02 | 0.04 | 0.05 | 0.06 | 0.05 | 0.09 | 0.10 | 0.13 | 0.19 | 0.28 | 0.38 | 0.66 | 2.35 | 91.74 |
| Quartz | 0.00 | 1.34 | 0.18 | 0.11 | 0.08 | 0.05 | 0.06 | 0.04 | 0.03 | 0.03 | 0.04 | 0.03 | 0.03 | 0.03 | 0.02 |
| Mica | 0.00 | 0.13 | 0.02 | 0.01 | 0.01 | 0.01 | 0.01 | 0.01 | 0.01 | 0.01 | 0.01 | 0.00 | 0.00 | 0.00 | 0.00 |
| Kaolinite | 0.00 | 0.01 | 0.01 | 0.03 | 0.01 | 0.01 | 0.01 | 0.04 | 0.32 | 0.10 | 0.09 | 0.06 | 0.07 | 0.12 | 0.19 |
| Others | 0.00 | 0.03 | 0.01 | 0.05 | 0.01 | 0.08 | 0.02 | 0.03 | 0.01 | 0.07 | 0.03 | 0.04 | 0.02 | 0.03 | 0.02 |
| Total | 0.00 | 1.53 | 0.26 | 0.26 | 0.16 | 0.20 | 0.20 | 0.22 | 0.50 | 0.41 | 0.44 | 0.51 | 0.78 | 2.54 | 91.97 |

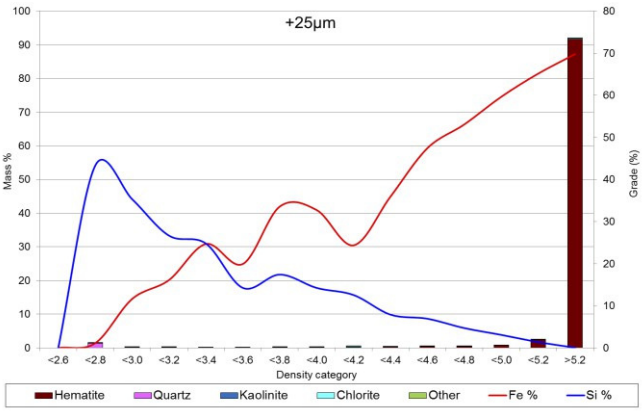

APPENDIX II - Milled Flotation Feed Sample

**Mass percent in liberation class - Hematite**

*Table vii: Hematite liberation data for milled flotation feed sample (-25 µm).*

| | Hematite liberation class | | | | | | | | | | |
|---|---|---|---|---|---|---|---|---|---|---|---|
| | Combined | <10 | <20 | <30 | <40 | <50 | <60 | <70 | <80 | <90 | >90 |
| % Fe Distribution | 66.84 | 4.05 | 18.35 | 27.42 | 35.49 | 42.80 | 48.51 | 54.16 | 59.29 | 63.89 | 69.75 |
| Fe deportment | 66.84 | 0.09 | 0.14 | 0.18 | 0.20 | 0.24 | 0.26 | 0.30 | 0.47 | 1.03 | 63.94 |
| Mass Fe Distribution | 100.00 | 0.14 | 0.21 | 0.27 | 0.29 | 0.36 | 0.39 | 0.44 | 0.71 | 1.54 | 95.65 |
| % Si Distribution | 1.62 | 37.02 | 27.96 | 21.80 | 17.38 | 14.09 | 9.78 | 7.43 | 4.72 | 2.36 | 0.07 |
| Si deportment | 1.62 | 0.85 | 0.22 | 0.14 | 0.10 | 0.08 | 0.05 | 0.04 | 0.04 | 0.04 | 0.06 |
| Mass Si Distribution | 100.00 | 52.66 | 13.41 | 8.76 | 5.98 | 4.86 | 3.28 | 2.52 | 2.33 | 2.34 | 3.86 |
| % Al Distribution | 0.12 | 2.12 | 1.45 | 1.21 | 1.26 | 1.13 | 1.01 | 0.86 | 0.62 | 0.50 | 0.02 |
| Al deportment | 0.12 | 0.05 | 0.01 | 0.01 | 0.01 | 0.01 | 0.01 | 0.00 | 0.00 | 0.01 | 0.02 |
| Mass Al Distribution | 100.00 | 39.03 | 8.97 | 6.31 | 5.61 | 5.03 | 4.38 | 3.77 | 3.97 | 6.40 | 16.54 |
| % K Distribution | 0.01 | 0.19 | 0.17 | 0.11 | 0.08 | 0.13 | 0.06 | 0.03 | 0.03 | 0.02 | 0.00 |
| K deportment | 0.01 | 0.00 | 0.00 | 0.00 | 0.00 | 0.00 | 0.00 | 0.00 | 0.00 | 0.00 | 0.00 |
| Mass K Distribution | 100.00 | 49.60 | 14.75 | 8.20 | 4.81 | 8.13 | 3.90 | 1.83 | 2.31 | 2.83 | 3.64 |
| % P Distribution | 0.05 | 0.58 | 0.91 | 1.35 | 0.82 | 0.43 | 0.74 | 0.29 | 0.26 | 0.14 | 0.00 |
| P deportment | 0.05 | 0.01 | 0.01 | 0.01 | 0.00 | 0.00 | 0.00 | 0.00 | 0.00 | 0.00 | 0.00 |
| Mass P Distribution | 100.00 | 27.26 | 14.37 | 18.00 | 9.35 | 4.87 | 8.20 | 3.28 | 4.21 | 4.76 | 5.69 |
| Density | 5.11 | 2.84 | 3.21 | 3.51 | 3.78 | 4.00 | 4.30 | 4.52 | 4.78 | 5.02 | 5.29 |
| | Mineral mass percent | | | | | | | | | | |
| Hematite | 95.42 | 0.09 | 0.19 | 0.25 | 0.27 | 0.33 | 0.37 | 0.42 | 0.67 | 1.45 | 91.38 |
| Quartz | 3.06 | 1.67 | 0.43 | 0.28 | 0.18 | 0.15 | 0.10 | 0.07 | 0.06 | 0.06 | 0.07 |
| Kaolinite | 0.16 | 0.11 | 0.01 | 0.01 | 0.01 | 0.00 | 0.00 | 0.00 | 0.00 | 0.00 | 0.00 |
| Chlorite | 0.91 | 0.24 | 0.08 | 0.06 | 0.06 | 0.05 | 0.04 | 0.04 | 0.05 | 0.08 | 0.21 |
| Other | 0.45 | 0.18 | 0.06 | 0.06 | 0.04 | 0.02 | 0.03 | 0.01 | 0.02 | 0.02 | 0.02 |
| Total | 100.00 | 2.30 | 0.77 | 0.65 | 0.56 | 0.56 | 0.54 | 0.55 | 0.80 | 1.61 | 91.67 |
| | Normalized mineral mass percent | | | | | | | | | | |
| Hematite | 100.00 | 0.10 | 0.20 | 0.26 | 0.29 | 0.35 | 0.39 | 0.44 | 0.70 | 1.52 | 95.76 |
| Quartz | 100.00 | 54.52 | 13.93 | 9.05 | 5.99 | 4.81 | 3.14 | 2.34 | 2.11 | 1.83 | 2.28 |
| Kaolinite | 100.00 | 70.78 | 8.85 | 6.27 | 4.20 | 2.98 | 3.08 | 1.69 | 0.63 | 0.94 | 0.58 |
| Chlorite | 100.00 | 26.76 | 8.91 | 6.30 | 6.33 | 5.50 | 4.91 | 4.89 | 5.28 | 8.51 | 22.61 |
| Other | 100.00 | 39.78 | 13.91 | 13.17 | 7.81 | 4.99 | 6.17 | 2.61 | 3.45 | 3.67 | 4.46 |

**Grade and yield vs. hematite liberation.**

*Table viii: Mass percent cumulative Fe and mass percent cumulative sample yield versus hematite liberation class for milled flotation feed sample (-25 µm).*

| | | Discrete Analysis | | | | | | | | | |
|---|---|---|---|---|---|---|---|---|---|---|---|
| %Liberation | Combined | <10 | 10-20 | 20-30 | 30-40 | 40-50 | 50-60 | 60-70 | 70-80 | 80-90 | >90 |
| %Fe | 66.84 | 4.05 | 18.35 | 27.42 | 35.49 | 42.80 | 48.51 | 54.16 | 59.29 | 63.89 | 69.75 |
| %Si | 1.62 | 37.02 | 27.96 | 21.80 | 17.38 | 14.09 | 9.78 | 7.43 | 4.72 | 2.36 | 0.07 |
| Mass%(yield) | 100.00 | 2.30 | 0.77 | 0.65 | 0.56 | 0.56 | 0.54 | 0.55 | 0.80 | 1.61 | 91.67 |
| Density of Fraction | 5.11 | 2.84 | 3.21 | 3.51 | 3.78 | 4.00 | 4.30 | 4.52 | 4.78 | 5.02 | 5.29 |
| | | | | Cumulative Analysis | | | | | | | |
| Cumulative % Fe | | 66.84 | 68.32 | 68.72 | 69.00 | 69.19 | 69.35 | 69.47 | 69.56 | 69.64 | 69.75 |
| Cumulative % Si | | 1.62 | 0.78 | 0.57 | 0.42 | 0.32 | 0.24 | 0.19 | 0.15 | 0.11 | 0.07 |
| Cumulative mass % (yield) | | 100.00 | 97.70 | 96.93 | 96.28 | 95.72 | 95.17 | 94.62 | 94.08 | 93.28 | 91.67 |

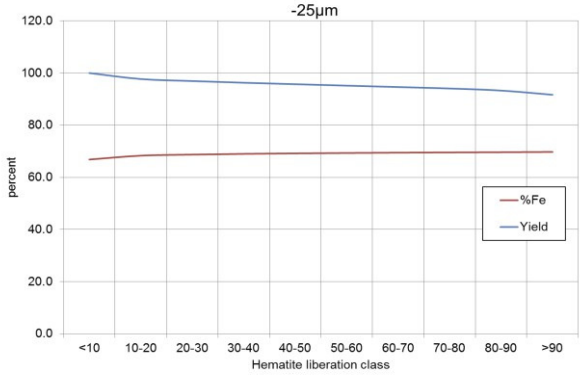


**Mass percent in density class**

*Table ix: Mass percent in density class together with elemental mass percent Fe and Si for milled flotation feed sample (-25 µm).*

| | | | | | Density Class | | | | | | | | | | |
|---|---|---|---|---|---|---|---|---|---|---|---|---|---|---|---|
| | <2.6 | <2.8 | <3.0 | <3.2 | <3.4 | <3.6 | <3.8 | <4.0 | <4.2 | <4.4 | <4.6 | <4.8 | <5.0 | <5.2 | >5.2 |
| % Fe | 0.00 | 1.73 | 12.68 | 19.22 | 27.30 | 30.95 | 38.46 | 41.83 | 31.59 | 38.66 | 45.69 | 53.91 | 60.04 | 65.67 | 69.80 |
| % Si | 0.00 | 43.77 | 37.06 | 30.55 | 26.47 | 20.51 | 18.09 | 15.35 | 12.80 | 8.23 | 6.42 | 4.88 | 3.25 | 1.40 | 0.04 |
| Average Density | 0.00 | 2.66 | 2.89 | 3.09 | 3.30 | 3.50 | 3.71 | 3.90 | 4.07 | 4.30 | 4.50 | 4.70 | 4.90 | 5.13 | 5.30 |
| | | | | | Mineral mass percent | | | | | | | | | | |
| Hematite | 0.00 | 0.04 | 0.08 | 0.13 | 0.15 | 0.16 | 0.17 | 0.20 | 0.22 | 0.26 | 0.36 | 0.46 | 0.77 | 2.98 | 89.43 |
| Quartz | 0.00 | 1.47 | 0.36 | 0.30 | 0.21 | 0.15 | 0.11 | 0.10 | 0.08 | 0.06 | 0.05 | 0.04 | 0.04 | 0.06 | 0.02 |
| Mica | 0.00 | 0.10 | 0.01 | 0.01 | 0.01 | 0.01 | 0.01 | 0.01 | 0.00 | 0.00 | 0.00 | 0.00 | 0.00 | 0.00 | 0.00 |
| Kaolinite | 0.00 | 0.00 | 0.00 | 0.03 | 0.01 | 0.01 | 0.01 | 0.02 | 0.25 | 0.08 | 0.08 | 0.06 | 0.06 | 0.13 | 0.17 |
| Others | 0.00 | 0.02 | 0.01 | 0.03 | 0.01 | 0.04 | 0.02 | 0.01 | 0.02 | 0.09 | 0.08 | 0.04 | 0.03 | 0.03 | 0.02 |
| Total | 0.00 | 1.63 | 0.47 | 0.49 | 0.40 | 0.37 | 0.32 | 0.33 | 0.57 | 0.50 | 0.57 | 0.61 | 0.91 | 3.19 | 89.64 |

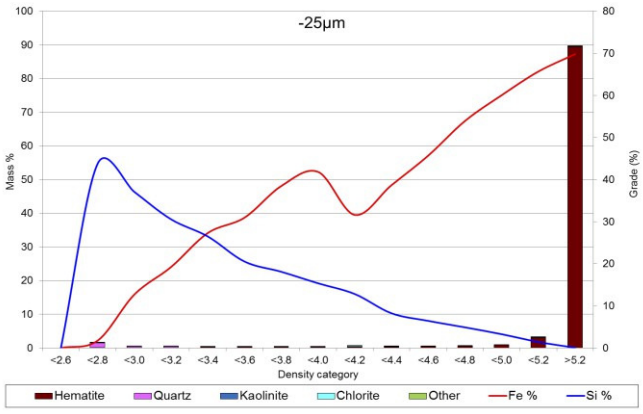

## 7.7 Appendix G: Revised flotation test raw data results

The tabulated results include the XRF analysed data for the flotation testwork conducted at various milling times, including a control sample, a five minute milled sample and, a 15 minute milled sample. The control sample was floated as is, i.e. after removal of the fines. For these tests the reagent dosage was kept constant at a pH of 9,5, starch at 400 g/t and a 100 g/t amine.

| Sample - Control | Fe2O3 (%) | Fe (%) | SiO2 (%) | K2O (%) | Al2O3 (%) | P2O5 (%) | SO3 (%) | MnO (%) | TiO2 (%) | CaO (%) | |
|---|---|---|---|---|---|---|---|---|---|---|---|
| **Feed** | 92.97 | 64.90 | 4.07 | 0.43 | 1.68 | 0.17 | 0.03 | 0.23 | 0.18 | 0.21 | 100 |
| **AM14CONC** | 92.46 | 64.55 | 3.64 | 0.37 | 1.32 | 0.16 | 0.04 | 0.26 | 0.18 | 0.21 | 98 |
| | 93.70 | 65.41 | 3.69 | 0.38 | 1.34 | 0.16 | 0.04 | 0.26 | 0.19 | 0.22 | 100 |
| **AM14CONC** | 92.75 | 64.75 | 3.47 | 0.37 | 1.29 | 0.16 | 0.03 | 0.25 | 0.18 | 0.21 | 98 |
| | 93.90 | 65.55 | 3.51 | 0.37 | 1.31 | 0.16 | 0.03 | 0.26 | 0.18 | 0.21 | 100 |
| **AM14OF1** | 84.23 | 58.80 | 10.82 | 0.75 | 2.30 | 0.18 | 0.08 | 0.37 | 0.17 | 0.26 | 99 |
| **30 seconds** | 84.90 | 59.27 | 10.90 | 0.76 | 2.32 | 0.18 | 0.08 | 0.37 | 0.17 | 0.26 | 100 |
| **AM14OF2** | 85.67 | 59.81 | 9.92 | 0.73 | 2.27 | 0.18 | 0.06 | 0.26 | 0.18 | 0.23 | 99 |
| **60 seconds** | 86.05 | 60.07 | 9.96 | 0.73 | 2.28 | 0.18 | 0.06 | 0.26 | 0.18 | 0.23 | 100 |
| **AM14OF3** | 85.48 | 59.67 | 9.81 | 0.75 | 2.30 | 0.18 | 0.06 | 0.26 | 0.19 | 0.24 | 99 |
| **90 seconds** | 86.09 | 60.10 | 9.88 | 0.75 | 2.31 | 0.18 | 0.06 | 0.26 | 0.19 | 0.24 | 100 |
| **AM14OF4** | 84.29 | 58.84 | 9.98 | 0.80 | 2.27 | 0.17 | 0.05 | 0.26 | 0.18 | 0.23 | 98 |
| **``120 seconds** | 85.77 | 59.88 | 10.16 | 0.81 | 2.31 | 0.18 | 0.05 | 0.26 | 0.18 | 0.24 | 100 |

The results include the XRF data for the floated sample which was milled for five minutes. Note that the fines was screened out prior to milling.

| Sample (5 min Milled) | Fe2O3 (%) | Fe (%) | SiO2 (%) | K2O (%) | Al2O3 (%) | P2O5 (%) | SO3 (%) | MnO (%) | TiO2 (%) | CaO (%) | |
|---|---|---|---|---|---|---|---|---|---|---|---|
| **Feed** | 93.10 | 65.00 | 4.25 | 0.25 | 1.33 | 0.13 | 0.03 | 0.11 | 0.11 | 0.12 | 100 |
| **AM15CONC** | 94.74 | 66.14 | 2.33 | 0.33 | 1.16 | 0.15 | 0.03 | 0.25 | 0.18 | 0.19 | 99 |
| | 95.29 | 66.52 | 2.35 | 0.33 | 1.17 | 0.15 | 0.03 | 0.25 | 0.19 | 0.20 | 100 |
| **AM15CONC** | 94.77 | 66.16 | 2.36 | 0.31 | 1.11 | 0.15 | 0.04 | 0.26 | 0.19 | 0.20 | 99 |
| | 95.32 | 66.54 | 2.37 | 0.31 | 1.12 | 0.15 | 0.04 | 0.26 | 0.19 | 0.20 | 100 |
| **AM15OF1** | 88.11 | 61.51 | 9.18 | 0.57 | 1.86 | 0.16 | 0.04 | 0.25 | 0.19 | 0.22 | 101 |
| **30 seconds** | 87.54 | 61.11 | 9.12 | 0.57 | 1.85 | 0.16 | 0.04 | 0.25 | 0.19 | 0.22 | 100 |
| **AM15OF2** | 88.58 | 61.84 | 7.87 | 0.57 | 1.85 | 0.17 | 0.04 | 0.25 | 0.18 | 0.23 | 100 |
| **60 seconds** | 88.74 | 61.95 | 7.88 | 0.57 | 1.86 | 0.17 | 0.04 | 0.25 | 0.18 | 0.23 | 100 |
| **AM15OF3** | 90.25 | 63.00 | 6.80 | 0.54 | 1.78 | 0.16 | 0.04 | 0.26 | 0.19 | 0.22 | 100 |
| **90 seconds** | 89.98 | 62.82 | 6.78 | 0.54 | 1.77 | 0.16 | 0.04 | 0.26 | 0.19 | 0.22 | 100 |
| **AM15OF4** | 90.92 | 63.47 | 6.43 | 0.52 | 1.78 | 0.17 | 0.05 | 0.26 | 0.19 | 0.25 | 101 |
| **120 seconds** | 90.38 | 63.09 | 6.39 | 0.51 | 1.77 | 0.17 | 0.05 | 0.26 | 0.19 | 0.25 | 100 |

The XRF analysis data for the flotation tests conducted after 15 minutes of milling is given. Note that the fines was screened out prior to milling.

| Sample 15 min Milled | Fe2O3 (%) | Fe (%) | SiO2 (%) | K2O (%) | Al2O3 (%) | P2O5 (%) | SO3 (%) | MnO (%) | TiO2 (%) | CaO (%) | |
|---|---|---|---|---|---|---|---|---|---|---|---|
| **Feed** | 93.10 | 65.00 | 4.25 | 0.25 | 1.33 | 0.13 | 0.03 | 0.11 | 0.11 | 0.12 | 100 |
| **AM16CONC** | 94.55 | 66.00 | 1.89 | 0.26 | 1.02 | 0.16 | 0.03 | 0.26 | 0.17 | 0.20 | 99 |
| | 95.92 | 66.96 | 1.91 | 0.26 | 1.03 | 0.16 | 0.03 | 0.26 | 0.17 | 0.21 | 100 |
| **AM16CONC** | 94.51 | 65.98 | 1.90 | 0.26 | 0.98 | 0.14 | 0.04 | 0.27 | 0.18 | 0.21 | 99 |
| | 95.94 | 66.98 | 1.93 | 0.26 | 0.99 | 0.14 | 0.04 | 0.27 | 0.18 | 0.21 | 100 |
| **AM16OF1** | 86.34 | 60.28 | 10.22 | 0.61 | 2.02 | 0.17 | 0.05 | 0.26 | 0.19 | 0.24 | 100 |
| **30 seconds** | 86.23 | 60.20 | 10.20 | 0.61 | 2.02 | 0.17 | 0.05 | 0.25 | 0.19 | 0.24 | 100 |
| **AM16OF2** | 89.98 | 62.82 | 7.57 | 0.56 | 1.79 | 0.17 | 0.04 | 0.26 | 0.19 | 0.24 | 101 |
| **60 seconds** | 89.20 | 62.27 | 7.50 | 0.56 | 1.77 | 0.17 | 0.04 | 0.26 | 0.19 | 0.24 | 100 |
| **AM16OF3** | 91.04 | 63.56 | 6.36 | 0.50 | 1.71 | 0.17 | 0.05 | 0.26 | 0.19 | 0.20 | 101 |
| **90 seconds** | 90.58 | 63.23 | 6.32 | 0.49 | 1.70 | 0.17 | 0.05 | 0.26 | 0.19 | 0.20 | 100 |
| **AM16OF4** | 94.62 | 66.06 | 2.56 | 0.49 | 1.64 | 0.16 | 0.04 | 0.26 | 0.19 | 0.22 | 100 |
| **120 seconds** | 94.41 | 65.91 | 2.55 | 0.49 | 1.63 | 0.16 | 0.04 | 0.26 | 0.19 | 0.22 | 100 |

Results for flotation conducted at various milling times follows. The flotation masses were weighed after 30, 60, 90 and 120 seconds during flotation, which was used to calculate the concentrate grade and recovery over time.

| Mass Rec | AM14 | AM15 | AM16 |
|---|---|---|---|
| **OF1 - 30 seconds** | 9.42 | 37.77 | 40.68 |
| **OF2 - 60 seconds** | 20.78 | 52.92 | 65.78 |
| **OF3 - 90 seconds** | 15.51 | 34.36 | 44.39 |
| **OF4 - 120 seconds** | 7.46 | 25.62 | 26.83 |
| **OF5** | - | - | 13.57 |
| **CONC** | 430.38 | 270.57 | 189.27 |
| **Total** | 483.55 | 421.24 | 380.52 |

The following includes the raw data for the flotation tests conducted on material after a fixed milling time of 25 minutes with varying amine and starch dosages.

| Sample | MnO (%) | TiO2 (%) | Fe (%) | K2O (%) | P (%) | SiO2 (%) | Al2O3 (%) | CaO (%) | MgO (%) | Na2O (%) | S (%) |
|---|---|---|---|---|---|---|---|---|---|---|---|
| **FEED** | 0.071 | 0.19 | 65.51 | 0.394 | 0.056 | 4.01 | 2.074 | 0.147 | 0.044 | 0.017 | 0.019 |
| **50 g/t amine T** | 0.043 | 0.213 | 62.43 | 0.623 | 0.059 | 7.72 | 1.84 | 0.14 | 0.097 | 0.025 | 0.026 |
| **50 g/t amine P** | 0.086 | 0.173 | 65.89 | 0.395 | 0.059 | 3.6 | 2.103 | 0.131 | 0.038 | 0.01 | 0.012 |
| **75 g/t amine T** | 0.061 | 0.219 | 63.1 | 0.69 | 0.069 | 8.03 | 3.24 | 0.165 | 0.137 | 0.033 | 0.029 |
| **75 g/t amine P** | 0.09 | 0.178 | 66.32 | 0.372 | 0.056 | 2.81 | 1.725 | 0.131 | 0.036 | 0.015 | 0.012 |
| **100 g/t amine T** | 0.051 | 0.254 | 63.42 | 0.608 | 0.053 | 7.42 | 3.28 | 0.121 | 0.056 | 0.013 | 0.012 |
| **100 g/t amine P** | 0.092 | 0.155 | 66.811 | 0.207 | 0.056 | 1.92 | 1.33 | 0.145 | 0.037 | 0.014 | 0.012 |
| **125 g/t amine T** | 0.052 | 0.25 | 63.53 | 0.615 | 0.053 | 7.03 | 3.02 | 0.122 | 0.056 | 0.018 | 0.011 |
| **125 g/t amine P** | 0.086 | 0.156 | 67.077 | 0.175 | 0.051 | 1.56 | 1.203 | 0.129 | 0.03 | 0.017 | 0.01 |
| **200 g/t starch T** | 0.055 | 0.266 | 64.26 | 0.703 | 0.055 | 3.93 | 3.24 | 0.119 | 0.062 | 0.022 | 0.014 |
| **200 g/t starch P** | 0.099 | 0.165 | 66.547 | 0.226 | 0.057 | 2.53 | 1.235 | 0.157 | 0.032 | 0.011 | 0.012 |
| **400 g/t starch T** | 0.051 | 0.254 | 62.58 | 0.608 | 0.053 | 7.42 | 3.28 | 0.121 | 0.056 | 0.013 | 0.012 |
| **400 g/t starch P** | 0.092 | 0.155 | 66.811 | 0.207 | 0.056 | 1.92 | 1.33 | 0.145 | 0.037 | 0.014 | 0.012 |
| **600 g/t starch T** | 0.047 | 0.278 | 62.56 | 0.734 | 0.054 | 6.95 | 3.65 | 0.117 | 0.067 | 0.021 | 0.013 |
| **600 g/t starch P** | 0.084 | 0.168 | 66.32 | 0.242 | 0.053 | 2.61 | 1.36 | 0.132 | 0.038 | 0.017 | 0.011 |
| **800 g/t starch T** | 0.054 | 0.27 | 62.53 | 0.796 | 0.054 | 7.62 | 4.065 | 0.12 | 0.069 | 0.015 | 0.013 |
| **800 g/t starch P** | 0.089 | 0.16 | 66.063 | 0.233 | 0.052 | 3.12 | 1.326 | 0.13 | 0.037 | 0.016 | 0.012 |

## 7.8 Appendix H: Safety and chemical disposal

### 7.8.1 Safety

As there are agitating components, compressed air, chemicals, glass and hot ovens to be used, safety is an important factor to consider. For working with both the laboratory scale test rigs and the automatic splitters, the proper PPE used included a lab coat, closed shoes, long pants, gloves, and safety glasses. When using the ovens, heat resistant gloves were a must. In addition, all of the MSDS documentation for all the chemicals used is included in this document under the appendices, as well as in a file that is placed at the relevant test equipment for ease of access during emergencies.

The reagents were stored and locked away in safe storage. Fire extinguishers were also placed in close vicinity of the test equipment, as all of the reagents are flammable to some extent.

Finally, hazard identification risk assessments were done prior to working on any test equipment, according to the safety standards of the University of Pretoria.

### 7.8.2 Disposal of chemicals and samples

All organic and inorganic chemicals were disposed of in a single five litre bottle and concealed until the end of the project. The reagents were then disposed of according to the disposal method stipulated in the MSDS documents. The same goes for the inorganic reagents, except that another container was used.

## 7.9 Appendix I: AZMET and ENPROTEC LSTK proposals

### 7.9.1 Enprotec proposal

ENPROTEC
CREATIVE THINKING, NEW POSSIBILITIES

1 Mill str, Middelburg, Mpumalanga, South Africa
PO Box 14946, Witbank, Middelburg 1050, South Africa
Tel: 013 246 1389
Fax: 013 246 1070
Email: info@enprotec.co.za
www.enprotec.co.za

20 October 2015

Subject: 20% Budget Estimate for a 100 tph Iron Flotation, Product Filtration and Discard Filtration Plant

Mornè Kruger, currently a student at the University of Pretoria, whom is currently busy with his M.Eng requested a 20 % budget estimate quotation for a flotation, product filtration and tails filtration plant for a 100 tph iron ore plant.

ENPROTEC (ENVIRONMENTAL AND PROCESS TECHNOLOGIES) was established based on the need for a mineral processing company with the capability to provide solutions for the recovery of ultra-fine minerals [i.e., coal, platinum, iron ore etc.] and we pride ourselves on our knowledge and experience to provide sustainable and viable solutions to our clients.

ENPROTEC has the capability to carry out environmental, economic and technical feasibility studies to determine the most viable solution to turn waste stream into a viable product stream.

The company operates from three key fields: the Projects and Engineering Services Division, the Operations Management Division and the Process Equipment Division.

ENPROTEC has conducted complete turnkey solutions for various clients: including Anglo American, Northam, Glencore, SASOL, Jindal, Keaton Energy, BECSA, EVRAS (Vametco), etc.

*100 tph Flotation, Product Filtration and Discard Filtration Plant*

The following design information was received from Morne Kruger (based on laboratory test work):

- Desliming Cyclone Plant
  - Design feed tonnage - 100 tph (iron ore)
  - Feed D80 - 38 micron
  - Product D80 - 25 micron
  - Recovery to U/F - 60%
  - Main feed solids content - 30% (w/w)
- Flotation Plant
  - Design feed tonnage - 40 tph
  - Yield to product - 50%
- Product Filtration
  - Design feed tonnage - 80 tph
  - Feed solids content - 14% solids (w/w)
- Discard Filtration
  - Design feed tonnage - 20 tph
  - Feed solids content - 30% solids (w/w)

Based on the design information the following 20% budget estimate for the Capital Expenditure (CAPEX) is tabulated below:

| Plant Area | Estimated Capital Cost |
|---|---|
| **Desliming Cyclone Plant** | R 15 000 000.00 |
| **Flotation Plant** | R 20 000 000.00 |
| **Flotation Product Circuit** | |
| Product thickener | R 15 000 000.00 |
| Product Filter Plant | R 60 000 000.00 |
| **Flotation Tailing Circuit** | |
| Tails thickener | R 11 000 000.00 |
| Tailings Filter Plant | R 20 000 000.00 |

Based on the design information the following 20% budget estimate for the Operational Expenditure (OPEX) is tabulated below:

| Description | Cost | | Unit |
|---|---|---|---|
| **Flotation Amine** | R | 1.40 | R/feed ton |
| **Flotation Starch** | R | 1.44 | R/feed ton |
| **Flotation Modifier** | R | 10.00 | R/feed ton |
| **Flotation Plant Maintennce** | R | 1.48 | R/feed ton |
| **Product Thickener** | R | 1.32 | R/feed ton |
| **Product Filter Plant** | R | 4.40 | R/feed ton |
| **Tailings Thickener** | R | 0.33 | R/feed ton |
| **Tailings Filter Plant** | R | 1.50 | R/feed ton |
| **Electricity** | R | 28.00 | R/feed ton |
| **Railage** | R | 76.00 | R/feed ton |
| **Labour** | R | 5.11 | R/feed ton |

## Inclusions

- Project Management incl. P's and G's
- Design
- Procurement and Supply
- Installation
- Commissioning

This is inclusive of civil works, mechanical works, structural works, electrical works as well as control and instrumentation.

## Exclusions

- Earthworks

Hope you find the above in order,

J Jacobs
ENPROTEC

### 7.9.2 AZMET proposal

AZMET TECHNOLOGY & PROJECTS

20 October 2015

Subject: 20% Budget Estimate for a 40 tph Iron Flotation, Product Filtration and Discard Filtration Plant

Mornè Kruger, currently a student at the University of Pretoria, whom is currently busy with his M.Eng requested a 20 % budget estimate quotation for a milling circuit for a 40 tph iron ore plant.

AZMET Technology and Projects (Pty) Ltd's executive team has more than 50 years collective experience within the mining and mineral sectors.

Our industry knowledge and experience, linked to a sound fundamental understanding of numerous metallurgical processes, ensures feasible and economically viable solutions to our clients.

AZMET distinguishes itself by constantly striving to provide clients with the latest technologies and designs that will maximize profit and minimize cost, with an unparalleled safety and environmental consciousness.

*100 tph Flotation, Product Filtration and Discard Filtration Plant*

The following design information was received from Morne Kruger (based on laboratory test work):

- Milling Plant
  - Design feed tonnage - 40 tph (iron ore)
  - Feed D80 - 75 micron
  - Product D80 - 20 micron
  - Main feed solids content - 30% (w/w)
- Including recirculation system (Sizing Cyclone Plant)

Based on the design information the following 20% budget estimate for the Capital Expenditure (CAPEX) in South Africa is tabulated below. These estimates are based on our in-house database information for similar process parameters:

| Plant Area | Estimated Capital Cost |
|---|---|
| **Milling Plant** | R 54 000 000.00 |
| **Sizing cyclone** | R 10 000 000.00 |

Based on the design information the following 20% budget estimate for the Operational Expenditure (OPEX) is tabulated below:

| Description | Cost | | Unit |
|---|---|---|---|
| **Milling (incl. cyclones)** | R | 24.00 | R/feed ton |
| **Milling Plant Maintenance** | R | 20.00 | R/feed ton |

**Inclusions**

- Project Management incl. P's and G's
- Design
- Procurement and Supply
- Installation
- Commissioning

This is inclusive of civil works, mechanical works, structural works, electrical works as well as control and instrumentation.

**Exclusions**

- Earthworks

Hope you find the above in order,

Barry
AZMET